The Dissertation Committee for Daniel James Ellenberger Certifies that this is the approved version of the following dissertation:

Processing Challenging Active Pharmaceutical Ingredients And Polymers By KinetiSol® To Produce Amorphous Solid Dispersions With Improved In-Vitro And In-Vivo Performance

Committee:

Robert Williams, Supervisor

Feng Zhang

Zhengrong Cui

Christopher Frei

Dave Miller

Processing Challenging Active Pharmaceutical Ingredients And Polymers By Kinetisol® To Produce Amorphous Solid Dispersions With Improved In-Vitro And In-Vivo Performance

by

Daniel James Ellenberger

Dissertation

Presented to the Faculty of the Graduate School of

The University of Texas at Austin

in Partial Fulfillment

of the Requirements

for the Degree of

Doctor of Philosophy

The University of Texas at Austin

December 2017

Dedication

To Cathleen, Roscoe, Molly, Jane, Ed, Cookie, and George

Acknowledgements

I would first like to thank Dave Miller, my mentor for the last 4.5 years of my professional and academic career. You have shown tremendous patience as I talk through all of my thoughts and theories with every bit of data generated. Whenever there was interesting data or information to pursue, you enabled pursuit of it in whatever way possible. The value you place in continuing education is why I am completing the educational work for which this manuscript is a culmination of that effort. I am also thankful that you passed on your favorite pet project (vemurafenib) and turned me loose to explore it.

I would also like to thank Dr. Williams, my supervisor during my time as a graduate student at the university. You may not realize it, but you've had a role in nearly every part of my career from my first job at PharmaForm in 2009 to joining DisperSol in 2013 to joining your research group in 2015. You were a check on my industry perspective and helped train me to communicate in a meaningful way with other scientists. I also want to thank you for your patience and work over the last few months as everything has wrapped up all at once.

A large thank you is also owed to Sandra Kucera. You are my work bff and I appreciate that we get along as well as we do. You have been a sounding board for ideas and have provided invaluable feedback and insight. I am also especially thankful for your collaboration and help on the ritonavir and lubricant projects.

There are several other individuals at DisperSol Technologies who deserve recognition as well. To Devon McDonald, your help with training and support on operation of the KinetiSol units was invaluable. You provided insight whenever I needed assistance with troubleshooting and assistance with lubricant sample generation. To Jordan Tuz, Jonathon DenBeste, Adam Mincey, and Jonathon Risso, I would like to thank all of you for your help in operating the manufacturing scale of the process. To Tracy Day, your help with initial development of our lab scale MBP process was very beneficial. To Drew Barhydt, your efforts during a summer of failed projects and MBP production was of great help. To Doran Pennington, your assistance with dissolution analysis and listening to my ramblings as I tried to explain experimental observations was very appreciated. To Gershon Yaniv, thank you for being the person to initially plant the seed and nudge me into joining the graduate program at the university. Without this, none of the efforts in this work would have been possible. To Chris Brough, your insight into the mechanisms of the technology helped to explain and troubleshoot issues as I worked through my projects. Thank you to all of you for your help.

I also owe a huge thank you to John Koleng. Your timely loan of an entire dissolution apparatus during a time of crisis kept multiple projects on track. Thank you so very much.

Many other individuals played a role in helping projects. Dr. Matt Nethercott and Dr. Eric Munson of Kansas Analytical Services collected SSNMR data and helped with interpretation of this advanced technique. Dr. Oksana and Dr. Konstantin Tsinman of Pion Inc. were invaluable in their help with designing and performing FLUX based experiments.

Daniel Moriaga, Ashlee Branuagh, Dr. Dwight Romanovicz, and Dr. Alan Watts all provided valuable equipment training that enabled the work contained within this work.

I also owe a thank you to Yolanda Camacho, Stephanie Crouch, and Charmarie Burke for their help in cutting through the red tape that is administration, paperwork, and scheduling.

To Zach Warnken and Hannah O'Mary, I am glad that I was able to survive and complain about a number of classes with y'all.

Finally, and most importantly, I need to thank Cathleen. Thank you so much for putting up with the extra/atypical hours, the stress and the occasional crankiness. Thank you so much for being my alarm clock when late hours were required. Thank you for being a voice of encouragement as I have worked through this program. Your love and support has meant the world to me. You are my partner in crime and in life.

Processing Challenging Active Pharmaceutical Ingredients And Polymers By Kinetisol® To Produce Amorphous Solid Dispersions With Improved In-Vitro And In-Vivo Performance

Daniel James Ellenberger, Ph.D.

The University of Texas at Austin, 2017

Supervisor: Robert O. Williams III

KinetiSol processing is an emerging technology for processing amorphous solid dispersions for pharmaceutical delivery of poorly water soluble drugs. Chapter 1 reviews the current literate around the application of this technology and provides insights into its benefits to pharmaceutical product development for poorly water soluble drugs.

In Chapter 2, KinetiSol processing was used to render amorphous the poorly water soluble drug vemurafenib. Vemurafenib was challenging because conventional processes of pharmaceutical amorphous dispersions (hot melt extrusion and spray drying) were unable to render formulations containing this molecule amorphous and a non-ideal solvent-controlled coprecipitation process was utilized in production of its commercial product. Material generated by the KinetiSol process had particle morphology that differentiated it from the commercial particles. In-vitro and in-vivo performance analysis of the KinetiSol and commercial materials demonstrated enhanced product performance and drug exposure for the materials processed by KinetiSol.

In Chapter 3, KinetiSol processing produced a high drug load formulation of the anti-viral and pharmacokinetic boosting drug, ritonavir. The amorphous solid dispersion of ritonavir was demonstrated as amorphous and intimately mixed by sensitive analysis such as solid state nuclear magnetic resonance. During comparison to the commercial product for ritonavir, transmembrane flux analysis revealed similar permeation rates for both dosages. Subsequent in-vivo pharmacokinetic analysis in dogs resulted in equivalent exposure for the test and reference products with a small reduction in maximum plasma concentration. It was concluded that the tablet generated in the study could serve as a pharmacokinetic booster with tablet mass reduced by approximately half.

In Chapter 4, the extent of a surprising pharmacokinetic result with a lubricant was investigated. The result was surprising as lubricants such as magnesium stearate are typically understood to hinder performance in dosage forms containing poorly soluble drugs and are typically avoided, but the original result showed a significant increase in exposure. The study evaluated several additional cases and demonstrated positive effects of lubricant inclusion for weak acid, neutral, and weak base example compounds. Additionally, the study evaluated additional components not classified as pharmaceutical lubricants but with similar physiochemical properties to magnesium stearate and demonstrated similar positive benefits for these additional compounds.

Table of Contents

List of Tables

List of Figures

Chapter 1: Expanding the Application and Formulation Space of Amorphous Solid Dispersions with KinetiSol®: A Review

1.1 Abstract:

Due to the high number of poorly soluble drugs in the development pipeline, novel processes for delivery of these challenging molecules are increasingly in demand. One such emerging method is KinetiSol, which utilizes high shear to produce amorphous solid dispersions. The process has been shown to be amenable to difficult to process active pharmaceutical ingredients with high melting points, poor organic solubility, or sensitivity to heat degradation. Additionally, the process enables classes of polymers not conventionally processable due to their high molecular weight and/or poor organic solubility. Beyond these advantages, the KinetiSol process shows promise with other applications, such as the production of amorphous mucoadhesive dispersions for delivery of compounds that would also benefit from permeability enhancement.

1.2 Introduction:

There is a growing need for aqueous solubility enhancement of active pharmaceutical ingredients (APIs). It is estimated that approximately 70-90% of drugs in development (1, 2) and 40% of currently marketed products (3) are solubility challenged. These drugs fall into class II and class IV of the Biopharmaceutical Classification System (BCS) for which solubility enhancement can

be used to improve oral bioavailability. In the case of BCS class IV compounds, permeability also presents a challenge for effective drug delivery. (4) Lipinski et al. established the rule of five to help predict which APIs coming out of drug discovery and development would be predicted to be challenging based on solubility and permeability considerations. (5) However, recent trends have shown that molecules coming out of development are more likely to be beyond the rule of five or just below the margins of the rule of five. Even though these below the margins drugs meet the rule of 5 criteria, they remain a challenge to develop. Within this trend, highly lipophilic compounds and higher molecular weight compounds are increasingly common. (6) Filed patent applications on drug molecules show on average higher molecular weights and lipophilicity than what is present in commercially approved products indicating high rates of attrition as products move from discovery through development. (7) These molecules tend to be solvation limited and benefit from the application of solubility-enabled formulations to ensure bioavailability. (8) These solubility-enabled formulations address the challenges of poorly soluble molecules by improving drug release rate and/or solubility. Further compounding the problem is growing demand for high dose molecules, particularly in the therapeutic area of oncology. (9) These high dose systems require high drug loadings in the delivery vehicle in order to achieve acceptable pill burden. (10)

A common conceptual approach for solubility enhancement is the use of a spring-parachute model wherein the drug is rapidly released into solution in a supersaturated state above its equilibrium solubility and then maintained in this state for as long as possible. (11, 12) A schematic diagram for this is depicted in Figure 1.1. To meet this model, there are crystalline approaches, non-polymeric approaches, and amorphous solid dispersion approaches. Crystalline

approaches include: salts, polymorphs, particle size reduction (13), nano-crystal formation (10, 14), salts and co-crystals (15, 16). However, these processes only impact the spring portion of the model and poorly soluble drugs will have a strong tendency to rapidly precipitate and thus limiting exposure in patients. Non-polymeric approaches include: lipids (17), cyclodextrins (2), and self-emulsifying systems (18). However, these dosages are either limited by carrier solubility in water (19) or suffer inadequate drug loads to meet the needs of many of today's challenging molecules (10).

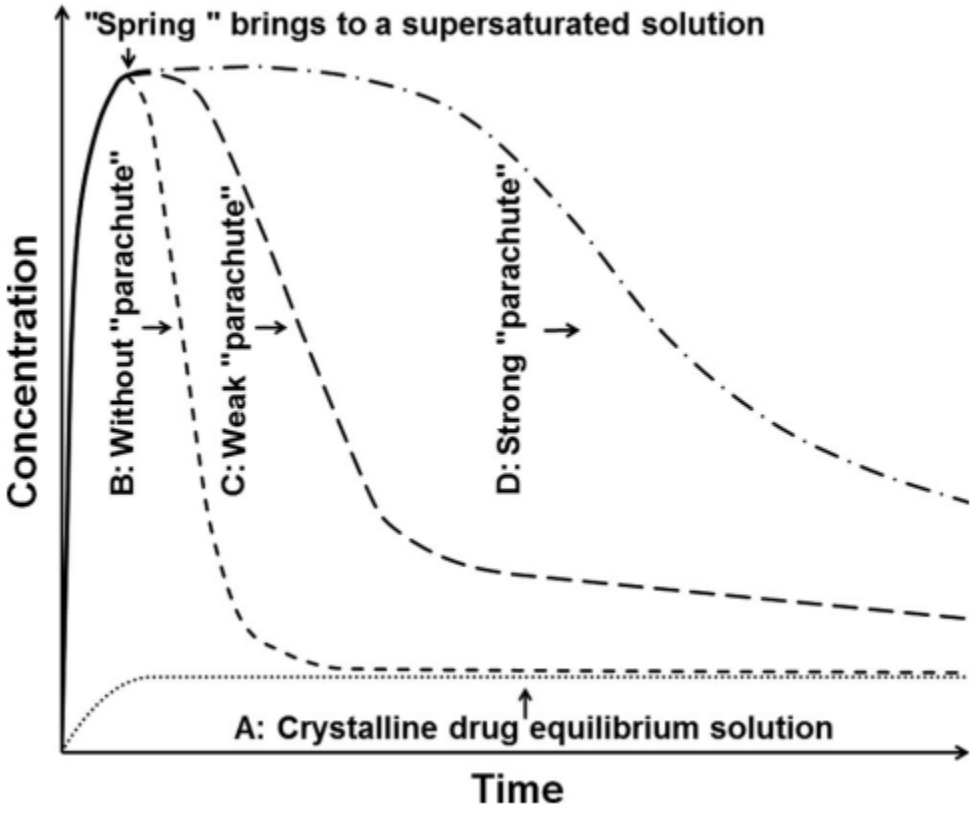

Figure 1.1: Concept Diagram for Spring-Parachute Approach to Solubility Enhancement. Reprinted with permission from (10).

Amorphous solid dispersions (ASDs) have greatly increased in importance due to the physiochemical properties becoming more challenging and increasing doses limiting the applicability of more traditional routes of solubility enhancement. In the ASD approach, drug is converted to an amorphous state and, ideally, molecularly dispersed in a pharmaceutical polymer. The amorphous form puts the drug in a higher energy state in which dissolution and solubility are more favored. The polymer acts to stabilize the drug in the thermodynamically unfavorable amorphous state as well as to provide in-solution stability through drug-polymer interactions. (20, 21) As Miller et al. notes, this amorphous approach does not come at the expense of drug permeability as with other solubility enhancement approaches, i.e., lipid-based systems. (22) Spray-drying (23-25) and hot-melt extrusion (26, 27) are common methods of producing amorphous solid dispersions; however, these approaches are not without their own limitations. Spray-drying is limited by the organic solubility of the drug substance or polymer carrier in common organic solvents. If the API is organic solubility limited, then spray-drying cannot be used for that molecule as seen with the case study vemurafenib described in detail later in this manuscript. (25, 28) As the size and lipophilicity of drug substances continues to increase, inadequate organic solubility will be an increasingly common barrier. The formulation space is also narrowed by poor organic solubility of some polymers/pharmaceutical additives or by too viscous of feed solutions for atomization with other polymer options (e.g. high molecular weight hydroxypropyl methylcellulose). (29) When hot melt extrusion (HME) was first introduced, it was described as a “renaissance” for amorphous solid dispersion technology. Due to economic, environmental, and safety considerations, thermal processes like hot melt extrusion are preferred over solvent based processing like spray drying. (30) However, it has since been realized that the process can be challenging for high melting point APIs, thermally labile materials, and viscous

polymers. (31) As a result, solvent processing is commonly employed due to the described limitations of the hot melt extrusion process. With the increasing presence of molecules needing enabled formulations such as amorphous solid dispersions, it is of importance to have a toolbox of techniques to provide enablement. It is also imperative for these challenging molecules that the formulation space be maximized with the widest range of parachutes available.

To address the growing number of challenging compounds in development and their formulations, a novel technology, KinetiSol, was developed for production of amorphous solid dispersions. KinetiSol utilizes a fusion-based approach to produce amorphous material by rotation of a set of protruding blades to apply friction and shear to the material being processed at an order of magnitude higher than realized by hot melt extrusion. These non-heat energy inputs enable the components to be rendered amorphous at temperatures often well below the melting point of the compound and at fast solubilization rates. (32) KinetiSol has also been applied to materials that are typically difficult to process into an amorphous solid dispersion, including: high melting point APIs, thermally labile components, viscous polymers, and materials with poor organic solvent solubility. Subsequent sections will examine multiple of these case studies. Figure 1.2 illustrates conceptual diagrams for how the formulation space has been expanded by KinetiSol as it relates to the conventionally used hot melt extrusion and spray drying processes. Additionally, the initial KinetiSol research was conducted on industry-scale plastics equipment to assess feasibility of the process. The technology had to be scaled down for pharmaceutical applications which is the opposite of most pharmaceutical technologies. (33) In the plastics space, it has already been proven to be viable for large-scale manufacturing and was

modified for smaller scale pharmaceutical applications, similar to the hot melt extrusion precedent. (30)

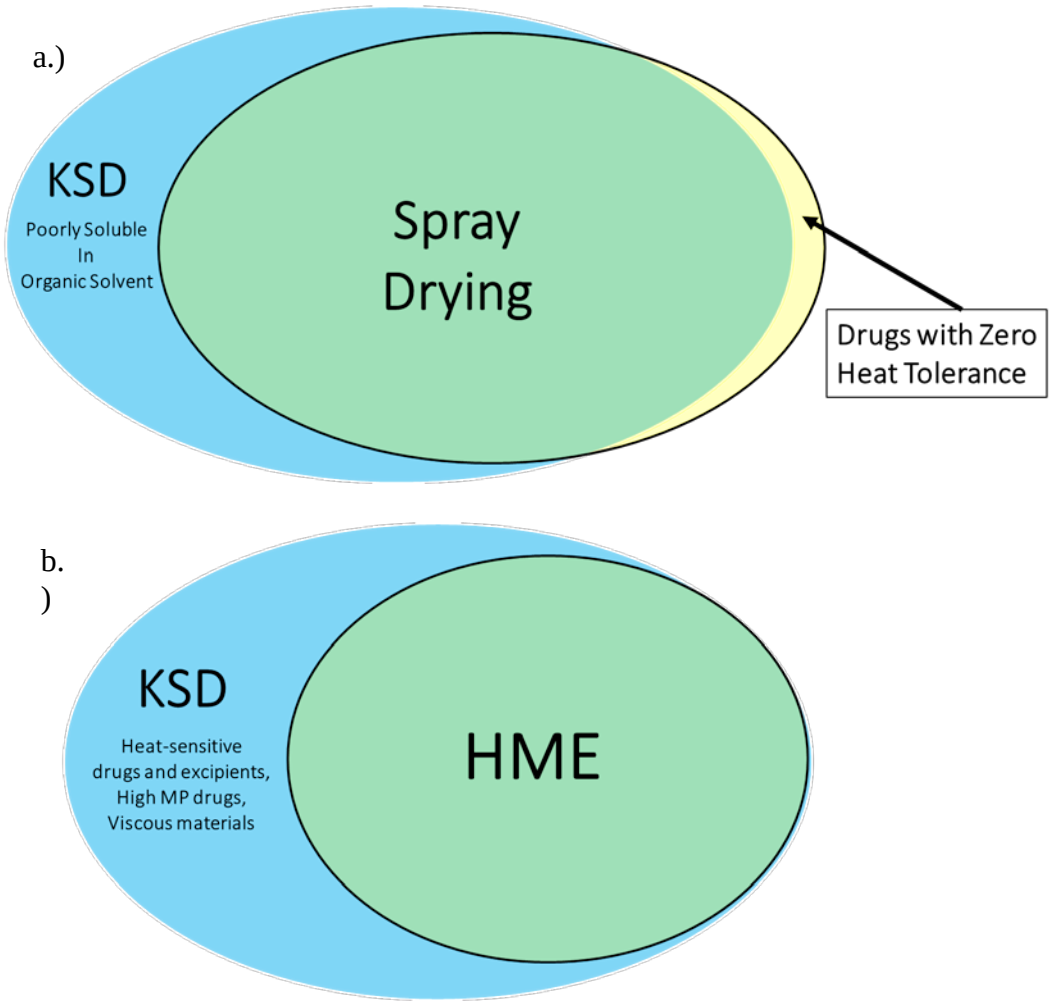

Figure 1.2: Conceptual Diagrams of the Expanded Formulation Space as it Pertains to the Following Process Comparisons: a. KinetiSol and Spray Drying and b. KinetiSol and Hot Melt Extrusion

1.3 Materials, Processing, and Equipment Used by KinetiSol

1.3.1 Materials:

1.3.1.1 APIs Used in KinetiSol Processing:

KinetiSol can be applied to compounds requiring an amorphous solid dispersion, even compounds that would traditionally be a challenge due to high melting point, organic solvent solubility, or thermal instability. As noted in Figure 1.2, it provides unique value to those that cannot be melt extruded due to melting point or thermal instability or those without organic solvent compatibility. Figure 1.3 shows a conceptual matrix for the applicability of spray drying, hot melt extrusion, and KinetiSol as it pertains to API properties of melting point and organic solubility. Further discussion of processing challenging APIs will be covered in case studies later in the manuscript. A summary of APIs used in KinetiSol processing along with their melting points is provided in Table 1.1. It should be noted that the process is not limited to this list as KinetiSol has been used with many more molecules which have not been made publicly available.

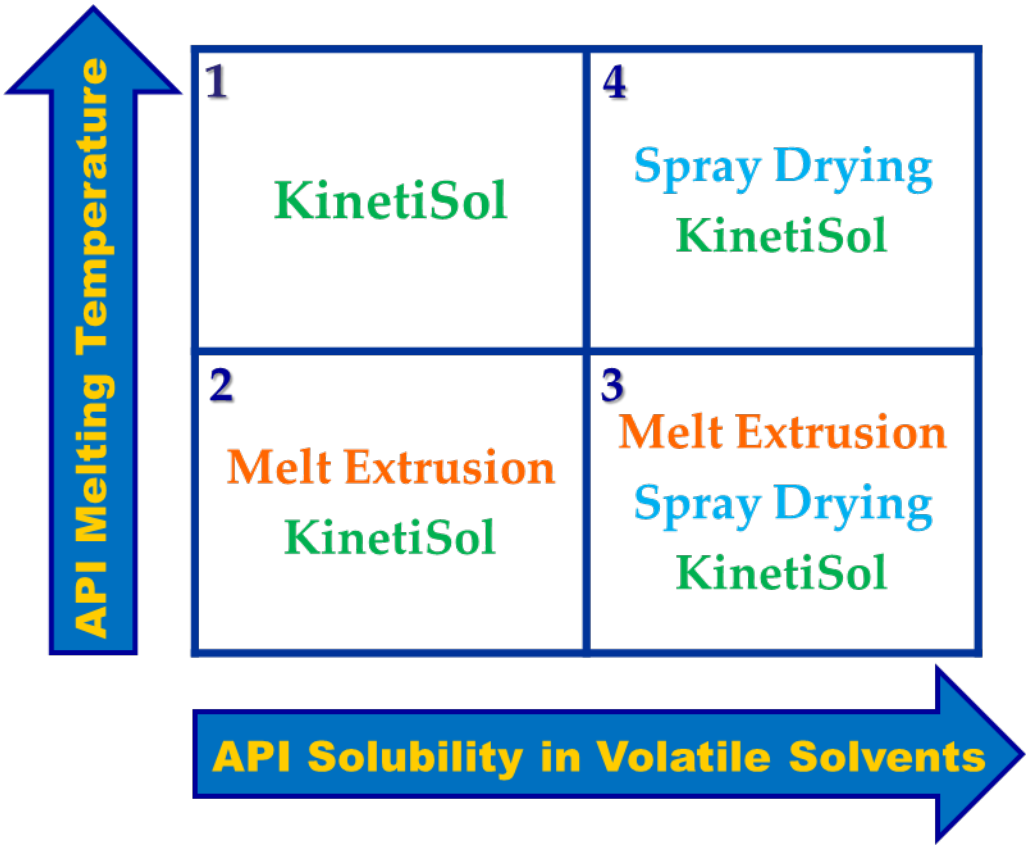

Figure 1.3: Conceptual Matrix for Applicability of Amorphous Solid Dispersion Technologies in Response to API Properties. Adapted from (129).

Active	Melting Point (°C)	KinetiSol Example(s)
Acetaminophen	169 (117)	(33)
AKBA	295 (77)	(37, 77)
Carbamazepine	190 (118)	(38, 46)
Deferasirox	263 (119)	(62)
Griseofulvin	217 (120)	(43, 89)
Hydrocortisone	220 (121)	(43, 44)
Indomethacin	162 (122)	(33)
Itraconazole	170 (84)	(34, 38, 43, 50, 84, 88, 102, 103)
Ketoconazole	146 (123)	(33)
Meloxicam	270 (64)	(64)
Nifedipine	171 (47)	(47)
Ritonavir	120 (56)	(37, 56)
ROA	230 (45)	(45)
Tetrabenazine	126 (124)	(39)
Vemurafenib	272 (72)	(76)

Table 1.1: Disclosed Active Pharmaceutical Ingredients used in KinetiSol Processing (citation is parenthesis).

1.3.1.2 Polymers Used in KinetiSol Processing:

KinetiSol can be used with all polymers commonly used in amorphous solid dispersions. Like with APIs, it expands the formulation space for spray drying and hot melt extrusion (as depicted in Figures 1.2 and 1.3) to include thermally labile, viscous, and organic solvent insoluble polymers. The spray drying process requires a mutual solvent for the API and polymer which can be a limiting factor on the formulation space. Additionally, some polymers, such as high viscosity hypromellose, are not amenable to the process as the feed solution becomes too viscous to form droplets. (29) To thermally process a viscous polymer by hot melt extrusion, the inclusion of a stability compromising processing aid is necessary. (31) The KinetiSol process has been shown to achieve amorphous solid dispersions with these polymers without this inclusion. (34) Additional discussion of processing challenging polymeric carriers will be discussed in a later applications section. A summary of polymers that have been used in KinetiSol processing is provided in Table 1.2.

Polymer	Abbreviation /Trade Name	Grades Processed	Molecular Weight (g/mol)	Tg (°C)	Tm (°C)	Degradation Onset (°C)	KinetiSol Example(s)
Carbomer	Carbopol	974P (110)	700,000-4,000,000,000	100-105	N/A	260	(43, 50, 125)
		71G (110)	700,000-4,000,000,000	100-105	N/A	260	(111)
Methacrylic Acid Copolymers	Eudragit	L100-55 (31)	320,000	111	N/A	176	(33, 43, 45, 50, 77)

Table 1.2: Disclosed Polymers Used in KinetiSol Processing. References in parentheses.

Polymer	Abbreviation /Trade Name	Grades Processed	Molecular Weight (g/mol)	Tg (°C)	Tm (°C)	Degradation Onset (°C)	KinetiSol Example(s)
Hypromellose	HPMC	E3 (126, 127)	20,000	170-180	N/A	200	(39, 44)
		E5 (89)	28,700	170-180	N/A	200	(39, 43, 44, 76, 89)
		E15 (89)	60,300	170-180	N/A	200	(39, 89)
		E50 (89)	86,700	170-180	N/A	200	(33, 34, 39, 88, 89)
		E4M (88, 126)	323,200	180	N/A	200	(88)

Table 1.2, cont.

Polymer	Abbreviation /Trade Name	Grades Processed	Molecular Weight (g/mol)	Tg (°C)	Tm (°C)	Degradation Onset (°C)	KinetiSol Example(s)
Hypromellose Acetate Succinate	HPMCAS	LF (128)	10,000-500,000	120	N/A	258-276	(37, 45, 47, 76, 77, 84)
		MF (128)	10,000-500,000	120	N/A	258-276	(37, 47, 77, 84)
		HF (128)	10,000-500,000	120	N/A	258-276	(47, 84)
Copovidone	PVP/VA	VA64 (31)	45,000-70,000	105	N/A	270	(39, 43, 44, 56, 76)

Table 1.2, cont.

Polymer	Abbreviation /Trade Name	Grades Processed	Molecular Weight (g/mol)	Tg (°C)	Tm (°C)	Degradation Onset (°C)	KinetiSol Example(s)
Polyvinyl Alcohol	PVA	4-88 (99)	31,000	40-80	180-240	180	(56, 102, 103)
		5-88 (99)	37,000	40-80	180-240	180	(103)
		8-88 (99)	67,000	40-80	180-240	180	(103)
		18-88 (99)	130,000	40-80	180-240	180	(103)
		4-38 (99)	Not available	40-80	180-240	180	(102)
		4-75 (99)	Not available	40-80	180-240	180	(102)
		4-98 (99)	27,000	40-80	180-240	180	(102)

Table 1.2, cont.

Polymer	Abbreviation /Trade Name	Grades Processed	Molecular Weight (g/mol)	Tg (°C)	Tm (°C)	Degradation Onset (°C)	KinetiSol Example(s)
Povidone	PVP	K17 (31)	7,000-11,000	140	N/A	217	(89)
		K30 (31)	44,000-54,000	160	N/A	171	(33, 38, 43, 89)
		K90 (31)	1,000,000-1,500,000	177	N/A	194	(89)
Soluplus	Soluplus	N/A (31)	90,000-140,000	72	N/A	278	(46, 64, 77)

Table 1.2, cont.

1.3.1.3 Additives Used in KinetiSol Processing:

Several classes of pharmaceutical additives are important for amorphous solid dispersions and have been used in the KinetiSol process. These additives include:

- Surfactants – are well understood for their use in amorphous solid dispersions. They have a beneficial synergistic effect on drug concentration with polymers through promotion of micelles and colloids to prevent crystallization in solution. (35, 36) Docusate sodium is one such example explored by KinetiSol. (37)
- Release modifiers – these agents can be included to create particles or a monolithic dosage form in which water ingress is hindered and drug release is slowed. An example of this application is glyceryl behenate. (38)
- Chemical stabilizers – these include functional categories like anti-oxidants, pH modifiers, and free radical scavengers. The case study for tetrabenazine includes multiple applications in this role. (39)
- Lubricants – these act as processing aids and improve KinetiSol product discharge (yield). One such example is sodium stearyl fumarate (39), although others like magnesium stearate have been explored by the authors as well.
- Moisture scavengers – as their name implies, these absorb and bind water in the dosage form and improve storage stability. (40, 41) This is seen in the amorphous dispersion of a Norvir®, an approved product for ritonavir. (42)

1.3.2 KinetiSol Processing and Equipment:

1.3.2.1 KinetiSol Processing

KinetiSol processing occurs in a cylindrical chamber with a horizontally aligned shaft. A simplified schematic diagram of the chamber is shown in Figure 1.4. The shaft has a set of protruding blades that undergo controlled rotation to initiate processing of pharmaceutical material. On the outer surface of the chamber, a probe is mounted that monitors the temperature of the pharmaceutical material in real time with rapid process feedback. Doors are engineered into the bottom of the chamber which are designed to rapidly open to allow for quick material discharge with the sample being carried out by centrifugal force imparted by the process. Individual KinetiSol units are described in the following sections.

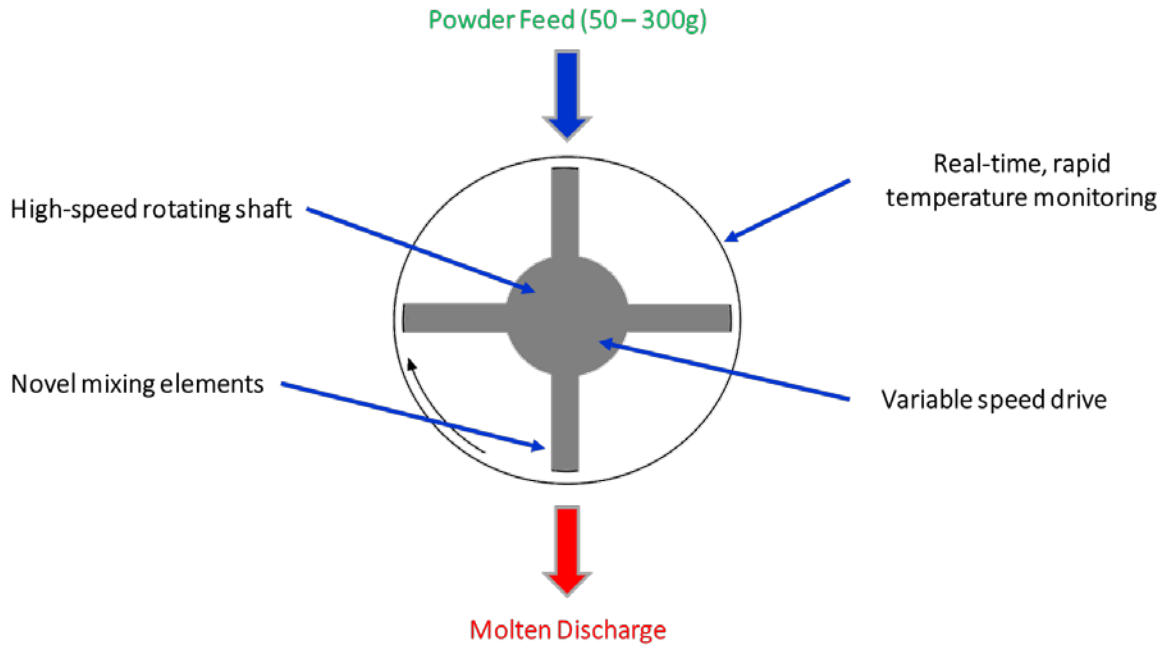

Figure 1.4: Simplified Schematic Diagram for a KinetiSol Compounder

In the typical KinetiSol process, the workflow progresses through:

1. Charging the material – the formulation blend is loaded into the chamber which is then plugged to seal the machine.

2. Control parameters – these are input to the unit to dictate the execution of the process. These parameters are described in detail below.

3. Process initiation - the operator triggers the process and rotation of the blades commences automatically.

4. Discharge – the doors of the unit rapidly open and material is ejected.

5. Quenching – the molten mass can be quenched in a variety of ways, most involving pressing the material to a flat disk to maximize the surface area and heat transfer out of the sample. Manual quenching can be performed by an operator transferring the molten mass to the

surface between two metal plates with pressures applied by the operator or a pneumatic press. Automatic quenching can also be used to quench the sample as it ejects from the unit.

6. Milling – the quenched sample is milled to reduce sample particle size to the desired outcome.

For operation in batch mode, steps 1, 2, 3, and 5 are manually executed by an equipment operator for each aliquot of material. In semi-continuous mode, blended material is loaded into a feed system and parameters are input to the system. The unit runs a described number of batches consecutively operating steps 1-5 autonomously. This mode of operation allows large quantities of materials to be processed without intervention from technicians.

The KinetiSol process has several control parameters that are adjusted to achieve desired processing outcomes:

- Rpm controls the rotational speed of the blades in the chamber. Lower rotational speeds may be beneficial for samples that are shear sensitive, are low viscosity, or need longer processing times to be rendered amorphous. Higher rotational speeds benefit systems that include viscous polymers, require more frictional energy input to become molten, or need higher shear rates.
- Temperature provides feedback on the state of the material in the chamber. Temperature change is influenced by the rpm of the process and can rise rapidly to the desired ejection temperature. As a processing parameter, when the pre-set temperature is reached the sample is ejected.

- Time can be used to control how long the process occurs. This can be useful for maintaining mixing conditions or controlling the duration of time that a sample is exposed to aggressive conditions. (33)

The temperature of the chamber is plotted against run time to create a processing profile for the batch. Figure 1.5 shows processing profiles from an example DOE in which rpm and ejection temperature parameters were modified from run to run. As shown in these processing profiles, rpm influences the duration of both the overall process and the time before temperature increase occurs as well as the rate of temperature increase. Higher rpms promote shorter processing times and increased rate of temperature gain.

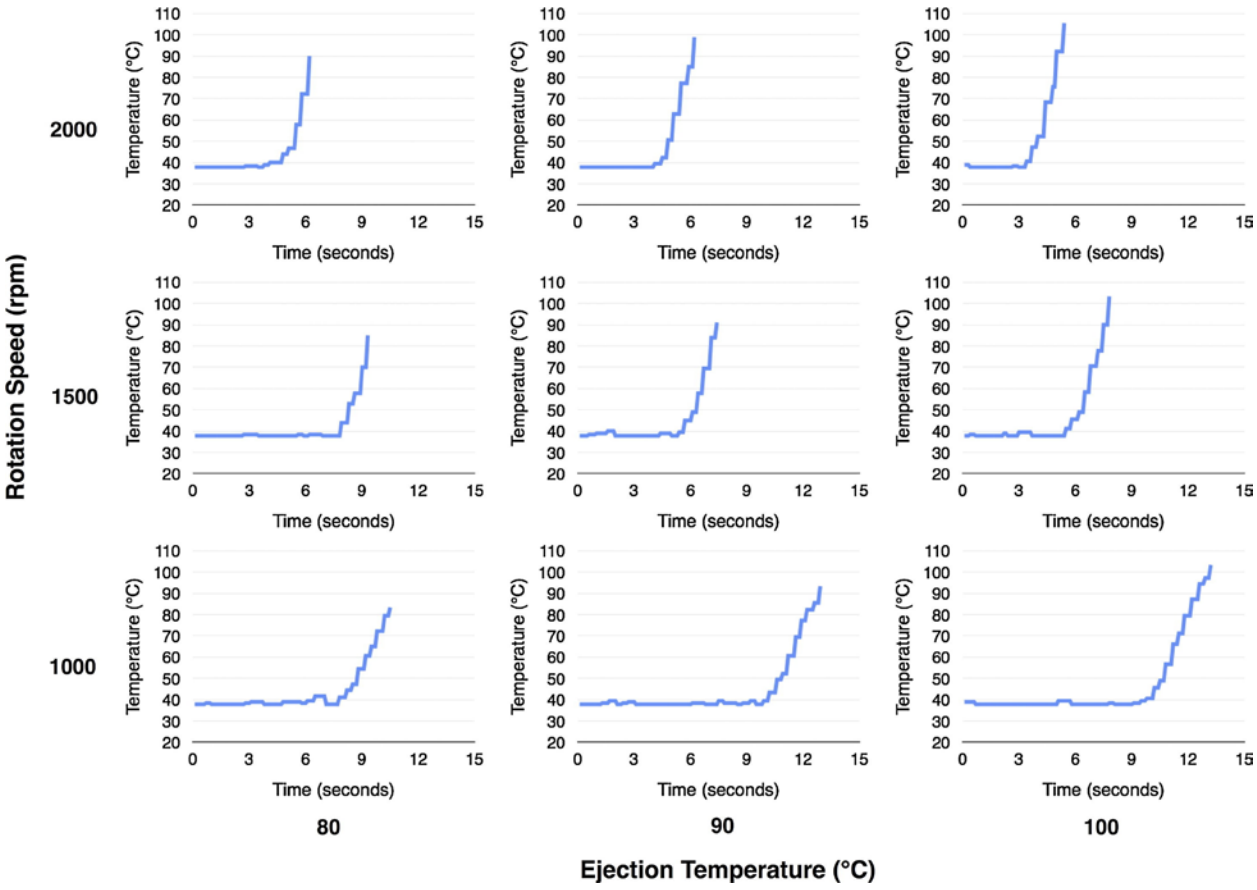

Figure 1.5: Sample KinetiSol Profiles. Reprinted with permission from (56).

1.3.2.2 KinetiSol Equipment

KinetiSol Research Formulator, KBC20:

As the smallest size unit, the KinetiSol Research Formulator was designed with formulation screening and feasibility assessment in mind. Batch size in the Formulator ranges from 7 to 15g which minimizes the use of material when compared to other units for KinetiSol processing. The

entire chamber and blades are easily replaceable allowing for chambers to be swapped in from batch to batch to improve throughput. This enables rapid processing of formulations without the need to clean equipment between each composition. Feed and quenching operations are conducted manually, but the process is monitored and executed in real time by a computer monitoring system. Processing time for each batch is typically between 5 and 20 seconds. The system is dimensionally smaller than other KinetiSol units as seen in the image of a Formulator shown in Figure 1.6.

Figure 1.6: Photograph of the KinetiSol Formulator, KBC20

KinetiSol Batch Compounder, KBC250:

At the time of this writing, most of the published research and patents with KinetiSol was conducted on a Batch Compounder unit. The batch size in the Batch Compounder ranges from 50 to 350g. The unit can be used to facilitate preclinical and early stage clinical supply with up to 10 kg of manufactured material being reasonable. Scale-up of processing parameters from the Formulator unit principally involves applying a linear scaling factor to the rotational speed, with all other parameters remaining the same. Like the Formulator, feed and quenching operations are conducted manually with control in real time by a computer monitoring system. Processing time is typically between 5 and 20 seconds for each batch. An image of a Batch Compounder is shown in Figure 1.7.

Figure 1.7: Photograph of the KinetiSol Batch Compounder, KBC250

KinetiSol Continuous Compounder, KCC250:

The KinetiSol Continuous Compounder is designed with large scale manufacturing options in mind. The geometry and size of the unit matches that of the Batch Compounder. Thus, process development is streamlined when transitioning to high-volume manufacturing because there is no scale-up required, just optimization for continuous processing. Batch size is also 50 to 350g and processing conditions developed on a Batch Compounder directly translate to the Continuous Compounder. However, the unit is equipped with an automated feed and quenching system which greatly increases the throughput, up to 40 kg/hr. The unit's size is 34" x 75" x 60" which potentially enables multiple units to be set up in a single processing suite to increase throughput further if necessary. The unit has the capability to supply materials for Good Manufacturing Practices (GMP) Phase I through commercial manufacturing. As is the case for all KinetiSol units, processing time is typically between 5 and 20 seconds for each batch. The system is configured so that the next batch begins feeding automatically as soon as the ejection door closes from the previous batch. An image of a Continuous Compounder is shown in Figure 1.8.

Figure 1.8: Photograph of the KinetiSol Continuous Compounder, KCC250

Processing and equipment information and photos provided by DisperSol Technologies, LLC

1.4 APPLICATIONS

The KinetiSol process can be applied to drug substances and polymers to produce amorphous solid dispersions. However, it is unique in its ability to process: high melting point drugs, thermally labile APIs and polymers, drugs/polymers with poor organic solubility, and high molecular weight viscous polymers. These applications represent an expansion of the formulation space over conventional hot melt extrusion and spray drying approaches. Each of these unique capabilities will be explored in the subsequent sections.

The KinetiSol process has been utilized to generate amorphous solid dispersions for many active pharmaceutical ingredients. When the process was first applied to pharmaceutical compositions,

feasibility was immediately established for a number of active pharmaceutical ingredients including: acetaminophen, griseofulvin, hydrocortisone, itraconazole, indomethacin, and ketoconazole. (33, 43) After the initial assessment, additional studies were performed to compare the novel process of KinetiSol to the more established thermal process of hot melt extrusion. (44, 45) In addition to the traditional processing polymers explored in these studies, other options such as Soluplus® (46) and low-substituted hydroxypropylcellulose (L-HPC) (47) were also found to be amenable to the KinetiSol process. Other studies have shown the process is agreeable to the inclusion of additives, e.g. anti-oxidants for degradation protection, to provide additional functionality to the produced amorphous solid dispersions. (39)

Subsequent sections will focus on compositions that present unique challenges for processing into amorphous solid dispersions.

1.4.1 API Challenges

1.4.1.1 Thermally Labile APIs

Thermally labile active pharmaceutical ingredients are susceptible to drug substance degradation during processing by thermal techniques. Common strategies to reduce thermal degradation include: lowering of processing temperatures (often through inclusion of plasticizers), shortening processing times, and inclusion of additives to inhibit the mechanism of degradation. KinetiSol has the innate advantage of processing at lower temperatures and for residence times in the range

of seconds rather than minutes which gives it a unique advantage over other thermal processing techniques. (26, 31, 48-51) Figure 1.9 shows an overlay of a KinetiSol profile with a HME profile for a similar composition. It is apparent from this figure that the amount of total thermal exposure of a KinetiSol sample is significantly less than that required by the HME process. As exposure to thermal conditions increases, the risk of API degradation increases and the process becomes less viable. Some examples of thermally labile APIs processed by KinetiSol follow.

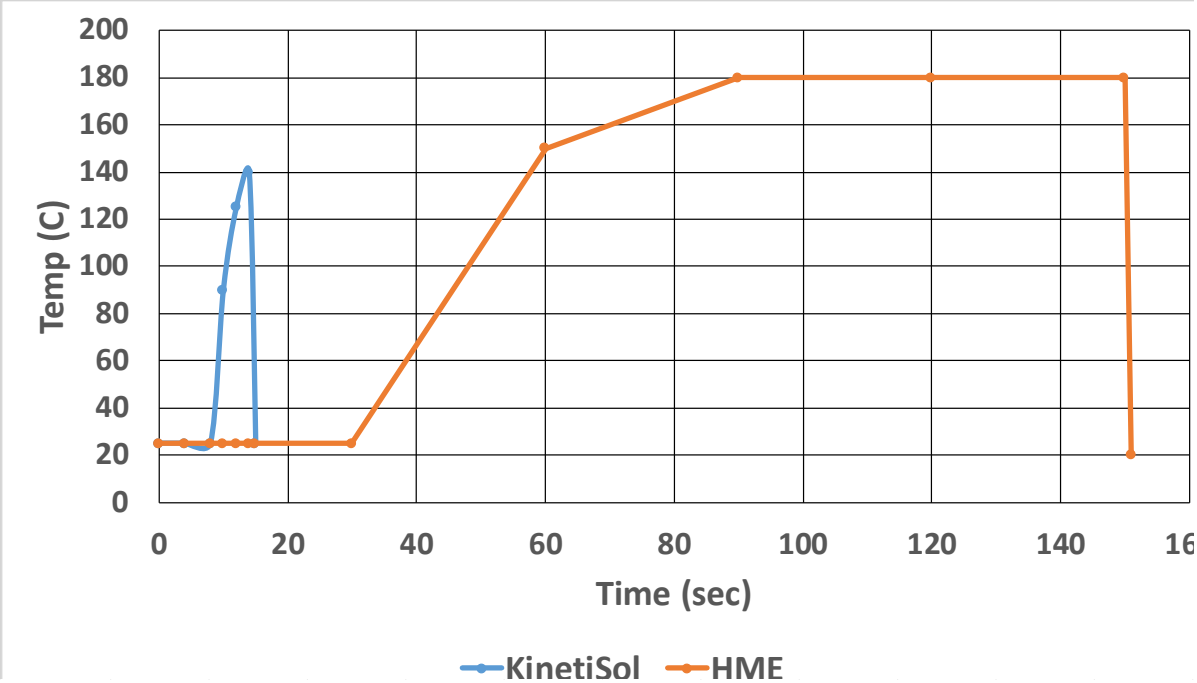

Figure 1.9: Comparison of Temperature Vs. Time Plots Depicting Total Thermal Exposure of an Itraconazole-HPMC E5 System when Processed by Both Hot Melt Extrusion and KinetiSol. KinetiSol plot adapted from (34). Hot melt extrusion plot approximated from temperature and instrument configures described in (86, 130, 131).

Tetrabenazine:

In patent application WO/2015/175505 filed by Miller et al., thermally labile tetrabenazine was processed by KinetiSol. Tetrabenazine is used for treatment of chorea in patients with Huntington's disease and is available as Xenazine®, the only FDA approved product for this treatment. Xenazine is an immediate release product of the weakly basic tetrabenazine in which patients are exposed to an initially high amount of tetrabenazine due to extensive gastric solubility, rapid and complete absorption, and then swift elimination. A significant challenge is that dosing of tetrabenazine is limited by the onset of side effects which correlate to Cmax, and patients are individually dose titrated until onset occurs. For many patients, this results in a lowering of dose and an overall reduction in efficacy. Thus, there is a demonstrated need for improved formulation with modified release properties to produce higher drug solubility in pH neutral environments and blunted Cmax, but with similar AUC in respect to Xenazine.

A new, modified release formulation for tetrabenazine was pursued using the KinetiSol process. Several compositions were explored including various grades of HPMC and in some instances copovidone was included as a secondary polymer. It became apparent during development that oxidative thermal degradation was a challenge that needed to be overcome. Both formulation and process approaches were employed to overcome this barrier. For formulation approaches, combinations of butylated hydroxytoluene, butylated hydroxyanisole, and sodium ascorbate were added to the amorphous solid dispersion as antioxidants to counteract this route of degradation. From a process approach, the compounder chamber was purged with dry nitrogen gas prior to processing. This step reduced the amount of oxygen available in the process, particularly when the sample was at elevated temperatures. The results of the combined formulation and process

adjustments resulted in several tetrabenazine amorphous solid dispersions with acceptable impurity profiles.

The goals of the tetrabenazine amorphous solid dispersions were to provide controlled release of the drug that was less dependent on pH and to reduce Cmax without sacrificing systemic exposure. In-vitro and in-vivo analyses were conducted on the KinetiSol samples. As shown in Figure 1.10, pH change dissolution studies demonstrated that Xenazine behaved as expected with complete immediate release in the acid phase of the test followed by rapid precipitation to the equilibrium solubility of tetrabenazine of approximately 30 µg/mL in media with pH greater than 4. By contrast, the modified release formulations produced by KinetiSol released across a range of concentrations during the 2 hours in gastric media, and were followed by equilibrium in-solution concentrations as high as 50 µg/mL after conversion to neutral media. These four test articles demonstrated that tetrabenazine can be formulated to release across a range of concentrations in the gastric phase with continued drug release and exposure during intestinal transit. Samples were also formulated into tablets and dosed to fasted male beagle dogs and multiple articles showed promising data for Cmax reduction with similar AUC to Xenazine and were selected for dosing in healthy fasted human volunteers. Table 1.3 summarizes these healthy volunteer results. Formulations containing HPMC E3, HPMC E5, and HPMC E15/VA64 had AUC values that were within 5% of Xenazine, but had Cmax values that were 66%, 55%, and 45% of Xenazine's Cmax, respectively. These three formulations show the potential to be titrated to higher doses in patients before side effect onset which would allow for increased exposure and presumably reduction in chorea symptoms in those with Huntington's disease. (39)

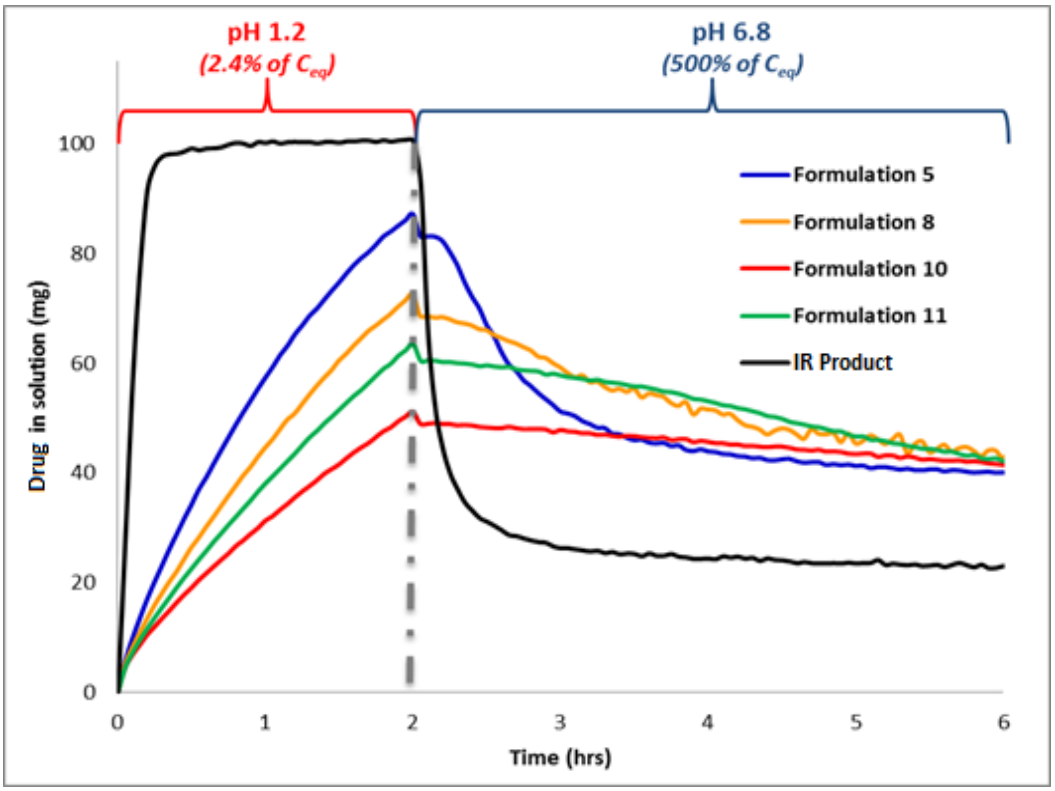

Figure 1.10: Non-Sink Gastric Transfer Dissolution Testing of Tetrabenazine Modified Release Formulations and the Approved IR Product, Xenazine. At pH 1.2, tetrabenazine dissolved to a level of 2.4% of its equilibrium solubility, whereas at pH 6.8, tetrabenazine dissolved to a level of 500% of its equilibrium solubility. Adapted from (39).

Formulation	Xenazine	HPMC E3	HPMC E5	HPMC E50/VA64	HPMC E15/VA64
tmax (h)	1.25 (36%)	3.04 (24%)	3.79 (22%)	3.58 (34%)	3.71 (34%)
Cmax (ng/mL)	51.56 (64%)	34.20 (56%)	28.40 (37%)	20.99 (55%)	23.37 (48%)
AUC0→∞ (hr·ng/mL)	248.4 (63%)	240.5 (54%)	252.7 (70%)	201.8 (54%)	238.8 (54%)

Table 1.3: Human Pharmacokinetic Study Results for Dosing of KinetiSol Modified Release Formulations of Tetrabenazine and the FDA Approved Xenazine. Adapted from (39).

Ritonavir:

Ritonavir (RTV) is a poorly soluble, weakly basic active pharmaceutical ingredient that has been processed into a number of commercial products by hot melt extrusion (52, 53) and has seen application as a permeability enhancer. (54) Studies have shown that ritonavir is shear sensitive, experiencing chemical instability during high shear conditions. (55) A shear sensitive molecule presents a unique challenge to KinetiSol compared to hot melt extrusion as the process utilizes shear an order of magnitude higher. Preformulation work by LaFountaine et al. found that ritonavir was thermally stable up to a temperature of 160°C after which significant chemical degradation was observed. Tertiary systems containing polyvinyl alcohol, copovidone, and ritonavir were processed by KinetiSol with rotational speeds varying from 1000 to 2000 rpm and ejection temperatures from 80°C to 100°C. All but the lowest energy input (1000 rpm and 80°C) were found to be amorphous with respect to ritonavir. Degradation was observed to increase with increasing energy input with the strongest contribution to degradation coming through shear input. This data is depicted in Figure 1.11. However, a number of amorphous compositions were able to be processed by KinetiSol that exhibited acceptable levels of ritonavir purity. (56)

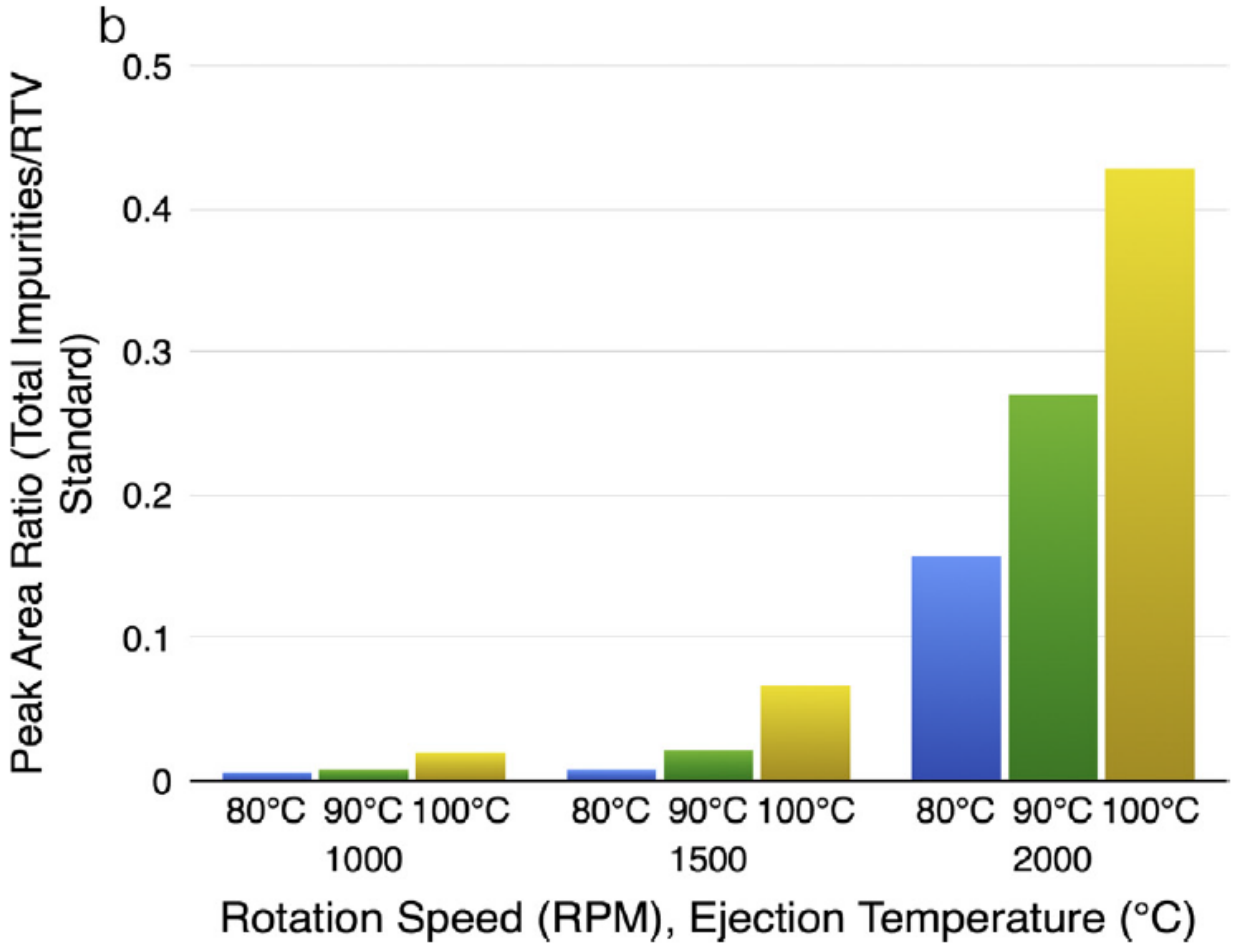

Figure 1.11: Ritonavir Impurities as a Function of Rotation Speed and Ejection Temperature. Reprinted with permission from (56).

Due to processing limitations, polyvinyl alcohol is a little utilized polymer in amorphous solid dispersions and is further explored in the related polymer section below.

A ritonavir amorphous solid dispersion was also explored for use in a combination product with acetyl-11-keto-beta-boswellic acid (AKBA). In the commercial product Norvir, an amorphous dispersion of ritonavir is included with 15% w/w drug loading in its amorphous phase. (42) For

the RTV-AKBA combination product, this drug load was calculated to be inadequate for the intended design and a new formulation was required. An amorphous 30:65:5 RTV:HPMCAS:docusate sodium formulation was developed to increase the drug load. Dissolution results of this amorphous solid dispersion are shown in Figure 1.12. While the enteric nature of the formulation limited its release in the acid phase, pH change to 6.8 initiated rapid drug release with equilibrium solubility essentially equivalent to that of the crushed Norvir tablet. Both samples are well above the literature reported value of ritonavir at 1 µg/mL in pH 6.8 media. The profile was also in sync with the AKBA release profile ensuring similar time and location exposure in-vivo. This new formulation matched the drug load and dissolution requirements for a fixed-dose combination product with AKBA. (37) The AKBA portion of the combination product is further explored in its section below.

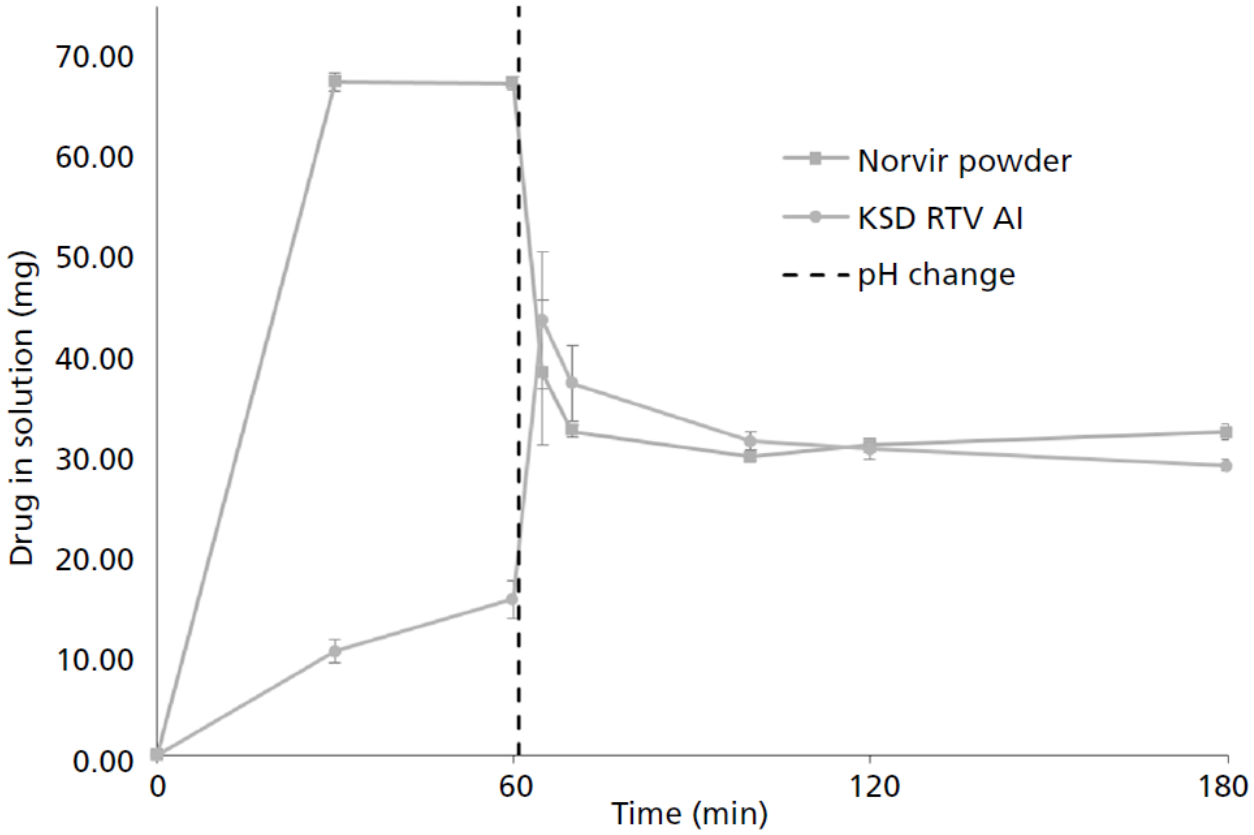

Figure 1.12: pH Change Dissolution Profiles of KinetiSol Ritonavir Amorphous Intermediate as Compared to Crushed Norvir. Reprinted with permission from (37).

Hydrocortisone:

Hydrocortisone is a thermally labile active pharmaceutical ingredient which has been previously studied as a component in amorphous films. During these studies, films containing hydrocortisone produced by hot-melt extrusion were found to have significant oxidative degradation at elevated temperatures. (57) DiNunzio et al. hypothesized that thermal degradation was related to cumulative exposure during hot melt extrusion and that processing by the

relatively shorter KinetiSol would yield product with significantly reduced degradation. Preformulation work conducted using optical hot stage imaging revealed that copovidone allowed processing at a temperature of 160°C while HPMC required a processing temperature of 180°C which posed a higher risk for degradation. These results are depicted in Figure 1.13. Thus, copovidone was selected as the carrier for subsequent studies.

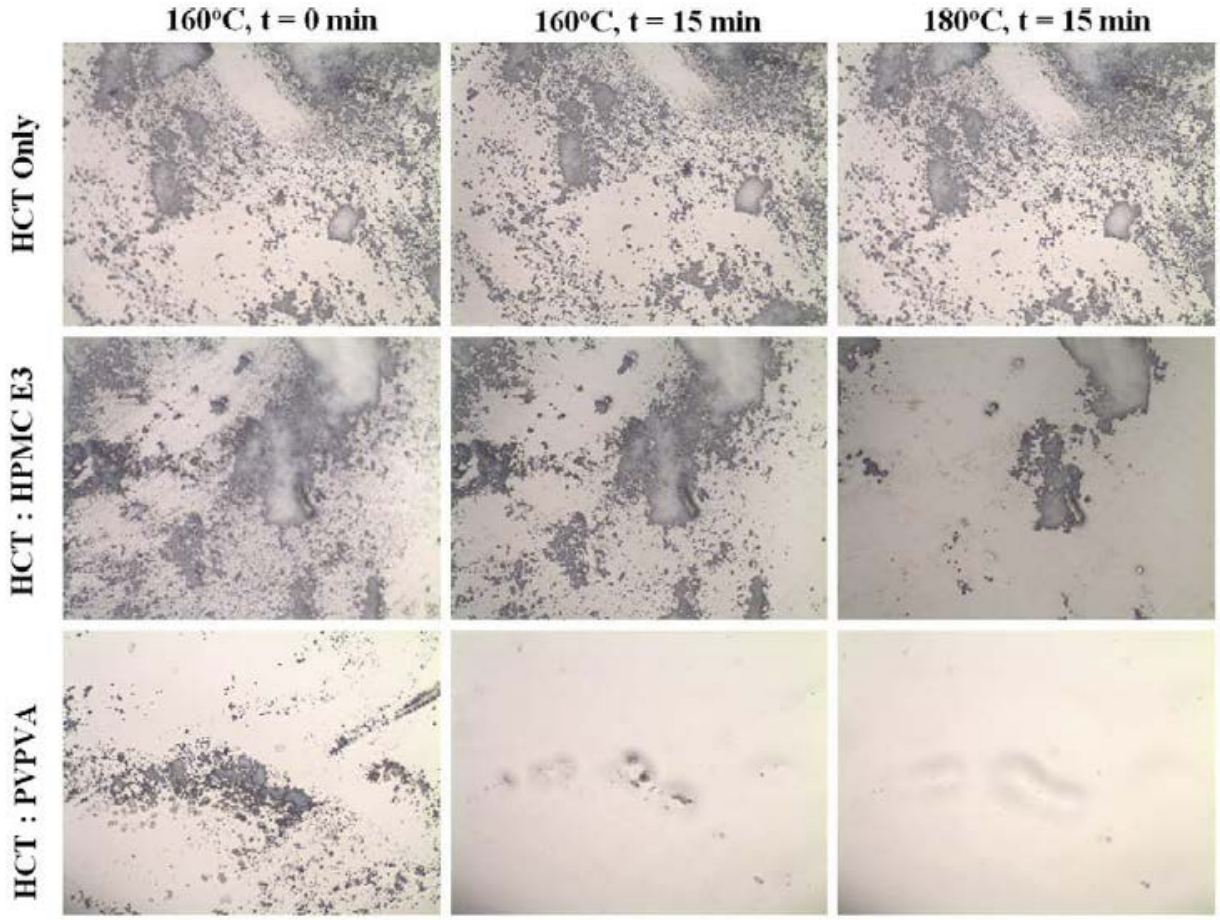

Figure 1.13: Optical Microscopy Analysis for Miscibility of Hydrocortisone (HTC) with HPMC E3 and Copovidone (PVPVA). Reprinted with permission from (44).

Compositions of hydrocortisone-copovidone were prepared by both hot melt extrusion and KinetiSol. The KinetiSol material had reduced degradation compared to the hot-melt extrusion material which the authors ultimately attributed to reduced processing temperature and shorter residence times in the process (less than 30 seconds total with temperatures above 130°C for under 5 seconds). (44) Thus, it was concluded that for the thermally labile hydrocortisone, KinetiSol offered favorable processing conditions for generation of an amorphous solid dispersion.

ROA:

Another investigation into a thermally labile API was conducted by Hughey et al. on a Roche research compound, ROA. Preformulation studies for ROA demonstrated that it was susceptible to thermal and acidic degradation at elevated temperatures. Initially, the authors processed ROA by hot melt extrusion with Eudragit® L100-55 and HPMCAS as the polymeric carriers. However, they found that ROA was processable into an amorphous dispersion containing L100-55 only with the inclusion of a plasticizer (triethyl citrate) or when ROA was micronized during pre-processing. (45) The inclusion of plasticizers in amorphous compositions is known to increase the molecular mobility of the system through lowering the glass transition temperature of the system. This can ultimately lead to phase separation and recrystallization. (58) It could not be rendered fully amorphous at all with HPMCAS. For both compositions by hot melt extrusion, unacceptable levels of ROA related impurities were observed. By contrast, when processed by KinetiSol, both compositions were generated as substantially amorphous with significantly better impurity profiles compared to the hot melt extrusion compositions. Ultimately, amorphous

compositions by both methods could produce approximately threefold higher equilibrium solubility for ROA in aqueous solution. However, the KinetiSol process could realize these solubility gains without sacrificing chemical stability of the drug substance. (45)

1.4.1.2 High Melting Point APIs

Active pharmaceutical ingredients with high melting points represent a challenge to conventional methods for thermal processing, like hot melt extrusion. The challenges with processing these high melting point molecules through thermal processing (without the inclusion of processing aids) has been extensively documented. (31, 51, 59-61) However, a number of examples exist for which the high shear process, KinetiSol, can render these actives amorphous at temperatures significantly below their melting point and without the inclusion of processing aids. Some of these examples are expanded on below.

Deferasirox:

An example of a high melting point drug successfully processed by KinetiSol is deferasirox, as demonstrated in patent application WO/2016/205658. Deferasirox (DFX) is an orally delivered iron chelator used in the treatment of chronic iron overload in patients who are receiving long-term blood transfusions. It is commercially available in the United States as Exjade® and Jadenu®. Deferasirox delivery from these dosage forms is noted as having highly variable delivery stemming from issues with the pH dependent solubility of the molecule. As a weak acid, deferasirox has poor gastric solubility which can lead to drug aggregate formation limiting

intestinal absorption. (62) Deferasirox is also a high dose therapy (up to 40mg/kg/day) and when coupled with solubility challenges leads to ~30% of patients absorbing the drug poorly and not responding to treatment. This unmet need of improving bioavailability for these non-responder patients is where an improved formulation would have significant value. (63) It was hypothesized that an amorphous solid dispersion of deferasirox would hinder drug aggregate formation and improve bioavailability. However, processing deferasirox by hot melt extrusion would represent a significant challenge as deferasirox's melting point of 264-265°C would require processing temperature that would degrade the polymers employed. Spray drying deferasirox is challenging as it has limited solubility in organic solvents commonly used in the spray drying process.

The KinetiSol process was deployed to generate amorphous solid dispersions of deferasirox. Systems containing deferasirox and one or more of copovidone, HPMCAS, and Eudragit were manufactured with deferasirox drug loads of 40-60%, except in the case of binary deferasirox/HPMCAS where maximal drug load was 20%. These systems were found to be fully amorphous by x-ray powder diffraction and maintained a lack of crystallinity for 2 months of storage at 40°C/75% R.H. in an open container. Modulated differential scanning calorimetry showed all systems as single phase with sufficiently high Tgs to suggest samples would be stable at typical storage conditions. High performance liquid chromatography analysis for purity showed that all samples were >99.9% pure with respect to deferasirox except for the binary deferasirox/Eudragit system which had a purity of 99.5%. These high levels of purity were possible due to the short processing time (<10 seconds at elevated temperature) and low ejection

temperature (170°C, approximately 90°C below melting temperature) which would have been challenging to replicate by hot melt extrusion.

The amorphous intermediates, neat API, and Jadenu were tested for in-vitro performance by pH change dissolution from pH 1.1 to pH 6.8. The results are shown in Figure 1.14. None of the tested dosage forms had any detectable release of deferasirox during the acid phase of the test. After the pH change, neat API, Exjade and Jadenu surprisingly showed release only up to 25% of the theoretical load of deferasirox. By contrast, drug from the amorphous dosage forms released to approximately 80% of theoretical drug load demonstrating a clear advantage of amorphous delivery of deferasirox over its crystalline form. Using the amorphous dispersions, a range of tablets were made that had properties that varied from disintegrated to eroding performance. Thus, DFX delivery could likely be modulated to fit the needs of optimal pharmacokinetic performance.

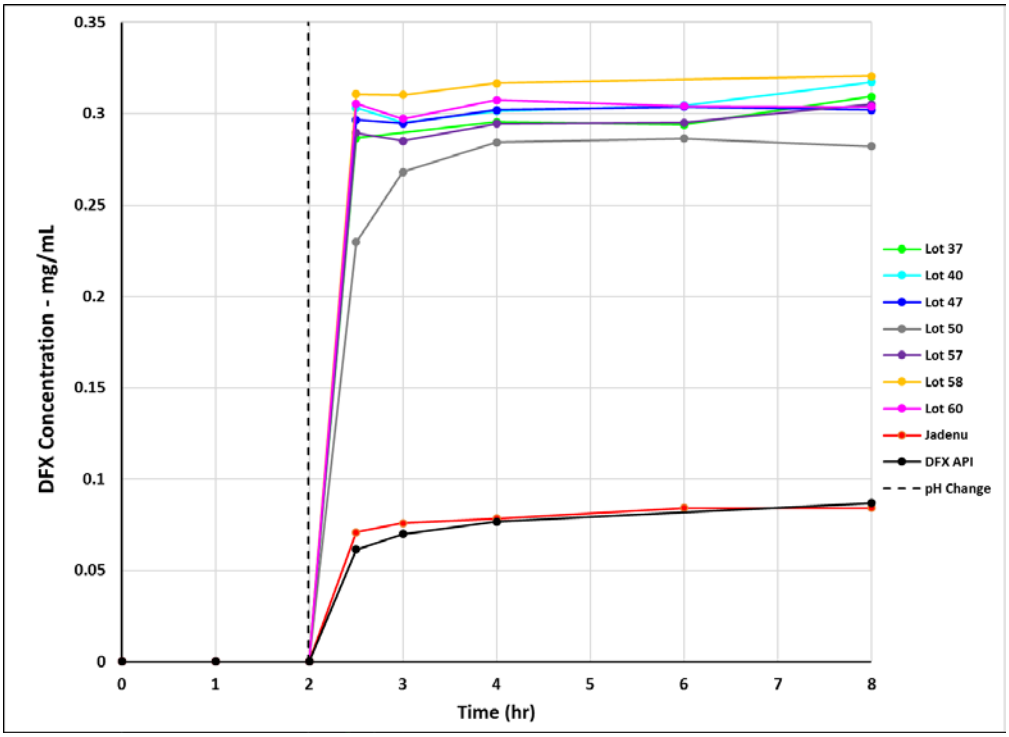

Figure 1.14: pH Change Dissolution Testing of Deferasirox Amorphous Solid Dispersion Intermediates Produced by KinetiSol as Compared to the FDA Approved Jadenu and Neat API. Reprinted from (62).

For initial in-vivo testing, two tablet formulations were dosed at 36 mg/kg in a fasted dog model against Exjade and Jadenu. The plasma concentration profile for DFX is shown in Figure 1.15 and both formulations exhibited >300% increase in deferasirox exposure. Following the dog study, two formulations were dosed in a crossover study in healthy human volunteers under fasted conditions. The results of this PK study are summarized in Table 1.4. Both formulations exhibited approximately 30% higher Cmax, 17% higher AUC, and reduced variability relative to Jadenu. Notably, while many test subjects had similar exposure to both Jadenu and the KinetiSol formulations, multiple patients exhibited a substantial reduction of Jadenu exposure compared to

the KinetiSol dosage. These results may represent a response in a non-responder population. Thus, it was demonstrated that an amorphous solid dispersion of deferasirox processed by KinetiSol could be utilized for superior delivery and clinical efficacy. (62)

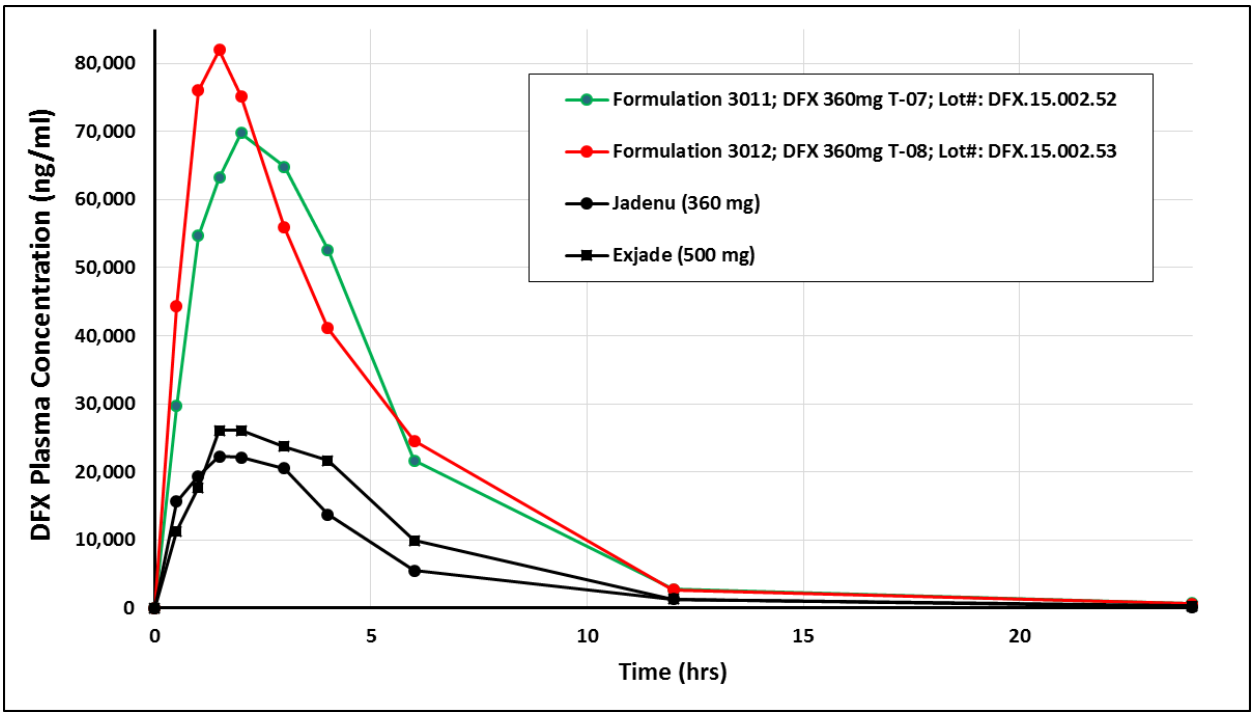

Figure 1.15: Deferasirox Blood Plasma Concentrations in Fasted Beagle Dogs of KinetiSol Produced Tablets Against Exjade and Jadenu at 36 mg/kg

Parameter (Units)	Formulation 30011		Formulation 30012		Reference (Jadenu)	
	Mean	**(C.V. %)**	**Mean**	**(C.V. %)**	**Mean**	**(C.V. %)**
Cmax (ng/mL)	55.636	(25.4)	58.019	(27.2)	45.071	(38.8)
Tmax (hours)a	3.50	(2.50-5.00)	4.00	(2.50-5.00)	2.50	(1.50-5.00)
AUC0-∞ (ng·h/mL)	590.016	(31.9)	556.538	(31.8)	542.527	(46.4)

Table 1.4: Pharmacokinetic Evaluation in a Crossover Study in Healthy Human Subjects Comparing Two KinetiSol Formulations to the Reference Product Jadenu Dosed at 14 mg/kg. Adapted from (62).

Meloxicam:

Meloxicam is a high melting point molecule (270°C) (64) for which there is an interest to form solid dispersions to aid in solubility enhancement. (65-69) After preformulation work to screen for a carrier that promoted solubility in aqueous media and had good miscibility for processing, Hughey et al. moved forward with development of a 10% meloxicam amorphous solid dispersion with Soluplus. As part of the development, the authors also processed and compared the formulations by hot melt extrusion. It was found that hot melt extrusion could not render the high melting point drug substance into an amorphous composition even with recirculation for 2 minutes at 175°C. The purity of the drug substance at these conditions was 87% which indicated substantial degradation of meloxicam. (64) In a separate hot melt extrusion study, a binary

amorphous solid dispersion was produced with 10% meloxicam in copovidone. Through rigorous process optimization and extruder design, purity was reduced as far as possible (recovery 96.7%), but it was not until the addition of the base meglumine to chemically stabilize meloxicam that an acceptable purity level was reached. (70) However, additives can negatively impact the physical stability of amorphous solid dispersions and meglumine has been shown to act as a destabilizer in some systems. (71) By contrast, amorphous compositions could be processed by KinetiSol with substantially less degradation. Compositions were processed as low as 110°C with a total processing time of less than 25 seconds. For KinetiSol, the strongest correlation between processing conditions and degradation was ejection temperature with all compositions at 110°C having 98% or greater purity. While the key study parameters (rpm and ejection temperature) were probed for their impacts, the process was not fully optimized and it is likely that with additional experimentation that the impurities could be reduced to negligible levels. (64) This case study demonstrated the capability of KinetiSol to produce an amorphous dispersion of a high melting point compound when the more limited processing space of hot melt extrusion required the addition of an additional component to overcome.

Vemurafenib:

Vemurafenib is BCS Class II/IV drug for which a clear need for an amorphous form exists as it has <2 μg/mL solubility in aqueous vehicles. However, as noted by Shah et al., its high melting point of 272°C and poor organic solubility of <6 mg/mL in solvents amenable to spray drying make it a challenging entity for processing into an amorphous dispersion by conventional means (e.g., hot melt extrusion and spray drying). (72) In the case of hot melt extrusion, the highest

reported drug loading achieved with vemurafenib was 10% w/w in a binary copovidone amorphous solid dispersion. Drug load could be increased as high as 20-25% with the inclusion of 5-15% glyceryl monostearate, a plasticizer. (73) Additionally, clinical trial results dictated a dosing of 960 mg (4 x 240 mg tablets) of amorphous vemurafenib twice-daily in patients. (74) This high dose requirement limits the application of hot melt extrusion and created a driver for an approach that could yield an amorphous solid dispersion with higher drug load.

A novel process of solvent-controlled coprecipitation was developed in which an amorphous solid dispersion of 30/70 vemurafenib/HPMCAS-LF was precipitated in an anti-solvent (acidified aqueous media) from dimethylacetamide. (72) However, this process has a number of limitations including: the requirement of ionic polymers, difficulty in developing suitable solvent/anti-solvent systems, inability to include solubility/permeability enhancers in the dispersion, and stability risks due to matrix exposure to water during preparation. (75) In the case of Zelboraf® (vemurafenib) development, the formulation space was limited to HPMCAS, Eudragit, and hypromellose phthalate. (72) It is plausible that an optimized formulation with improved bioavailability and lower dosing exists outside of this narrow domain.

Despite the difficulties with processing vemurafenib by other amorphous solid dispersion approaches, several amorphous compositions of vemurafenib have been made utilizing KinetiSol, as described in WO/2016/073421. An equivalent composition to the solvent-controlled coprecipitation process was developed. The composition was found to be amorphous by X-ray powder diffraction and with a similar Tg by modulated differential scanning calorimetry. Dissolution performance testing mimicking the work described by Shah et al.

showed similar performance between the precipitated and KinetiSol produced materials. Additional compositions were prepared utilizing HPMC E5 and PVP VA64 as carrier polymers with additional batches produced with docusate sodium as an internal component in the amorphous dispersion. These batches were shown to be amorphous and demonstrated the capacity for KinetiSol to produce additional formulations not achievable by other means, whether it be conventional or the novel solvent-controlled coprecipitation process. (76) The expanded formulation space enabled by KinetiSol presents the possibility of an improved vemurafenib formulation with reduced dosing and patient pill burden.

AKBA:

3-acetyl-11-keto-beta-boswellic acid (AKBA) is a poorly aqueous soluble (77), high melting point (295°C) compound with increasing interest. (78) Historically, all of the boswellic acids have been known to have anti-inflammatory properties (79) while more recently AKBA has gained attraction for its promising anti-tumor properties. (80) To better deliver AKBA, Bennett et al. explored amorphous solid dispersions for solubility enhancement of this molecule. During thermal preformulation evaluations, the authors identified that the processing conditions required to thermally process AKBA by hot melt extrusion would pose significant risk to polymer and drug degradation. In moving forward, Bennett et al. processed amorphous compositions containing AKBA with various polymeric carriers: HMPCAS-LF, HPMCAS-MF, Eudragit L100-55, and Soluplus. Additionally, all compositions were prepared with docusate sodium in the amorphous dispersion to act as a surfactant for further improvement of aqueous solubility. For all compositions, the resulting material was substantially amorphous and possessed

acceptable recovery of the drug substance which validated the feasibility of KinetiSol to process compositions of AKBA. As a comparator, equivalent compositions were produced by rotary evaporation. In-vitro dissolution studies demonstrated that both processing methods significantly enhanced solubility of AKBA. However, the authors also identified that for some compositions there were surface morphology differences that resulted in a performance difference of the rotary evaporated material compared to material produced by KinetiSol. These results carried over to an in-vivo rat study in which oral absorption was seen at levels approximately 18-fold higher than crystalline AKBA. (77)

However, recent literature has shown that permeability of AKBA is also a significant limitation in its delivery. (81) Specifically, Kruger et al. demonstrated that metabolic enzymes in the intestinal tract led to extensive metabolism of the compound. (82) Miller et al. hypothesized that inhibition of these metabolic enzymes could be utilized to enhance the permeability of AKBA, further boosting its oral bioavailability. (37) Ritonavir was known to be an effective CYP3A enzyme inhibitor as evidenced by its success with Kaletra, a combination product which included amorphous ritonavir to boost the permeability of the highly metabolized lopinavir. (53) To this end, Miller et al. (37) processed amorphous compositions of AKBA like the work performed by Bennett et al. (77) as well as separate amorphous dispersions for ritonavir by KinetiSol. Tablets were made of the blended amorphous dispersions and dosed in an in-vivo dog study. The combination of enhanced solubility from amorphous AKBA as well as the enzyme inhibition from ritonavir yielded oral absorption approximately 4 times the AKBA composition alone and 24 times the crystalline drug. See Figure 1.16 for the plasma concentration profiles. These results demonstrated the utility of KinetiSol processing to enhance oral absorption of the challenging

AKBA molecule through both solubility enhancement by amorphous dispersion and delivery of a solubility challenged enzyme inhibitor. (37)

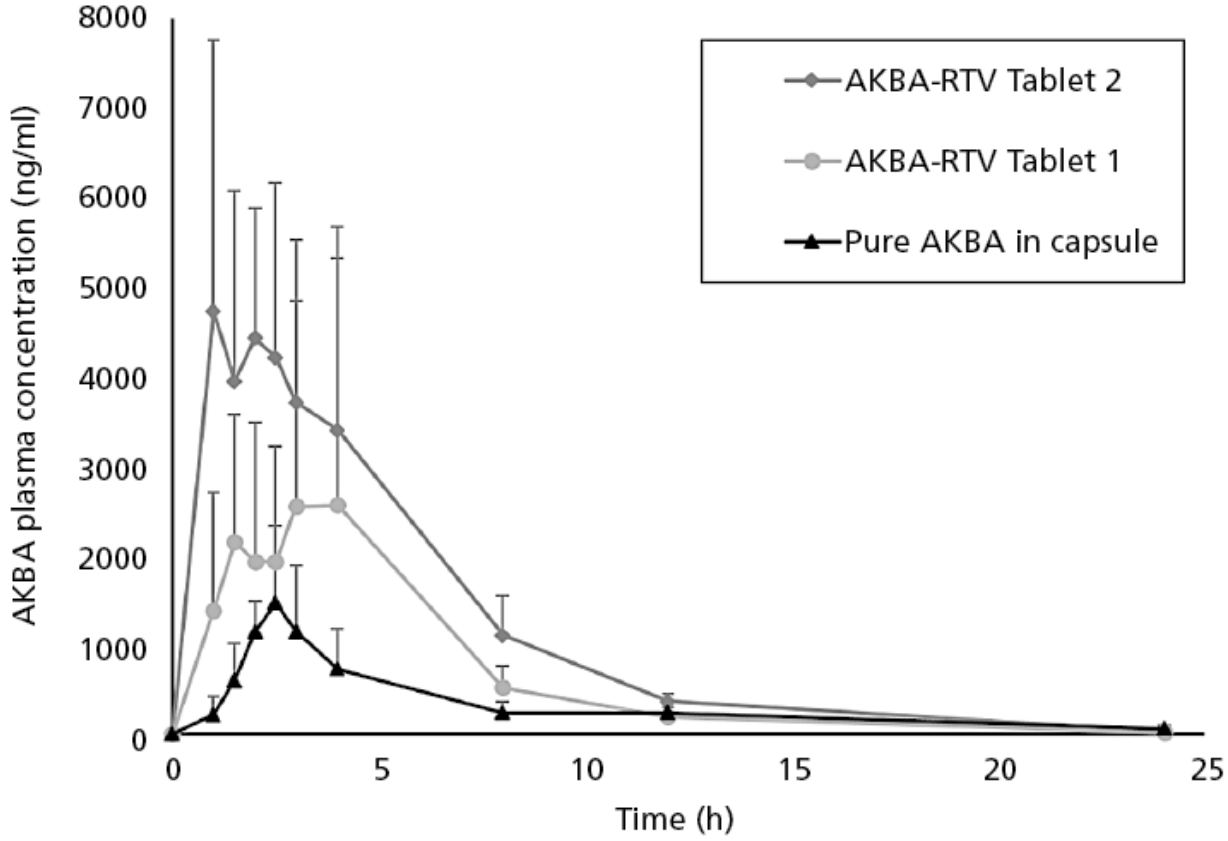

Figure 1.16: Plasma Concentrations of AKBA-RTV Tablets Against Pure AKBA in a Fasted In-Vivo Dog Model. Reprinted with permission from (37).

1.4.2 Polymeric Excipient Challenges

1.4.2.1 High Molecular Weight, Viscous Polymers

High molecular weight polymers have been demonstrated to be challenging to process by thermal methods such as hot melt extrusion. (31, 51, 59-61) However, these polymers are desirable for use in amorphous solid dispersions as a number of studies have demonstrated the benefit of increased molecular weight and solubility gains. (34) This benefit has been attributed to inhibition of precipitation through drug-polymer interactions, steric hindrance of the active pharmaceutical ingredient, and improved shielding from dissolution/recrystallization during the gelling process. (83-85) Many studies have been performed utilizing KinetiSol to process amorphous solid dispersions with high molecular weight polymers to enhance drug release and oral absorption. These are discussed below.

Feasibility of Processing HPMC E50 by Thermal Processing Methods:

Hughey et al. conducted a series of experiments to compare the feasibility of processing compositions containing high molecular weight HPMC E50 by hot melt extrusion and KinetiSol. Compositions of 1:2 itraconazole:HPMC E50 were attempted by hot melt extrusion using a Minilab II extruder. Processing temperature was maintained at 180°C with screw rotation at 150 rpm without recirculation. This processing temperature was found to be necessary as lower temperatures resulted in torque loads that exceeded the capacity of the instrument. At this processing temperature, significant browning of the material was observed with subsequent

analysis determining that there was an 18.4% loss in molecular weight of the polymer. Additionally, to assess the presence of metals in the dispersion caused by strain on the extruder, metals analysis of the composition was conducted and the HME composition was found to have 450 ppm of iron with detectable levels of chromium, nickel, copper, and zinc present as well. Between the significant degradation of the polymer and the presence of metals in the dispersion indicated a lack of feasibility for hot melt extrusion to process the desired composition. (34)

Subsequently, Hughey et al. processed the same composition by KinetiSol at 1750 and 2250 rpm and ejections temperatures of 120 and 180°C. Degradation of the polymer was also observed in these samples with statistical correlations to both ejection temperature and rotational speed. However, size exclusion analysis showed a reduction of 12.8% in molecular weight, an improvement on the best-case result obtained from hot melt extrusion. Metals analysis was also conducted on the KinetiSol material. Iron was found a level of 21 ppm, significantly less than the hot melt extrusion result, with none of the other metals detected in the composition. (34) These results indicated the challenge in processing high molecular weight HPMC E50 by hot melt extrusion and the potential feasibility of KinetiSol in this area.

HPMC E50 and E4M Delivery of Itraconazole:

Itraconazole is a poorly soluble BCS class II drug used in the commercial Onmel® product as an antifungal agent. In this product, itraconazole is delivered orally as a tablet containing an amorphous solid dispersion of the drug with HPMC E5. (86) Given the potential of higher molecular weight polymers to further enhance solubility (87), Keen et al. hypothesized that an

amorphous solid dispersion of itraconazole in HPMC E50 or E4M could provide equivalent or better oral absorption than Onmel without conflicting with the product patent. As shown in the previous section, HPMC E50 was not processable with itraconazole by hot melt extrusion. The authors utilized KinetiSol to process amorphous solid dispersions of itraconazole. The amorphous dispersions were milled and a series of tablet dispersions were developed which yielded tablets that were non-disintegrating and resulted in viscous gel formation. In-vitro analysis showed a significant reduction in drug dissolved in acid compared to Onmel, despite itraconazole's affinity for dissolution in acidic media. This was attributed to the controlled release nature of the viscous gel formed by the higher molecular weight HPMC. In a number of examples, tablets from the higher molecular weight dispersions resulted in supersaturation maintenance well into neutral phase whereas the Onmel product approached no drug in solution during this phase (88). This data has been reproduced in Figure 1.17.

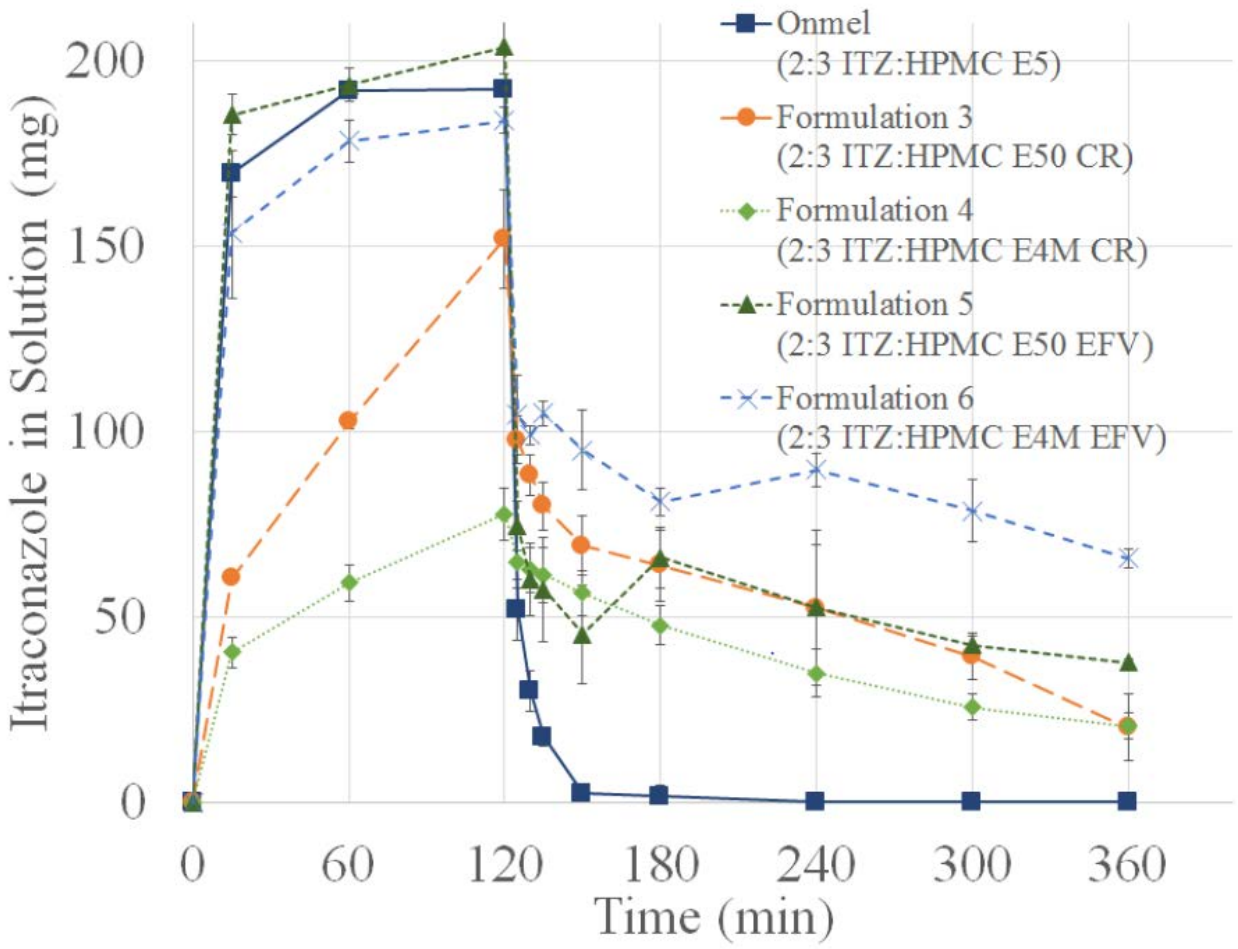

Figure 1.17: In-vitro Testing of High Molecular Weight HPMC Compositions Containing Itraconazole. Reproduced from (88).

Two lead candidates (one of each polymer type) were selected based on small volume dissolution performance for study in an in-vivo dog model. In this model, the E4M dispersion performed similarly to the Onmel product. The E50 controlled release tablet appeared to outperform the comparator product, but the sample size was too small to obtain statistically significant results. The plasma concentration profiles are reproduced in Figure 1.18. (88)

However, these results demonstrate the utility of KinetiSol to produce alternative formulations that may have more desirable properties such as controlled release or superior supersaturation.

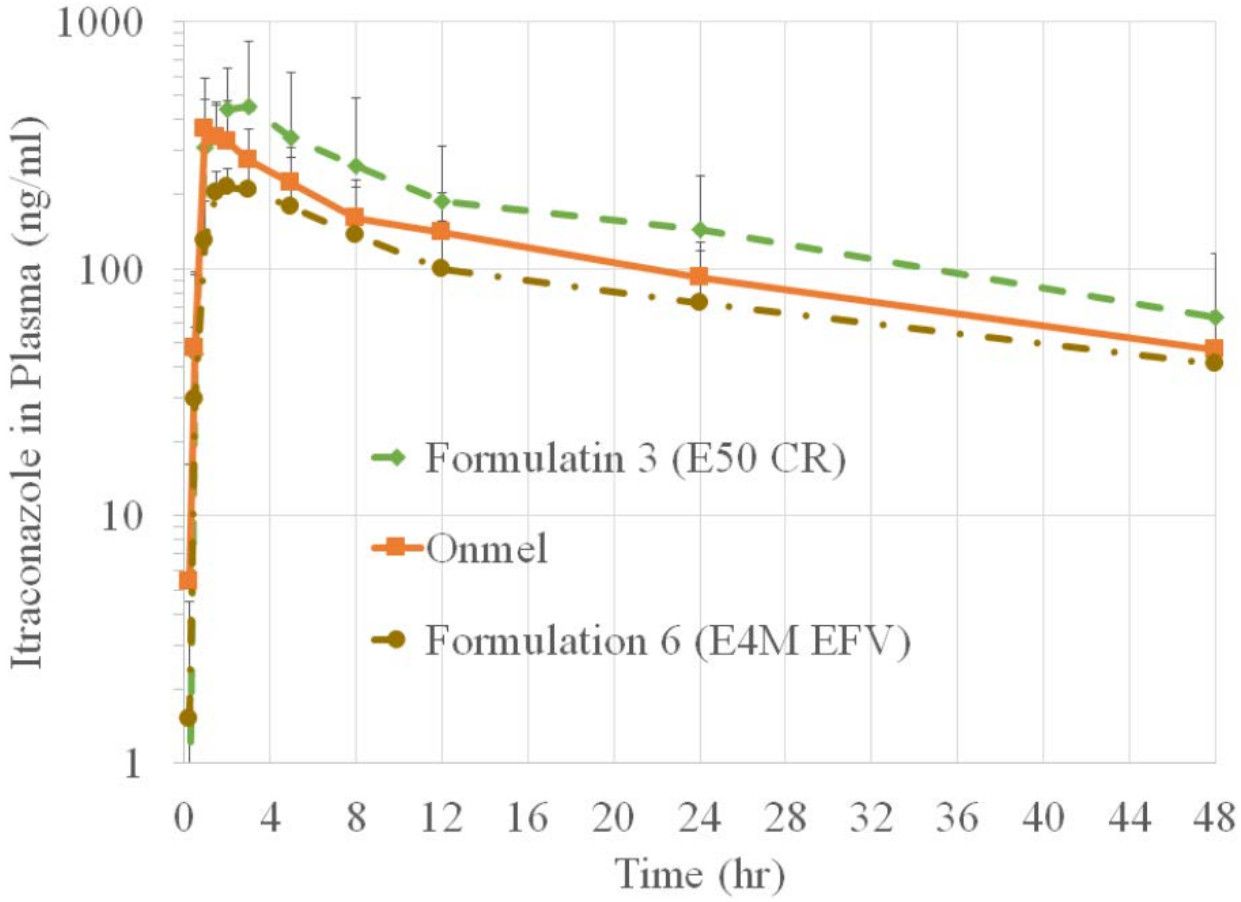

Figure 1.18: In-Vivo Performance in Dog Model of High Molecular Weight HPMC Compositions Containing Amorphous Itraconazole. Reproduced from (88).

Processing Evaluation for Various Grades of PVP and HPMC:

In another study, LaFountaine et al. examined the capability of hot melt extrusion and KinetiSol to process compositions containing various grades of povidone (K17, K30, and K90) and HPMC

(E5, E15, and E50) with a model compound, griseofulvin, at various drug loads (10-40%). Due to processing challenges, namely high torque and high pressure, only K17 and HPMC E5 were processable but hot melt extrusion. By contrast, all compositions could be processed by KinetiSol into amorphous solid dispersions except for K30 at 40% drug load. Also, for K17 and HPMC E5, hot melt extrusion could only process amorphous compositions at drug loads of 10 and 20% while KinetiSol could process compositions up to 40% drug load. The authors cited the high shear output of KinetiSol as the most likely explanation for its ability to process these challenging compositions. (89)

1.4.2.2 Thermally Labile Polymers

Like thermally labile active pharmaceutical ingredients, carrier polymers are often susceptible to degradation during thermal processing. (59-61, 90) Similar strategies exist for minimizing this degradation through lowering the processing temperature, inclusion of plasticizers, and shortening processing times. The same advantages that KinetiSol has for processing thermally labile APIs (lower processing temperatures and shorter processing times as seen in Figure 1.9) apply to thermally sensitive polymers as well. (31, 51) A number of examples have already been discussed in this work, most notably the work by Hughey et al. with HPMC E50. Additional examples follow.

HPMCAS:

HPMCAS is a hydroxypropylmethylcellulose based polymer with substitution of acetyl and succinoyl groups. Three grades are primarily available and are described in Table 1.5. Depending on the degree of substitution of acetyl and succinoyl, the pH solubility profile of the polymer is impacted and the polymers exhibit various degrees of enteric release. (91) These functional groups, predominantly acetyl, have been shown to promote improved drug solubility through hydrophobic interactions with the drug preventing recrystallization. (21)

Grade	% Acetyl Substitution	% Succinoyl Substitution	pH
L	7	16	>5.5
M	9	12	>6.0
H	12	6	>6.8

Table 1.5: Acetyl and Succinoyl Substitutions of HPMCAS and Resulting pH of Dissolution of Polymer. Data summarized from (91).

When processing amorphous solid dispersions with HPMCAS, it is important to not change the functional group substitutions to maintain desired pH and recrystallization inhibition properties. A study was conducted with the three primary grades of HPMCAS used in hot melt extrusion at various temperature and rpm conditions. As a result of processing, all three grades showed an increase in free acetic and succinic acid which was indicative of degradation of the acetyl and succinoyl groups. The H grade, in particular, showed significantly increased dissolution time

after processing which would concurrently limit drug release in an amorphous solid dispersion system. (91) Review conducted by LaFountaine et al. found that HPMCAS possesses no suitable extrudable range as it requires temperatures above 170°C to sufficiently reduce its melt viscosity but degradation onset occurs as low 180°C. (31) This limitation of HPMCAS presents a challenge when processing high melting point drugs like telaprevir (246°C) (92), ivacaftor (292°C) (93), and vemurafenib (272°C) (72) in hot melt extrusion. Alternative processes were pursued to make commercial products with spray drying used to make Incivek® (telaprevir) and Kalydeco® (ivacaftor) (28) and solvent controlled coprecipitation to make Zelboraf (vemurafenib). (72)

Like its success with viscous, high molecular weight polymers, KinetiSol has been used to process amorphous solid dispersions containing HPMCAS. In the vemurafenib example previously described, the sample containing 70% HMPCAS-L was ejected at 180°C after approximately 7 seconds of processing time. While the polymer reached the reported degradation onset during processing, the process ejected sample as it reached this level and the overall processing time was minimal which limited degradation. (76) In the previously described ritonavir example, both the HPMCAS polymer and the drug substance are susceptible to thermal degradation. However, the process only required a final temperature of 90°C to render the sample fully amorphous. This value was substantially below the degradation onsets for both the drug and HPMCAS. The study demonstrated a case where KinetiSol enabled the processing of a composition approximately 80°C below the polymeric carrier's minimum operating temperature. This occurred as a result of KinetiSol high shear reducing the melt viscosity of HPMCAS without the application of heat. (81)

Eudragit L100-55:

Eudragit L100-55, an anionic methacrylic acid polymer, has been studied for its use in solubility enhancement of poorly water soluble drugs with thermal processing into an amorphous solid dispersion as a common outcome. (94-97) In an ideal iteration, plasticizer would not be used to process the composition due to its potential negative effects on physical stability of the composition. (58) However, Eudragit L100-55 presents a challenge for thermal processing as it is known to undergo side chain degradation at 155°C with backbone structural loss starting at 180°C. (98)

In a study conducted by DiNunzio et al., compositions of Eudragit L100-55 with itraconazole were assessed by hot melt extrusion and KinetiSol to determine the impact of thermal processing on the polymer's integrity. An initial finding of the study was the requirement of a plasticizer (triethyl citrate) was necessary to render compositions amorphous by hot melt extrusion but was not necessary for the same compositions by KinetiSol. The impact of this was a reduction of the glass transition temperature in the hot melt extrusion to dispersion to approximately 54°C whereas the material produced by KinetiSol had a glass transition temperature of 101°C. Ultimately, recrystallization of the hot melt extrusion composition was observed at accelerated stability conditions. As expected, no recrystallization was observed for the KinetiSol compositions. (50)

Degradation of Eudragit L100-55 due to processing was also examined with specific focus on methacrylic acid functionality. Neat L100-55 was found to have 48.6% methacrylic acid units while the materials from hot melt extrusion and KinetiSol had 47.3% and 47.4% respectively. It is interesting to note that the hot melt extrusion sample was processed at 130°C (below the Eudragit degradation onset) while the KinetiSol process briefly went to 158°C. The degradation between the two samples was comparable but the KinetiSol process had the advantage of processing without a plasticizer which enabled it to have acceptable physical stability.

1.4.2.3 Polyvinyl Alcohol

A polymer whose application for amorphous solid dispersions that has not been extensively explored is polyvinyl alcohol (PVA). The reason for this is that PVA is difficult to process into amorphous solid dispersions by conventional means (spray drying and hot melt extrusion). Spray drying is challenging because the polymer is practically insoluble in organic solvents used in spray drying. (99) Thermal processing is difficult as PVA does not soften until reaching its melting point at which degradation onset can occur. (100, 101) However, PVA is an attractive polymer as it can modified by degree of polymerization (impacting solution viscosity) and the degree of hydrolysis. For example, PVA 4-88 has a 4% solution viscosity of 4 mPa*s and the functional groups have been 88% hydrolyzed (leaving 12% as acetate). (99, 102) This flexibility in substitution would theoretically allow for varying levels of sites for hydrophobic or hydrophilic interaction to aid in solubilizing poor soluble drugs. (56)

Brough et al. hypothesized that PVA could be processed into amorphous solid dispersions by KinetiSol. Itraconazole was selected as a model compound for the investigation. An initial study was carried out with 20% itraconazole to determine the ideal level of hydrolysis for solubility enhancement using PVA 4-38, 4-75, 4-88, and 4-98. While 4-98 showed some trace crystallinity upon processing, the other three compositions were found to be processable into amorphous solid dispersions by KinetiSol. Of these compositions, the 88% substituted grade had the greatest solubility enhancement by in-vitro dissolution testing. (102) A subsequent study investigated the impact of molecular weight (viscosity) and drug load on performance of 88% substituted grades of PVA. Specifically, grades 4-88, 5-88, 8-88, and 18-88 were evaluated by dissolution testing with PVA 4-88 having the best supersaturation properties of the 4 grades analyzed. Drug load dissolution studies showed that drug supersaturation was decreased with increasing drug load. (103) These studies demonstrated both the feasibility of processing amorphous solid dispersions containing PVA and the positive benefit for drug supersaturation with PVA 4-88.

In another study by LaFountaine et al., the potential degradation of PVA when processed by KinetiSol was explored. Of particular interest was the degradation of PVA related to its degree of hydrolysis. PVA-ritonavir compositions were exposed to a range of rotational speeds (1000-2000 rpm) and ejection temperatures (80-100°C). For all the processed samples except 1000 rpm/80°C ejection temperature, compositions were successfully rendered amorphous with respect to ritonavir. Ritonavir was separated out and in-solution 13C NMR analysis was conducted on the remaining sample. The analysis noted no change in the degree of hydrolysis of PVA. (56) However, it should be noted that the processing temperatures used in this study are significantly below the known degradation of PVA.

1.4.3 Other Applications

1.4.3.1 Direct Compression

To facilitate controlled release of a drug substance, approaches such as granules, pellets, and monolithic tablets have been utilized. (27, 104, 105) A key aspect is inhibition of recrystallization within the matrix due to water ingress. (106) Keen et al. studied the impact of glyceryl behenate, a modified release agent, in various hydrophilic dosage forms with one iteration comprised of monolithic tablets directly compressed from molten mass ejected from the KinetiSol process. The composition consisted of carbamazepine or itraconazole as model drugs, povidone K30 as the polymeric carrier, and glyceryl behenate which acted as a plasticizer as well as a modified release agent. In the case of itraconazole, a unique result was observed as zero-order release was achieved for the molded tablet, even without glyceryl behenate present in the dosage form. The authors hypothesized that the hydrophobic nature of itraconazole acted as a release modifier. Additionally, it was suggested that there was an advantage in a directly molded dispersion over a compressed tablet as the compressed tablet would have pores in which water could ingress causing recrystallization of the drug in the matrix and blunted release. (38) Thus, the direct compression of molten mass into a monolithic tablet is another potential application of the KinetiSol process.

1.4.3.2 Mucoadhesive Dispersions

Carbopol® is a cross-linked polyacrylic acid that has been utilized for delivery of molecules, predominantly peptides, to the intestinal region through the use mucoadhesion as an enhancement to delivery of challenging molecules. Specifically, the mucoadhesive patch adheres to the intestinal lining and promotes intimate interaction between the molecule being delivered and the intestinal membrane. (107-109) In relation to amorphous solid dispersions, Carbopol is a high melting point drug (110) which as noted elsewhere in this work poses a challenge for processing by hot melt extrusion. LaFountaine et al. hypothesized that KinetiSol could be utilized to process a binary composition of carbopol with a poorly soluble drug. Itraconazole was selected as a model due to its ease of processing and its extensive use as a model compound. (111)

The authors processed binary compositions at drug loads of 10, 20, and 30% drug load. Trace crystallinity was observed at 40% drug load and this composition was excluded from future analysis. (111) Due to the hydrophobic nature of itraconazole, it was suspected that water ingress would be more limited in higher drug loads similar to the work molded tablet discussed in the previous section. (38) This was verified by contact angle analysis which showed not only did contact angle increase as a function of drug load, but also that KinetiSol processed material had a higher contact angle than equivalent physical mixtures. The authors posited that this was due to greater homogeneity of the samples with itraconazole dispersed at the molecular level. (111)

Investigation of the mucoadhesive properties of the dispersions was evaluated by measuring the adherence of compressed dispersion to freshly excised porcine intestine. Analysis was conducted by Texture Analyzer to determine the work of adhesion, or how strongly the tablet bound to the membrane. When sufficient wetting time was allowed (greater than 30 minutes with incubation), all dispersions adhered to the membrane. However, subsequent in-vivo analysis in a rat model showed lower itraconazole absorption than was expected. The authors attributed this to the lower pH in rats compared to humans as well as the low fluid volume. A necropsy study verified that the tablets adhered to the intestinal in the dosed rats as intended. Future analysis in a different model would be necessary to evaluate the efficacy of the delivery platform for delivering amorphous solid dispersions through mucoadhesion to the intestinal wall. (111) However, this is an attractive delivery platform for which KinetiSol is uniquely positioned to process.

1.4.3.3 Porosity Enhancement

For thermally based techniques, there is a growing interest in modifying the process of amorphous solid dispersion generation in a manner that increases the resulting product's porosity and surface area. The increase in surface area from pores can lead to substantially increased dissolution rates, a desirable outcome for many dosage forms. (112, 113) A number of approaches have been employed with hot melt extrusion to create porosity in extrudate including sodium bicarbonate (114), supercritical carbon dioxide (115, 116) and nitrogen. (113) In a study conducted by LaFountaine et al., griseofulvin was processed with povidone K17 and HPMC E5 into amorphous solid dispersions by both hot melt extrusion and KinetiSol. As shown in Figure 1.19, porosity was apparent in x-ray computed tomography and scanning electron microscopy

images of the sample for the KinetiSol material. Further analysis showed that none of the hot melt extrusion products showed signs of porosity, but all the KinetiSol samples had at least some qualitatively observed porosity. It was hypothesized that the porosity was due to entrapped air in the molten mass and that the content could be modulated with modifications to quenching; however, this was not explored further. (89)

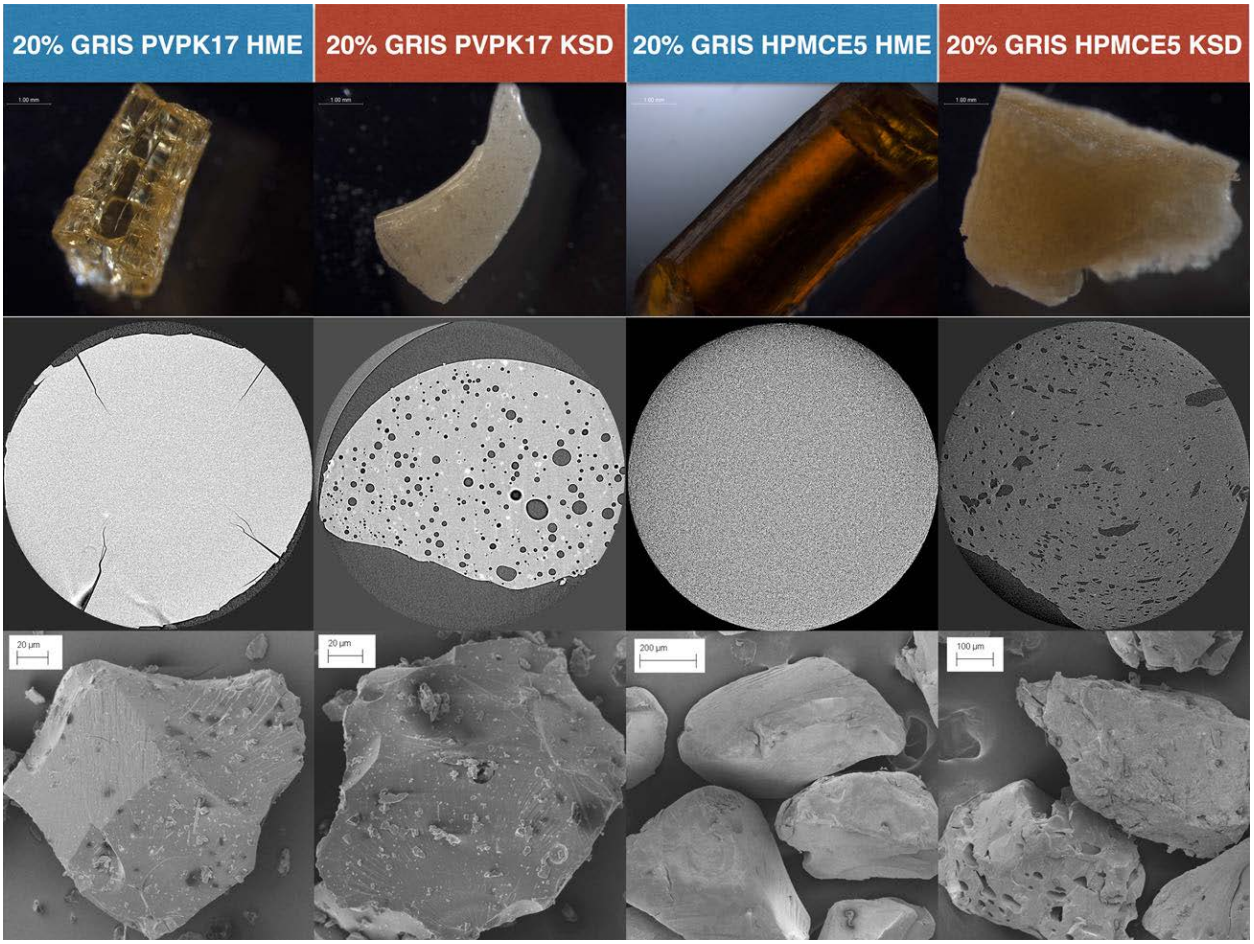

Figure 1.19: Stereo Microscopy, X-Ray Computed Tomography, and Scanning Electron Microscopy Images of Amorphous Dispersions Generated by Hot Melt Extrusion and KinetiSol. Reprinted with permission from (89).

1.5 CONCLUSION

As the number and complexity of poorly soluble drugs in pharmaceutical development increases, there exists increasing demand for solubility enabled delivery of these compounds. However, there is a growing void in this space as the conventional approaches of hot melt extrusion and spray drying now face limitations. KinetiSol has been shown to be an emerging technology that is beginning to fill this void. It has demonstrated its capability in handling high melting point and/or organic solvent insoluble APIs, thermally labile materials, and viscous polymers as well as the promise of other applications. These capabilities have expanded the formulation space beyond what was previously viable.

1.6 REFERENCES

1. Ku MS, Dulin W. A biopharmaceutical classification-based Right-First-Time formulation approach to reduce human pharmacokinetic variability and project cycle time from First-In-Human to clinical Proof-Of-Concept. Pharmaceutical development and technology. 2012;17(3):285-302.

2. Loftsson T, Brewster ME. Pharmaceutical applications of cyclodextrins: basic science and product development. Journal of pharmacy and pharmacology. 2010;62(11):1607-21.

3. Williams HD, Trevaskis NL, Charman SA, Shanker RM, Charman WN, Pouton CW, et al. Strategies to address low drug solubility in discovery and development. Pharmacological reviews. 2013;65(1):315-499.

4. Amidon GL, Lennernäs H, Shah VP, Crison JR. A theoretical basis for a biopharmaceutic drug classification: the correlation of in vitro drug product dissolution and in vivo bioavailability. Pharmaceutical research. 1995;12(3):413-20.

5. Lipinski CA. Drug-like properties and the causes of poor solubility and poor permeability. Journal of pharmacological and toxicological methods. 2000;44(1):235-49.

6. Bergström CA, Charman WN, Porter CJ. Computational prediction of formulation strategies for beyond-rule-of-5 compounds. Advanced drug delivery reviews. 2016;101:6-21.

7. Leeson PD. Molecular inflation, attrition and the rule of five. Advanced drug delivery reviews. 2016;101:22-33.

8. Jain N, Yalkowsky SH. Estimation of the aqueous solubility I: Application to organic nonelectrolytes. Journal of pharmaceutical sciences. 2001;90(2):234-52.

9. Di L, Fish PV, Mano T. Bridging solubility between drug discovery and development. Drug Discovery Today. 2012;17(9):486-95.

10. He Y, Ho C. Amorphous solid dispersions: utilization and challenges in drug discovery and development. Journal of pharmaceutical sciences. 2015;104(10):3237-58.

11. Guzmán HR, Tawa M, Zhang Z, Ratanabanangkoon P, Shaw P, Gardner CR, et al. Combined use of crystalline salt forms and precipitation inhibitors to improve oral absorption of celecoxib from solid oral formulations. Journal of pharmaceutical sciences. 2007;96(10):2686-702.

12. Bevernage J, Brouwers J, Brewster ME, Augustijns P. Evaluation of gastrointestinal drug supersaturation and precipitation: strategies and issues. International journal of pharmaceutics. 2013;453(1):25-35.

13. Jinno J-i, Kamada N, Miyake M, Yamada K, Mukai T, Odomi M, et al. Effect of particle size reduction on dissolution and oral absorption of a poorly water-soluble drug, cilostazol, in beagle dogs. Journal of controlled release. 2006;111(1):56-64.

14. Brough C, Williams Iii RO. Amorphous solid dispersions and nano-crystal technologies for poorly water-soluble drug delivery. International Journal of Pharmaceutics. 2013;453(1):157-66.

15. Banik M, Gopi SP, Ganguly S, Desiraju GR. Cocrystal and salt forms of furosemide: solubility and diffusion variations. Crystal Growth & Design. 2016;16(9):5418-28.

16. Kuminek G, Cao F, da Rocha ABdO, Cardoso SG, Rodríguez-Hornedo N. Cocrystals to facilitate delivery of poorly soluble compounds beyond-rule-of-5. Advanced drug delivery reviews. 2016;101:143-66.

17. Savla R, Browne J, Plassat V, Wasan KM, Wasan EK. Review and analysis of FDA approved drugs using lipid-based formulations. Drug Development and Industrial Pharmacy. 2017:1-16.

18. Singh B, Bandopadhyay S, Kapil R, Singh R. Self-emulsifying drug delivery systems (SEDDS): formulation development, characterization, and applications. Critical Reviews™ in Therapeutic Drug Carrier Systems. 2009;26(5).

19. Shi Y, Porter W, Merdan T, Li LC. Recent advances in intravenous delivery of poorly water-soluble compounds. Expert opinion on drug delivery. 2009;6(12):1261-82.

20. Ilevbare GA, Xu W, John CT, D Ormes J, Kuiper JL, Templeton AC, et al. Solubility and Dissolution Considerations for Amorphous Solid Dispersions. Pharmaceutical Sciences Encyclopedia. 2015.

21. Ueda K, Higashi K, Yamamoto K, Moribe K. Inhibitory effect of hydroxypropyl methylcellulose acetate succinate on drug recrystallization from a supersaturated solution assessed using nuclear magnetic resonance measurements. Molecular pharmaceutics. 2013;10(10):3801-11.

22. Miller JM, Beig A, Carr RA, Spence JK, Dahan A. A win–win solution in oral delivery of lipophilic drugs: supersaturation via amorphous solid dispersions increases apparent solubility without sacrifice of intestinal membrane permeability. Molecular pharmaceutics. 2012;9(7):2009-16.

23. Friesen DT, Shanker R, Crew M, Smithey DT, Curatolo W, Nightingale J. Hydroxypropyl methylcellulose acetate succinate-based spray-dried dispersions: an overview. Molecular pharmaceutics. 2008;5(6):1003-19.

24. Moser J, Broyles J, Liu L, Miller E, Wang M. Enhancing bioavailability of poorly soluble drugs using spray dried solid dispersions Part I. Am Pharm Rev. 2008;11:70-1.

25. Paudel A, Worku ZA, Meeus J, Guns S, Van den Mooter G. Manufacturing of solid dispersions of poorly water soluble drugs by spray drying: formulation and process considerations. International journal of pharmaceutics. 2013;453(1):253-84.

26. Crowley MM, Zhang F, Repka MA, Thumma S, Upadhye SB, Kumar Battu S, et al. Pharmaceutical applications of hot-melt extrusion: part I. Drug development and industrial pharmacy. 2007;33(9):909-26.

27. Repka MA, Battu SK, Upadhye SB, Thumma S, Crowley MM, Zhang F, et al. Pharmaceutical applications of hot-melt extrusion: Part II. Drug development and industrial pharmacy. 2007;33(10):1043-57.

28. Miller DA, Ellenberger D, Gil M. Spray-Drying Technology. Formulating Poorly Water Soluble Drugs: Springer; 2016. p. 437-525.

29. Broadhead J, Edmond Rouan S, Rhodes C. The spray drying of pharmaceuticals. Drug Development and Industrial Pharmacy. 1992;18(11-12):1169-206.

30. Leuner C, Dressman J. Improving drug solubility for oral delivery using solid dispersions. European journal of Pharmaceutics and Biopharmaceutics. 2000;50(1):47-60.

31. LaFountaine JS, McGinity JW, Williams III RO. Challenges and strategies in thermal processing of amorphous solid dispersions: a review. AAPS PharmSciTech. 2016;17(1):43-55.

32. Miller DA, DiNunzio JC, Hughey JR, Williams III RO, McGinity JW. KinetiSol: a new processing paradigm for amorphous solid dispersion systems. Drug Dev Deliv. 2012;11(2011):22-31.

33. Miller DA. Improved oral absorption of poorly water-soluble drugs by advanced solid dispersion systems: University of Texas
2007.

34. Hughey JR, Keen JM, Miller DA, Brough C, McGinity JW. Preparation and characterization of fusion processed solid dispersions containing a viscous thermally labile polymeric carrier. International journal of pharmaceutics. 2012;438(1):11-9.

35. Vasconcelos T, Sarmento B, Costa P. Solid dispersions as strategy to improve oral bioavailability of poor water soluble drugs. Drug discovery today. 2007;12(23):1068-75.

36. Newman A, Knipp G, Zografi G. Assessing the performance of amorphous solid dispersions. Journal of pharmaceutical sciences. 2012;101(4):1355-77.

37. Miller DA, Keen JM, Brough C, Ellenberger DJ, Cisneros M, Williams RO, et al. Bioavailability enhancement of a BCS IV compound via an amorphous combination product containing ritonavir. Journal of Pharmacy and Pharmacology. 2015.

38. Keen JM, Hughey JR, Bennett RC, Jannin V, Rosiaux Y, Marchaud D, et al. Effect of tablet structure on controlled release from supersaturating solid dispersions containing glyceryl behenate. Molecular pharmaceutics. 2014;12(1):120-6.

39. Miller DA, Keen, Justin M, Brough, Chris, inventorTetrabenazine Modified Release Formulation2015.

40. Darji MA, Lalge RM, Marathe SP, Mulay TD, Fatima T, Alshammari A, et al. Excipient Stability in Oral Solid Dosage Forms: A Review. AAPS PharmSciTech. 2017:1-15.

41. Ambike AA, Mahadik K, Paradkar A. Spray-dried amorphous solid dispersions of simvastatin, a low Tg drug: in vitro and in vivo evaluations. Pharmaceutical research. 2005;22(6):990-8.

42. Berndl G, Rosenberg J, Liepold B, Fastnacht K, Jung T, Roth W, et al., inventors; Abbott Laboratories, assignee. Solid pharmaceutical dosage formulations. United States patent application 11/939,640. 2008 Jul 31.

43. Brough C, McGinity JW, Miller DA, DiNunzio JC, Williams RO, inventors; DisperSol Technologies, LLC, assignee. Thermo-kinetic mixing for pharmaceutical applications. United States patent 8486423 B2. 2013 Jul 16.

44. DiNunzio JC, Brough C, Hughey JR, Miller DA, Williams RO, McGinity JW. Fusion production of solid dispersions containing a heat-sensitive active ingredient by hot melt extrusion and Kinetisol® dispersing. European Journal of Pharmaceutics and Biopharmaceutics. 2010;74(2):340-51.

45. Hughey JR, DiNunzio JC, Bennett RC, Brough C, Miller DA, Ma H, et al. Dissolution enhancement of a drug exhibiting thermal and acidic decomposition characteristics by fusion processing: a comparative study of hot melt extrusion and KinetiSol® dispersing. AAPs Pharmscitech. 2010;11(2):760-74.

46. Hughey JR, Keen JM, Miller DA, Kolter K, Langley N, McGinity JW. The use of inorganic salts to improve the dissolution characteristics of tablets containing Soluplus®-based solid dispersions. European Journal of Pharmaceutical Sciences. 2013;48(4):758-66.

47. Hughey JR, Keen JM, Bennett RC, Obara S, McGinity JW. The incorporation of low-substituted hydroxypropyl cellulose into solid dispersion systems. Drug development and industrial pharmacy. 2015;41(8):1294-301.

48. Hughey JR, McGinity JW. Emerging Technologies to Increase the Bioavailability of Poorly Water-Soluble Drugs. Formulating Poorly Water Soluble Drugs: Springer; 2012. p. 569-602.

49. Miller DA, Keen JM. KinetiSol®-Based Amorphous Solid Dispersions. Amorphous Solid Dispersions: Springer; 2014. p. 567-77.

50. DiNunzio JC, Brough C, Miller DA, Williams RO, McGinity JW. Applications of KinetiSol® dispersing for the production of plasticizer free amorphous solid dispersions. European Journal of Pharmaceutical Sciences. 2010;40(3):179-87.

51. Keen JM, McGinity JW, Williams III RO. Enhancing bioavailability through thermal processing. International journal of pharmaceutics. 2013;450(1):185-96.

52. Chandanais R. Specialty drug approvals: Review of 2014 and a forecast for 2015. Pharmacy Today. 2015;21(1):50-1.

53. Corbett AH, Lim ML, Kashuba AD. Kaletra (lopinavir/ritonavir). Annals of Pharmacotherapy. 2002;36(7-8):1193-203.

54. Chen C, Lu X-H, Yan S, Chai H, Yao Q. HIV protease inhibitor ritonavir increases endothelial monolayer permeability. Biochemical and biophysical research communications. 2005;335(3):874-82.

55. Kessler T, Breitenbach J, Schmidt C, Degenhardt M, Rosenberg J, Krull H, inventors; Abbott Gmbh & Co., Kg, assignee. Process for producing a solid dispersion of an active ingredient. United States patent application 12/279,415. 2007 Mar 12.

56. LaFountaine JS, Jermain SV, Prasad LK, Brough C, Miller DA, Lubda D, et al. Enabling thermal processing of ritonavir–polyvinyl alcohol amorphous solid dispersions by KinetiSol® Dispersing. European Journal of Pharmaceutics and Biopharmaceutics. 2016;101:72-81.

57. Repka MA, Gerding TG, Repka SL, McGinity JW. Influence of plasticizers and drugs on the physical-mechanical properties of hydroxypropylcellulose films prepared by hot melt extrusion. Drug development and industrial pharmacy. 1999;25(5):625-33.

58. Hancock BC, Shamblin SL, Zografi G. Molecular mobility of amorphous pharmaceutical solids below their glass transition temperatures. Pharmaceutical research. 1995;12(6):799-806.

59. Gupta SS, Meena A, Parikh T, Serajuddin AT. Investigation of thermal and viscoelastic properties of polymers relevant to hot melt extrusion, I: Polyvinylpyrrolidone and related polymers. Journal of Excipients and Food Chemicals. 2014;5(1):32-45.

60. Meena A, Parikh T, Gupta SS, Serajuddin AT. Investigation of thermal and viscoelastic properties of polymers relevant to hot melt extrusion, II: Cellulosic polymers. Journal of Excipients and Food Chemicals. 2014;5(1):46-55.

61. Parikh T, Gupta SS, Meena A, Serajuddin AT. Investigation of thermal and viscoelastic properties of polymers relevant to hot melt extrusion, III: polymethacrylates and polymethacrylic acid based polymers. Journal of Excipients and Food Chemicals. 2014;5(1):56-64.

62. Miller DA, Keen JM, Kucera SU, inventors; DisperSol Technologies, LLC, assignee. Formulations of deferasirox and methods of making the same. United States patent application 15/185,888. 2016 Jun 17.

63. Chirnomas D, Smith AL, Braunstein J, Finkelstein Y, Pereira L, Bergmann AK, et al. Deferasirox pharmacokinetics in patients with adequate versus inadequate response. Blood. 2009;114(19):4009-13.

64. Hughey JR, Keen JM, Brough C, Saeger S, McGinity JW. Thermal processing of a poorly water-soluble drug substance exhibiting a high melting point: the utility of KinetiSol® dispersing. International journal of pharmaceutics. 2011;419(1):222-30.

65. Bashiri-Shahroodi A, Nassab PR, Szabó-Révész P, Rajkó R. Preparation of a solid dispersion by a dropping methodto improve the rate of dissolution of meloxicam. Drug development and industrial pharmacy. 2008;34(7):781-8.

66. Dehghan M, Jafar M. Improving dissolution of meloxicam using solid dispersions. Iranian journal of pharmaceutical research. 2010:231-8.

67. El-Badry M, Fathy M. Enhancement of the dissolution and permeation rates of meloxicam by formation of its freeze-dried solid dispersions in polyvinylpyrrolidone K-30. Drug development and industrial pharmacy. 2006;32(2):141-50.

68. Ghareeb MM, Abdulrasool AA, Hussein AA, Noordin MI. Kneading technique for preparation of binary solid dispersion of meloxicam with poloxamer 188. Aaps Pharmscitech. 2009;10(4):1206-15.

69. Vijaya Kumar SG, Mishra DN. Preparation and evaluation of solid dispersion of meloxicam with skimmed milk. Yakugaku Zasshi. 2006;126(2):93-7.

70. Haser A, Huang S, Listro T, White D, Zhang F. An approach for chemical stability during melt extrusion of a drug substance with a high melting point. International journal of pharmaceutics. 2017;524(1):55-64.

71. Gupta P, Bansal AK. Molecular interactions in celecoxib-PVP-meglumine amorphous system. Journal of pharmacy and pharmacology. 2005;57(3):303-10.

72. Shah N, Iyer RM, Mair HJ, Choi DS, Tian H, Diodone R, et al. Improved human bioavailability of vemurafenib, a practically insoluble drug, using an amorphous polymer-stabilized solid dispersion prepared by a solvent-controlled coprecipitation process. Journal of pharmaceutical sciences. 2013;102(3):967-81.

73. Albano AA, Desai D, Dinunzio J, Go Z, Iyer RM, Sandhu HK, et al., inventors; Hoffmann-La Roche Inc., assignee. Pharmaceutical composition with improved bioavailability for high melting hydrophobic compound. United States patent application 13/706,390. 2013 Jul 04.

74. Bollag G, Tsai J, Zhang J, Zhang C, Ibrahim P, Nolop K, et al. Vemurafenib: the first drug approved for BRAF-mutant cancer. Nature reviews Drug discovery. 2012;11(11):873.

75. Shah N, Sandhu H, Phuapradit W, Pinal R, Iyer R, Albano A, et al. Development of novel microprecipitated bulk powder (MBP) technology for manufacturing stable amorphous formulations of poorly soluble drugs. International journal of pharmaceutics. 2012;438(1):53-60.

76. Miller DA, Keen, Justin M, Brough, Chris, Kucera, Sandra U, and Ellenberger, Daniel J, inventorImproved Formulations of Vemurafenib and Methods of Making the Same2016.

77. Bennett RC, Brough C, Miller DA, O'Donnell KP, Keen JM, Hughey JR, et al. Preparation of amorphous solid dispersions by rotary evaporation and KinetiSol Dispersing: approaches to enhance solubility of a poorly water-soluble gum extract. Drug development and industrial pharmacy. 2015;41(3):382-97.

78. Karlina M, Pozharitskaya O, Kosman V, Ivanova S. Bioavailability of boswellic acids: in vitro/in vivo correlation. Pharmaceutical Chemistry Journal. 2007;41(11):569-72.

79. Safayhi H, Mack T, Sabieraj J, Anazodo MI, Subramanian LR, Ammon H. Boswellic acids: novel, specific, nonredox inhibitors of 5-lipoxygenase. Journal of Pharmacology and Experimental Therapeutics. 1992;261(3):1143-6.

80. Park B, Sung B, Yadav VR, Cho SG, Liu M, Aggarwal BB. Acetyl-11-keto-β-boswellic acid suppresses invasion of pancreatic cancer cells through the downregulation of CXCR4 chemokine receptor expression. International journal of cancer. 2011;129(1):23-33.

81. Krüger P, Kanzer J, Hummel J, Fricker G, Schubert-Zsilavecz M, Abdel-Tawab M. Permeation of Boswellia extract in the Caco-2 model and possible interactions of its constituents KBA and AKBA with OATP1B3 and MRP2. european journal of pharmaceutical sciences. 2009;36(2):275-84.

82. Krüger P, Daneshfar R, Eckert GP, Klein J, Volmer DA, Bahr U, et al. Metabolism of boswellic acids in vitro and in vivo. Drug Metabolism and Disposition. 2008;36(6):1135-42.

83. Raghavan S, Trividic A, Davis A, Hadgraft J. Crystallization of hydrocortisone acetate: influence of polymers. International journal of pharmaceutics. 2001;212(2):213-21.

84. DiNunzio JC, Hughey JR, Brough C, Miller DA, Williams III RO, McGinity JW. Production of advanced solid dispersions for enhanced bioavailability of itraconazole using KinetiSol® Dispersing. Drug development and industrial pharmacy. 2010;36(9):1064-78.

85. Tanaka N, Imai K, Okimoto K, Ueda S, Tokunaga Y, Ibuki R, et al. Development of novel sustained-release system, disintegration-controlled matrix tablet (DCMT) with solid dispersion granules of nilvadipine (II): in vivo evaluation. Journal of controlled release. 2006;112(1):51-6.

86. Baert LEC, Verreck G, Thoné D, inventors; Janssen Pharmaceutica NV, assignee. Antifungal compositions with improved bioavailability. United States patent 6,509,038. 2003 Jan 21.

87. Miller DA, DiNunzio JC, Yang W, McGinity JW, Williams III RO. Enhanced in vivo absorption of itraconazole via stabilization of supersaturation following acidic-to-neutral pH transition. Drug development and industrial pharmacy. 2008;34(8):890-902.

88. Keen JM. Development of Itraconazole Tablets Containing Viscous KinetiSol® Solid Dispersions: in vitro and in vivo Analysis in Dogs. AAPS PharmSciTech. In press, forthcoming 2017.

89. LaFountaine JS, Prasad LK, Brough C, Miller DA, McGinity JW, Williams III RO. Thermal processing of PVP-and HPMC-based amorphous solid dispersions. AAPS PharmSciTech. 2016;17(1):120-32.

90. Kolter K, Karl M, Gryczke A, Ludwigshafen am Rhein B. Hot-melt extrusion with BASF pharma polymers: extrusion compendium: BASF; 2012.

91. Sarode AL, Obara S, Tanno FK, Sandhu H, Iyer R, Shah N. Stability assessment of hypromellose acetate succinate (HPMCAS) NF for application in hot melt extrusion (HME). Carbohydrate polymers. 2014;101:146-53.

92. Kwong AD, Kauffman RS, Hurter P, Mueller P. Discovery and development of telaprevir: an NS3-4A protease inhibitor for treating genotype 1 chronic hepatitis C virus. Nature biotechnology. 2011;29(11):993-1003.

93. Hadida S, Van Goor F, Dinehart K, Looker AR, Mueller P, Grootenhuis PD. Case history: Kalydeco®(VX-770, Ivacaftor), a CFTR potentiator for the treatment of patients with cystic fibrosis and the G551D-CFTR mutation. Annu Rep Med Chem. 2014;49:383-98.

94. Maniruzzaman M, Morgan DJ, Mendham AP, Pang J, Snowden MJ, Douroumis D. Drug–polymer intermolecular interactions in hot-melt extruded solid dispersions. International journal of pharmaceutics. 2013;443(1):199-208.

95. Andrews GP, Jones DS, Diak OA, McCoy CP, Watts AB, McGinity JW. The manufacture and characterisation of hot-melt extruded enteric tablets. European journal of pharmaceutics and Biopharmaceutics. 2008;69(1):264-73.

96. Bruce C, Fegely KA, Rajabi-Siahboomi AR, McGinity JW. Crystal growth formation in melt extrudates. International journal of pharmaceutics. 2007;341(1):162-72.

97. Wyttenbach N, Janas C, Siam M, Lauer ME, Jacob L, Scheubel E, et al. Miniaturized screening of polymers for amorphous drug stabilization (SPADS): rapid assessment of solid dispersion systems. European Journal of Pharmaceutics and Biopharmaceutics. 2013;84(3):583-98.

98. Lin SY, Yu HL. Thermal stability of methacrylic acid copolymers of Eudragits L, S, and L30D and the acrylic acid polymer of carbopol. Journal of Polymer Science Part A: Polymer Chemistry. 1999;37(13):2061-7.

99. Mowiol Polyvinyl Alcohol. In: Clariant, editor. 1999.

100. Alexy P, Kachova D, Kršiak M, Bakoš D, Šimková B. Poly (vinyl alcohol) stabilisation in thermoplastic processing. Polymer Degradation and Stability. 2002;78(3):413-21.

101. Alexy P, Lacík I, Šimková B, Bakoš D, Prónayová Na, Liptaj T, et al. Effect of melt processing on thermo-mechanical degradation of poly (vinyl alcohol) s. Polymer Degradation and stability. 2004;85(2):823-30.

102. Brough C, Miller DA, Keen JM, Kucera SA, Lubda D, Williams III RO. Use of polyvinyl alcohol as a solubility-enhancing polymer for poorly water soluble drug delivery (part 1). AAPS PharmSciTech. 2016;17(1):167-79.

103. Brough C, Miller DA, Ellenberger D, Lubda D, Williams III RO. Use of Polyvinyl Alcohol as a Solubility Enhancing Polymer for Poorly Water-Soluble Drug Delivery (Part 2). AAPS PharmSciTech. 2016;17(1):180-90.

104. Tran PH-L, Tran TT-D, Park JB, Lee B-J. Controlled release systems containing solid dispersions: strategies and mechanisms. Pharmaceutical research. 2011;28(10):2353-78.

105. Reynolds TD, Mitchell SA, Balwinski KM. Investigation of the effect of tablet surface area/volume on drug release from hydroxypropylmethylcellulose controlled-release matrix tablets. Drug development and industrial pharmacy. 2002;28(4):457-66.

106. Tajarobi F, Larsson A, Matic H, Abrahmsén-Alami S. The influence of crystallization inhibition of HPMC and HPMCAS on model substance dissolution and release in swellable matrix tablets. European Journal of Pharmaceutics and Biopharmaceutics. 2011;78(1):125-33.

107. Banerjee A, Lee J, Mitragotri S. Intestinal mucoadhesive devices for oral delivery of insulin. Bioengineering & Translational Medicine. 2016.

108. Mansuri S, Kesharwani P, Jain K, Tekade RK, Jain N. Mucoadhesion: A promising approach in drug delivery system. Reactive and Functional Polymers. 2016;100:151-72.

109. Gupta V, Hwang BH, Lee J, Anselmo AC, Doshi N, Mitragotri S. Mucoadhesive intestinal devices for oral delivery of salmon calcitonin. Journal of Controlled Release. 2013;172(3):753-62.

110. Rowe RC, Sheskey PJ, Weller PJ. Handbook of pharmaceutical excipients. 2009. Hypromellose Page-438.

111. LaFountaine JSP, Leena K; Miller, Dave A; McGinity, James W; Williams, Robert O. Mucoadhesive Amorphous Solid Dispersions for Sustained Release of Poorly Water Soluble Drugs. European Journal of Pharmaceutics and Biopharmaceutics. 2017;113:157-67.

112. Sauceau M, Fages J, Common A, Nikitine C, Rodier E. New challenges in polymer foaming: A review of extrusion processes assisted by supercritical carbon dioxide. Progress in Polymer Science. 2011;36(6):749-66.

113. Dinunzio J. Applications of Melt-Extrusion for Continuous Manufacturing of Novel Drug Products. 2016 AAPS Annual Meeting & Exposition; Denver, CO2016.

114. Fukuda M, Peppas NA, McGinity JW. Floating hot-melt extruded tablets for gastroretentive controlled drug release system. Journal of controlled release. 2006;115(2):121-9.

115. Nikitine C, Rodier E, Sauceau M, Letourneau JJ, Fages J. Controlling the structure of a porous polymer by coupling supercritical CO2 and single screw extrusion process. Journal of applied polymer science. 2010;115(2):981-90.

116. Verreck G, Decorte A, Li H, Tomasko D, Arien A, Peeters J, et al. The effect of pressurized carbon dioxide as a plasticizer and foaming agent on the hot melt extrusion process and extrudate properties of pharmaceutical polymers. The Journal of supercritical fluids. 2006;38(3):383-91.

117. Sacchetti M. Thermodynamic analysis of DSC data for acetaminophen polymorphs. Journal of thermal analysis and calorimetry. 2000;63(2):345-50.

118. Rustichelli C, Gamberini G, Ferioli V, Gamberini M, Ficarra R, Tommasini S. Solid-state study of polymorphic drugs: carbamazepine. Journal of pharmaceutical and biomedical analysis. 2000;23(1):41-54.

119. Du Q, Xiong X, Suo Z, Tang P, He J, Zeng X, et al. Investigation of the solid forms of deferasirox: solvate, co-crystal, and amorphous form. RSC Advances. 2017;7(68):43151-60.

120. Zhou D, Zhang GG, Law D, Grant DJ, Schmitt EA. Thermodynamics, molecular mobility and crystallization kinetics of amorphous griseofulvin. Molecular pharmaceutics. 2008;5(6):927-36.

121. Cavalli R, Peira E, Caputo O, Gasco MR. Solid lipid nanoparticles as carriers of hydrocortisone and progesterone complexes with β-cyclodextrins. International journal of pharmaceutics. 1999;182(1):59-69.

122. Basavoju S, Boström D, Velaga SP. Indomethacin–saccharin cocrystal: design, synthesis and preliminary pharmaceutical characterization. Pharmaceutical research. 2008;25(3):530-41.

123. Souto E, Müller R. SLN and NLC for topical delivery of ketoconazole. Journal of microencapsulation. 2005;22(5):501-10.

124. Schopf C, inventor; E. Merck, assignee. Preparation of Quinolizine Derivatives. United States patent 3132147. 1964 May 5.

125. DiNunzio JC, Brough C, Miller DA, Williams RO, McGinity JW. Fusion processing of itraconazole solid dispersions by KinetiSol® dispersing: a comparative study to hot melt extrusion. Journal of pharmaceutical sciences. 2010;99(3):1239-53.

126. Coppens K, Hall M, Larsen P, Mitchell S, Nguyen P, Read M, et al., editors. Thermal and rheological evaluation of pharmaceutical excipients for hot melt extrusion. AAPS Annual Meeting and Exposition, Baltimore, MD; 2004.

127. Yang Y, Bi, Vivian, and Durig, Thomas. The Impact of HPMC Molecular Weight and Degree of Substitution on Crystallization Inhibition of Felodipine in Aqueous Media. AAPS: Ashland; 2015.

128. AquaSolve Hydroxypropylmethylcellulose Acetate Succinate. In: Ashland, editor. 2016.

129. Rahman M. The Use of Hot Melt Extrusion and Comparative Technologies in Preparing Solid Amorphous Dispersions and Controlled Release Dosage Forms. In: Leistritz, editor. Pharmaceutical Extrusion Seminar: Ashland; 2012.

130. Six K, Berghmans H, Leuner C, Dressman J, Van Werde K, Mullens J, et al. Characterization of solid dispersions of itraconazole and hydroxypropylmethylcellulose prepared by melt extrusion, part II. Pharmaceutical research. 2003;20(7):1047-54.

131. Berndl G, Degenhardt M, Mäegerlein M, Dispersyn G, inventors; Abbott Gmbh & Co. and Kg, assignee. Itraconazole compositions with improved bioavailability. United States patent 8,486,456. 2013 Jul 16.

Chapter 2: Improved Vemurafenib Dissolution and Pharmacokinetics as an Amorphous Solid Dispersion Produced by KinetiSol® Processing

2.1 Abstract

Vemurafenib is a poorly soluble, low permeability drug that has a demonstrated need for a solubility enhanced formulation. However, conventional approaches for amorphous solid dispersion production are challenging due to the physiochemical properties of the compound. A suitable and novel method for creating an amorphous solid dispersion, known as solvent-controlled coprecipitation, was developed to make material known as microprecipitated bulk powder (MBP). However, this approach has limitations in its processing and formulation space. In this study, it was hypothesized that vemurafenib can be processed by KinetiSol into the same amorphous formulation as MBP. The KinetiSol process utilizes high shear to rapidly process amorphous solid dispersions containing vemurafenib. Analysis of the material demonstrated that KinetiSol produced amorphous, single-phase material with acceptable chemical purity and stability. Values obtained were congruent to analysis conducted on the comparator material. However, the materials differed in particle morphology as the KinetiSol material was dense, smooth, and uniform while the MBP comparator was porous in structure and exhibited high surface area. The particles produced by KinetiSol had improved in-vitro dissolution and pharmacokinetic performance for vemurafenib compared to MBP due to slower drug nucleation and recrystallization which resulted in superior supersaturation maintenance during drug release. In the in-vivo rat pharmacokinetic study, both amorphous solid dispersions produced by

KinetiSol exhibited mean AUC values at least two-fold that of MBP when dosed as a suspension. It was concluded that the KinetiSol process produced superior dosage forms containing vemurafenib with the potential for substantial reduction in patient pill burden.

2.2 INTRODUCTION

Vemurafenib is administered in the treatment of the V600E mutation of the BRAF gene which leads to unresectable/metastatic melanoma in cancer patients (1, 2). It has also been demonstrated to reduce immunosuppression in addition to inhibition of tumor growth making it effective in tumor treatment. (3) The molecular structure of vemurafenib is shown in Figure 2.1 and some its key physiochemical properties related to drug delivery are listed in Table 2.1.

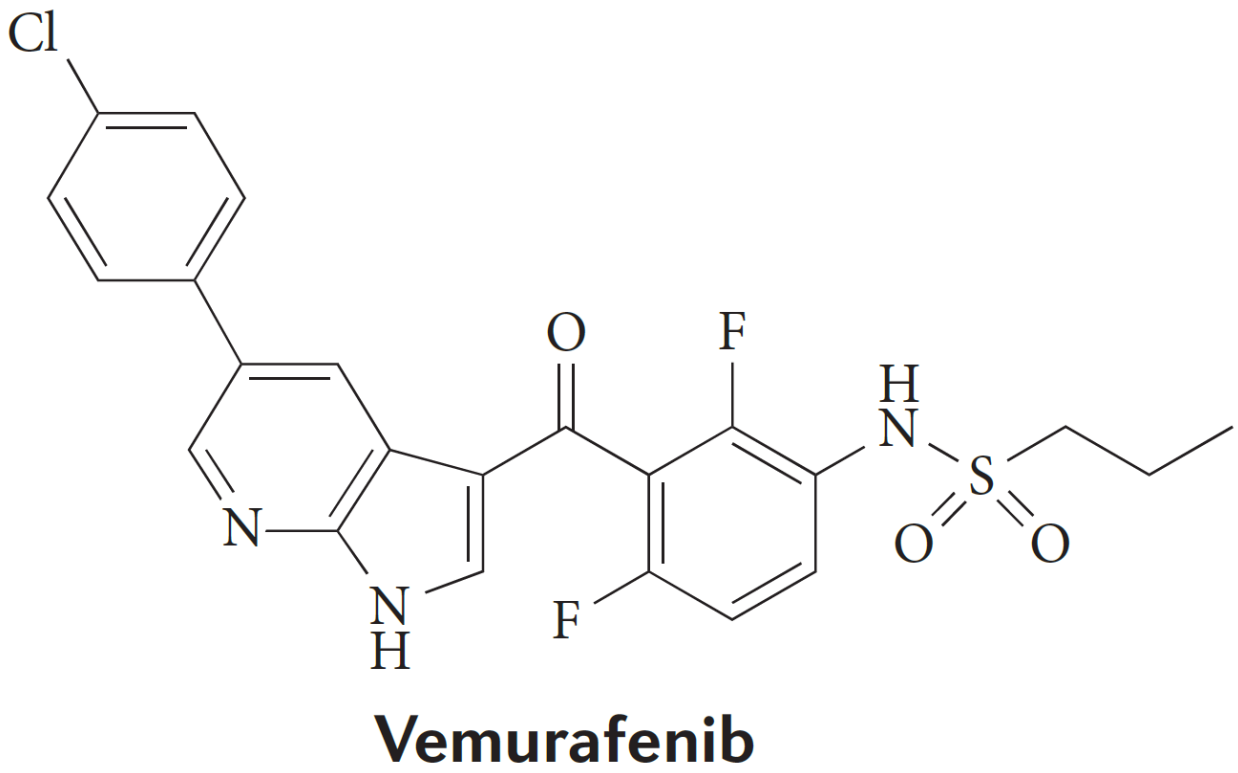

Figure 2.1: Structure of vemurafenib. Reproduced with permission from (60).

Molecular weight	489.93 Da
Melting point	272°C
BCS Classification	II/IV
Aqueous buffers (pH 3 and 7)	< 0.1 µg/mL
Fasted Simulated Intestinal Fluid (FaSSIF)	< 2 µg/mL
Log P	3.0

Table 2.1: Molecular properties of vemurafenib. Adapted with permission from (4).

Due to its physiochemical properties, vemurafenib represents a significant challenge for oral delivery and it is classified as a Class II or IV drug in the Biopharmaceutical Classification System (BCS). The aqueous solubility of crystalline vemurafenib is <0.1 µg/mL and does not exhibit pH dependence in a biologically relevant range. In fasted simulated intestinal fluid (FaSSIF), the equilibrium solubility remains low at <2 µg/mL. Vemurafenib has a log P value of 3.0 (4) which places it as a high permeability molecule with log P greater than 1.72. (5) This combination of parameters suggests that it should be classified as BCS Class II solubility challenged molecule. (6) However, in vitro testing found that vemurafenib demonstrated reduced permeability compared to a low permeability reference ranitidine in a Caco-2 cell model. (7) Thus, in practice it is a BCS Class IV solubility/permeability challenged molecule. (6) The molecular weight of vemurafenib is approximately 490 Daltons (4) which is just below the Lipinski rule of <500 Daltons. While not being counter to the multiple rule-of-5 criteria, the borderline nature of vemurafenib with multiple rules puts it in a class of molecules that are a challenge to formulate. (8) This difficulty is exhibited in clinical trial results. During initial phase I clinical trials, the crystalline form was found to be inadequate as the high dose patients were ingesting 1600 mg (32 capsules) of vemurafenib (9). Despite this very high administered dose (i.e., pill burden), efficacy was limited by low systemic drug concentrations, thus necessitating a solubility enhanced formulation to achieve the target therapeutic effect. Even with a solubility enhanced formulation, a clinical trial study found that 94% of the active vemurafenib was recovered in feces and 1% in urine, which was indicative of poor drug absorption. (10)

Several options exist for dissolution rate and solubility enhancement to improve the oral absorption of compounds like vemurafenib. The Noyes-Whitney equation indicates that the

dissolution rate of a drug is proportional to the concentration gradient as well as the particle surface area. Thus, the dissolution rate can be increased by increasing the surface area of the material. Particle size reduction can be used to achieve this goal (11, 12) with nano-crystal technology as an example of a more modern approach for dissolution rate enhancement and has led to several commercial products. (13) However, due to its low equilibrium solubility, dissolution rate is not the primary cause for poor oral absorption of vemurafenib, and apparent solubility enhancement was expected to provide greater delivery benefit. Lipid based formulations represent another approach for drug delivery in which the drug is solubilized in a lipid vehicle and administered orally. (14) However, lipid based formulations are often challenged by high dose drugs (15) and as clinical trials demonstrated, vemurafenib efficacy requires a prohibitively high dose. Another approach is to modify the parent molecule to create a prodrug for improved absorption. In the case of vemurafenib, prodrugs are being tested in animal models (16); however, little data is available and these types of modification can require targeted radiation to activate the dose. (17) An effective way to overcome solubility challenges, particularly for drugs requiring a high dose, is the use of an amorphous form of active pharmaceutical in an amorphous solid dispersion. Of the drugs that are currently in development, approximately 90% are thought to be poorly water-soluble and would benefit from solubility enhancement. (18, 19) An amorphous solid dispersion is a carrier-drug system (e.g., polymer carrier) in which the drug molecules are dispersed in an amorphous state most typically within an amorphous carrier matrix. (20) However, there are limitations and challenges with amorphous dispersion formulations including: method of preparation, reproducibility, formulation into dosage forms, manufacturing scale-up and stability. (21) Despite these challenges, many studies have shown improved solubility and bioavailability for drugs administered in the amorphous

form as compared to the crystalline state. (18) Due to its high dose requirement and poor aqueous solubility, an amorphous solid dispersion of vemurafenib represents an attractive approach for oral delivery of this challenging molecule.

Two predominant amorphous solid dispersion approaches are spray-draying and hot melt extrusion. Spray drying is a process by which the active pharmaceutical ingredient (API) and all excipients to be included in the amorphous dispersion are dissolved in a solvent system. This drug loaded solution is then sprayed as fine droplets into a drying chamber wherein solvent is quickly evaporated, resulting in an amorphous dispersion of the dissolved components. (22, 23) A significant limitation of the spray drying process is availability of a solvent in which all components demonstrate favorable solubility. Furthermore, the solvent system must be sufficiently volatile under typical spray drying conditions. To achieve suitable process efficiency, the solids load in the feed solution should be 5-50% (w/w) with >10% solids load being ideal. (22) This is particularly important for a high dose drug like vemurafenib in which large quantities need to be produced in order to meet the desired clinical and patient outcomes. Table 2.2 summarizes the solubility of vemurafenib in several organic solvents including the resulting calculated maximum drug % (w/w) in the feed solution and residual solvent classification of each solvent. As is apparent in the table, vemurafenib lacks suitable organic solubility in all of the listed common organic solvents except for dimethylacetamide (DMA). However, DMA is not suitable for the spray drying process due its high boiling point (166°C) (24) and it represents a safety and environmental hazard due to its residual solvent classification. (25) Thus, another amorphous solid dispersion approach is required for formulating vemurafenib.

Organic Solvent	Solvent Class	Solubility (mg/mL)	Maximum drug % (w/w) in Feed
Dimethylacetamide	2	>500	53.4
Methanol	2	4.57	0.6
Acetonitrile	2	1.40	0.2
Dichloromethane	2	1.95	0.1
Isopropanol	1	3.56	0.5
Acetone	1	<6	0.8

Table 2.2: Organic solvent classification, vemurafenib solubility, and maximum spray-drying feed drug load. Adapted from (4, 22)

The other approach for amorphous solid dispersion production is hot melt extrusion. This is a thermal-based process for which melting points, glass transition temperatures, and component viscosities are critical parameters. (26) As a general rule of thumb, formulations that contain components with melting points greater than 200°C are challenging to process by hot melt extrusion as they require higher extruder temperatures, reduced drug loads, and/or the addition of a plasticizer. (27) Based on polymer viscosity and degradation onset, none of the common polymeric carriers examined by LaFountaine et al. had an extrudable window greater than 200°C. (28) One specific example is hypromellose acetate succinate (HPMCAS), a polymer used to formulate amorphous solid dispersions with beneficial drug solubility properties related to interactions with acetyl and succinoyl groups. (29) However, HPMCAS has been shown to be sensitive to thermal degradation by melt extrusion leading to reduction in acetyl/succinoyl content as well as release of free acetic and succinic acid that may lead to drug degradation. (30) If drug load is reduced to accommodate the melt extrusion process, the result is increased pill burden for an already high dose drug to the patient. While plasticizers can be included during melt extrusion to lower the required processing temperature, the downside to their use is that they decrease the glass transition temperature of the system which can result in phase separation and eventually drug recrystallization. (31) Specific to vemurafenib, hot melt extrusion of vemurafenib was investigated by Albano et al. In their work, the maximum drug load of vemurafenib in a binary system was found to be only 10% (w/w) in a copovidone matrix. The drug load was increased to as high as 20-25% (w/w) only with the inclusion of 5-15% (w/w) glycerol monostearate, a plasticizer. (32) As it relates to drug load and plasticizer, these melt extrusion examples demonstrated the processing limits with vemurafenib by this technique.

Therefore, another amorphous solid dispersion approach was required in order to develop a suitable delivery platform for vemurafenib.

Ultimately, a solvent-controlled coprecipitation process was developed for vemurafenib. Utilizing the high solubility of vemurafenib in dimethylacetamide, vemurafenib and HPMCAS (L grade) were dissolved in this solvent at 30% (w/w) drug load. This feed solution was slowly added to an anti-solvent, 0.01N hydrochloric acid, which simultaneously precipitated the drug and polymer as an amorphous solid dispersion. After washing and drying steps, the final resulting product, known as microprecipitated bulk powder (MBP), was collected, and it exhibited an approximately 30-fold increase in equilibrium solubility as compared to the crystalline form of the drug. (4) This material was used to manufacture the U.S. Food and Drug Administration approved product, Zelboraf®, which is administered as four 870 mg total weight tablets at a dosing frequency of twice daily. (1, 33) The effectiveness of this process with other model compounds and investigational molecules has also been explored by the inventors. During these studies, limitations with the process have been identified. From a drug perspective, the process is limited to molecules that are not susceptible to acidic degradation and have poor solubility in acidic media. This means that the process is not viable for many weakly basic drugs, many of whom have poor solubility in neutral gastrointestinal conditions where absorption is favored. Another significant limitation of the coprecipitation process is that it requires ionic polymers, which potentially restricts the choice of polymers that may be more favorable for solubility or stability. Finally, the final processing step involves the drying of aqueous solvent from the amorphous particles and a final water content of 2-3% is typically found. Both the drying process and the final water content can compromise the physical stability of the

amorphous solid dispersion, and hence drug recrystallization is a significant concern. (34) While the solvent-controlled coprecipitation process is used to prepare a suitable amorphous solid dispersion for vemurafenib, there remains an unmet need for a process that works for drugs like vemurafenib but are not amenable to solvent-controlled co-precipitation. There also exists an opportunity to expand the formulation space of vemurafenib amorphous solid dispersions.

One such process to address this need is KinetiSol. This process has been shown to work with drugs similar to vemurafenib that exhibit a high-melting point and low solubility in organic solvent. Figure 2.2 illustrates a process viability matrix for assessing processing technologies for APIs based on their melting point and solubility in organic solvent. In this scheme, vemurafenib fits in the upper-left quadrant for which hot-melt extrusion and spray-drying are not viable processes. Similar high melting point, low organic solubility drugs that have been processed by KinetiSol and fit in this category are meloxicam (35) and deferasirox (36). The process utilizes a fusion based approach where rotation of a set of protruding blades applies friction and shear forces to the material being processed. These energy inputs render the components amorphous at temperatures below the melting point of the compound and at fast solubilization rates. (37) Due to processing material at a lower temperature than the melting point of the drug, there is reduced degradation for thermally labile compounds. (38, 39) Processing times are significantly shortened and overall thermal exposure is lessened, especially as compared to hot melt extrusion (e.g., seconds versus minutes). (40) KinetiSol is also readily scalable as it was developed at a commercial scale and was scaled down for use in laboratory environments. (37) Unlike solvent-controlled coprecipitation, the process is amenable to numerous types of polymers, which allows

for significant expansion of the formulation space. Thus, it was hypothesized that KinetiSol is a viable processing technology for the production of amorphous solid dispersions of vemurafenib.

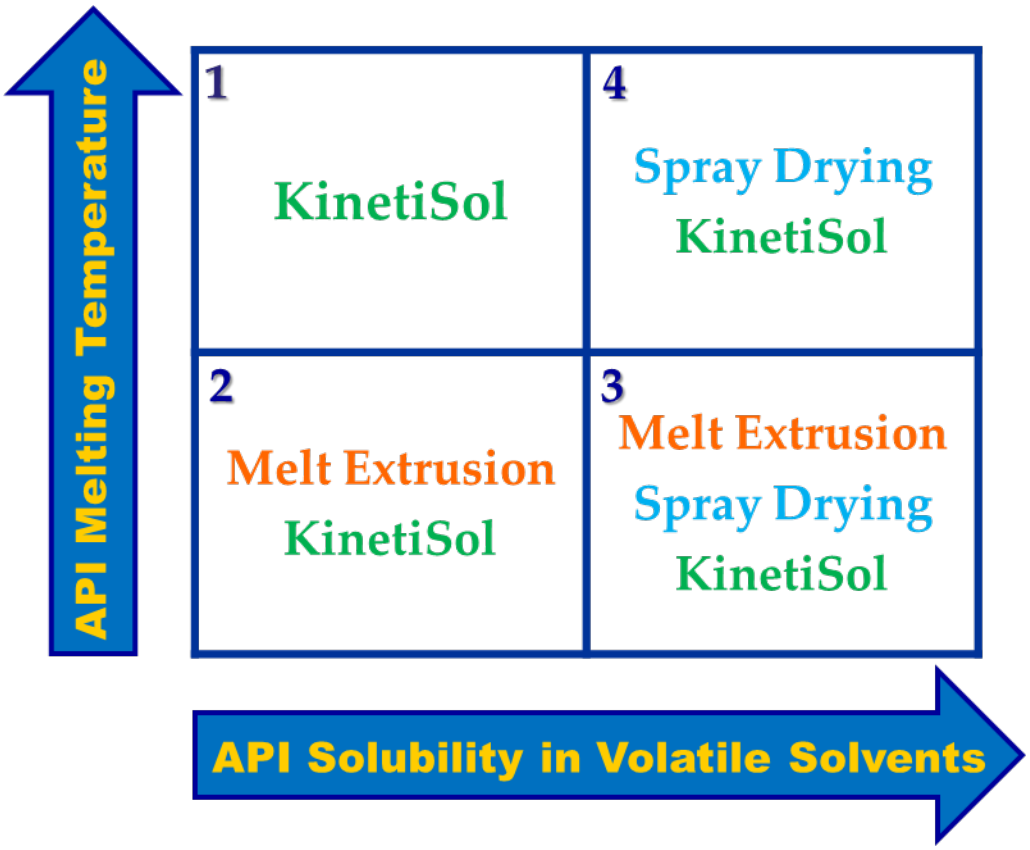

Figure 2.2: Amorphous solid dispersion viability matrix for API solubility and melting point. Reproduced from (61)

2.3 MATERIALS AND METHODS

2.3.1 Materials:

Vemurafenib API was obtained from Agno Pharma (Agno Pharma, Suzhou, Jiangsu, China). HPMCAS-LMP (L grade, medium particle size) was acquired from Shin-Etsu (Shin-Etsu Chemical Co., Tokyo, Japan). All chemicals used for MBP production were ACS grade and HPLC solvents were HPLC grade. FaSSIF dissolution media was prepared using FaSSIF, FeSSIF, and FaSSGF Powder (Biorelevant.com, Croydon, Surrey, UK)

2.3.2 MBP Preparation:

The process for MBP production provided by Shah et al. was used for production of amorphous vemurafenib material. (4, 34) Vemurafenib API and HPMCAS-LMP polymer were dissolved at 15% w/w level in dimethylacetamide (DMA). The solution was slowly added 0.01N hydrochloric acid (HCl) with continuous stirring. It was held in the range of 2-5°C and the DMA:0.01N HCl ratio did not exceed 1:10 w/w. Precipitated solids were collected by vacuum filtration and washed in triplicate with cold 0.01N HCl followed by triplicate washes of cold water. The MBP material was dried in a Jeio OF-22G forced air convection oven (Jeio Tech, Daejeon, South Korea) until a constant moisture content was achieved. A IR-30 moisture analyzer (Denver Instrument Company, Arvada, Colorado, USA) was utilized to measure moisture content. The sample was milled partway through the drying process to aid in drying and

to reduce the particle size to the intended result. Table 2.3 defines the acronyms used in this paper.

2.3.3 KinetiSol Processing:

A KinetiSol compounder (DisperSol Technologies, Georgetown, TX) was used to generate vemurafenib amorphous solid dispersions. API and polymer were pre-screened through a #30 mesh screen (≤300 μm) to rid the material of large particles. Material was prepared by hand mixing a blend of 30/70 vemurafenib/HPMCAS-LMP for 2 minutes and then charging into the compounder chamber. Inside the compounder chamber, a shaft with protruding blades was rotated a speed of 2400 rpm, without external heat addition, to impart frictional and shear forces to the sample material. Temperature of the mass was monitored using an infrared probe. When molten mass temperature reached a value of 180°C, the mass was rapidly ejected, collected, and pressed between two metal plates to rapidly quench the sample. This material was labeled KSD (KinetiSol Solid Dispersion) material.

2.3.4 Milling:

For <250 μm MBP and KSD samples, sample was broken into fragments and loaded into an IKA tube mill 100 (IKA, Staufen, Germany). Sample was processed for 1 minute at 5000 rpm. All milled material was subsequently passed through a #60 mesh screen (≤250 μm). Material >250 μm was cycled through the mill with the same parameters and this process of milling and sieve

was repeated until all material passed through the screen. The resulting material is henceforth known as KSD <250 (see, Table 2.3).

Abbreviation	Full Term
BCS	biopharmaceutical classification system
FaSSIF	fasted simulated intestinal fluid
API	active pharmaceutical ingredient
DMA	dimethylacetamide
HPMCAS	hypromellose acetate succinate
MBP	microprecipitated bulk powder
KSD	KinetiSol solid dispersion
KSD <250	KSD material <250 μm particle size
KSD Cryo	KSD material cryomilled
XRPD	x-ray powder diffraction
mDSC	modulated differential scanning calorimetry
Tg	glass transition temperature
SEM	scanning electron microscopy
PSD	particle size distribution
BET	Brunauer-Emmett-Teller theory
Cmax,diss	dissolution maximum concentration
tmax,diss	dissolution time of maximum concentration
Cmax	pharmacokinetic maximum concentration
tmax	pharmacokinetic time of maximum concentration
AUC0→24	area under the plasma curve from 0 to 24 hours
AUC0→∞	area under the plasma curve from 0 to infinity

Table 2.3: Acronyms Used in Manuscript

For cryomilling, approximately 5 g of samples was broken into fragments and fed into a stainless steel cryomill tube with impactor. The sealed tube was loaded into a SPEX 6775 Freezer/Mill (SPEX SamplePrep, Metuchen, NJ) and lowered into the pre-filled liquid nitrogen bath. After a pre-cool time of 1 minute, samples were impacted by oscillation at 10 cycles per second for 2 minute durations for a total of 10 iterations with 1 minute cooling time in between iterations. The sample was removed and used as is without further screening. The resulting material is referred to as KSD Cryo (see, Table 2.3).

2.3.5 X-Ray Powder Diffraction:

X-ray powder diffraction (XRPD) analysis was conducted using an Inel Equinox 100 X-ray diffractometer (INEL, Ardenay, France). Physical mixtures and milled, processed samples were loaded into aluminum sample holders and placed on a rotating stage. A Cu K Alpha radiation (λ = 1.5418 Å) x-ray tube was used with operating voltage of 42 kV and current of 0.8 mA. Data was collected with a curved radius detector in a 2Θ range of 2-110°. Data was collected and analyzed using Acquisition software (INEL, Ardenay, France).

2.3.6 Modulated Differential Scanning Calorimetry:

Thermal analysis was conducted by modulated differential scanning calorimetry (mDSC) with a Q20 Differential Scanning Calorimeter (TA Instruments, New Castle, DE, USA). Sample was prepared in a Tzero pan and sealed with Tzero lid. The target mass was approximately 5-10 mg

of sample per pan. Sample was equilibrated at a 35°C for 5 minutes after which the temperature was ramped at 3°C/minute to 300°C with a modulation of 0.3°C every 50 seconds. All data was collected with nitrogen as the sample purge gas. Samples were analyzed using Universal Analysis 2000 software (TA Instruments, New Castle, DE, USA).

2.3.7 Physical Stability Study:

Amorphous powders were loaded into aluminum X-ray sample holders and placed in a PH09 stability chamber (Darwin Chambers Company, St. Louis, MO, USA). Samples were held at 40°C/75% R.H. with no protection from moisture. Samples were removed and analyzed by X-ray powder diffraction at time points of 0, 1, and 3 months using XRPD method described previously. Immediately after analysis, the samples were returned to the stability chamber for storage.

2.3.8 HPLC Analysis:

A high performance liquid chromatography (HPLC) method was developed for chemical analysis of vemurafenib amorphous dispersions utilizing the stability indicating method from Chabda et al in 2013 as a starting point for method development. (41) A Dionex Ultimate 3000 HPLC system (Thermo Electron, Sunnyvale, CA, USA) was used for reverse-phase HPLC analysis. The HPLC column was a Kinetex 2.6u C8 100A column, P/N: 00C-4997-E0 (Phenomenex, Torrance, CA, USA). Mobile phase A was a 0.1% aqueous phosphoric acid

solution and mobile phase b was degassed acetonitrile. A gradient profile with flow rate of 1.5 mL/min was run for 16 minutes, the column was held at 40°C, and data was collected at a single wavelength of 254 nm. Samples were prepared at a nominal concentration of 0.1 mg/mL level with 80/20 Acetonitrile/Water as the standard/sample diluent. All samples were filtered through 0.2 um, 13 mm ID nylon syringe filters with GMF pre-filter, P/N: 6870-1302 (Whatman, Piscataway, NJ, USA), prior to analysis. Samples chromatography was analyzed using Chromeleon software, version 7.1 (Dionex, Bannockburn, IL, USA).

2.3.9 Scanning Electron Microscopy:

Powder samples were adhered to stubs with conductive carbon tape and the interior of a small unmilled quenched fragment was mounted to a stub at an angle using a combination of carbon and copper tape. Stubs with sample were sputter coated with platinum-palladium under argon gas to a thickness of 15 nm in a Cressington 208HR Sputter Coater (Cressington, Watford, UK). Scanning electron microscopy (SEM) was performed on coated samples in a Zeiss Supra40 Scanning Electron Microscope (Zeiss, Oberkochen, Germany). An accelerating voltage of 5 kV was used for all samples with the SE2 detector used for image capture. The stage was tilted so that the cross-section of the fragment sample was in-line with the imager.

2.3.10 Particle Size Distribution:

The particle size distribution (PSD) of the milled samples was analyzed in a Spraytec analyzer (Malvern Instruments, Malvern, UK). Samples were pre-loaded into gelatin capsules which were punctured to allow for sample exit and air flow escape. A feed pressure of 60 psi dry nitrogen was used to dose the powder into the unit. Acquisition was conducted with a 300 mm lens with acquisition triggered by transmission <98%.

2.3.11 Surface Area Analysis:

Particle surface areas were measured using a Monosorb Rapid Surface Area Analyzer model MS-25 (Quantachrome, Boynton Beach, Florida) and Brunauer–Emmett–Teller (BET) theory. For MBP and KSD Cryo samples, approximately 200 mg of material was loaded as 3 replicates into pre-dried U-tube glass sample cells. For the KSD <250 µm sample, approximately 1 gram of material was used. Samples were dried overnight at 35°C with outgassing under dry helium dioxide. Samples were re-weighed after outgassing. Surface area measurements were carried out by loading outgassed tubes into the analyzer one at a time and measuring the desorption phase of the absorption-desorption cycle. The sample surface area was divided by the outgassed sample mass to determine specific surface area.

2.3.12 Dissolution:

Amorphous solid samples were analyzed for dissolution performance via non-sink dissolution testing. A Distek 2500 dissolution tester (Distek, North Brunswick, NJ, USA) was used for testing. The apparatus was set up per guidelines from United States Pharmacopeia 38, Chapter 711 Dissolution, Apparatus 2. Fasted simulated intestinal fluid (FaSSIF), pH 6.5 dissolution media was prepared Biorelevant powder following manufacturer's instruction. 500 mL of the media was added to each dissolution vessel and allowed to equilibrate to 37°C. Samples were prepared by filling size 00 hypromellose Vcaps (Capsugel, Morristown, New Jersey, USA) with amorphous material containing an equivalent of 40 mg of vemurafenib API. Capsule samples were prepared in triplicate for each sample. Sample addition to vessels was performed using stainless steel sinkers and paddle revolution was immediately begun at 75 rpm. Data collection was done with a Spectra fiber optic UV system (Pion Inc., Billerica, MA, USA) with data collected every 5 minutes from 200-700 nm. The system was standardized by generation of a calibration curve by which 2 mg/mL vemurafenib in DMA stock solution was spiked into a stirred vessel containing FaSSIF media. Data was analyzed by AU Pro software (Pion Inc., Billerica, MA, USA) by second derivate analysis and a range of 308-318 nm for integration.

2.3.13 Pharmacokinetics in Male Sprague-Dawley Rats:

In-vivo non-crossover pharmacokinetic analysis in a fasted male Sprague-Dawley rat model was conducted at Absorption Systems (Exton, PA, USA). Samples were suspended in 0.5% methylcellulose in water at a concentration of 5 mg of vemurafenib per mL of vehicle. A target

dose of 25 mg/kg was administered to each arm of the study. The cryomilled arm was inadvertently dosed at 21.9 mg/kg. Each arm consisted of 4 rats who were blood sampled at time points: 15, 30 minutes, 1, 2, 3, 4, 6, 8, 12, and 24 hours. Sodium heparin was added as an anticoagulant and blood samples were spun down to collect plasma. The plasma samples were analyzed by LC-MS/MS for vemurafenib content. Pharmacokinetic parameters were determined using Phoenix WinNonlin v7.0 (Certara, Princeton, NJ, USA).

2.3.14 Statistical Analysis:

Statistical analysis of pharmacokinetic parameters was performed using JMP Pro statistical software v13. All data was log transformed to stabilize variance. Data was first assessed for normality by Goodness of Fit (Shapiro-Wilk W Test). The non-parametric Kruskal-Wallis test was used to detect the presence of a statistically significant difference between the 3 samples for Cmax, AUC0→24, and AUC0→∞. When a difference was detected, a post-hoc multiple comparisons procedure Dunn's test with the MBP sample as the control was used to check for differences against the KSD materials. Alpha level of 0.05 was used for all tests.

2.4 RESULTS

2.4.1 MBP and KSD Processing

MBP material was made per the methodology described above and that provided by Shah et al. (4) Visual observations of the process conform to the images presented in additional work by Shah et al. describing the process with additional molecules. (34) Sample yields of fully processed and milled material ranged from 70-80%. MBP moisture content was measured to be 2.76% by loss on drying.

Sample was prepared by the KinetiSol process and the processing profile is seen in Figure 2.3. The total processing time for the run was 11.4 seconds. A 90 gram batch size was used for the process with a process yield of 91%.

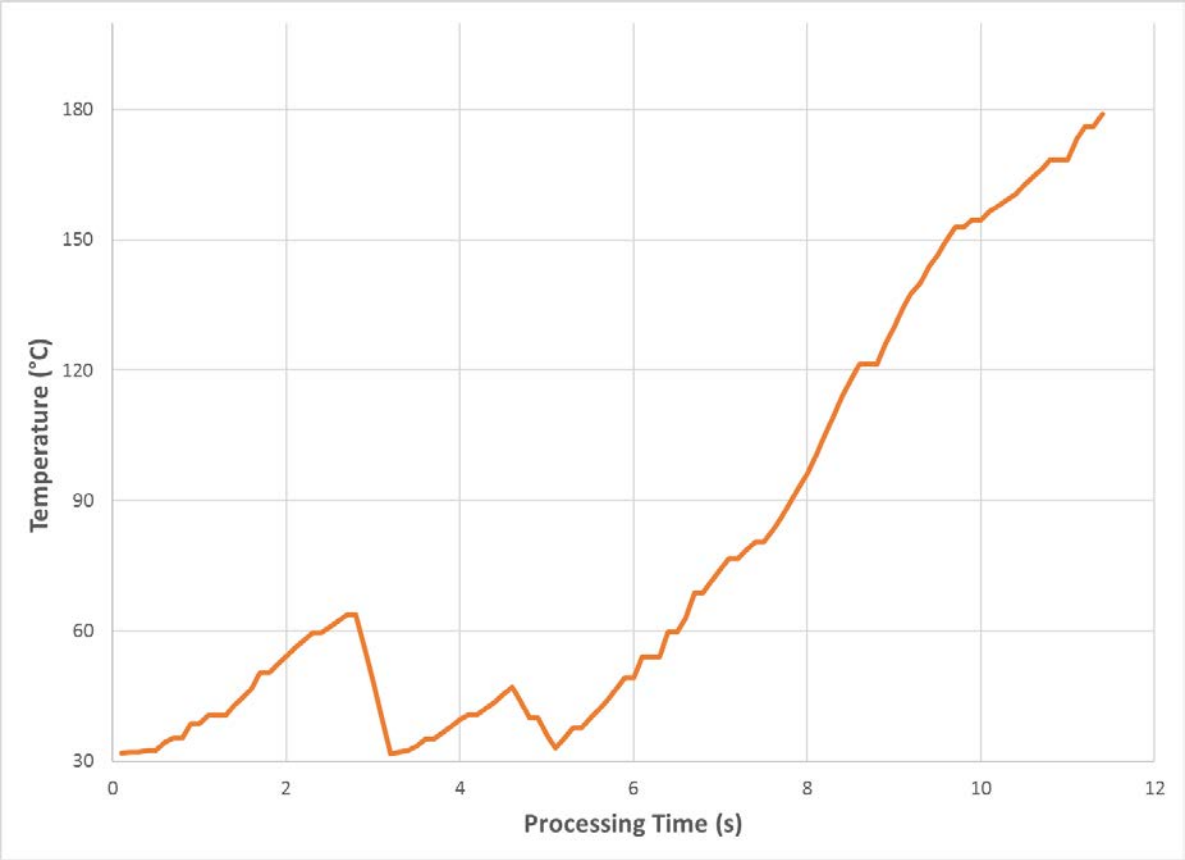

Figure 2.3: KinetiSol profile for processing an amorphous solid dispersion of vemurafenib at 2400 rpm

Sample milled in the IKA mill and passed through a 250 µm screen was labeled KSD <250 µm and sample milled in the cryomill was labeled KSD Cryo.

2.4.2 Solid State Characterization, Physical Stability, and Chemical Purity:

MBP and KSD material were analyzed by XRPD and overlaid with neat vemurafenib API. An overlay of the scans is shown in Figure 2.4. Crystalline vemurafenib had major peaks at 2theta

values of 9.3, 15.2, 19.3, and 24.6. No peaks related to crystalline vemurafenib, or of any kind, were detected by XRPD.

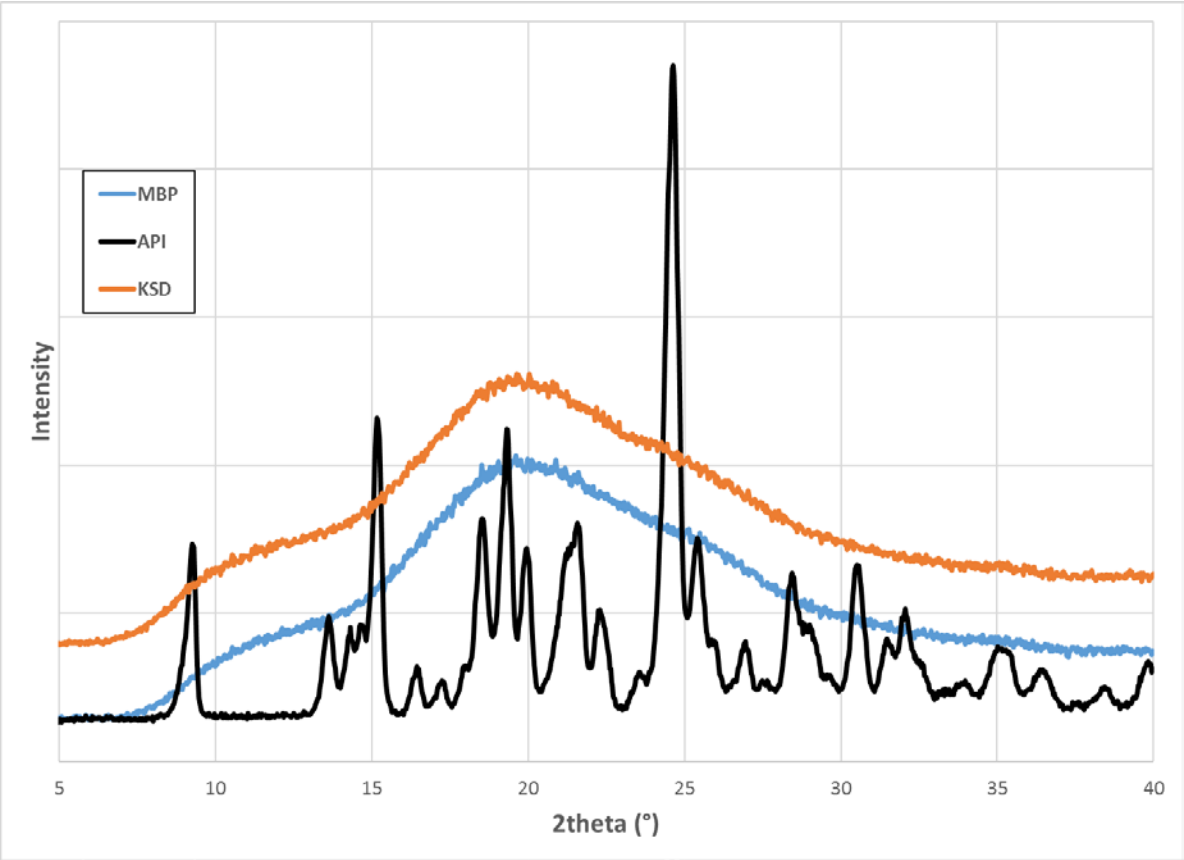

Figure 2.4: XRPD of neat vemurafenib, MBP, and KSD material (Scans are translated along the y-axis to aid in differentiation).

MBP and KSD materials were analyzed by mDSC and the reversing heat flow thermograms and are depicted in Figure 2.5. The glass transition temperature (Tg) was determined for MBP, KSD <250 µm, and KSD Cryo as 98.96°C, 99.15°C, and 101.10°C, respectively.

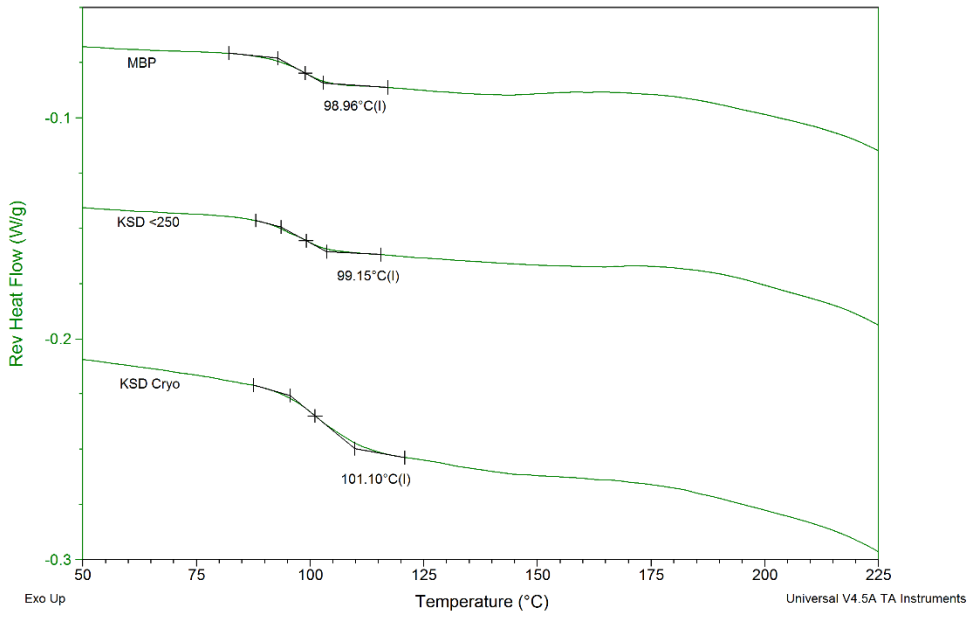

Figure 2.5: Reversing heat flow thermograms for modulated differential scanning calorimetry of KSD and MBP materials.

XPRD sample holders containing amorphous vemurafenib material were stored at 40°C/75% R.H. and were tested by the XPRD method at 0, 1, and 3 months. An overlay of the scans is shown in Figure 2.6. Scans are translated along the y-axis to aid in comparison.

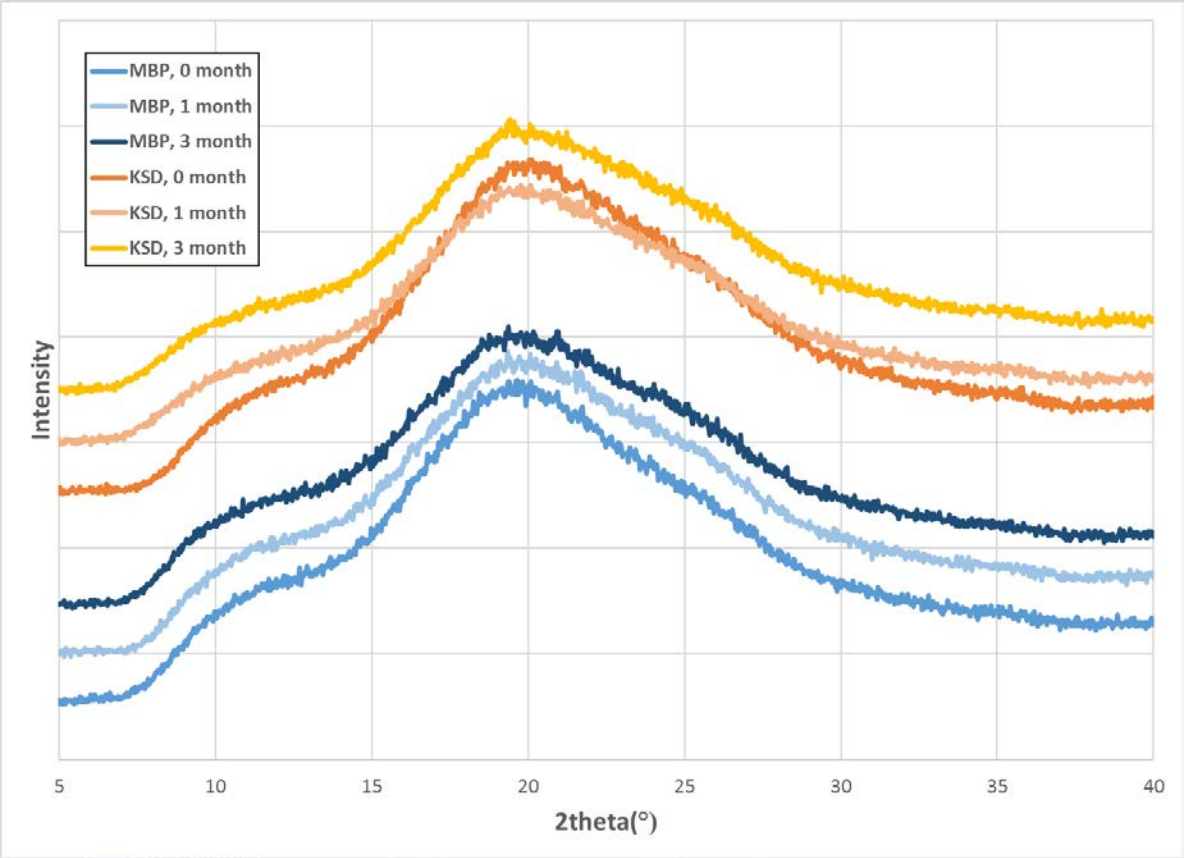

Figure 2.6: XRPD of stability samples stored at 40°C/75% R.H. for 0, 1, and 3 months in open container (Scans are translated along the y-axis to aid in differentiation).

Neat vemurafenib API, MBP and KSD samples were analyzed for purity based on % area by HPLC. The total % impurities for the neat API was 99.0%, MBP was 98.9%, and KSD was 98.9%.

2.4.3 Particle Morphology:

MBP and KSD samples were imaged for surface structure by SEM. The images are shown in Figure 2.7. Figure 2.7.a depicts a MBP particle which appeared to be solid particle with interconnected void space opening to the surface of the particle, similar to the spongy network structure as described by Shah et al. (4). This structure was observed across all MBP particles examined. Figure 2.7.b shows the KSD cryo material which contains a range of small particles sizes. These particles have smooth surfaces of uniform density without any visible pores. Figure 2.7.c is the outer surface of a large KSD <250 µm particle. On this outer surface, two large exposed pores are observed, but the rest of the material is uniform and smooth in appearance. In Figure 2.7.d, the upper right region contains an image of the cross-section of the quenched, but unmilled KSD sample at significantly lower magnification the other images. In this cross-section, many large, porous cavities are visible in the otherwise uniform mass. These cavities tended to aggregate near the edge of the cross-section.

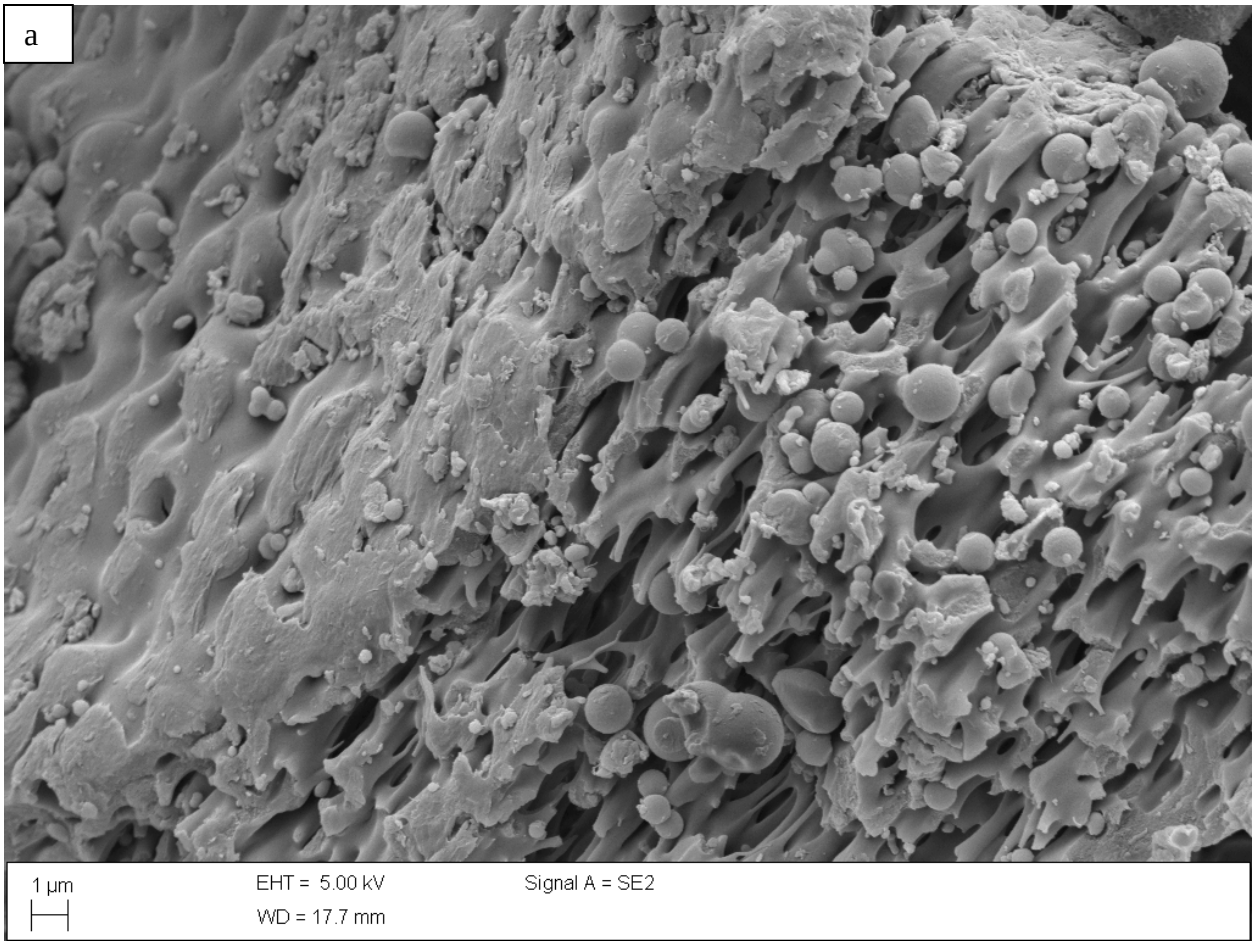

Figure 2.7: Scanning Electron Microscopy images of MBP and KSD materials for a. MBP material, b. KSD cryomilled material, c. KSD material, < 250 µm. Dark circles are large cavities as observed in the cross section of Figure 2.7.d, and d. c.

Unmilled cross section of quenched KSD material (upper right region, lower left region is carbon tape).

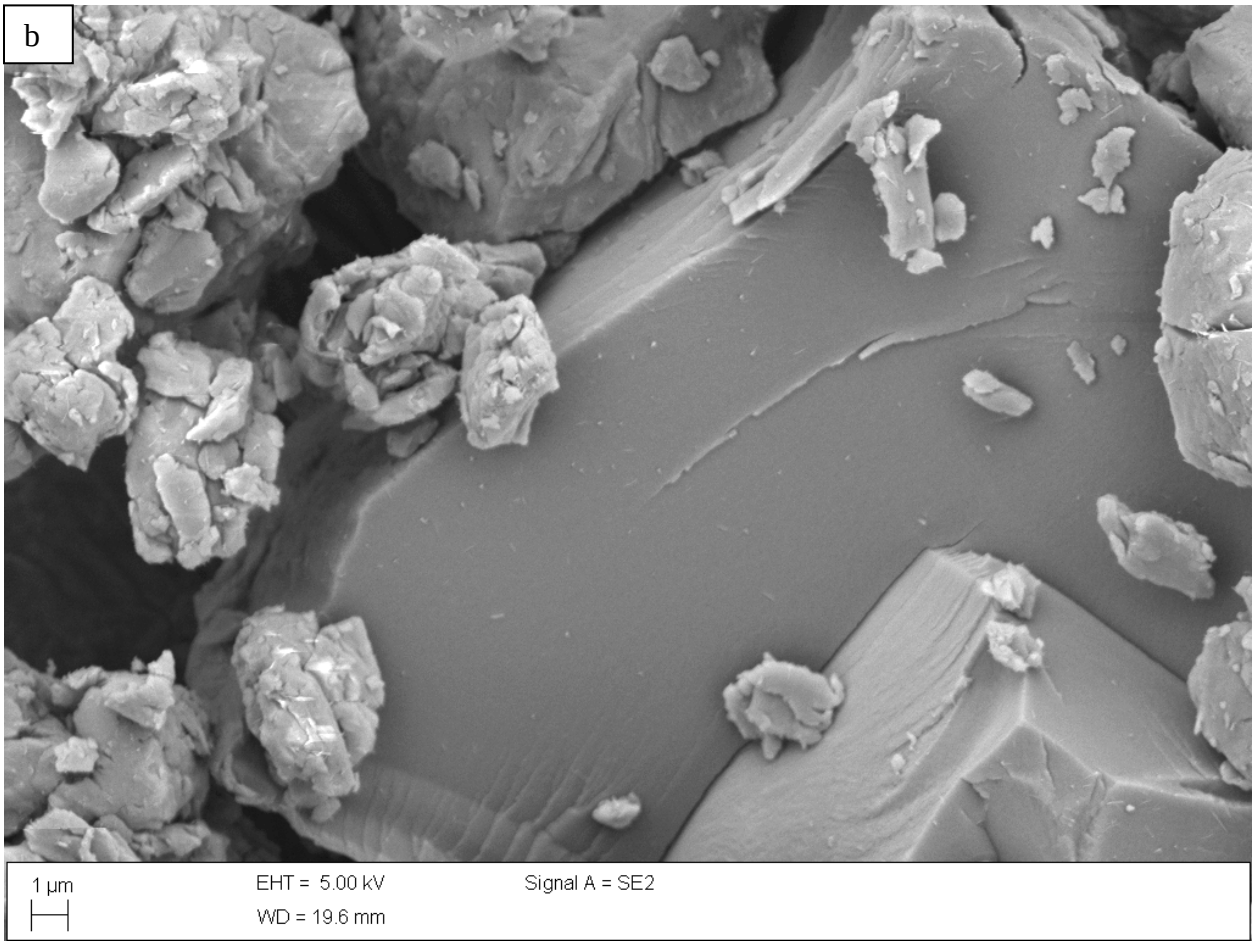

Figure 2.7, cont.

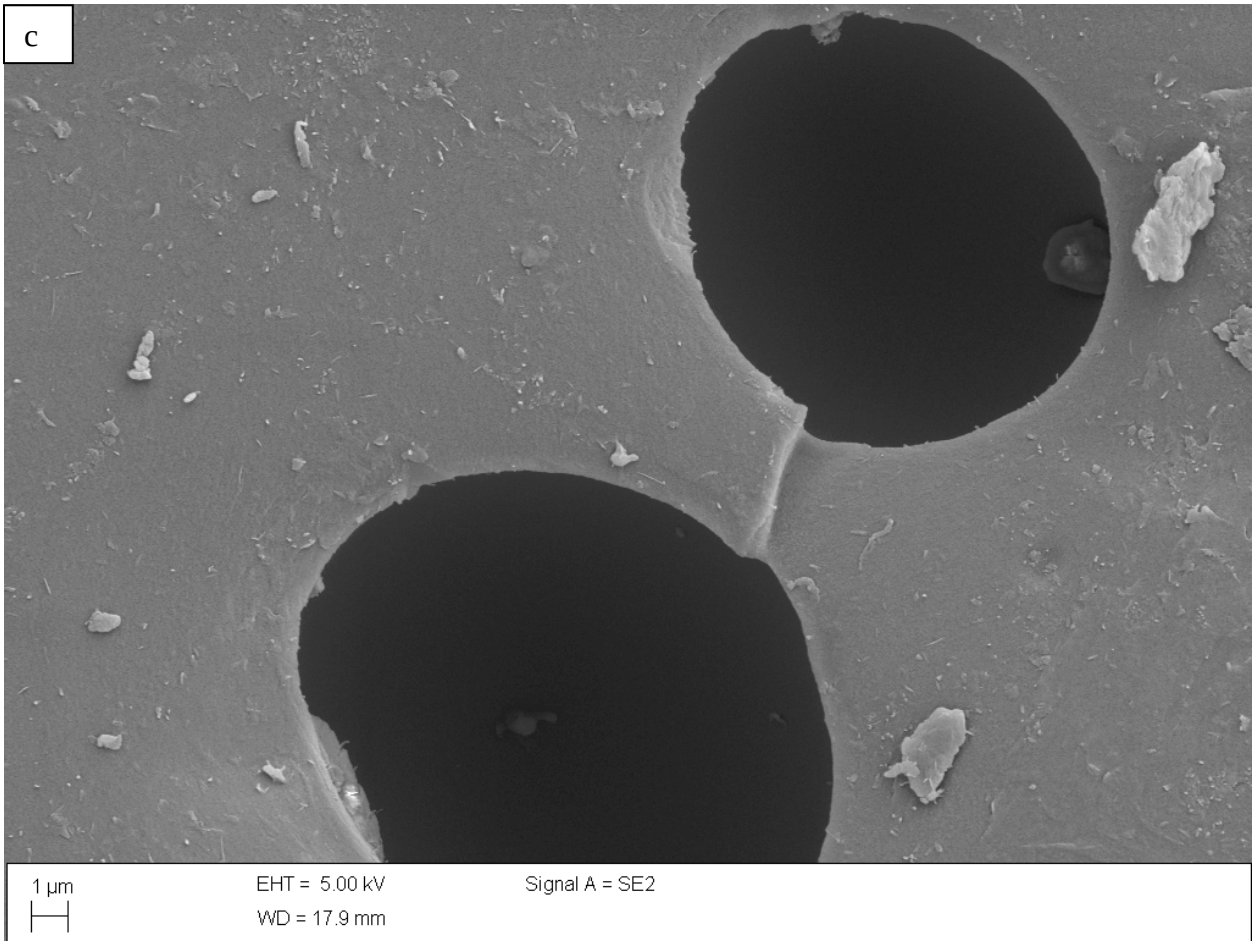

Figure 2.7, cont.

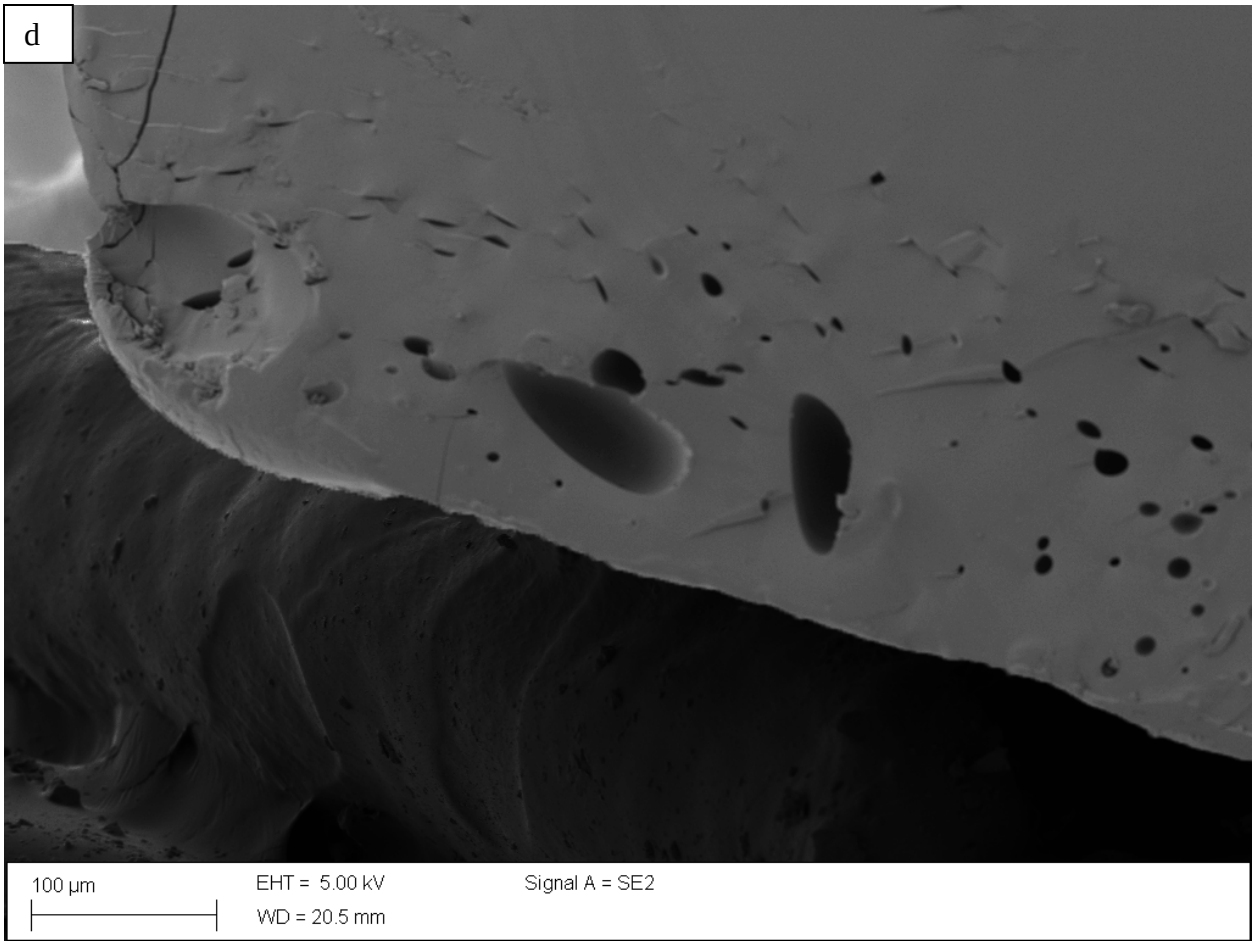

Figure 2.7, cont.

The D10, D50, and D90 values for particle size distribution are shown in Table 2.4. Specific surface areas are also listed. For the KSD <250 material, the surface area was below the limit of quantitation at 200 mg so the sample size was adjusted to 1 gram for sufficient material to measure surface area.

Sample	D10 (µm)	D50 (µm)	D90 (µm)	Specific Surface Area (m2/g)
MBP	2.39 ± 0.13	74.14 ± 1.68	220.90 ± 5.65	6.13 ± 0.05
KSD <250	14.02 ± 0.84	132.74 ± 3.43	300.79 ± 2.62	0.20 ± 0.02
KSD Cryo	2.14 ± 0.23	12.94 ± 1.42	78.96 ± 3.43	1.21 ± 0.06

Table 2.4: Particle size distribution and specific surface area for MBP and KSD amorphous solid dispersions of vemurafenib

2.4.4 In-Vitro Dissolution Testing:

Dissolution testing was conducted on MBP, KSD <250 µm, KSD Cryo and physical mixture material that was hand-filled into capsules so that each capsule contained 40 mg of vemurafenib API per capsule. Dissolution profiles are shown in Figure 2.8. The MBP and KSD Cryo materials had similar initial release rates although the MBP released to a Cmax,diss of 74.4 µg/mL at a tmax,diss of 3 hours, while the KSD Cryo material reached a Cmax,diss of 71.4 µg/mL at a tmax,diss of 6 hours. However, vemurafenib from the MBP material precipitated at a faster rate than the KSD Cryo sample and had less drug in solution by the 5-hour time point. Meanwhile, the KSD <250 µm material released drug at a slower rate reaching a Cmax,diss value of 54.0 µg/mL at a tmax,diss of 16 hours. For hours 14 through 24, the KSD <250 sample had more drug dissolved in solution than either the MBP or KSD Cryo material. The KSD <250

µm was visually less turbid than the MBP or KSD Cryo vessels and this scattering was reflected in the UV profiles collected by the fiber optic probes. The physical mixture only had minimally detectable drug level in solution throughout the duration of the dissolution test.

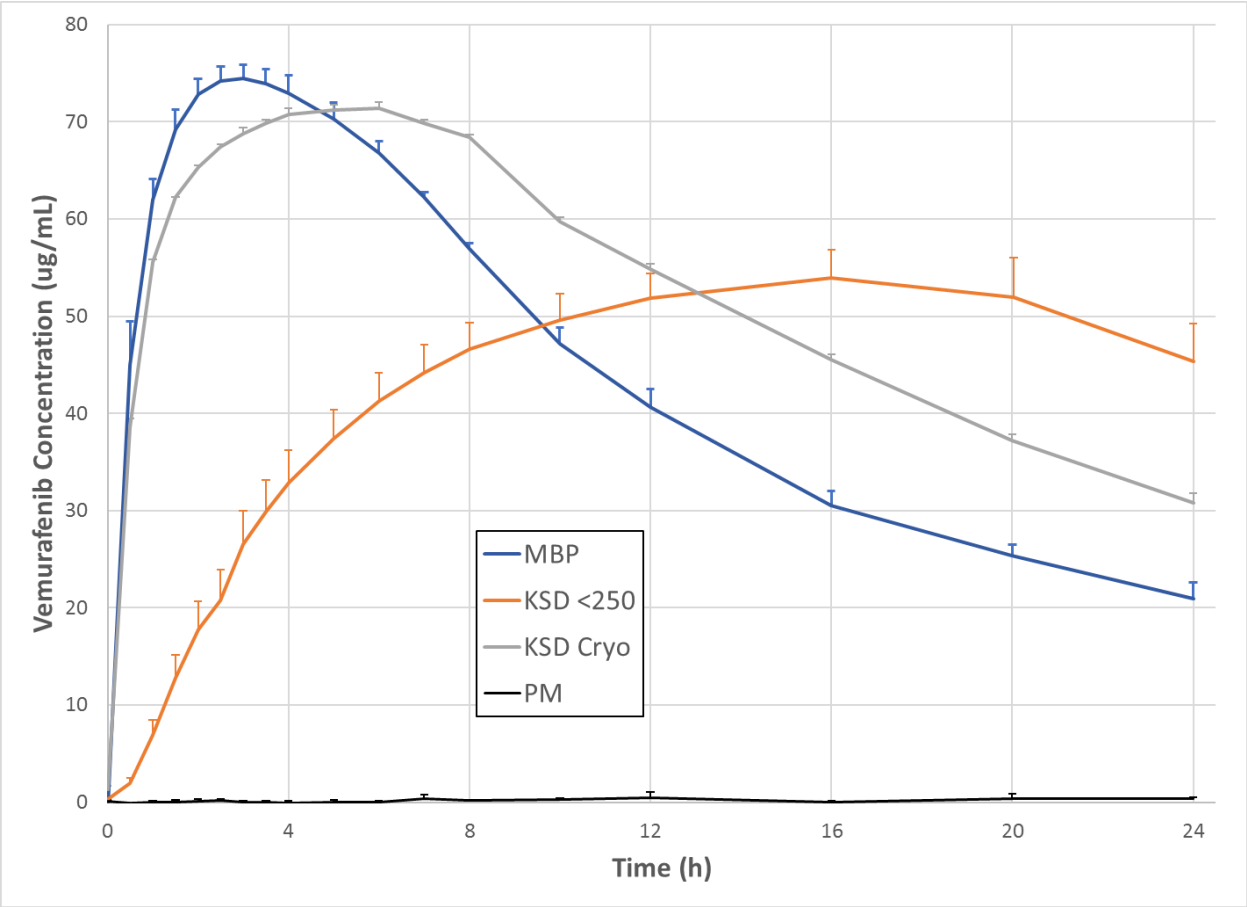

Figure 2.8: In-vitro dissolution of MBP and KSD amorphous solid dispersions and physical mixture of vemurafenib in pH 6.5 FaSSIF media

2.4.5 Pharmacokinetic Testing in Rats:

Figure 2.9 shows the plasma concentration levels of vemurafenib dosed by oral gavage of vemurafenib suspensions in fasted male Sprague-Dawley rats. Both KSD samples exhibited a higher Cmax than the MBP material and maintained higher plasma levels than MBP for 24 hours. Specifically, the average KSD Cryo value was higher than the average MBP value at each time point.

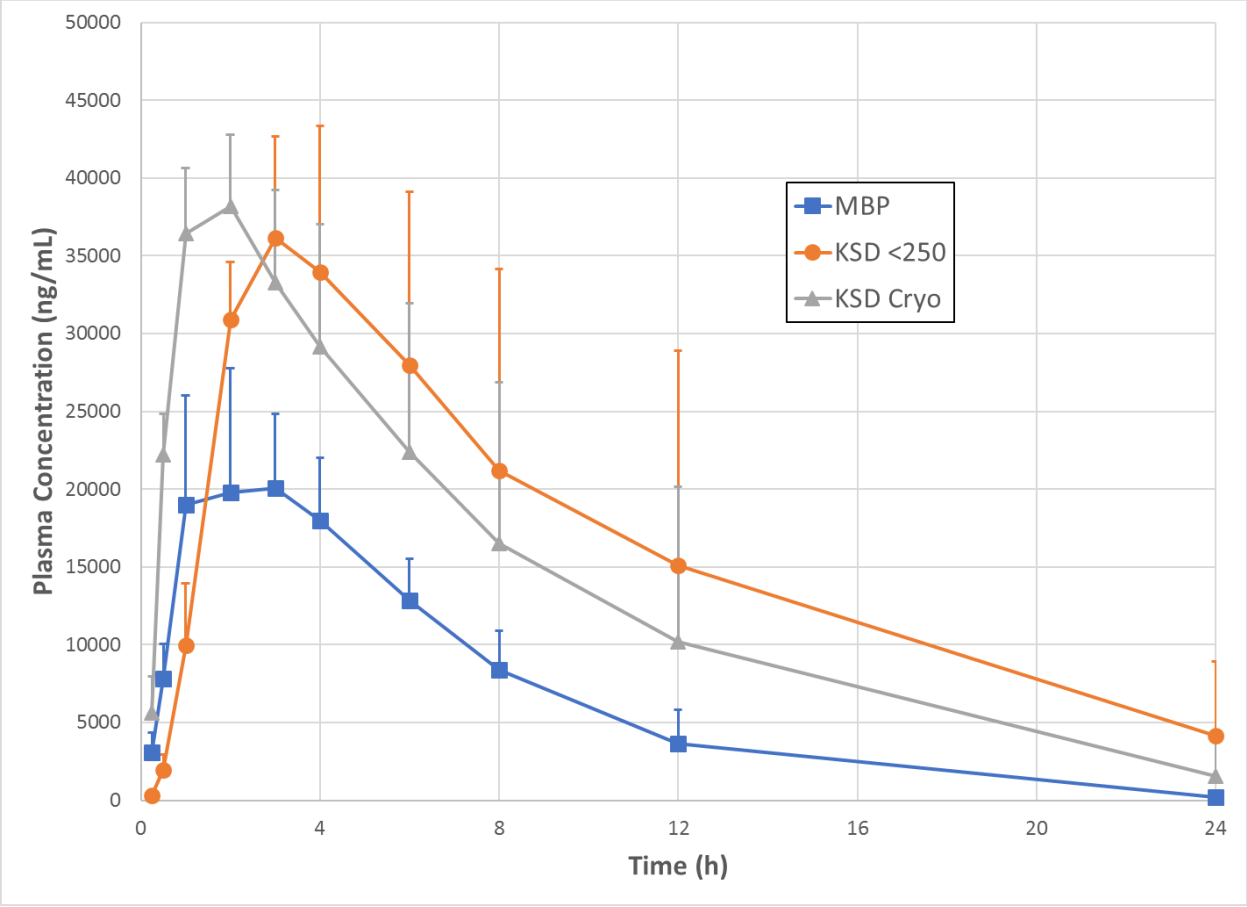

Figure 2.9: Vemurafenib plasma concentration in male Sprague-Dawley rats after oral administration of suspensions with target dosing of 25 mg/kg

Table 2.5 summarizes the calculated pharmacokinetic parameters from the plasma concentration data. Both KSD <250 and KSD Cryo materials had approximately 2-times the Cmax over MBP. The MBP material had a relative standard deviation (%RSD) of 24% which was similar to the KSD <250 material's %RSD of 20% while the KSD Cryo material had half the variability at 12%. For AUC, both KSD samples exhibited approximately 2.5-times the dose-normalized AUC value as compared to MBP. In this case, the % RSD was 29% for MBP, 63% for KSD <250, and 56% for KSD Cryo. For the KSD Cryo sample, dose-normalized AUC was calculated with the administered dose of 21.9 mg/kg. tmax was similar for MBP and KSD Cryo at 2.0 and 1.8 hours respectively but KSD <250 µm material had a tmax that was delayed until 3.5 hours.

Sample	MBP	KSD, <250 µm	KSD, Cryo
Dose (mg/kg)	25	25	20.9*
tmax (h)	2.0 ± 0.8	3.5 ± 0.6	1.8 ± 0.5
Cmax (ng/mL)	21,750 ± 5,171	37,250 ± 7,556	38,375 ± 4,492
Average Dose-normalized AUC0→∞ (hr·kg·ng/mL/mg)	6,661 ± 1,910	17,607 ± 11,060	16,738 ± 9,340

Table 2.5: Summary of calculated PK values for oral administration of MBP and KSD amorphous solid dispersions of vemurafenib in male Sprague-Dawley rats. *Suspension inadvertently dosed at 20.9 mg/kg instead of target 25 mg/kg.

Statistical results for MBP and KSD Cryo AUC parameters were found to be non-normally distributed, p-values: 0.033 and 0.031, respectively for AUC0→24 and 0.033 and 0.029 AUC0→∞. A statistically significant difference was not detected for either AUC parameter. A statistically significant difference was detected by the Kruskal-Wallis test for Cmax (p-value 0.039). However, when MBP was compared to KSD <250 and KSD Cryo, no specific statistical difference was detected (0.079 and 0.062).

2.5 DISCUSSION

2.5.1 Solid State and Chemical Purity:

The XPRD data in Figure 2.4 exhibits no crystalline peaks in either the MBP or KSD materials. Specifically, the diffractogram for both dispersions is absent the crystalline 2-theta (°) peaks that are associated with vemurafenib crystallinity as observed in the XPRD diffractogram of the neat API. This indicates that the materially has been rendered substantially amorphous by both processes. DSC could not verify the absence of crystalline vemurafenib as its melting point of 272°C exceeded the degradation onset of 204°C for HPMCAS (28) and polymer degradation events dominated the thermogram in the drug melting point region. However, mDSC was used for all amorphous solid dispersion samples to show a single Tg occurred at 99-101°C. The reversing heat flow thermograms are shown in Figure 2.5. These Tg values are consistent with the value obtained by Shah et al. for this MBP formulation, (4) indicating that the amorphous dispersions represent a single phase system with homogenous mixing of the drug and polymer. (42) Stability of the amorphous form is likely sufficient for both dispersions in light of literature recommending that samples be stored at least 50°C below the Tg of the system. (43, 44) This may allow storage of the amorphous dispersions up to ~48°C, which exceeds the typical accelerated storage condition of 40°C. In Figure 2.6, the stability data collected for MBP and KSD material showed no indication of crystallization peaks after 3 months at accelerated conditions in open container storage. The stable results show promise for the physical stability of the amorphous dispersions.

Comparison of the chemical purity of the amorphous dispersions to neat API indicates that vemurafenib undergoes minimal to no degradation when processed by both solvent-controlled coprecipitation and KinetiSol. MBP and KSD materials both had purity values 0.1% lower than neat API. These data demonstrated that KinetiSol can generate an amorphous solid dispersion of vemurafenib with a similar drug impurity profile to the solvent-controlled coprecipitation process utilized in manufacturing the commercial product.

2.5.2 Particle morphology

Based on the appearance of the resulting materials, it was suspected that differences in particle morphology exists between the two materials. The MBP material appeared sponge-like with a matrix of pores throughout the particles, similar to that described by Shah et al. (4). By contrast, the KinetiSol material appeared denser with no visible pores and was brittle when bent or compressed. The SEM images shown in Figure 2.7 confirm these observations. In Figure 2.7.a, the MBP material appears sponge-like with pores and channels running throughout the material, similar to images presented by Shah et al. (4) Based on this observation, it is expected that the sample exhibits high surface area on a mass basis and, per the Noyes-Whitney equation, a rapid drug dissolution rate. By contrast, the KSD materials both showed particles that lacked extensive pore networks with outer surface tending to be exposed. However, in the cross section shown in Figure 2.7.d., small pores were exposed near the edge when the quenched material was broken into smaller fragments. These observations are consistent with results previously observed by LaFountaine et al. with griseofulvin amorphous solid dispersion made by KinetiSol with hypromellose and povidone polymers. (45) These pores are sufficiently large that they were

completely eliminated by particle size reduction in the KSD Cryo samples and few remained in the larger KSD <250 particles. These pores are likely a function of the quenching processing causing entrapped air in the molten mass to be pressed towards the edges of the material. The outermost layers of the quenched sample were in direct contact with chilled plates and temperature likely decreased below the glass transition of the mass before the entrapped air reached this region. This caused the boundary to solidify before the entrapped air escaped, thus creating pores. It is plausible that control of these entrapped air pockets could be used to increase the surface area and modulate release properties of KSD materials with manipulation of the quench step of the process being a primary driver for this modification. However, this was beyond the scope of this study and was not explored further here.

The MBP, KSD <250, and KSD Cryo samples were milled to different particle sizes to investigate the effect of particle size on dissolution properties of the different materials. In a previous review by Huang and Williams, it was reported that for fusion-processed materials like KSD, milling is a significant contributor to surface area and release rate, whereas for porous materials like MBP and spray-dried dispersions, the pores were the primary driver of release rate with reduced impact from milling. (46) By particle size analysis, the MBP material had a D50 value of 74 µm and a D90 value of 221 µm. These values are in agreement with the D50 and D90 reported for milled MBP material of 60 µm and 220 µm, respectively. (4) The KSD Cryo material was predominantly fines with a D10 value similar to MBP at approximately 2 µm, but with a D50 of 14 µm, which was 20% of the measured D50 value for MBP. The D90 value of 79 µm was similar to the average diameter of a MBP particle. From this data and knowledge of particle appearances, the expectation was that reducing the KSD material particle size via cryo-

milling would result in a KSD sample with similar surface area to the MBP material. To test for this, analysis with Brunauer-Emmett-Teller (BET) theory was used to verify the surface area difference between the amorphous dispersions. (47, 48) Table 2.4 shows that MBP material had a specific surface area of approximately 6.1 m2/g which agreed with reported values for MBP particles of 6.2 m2/g. (49) This is compared to the KSD Cryo sample's specific surface area of approximately 1.2 m2/g. Despite an approximate 5-fold decrease in median particle size for the KSD Cryo material relative the MBP material, an approximately 5-fold increase in specific surface area was observed in the opposite direction of expectation based on particle diameter. Conventional evaluation of the Noyes Whitney equation indicates that the MBP material should release at approximately 5 times the rate of the KSD Cryo material. However, it is important to note that a substantial portion of the surface are of the MBP material is contained within the inner network of the material. Porous materials have been shown to have a dissolution rate slower than predicted by the Noyes-Whitney equation. (50) Studies conducted by Korsmeyer et al. and Cardamone et al. demonstrated that during dissolution, polymer dissolved and saturated the inner channels of a porous material which created viscous media in these channels for which drug dissolution was significantly slowed. (51, 52) Thus, despite MBP's high specific surface area, it was hypothesized that much of the gains in surface area are negated by this phenomenon. By contrast, the KSD <250 material was found to have a specific surface area of 0.2 m2/g. This surface area is congruent with results obtained by Dong et al. on similarly milled fusion-based material. (49) The expectation is that these particles can exhibit delayed release as compared to the MBP and KSD Cryo materials.

2.5.3 In-vitro and in-vivo performance testing

In-vitro dissolution analysis of the samples revealed interesting and unexpected results. First, it should be noted that a physical mixture of vemurafenib with HPMCAS-L exhibited almost no drug dissolution with the maximal observed concentration of 1.13 ± 0.14 µg/mL. This makes apparent the need for a solubility enhanced formulation of vemurafenib. The MBP and KSD Cryo material had very similar initial dissolution rates but the MBP material reached maximum release before the KSD Cryo material (tmax,diss 3 hours versus tmax,diss 6 hours). By contrast, the KSD <250 showed extended release properties in this dissolution media with a mean tmax,diss of 16 hours. This supports the theory posited by Huang and Williams that particle properties and release rate for fusion processed material can be modulated by post-processing milling conditions. (46) However, MBP material precipitated at a faster rate and to a greater extent than the KSD materials. An explanation for MBP's higher rate of precipitation is that within the interior of the particles, vemurafenib dissolved to saturation or supersaturation levels and remained at those levels due to lack of fluid exchange with bulk dissolution media. This lack of fluid exchange occurred because there was increased viscosity within the inner particle channels due to concurrent polymer dissolution as described by Korsmeyer et al. (51) In this microenvironment formed within the interior structure of the particle, vemurafenib was in contact with saturated or supersaturated media and the risk of recrystallization of undissolved vemurafenib increased. Additionally, in this microenvironment, supersaturated drug was susceptible to precipitation. Brouwers et al. described the following equation for the nucleation rate, Jn, of drug from solution:

$$J_n = N_0\, v \exp\left(\frac{-16\pi v^2 \gamma_{ns}^3}{3(k_b T)^3 (\ln(S))^2}\right)$$

as a function of N0, the number of molecules per unit volume, υ, the frequency of atomic vibration, γns, the surface energy of the boundary, kb, the Boltzmann's constant, T, the temperature, and S, the ratio of the drug concentration in solution to its equilibrium concentration. From this equation, a direct relationship exists between increases in the supersaturation ratio and resulting increases in the rate of nucleation. Once in bulk solution, these initial precipitates serve as sites for crystal growth with the greater number of nucleated particles in the MBP material resulting in increased precipitation rate. (53) By contrast, the KSD particles do not contain similar channels in which supersaturation can occur. Instead, the particles are expected to follow Noyes-Whitney behavior with drug diffusing away from the surface of the particle into bulk solution, thus minimizing localized supersaturation and nucleation risk. Based on the precipitation rate findings in this in-vitro study, in-vivo performance is expected to favor the KSD materials over the MBP particles.

The observations from the in-vitro dissolution work were consistent with the results of the male Sprague-Dawley rat study. The mean AUC0→∞ values were approximately 2 and 2.5 times larger than MBP for the KSD Cryo and KSD <250 samples respectively with approximately double Cmax for both samples as well. In addition, the KSD samples exhibited reduced Cmax variability compared to MBP, especially in the case of the KSD Cryo material. However, contrary to expectation, the opposite was true for AUC with substantially increased variability in the KSD groups. Rats are known to have variable gastrointestinal transit times with colon arrival time occurring from approximately 6 to 16 hours in the fasted rat model. (54) For all dosed samples, tmax occurred earlier than the minimum gastrointestinal transit time, which means that Cmax was not impacted by gastrointestinal transit time. For MBP, the variability in Cmax and

AUC were in agreement (24% and 29%, respectively), which suggests that variability in rat gastrointestinal transit time did not impact this dose as absorption was completed by the time variable transit time was a concern. The observed in-vitro precipitation corroborates this conclusion as MBP's increased precipitation negatively impacted drug absorption in rats with longer transit times as the amount of available drug to permeate was reduced. By contrast, the substantial increase in AUC variability in KSD <250 and KSD Cryo (63% and 56%, respectively) indicates that vemurafenib continued to be absorbed as the gastrointestinal transit time variability became a factor. Thus, the vemurafenib samples made by KinetiSol not only released to a greater maximal amount as exhibited by Cmax but also demonstrated behavior that correlates to prolonged absorption of the drug as compared to the MBP material. Additionally, it is important to note that the KSD Cryo sample was inadvertently dosed subpotently at 21.9 mg/kg instead of the intended 25.0 mg/kg. Despite this lower dosing amount, its mean AUC approximately doubled the AUC of the comparator MBP material and had the highest overall Cmax of the test articles. Given these results, if translatable to humans, the data suggest that this formulation produced by KinetiSol can reduce patient dosing from 4 tablets to 2 tablets at each dosing event. For the KSD Cryo and MBP materials, the initial similar release rate observed by in-vitro dissolution showed good correlation in the tmax pharmacokinetic values with the materials exhibiting maximal values at 1.8 and 2.0 hours respectively. However, the in-vitro dissolution method was a poor predictor of release rate for the KSD 250 material that had a tmax,diss of 16 hours by in-vitro dissolution, but an in-vivo tmax of 3.5 hours. A statistically significant difference was identified for Cmax per the Kruskal-Wallis test, but a multiple comparisons procedure Dunn's test was not able to determine which specific formulations were statistically different. The Dunn's test p-values for Cmax of MBP vs. KSD 250 and Cryo were

0.07 and 0.06, respectively. No differences were detected in AUC. The root cause for this was likely due to variance in the results as the rat PK study wasn't designed to have sufficient statistical power.

Data for in-vitro dissolution and in-vivo pharmacokinetic testing demonstrated that, for the same formulation, KinetiSol produced a superior product relative to the MBP material from the solvent-controlled coprecipitation method. Beyond the processing improvement imparted by KinetiSol, it is important to note that KinetiSol has also shown that it expands the formulation space for vemurafenib and allows the processing with non-ionic polymers and surfactants previously restricted by the solvent-controlled coprecipitation process. (55) The non-ionic polymers may improve drug absorption in the proximal small intestine over the enteric carrier studied in this paper, and the surfactant component can also aid in enhancing drug dissolution and equilibrium solubility. (56) Coupling the KinetiSol processing gains demonstrated in this study with this expanded formulation space opens the opportunity for a significantly improved vemurafenib drug product with substantially reduced pill burden. Current investigations into vemurafenib combination products for the treatment of advanced melanoma (57-59) represent a growing area of interest that benefits from the gains derived from KinetiSol processing and formulation space expansion.

2.6 CONCLUSION

This study found that KinetiSol processing produced vemurafenib amorphous solid dispersion material with similar purity and solid-state properties (amorphous and single-phase) as the

solvent-controlled coprecipitation process MBP. However, distinct differences were observed in the morphology of the particles produced by each of the processes with the KinetiSol generated materials representing dense particles without pores while the MBP material had significantly elevated surface area. These morphology differences resulted in intraparticle precipitation and subsequently more extensive precipitation of drug from the comparator MBP material. By comparison, the KSD particles exhibited reduced precipitation which led to improved dissolution and pharmacokinetic performance. Thus, KinetiSol produced a superior product that enhanced the delivery of the challenging vemurafenib molecule.

2.7 REFERENCES

1. Bollag G, Tsai J, Zhang J, Zhang C, Ibrahim P, Nolop K, et al. Vemurafenib: the first drug approved for BRAF-mutant cancer. Nature reviews Drug discovery. 2012;11(11):873.

2. Budha N, Frymoyer A, Smelick G, Jin J, Yago M, Dresser M, et al. Drug Absorption Interactions Between Oral Targeted Anticancer Agents and PPIs: Is pH-Dependent Solubility the Achilles Heel of Targeted Therapy? Clinical Pharmacology & Therapeutics. 2012;92(2):203-13.

3. Schilling B, Sucker A, Griewank K, Zhao F, Weide B, Görgens A, et al. Vemurafenib reverses immunosuppression by myeloid derived suppressor cells. International journal of cancer. 2013;133(7):1653-63.

4. Shah N, Iyer RM, Mair HJ, Choi DS, Tian H, Diodone R, et al. Improved human bioavailability of vemurafenib, a practically insoluble drug, using an amorphous polymer-stabilized solid dispersion prepared by a solvent-controlled coprecipitation process. Journal of pharmaceutical sciences. 2013;102(3):967-81.

5. Dahan A, Miller JM, Amidon GL. Prediction of solubility and permeability class membership: provisional BCS classification of the world's top oral drugs. The AAPS journal. 2009;11(4):740-6.

6. Amidon GL, Lennernäs H, Shah VP, Crison JR. A theoretical basis for a biopharmaceutic drug classification: the correlation of in vitro drug product dissolution and in vivo bioavailability. Pharmaceutical research. 1995;12(3):413-20.

7. Zelboraf® Tablets, Roche 2011 [cited FDA. Available from: https://www.accessdata.fda.gov/drugsatfda_docs/nda/2011/202429Orig1s000ClinPharmR.pdf.

8. Bergström CA, Charman WN, Porter CJ. Computational prediction of formulation strategies for beyond-rule-of-5 compounds. Advanced drug delivery reviews. 2016;101:6-21.

9. He Y, Ho C. Amorphous solid dispersions: utilization and challenges in drug discovery and development. Journal of pharmaceutical sciences. 2015;104(10):3237-58.

10. Goldinger SM, Rinderknecht J, Dummer R, Kuhn FP, Yang KH, Lee L, et al. A single-dose mass balance and metabolite-profiling study of vemurafenib in patients with metastatic melanoma. Pharmacology research & perspectives. 2015;3(2).

11. Mosharraf M, Nyström C. The effect of particle size and shape on the surface specific dissolution rate of microsized practically insoluble drugs. International Journal of Pharmaceutics. 1995;122(1-2):35-47.

12. Dokoumetzidis A, Macheras P. A century of dissolution research: from Noyes and Whitney to the biopharmaceutics classification system. International journal of pharmaceutics. 2006;321(1):1-11.

13. Brough C, Williams Iii RO. Amorphous solid dispersions and nano-crystal technologies for poorly water-soluble drug delivery. International Journal of Pharmaceutics. 2013;453(1):157-66.

14. Kalepu S, Manthina M, Padavala V. Oral lipid-based drug delivery systems–an overview. Acta Pharmaceutica Sinica B. 2013;3(6):361-72.

15. Fricker G, Kromp T, Wendel A, Blume A, Zirkel J, Rebmann H, et al. Phospholipids and lipid-based formulations in oral drug delivery. Pharmaceutical research. 2010;27(8):1469-86.

16. Xi N, Zhang Y, Wang Z, Lin T, Wang Q. Vemurafenib prodrugs suitable for oral and IV administration. AACR; 2014.

17. Horbert R, Pinchuk B, Davies P, Alessi D, Peifer C. Photoactivatable prodrugs of antimelanoma agent vemurafenib. ACS chemical biology. 2015;10(9):2099-107.

18. Vo CL-N, Park C, Lee B-J. Current trends and future perspectives of solid dispersions containing poorly water-soluble drugs. European journal of pharmaceutics and biopharmaceutics. 2013;85(3):799-813.

19. Benet LZ, Wu C-Y, Custodio JM. Predicting drug absorption and the effects of food on oral bioavailability. Bulletin Technique Gattefosse. 2006;99:9-16.

20. Van den Mooter G. The use of amorphous solid dispersions: A formulation strategy to overcome poor solubility and dissolution rate. Drug Discovery Today: Technologies. 2012;9(2):e79-e85.

21. Serajuddin A. Solid dispersion of poorly water-soluble drugs: Early promises, subsequent problems, and recent breakthroughs. Journal of pharmaceutical sciences. 1999;88(10):1058-66.

22. Miller DA, Ellenberger D, Gil M. Spray-Drying Technology. Formulating Poorly Water Soluble Drugs: Springer; 2016. p. 437-525.

23. Paudel A, Worku ZA, Meeus J, Guns S, Van den Mooter G. Manufacturing of solid dispersions of poorly water soluble drugs by spray drying: formulation and process considerations. International journal of pharmaceutics. 2013;453(1):253-84.

24. Gu S, Cai R, Luo T, Chen Z, Sun M, Liu Y, et al. A Soluble and Highly Conductive Ionomer for High-Performance Hydroxide Exchange Membrane Fuel Cells. Angewandte Chemie International Edition. 2009;48(35):6499-502.

25. Witschi C, Doelker E. Residual solvents in pharmaceutical products: acceptable limits, influences on physicochemical properties, analytical methods and documented values. European Journal of Pharmaceutics and Biopharmaceutics. 1997;43(3):215-42.

26. Haser A, DiNunzio JC, Martin C, McGinity JW, Zhang F. Melt Extrusion. Formulating Poorly Water Soluble Drugs: Springer; 2016. p. 383-435.

27. Brown C, DiNunzio J, Eglesia M, Forster S, Lamm M, Lowinger M, et al. Hot-melt extrusion for solid dispersions: composition and design considerations. Amorphous Solid Dispersions: Springer; 2014. p. 197-230.

28. LaFountaine JS, McGinity JW, Williams III RO. Challenges and strategies in thermal processing of amorphous solid dispersions: a review. AAPS PharmSciTech. 2016;17(1):43-55.

29. Curatolo W, Nightingale JA, Herbig SM. Utility of hydroxypropylmethylcellulose acetate succinate (HPMCAS) for initiation and maintenance of drug supersaturation in the GI milieu. Pharmaceutical research. 2009;26(6):1419-31.

30. Sarode AL, Obara S, Tanno FK, Sandhu H, Iyer R, Shah N. Stability assessment of hypromellose acetate succinate (HPMCAS) NF for application in hot melt extrusion (HME). Carbohydrate polymers. 2014;101:146-53.

31. Janssens S, Nagels S, Armas HNd, D'Autry W, Van Schepdael A, Van den Mooter G. Formulation and characterization of ternary solid dispersions made up of Itraconazole and two excipients, TPGS 1000 and PVPVA 64, that were selected based on a supersaturation screening study. European Journal of Pharmaceutics and Biopharmaceutics. 2008;69(1):158-66.

32. Albano AA, Desai D, Dinunzio J, Go Z, Iyer RM, Sandhu HK, et al. Pharmaceutical composition with improved bioavailability for high melting hydrophobic compound. F. Hoffmann-La Roche Ag; 2013.

33. Food and Drug Administration. Center for Drug Evaluation and Research. Clinical Pharmacology and Biopharmaceutics Review (s). 2011;202-429(0).

34. Shah N, Sandhu H, Phuapradit W, Pinal R, Iyer R, Albano A, et al. Development of novel microprecipitated bulk powder (MBP) technology for manufacturing stable amorphous formulations of poorly soluble drugs. International journal of pharmaceutics. 2012;438(1):53-60.

35. Hughey JR, Keen JM, Brough C, Saeger S, McGinity JW. Thermal processing of a poorly water-soluble drug substance exhibiting a high melting point: the utility of KinetiSol® dispersing. International journal of pharmaceutics. 2011;419(1):222-30.

36. Miller DA, Keen JM, Kucera SU, inventors; DisperSol Technologies, LLC, assignee. Formulations of deferasirox and methods of making the same. United States patent application 15/185,888. 2016 Jun 17.

37. Miller DA. Improved oral absorption of poorly water-soluble drugs by advanced solid dispersion systems: University of Texas
2007.

38. DiNunzio JC, Brough C, Hughey JR, Miller DA, Williams RO, McGinity JW. Fusion production of solid dispersions containing a heat-sensitive active ingredient by hot melt extrusion

and Kinetisol® dispersing. European Journal of Pharmaceutics and Biopharmaceutics. 2010;74(2):340-51.

39. Hughey JR, DiNunzio JC, Bennett RC, Brough C, Miller DA, Ma H, et al. Dissolution enhancement of a drug exhibiting thermal and acidic decomposition characteristics by fusion processing: a comparative study of hot melt extrusion and KinetiSol® dispersing. AAPs Pharmscitech. 2010;11(2):760-74.

40. Jain S, Patel N, Lin S. Solubility and dissolution enhancement strategies: current understanding and recent trends. Drug development and industrial pharmacy. 2015;41(6):875-87.

41. Chhabda PJ, Balaji M, Srinivasarao V, Rao KCA. Development and validation of a new simple and stability indicating RP-HPLC method for the determination of vemurafenib in presence of degradant products.

42. Qian F, Huang J, Hussain MA. Drug–polymer solubility and miscibility: stability consideration and practical challenges in amorphous solid dispersion development. Journal of pharmaceutical sciences. 2010;99(7):2941-7.

43. Hancock BC, Shamblin SL, Zografi G. Molecular mobility of amorphous pharmaceutical solids below their glass transition temperatures. Pharmaceutical research. 1995;12(6):799-806.

44. Yoshioka M, Hancock BC, Zografi G. Crystallization of indomethacin from the amorphous state below and above its glass transition temperature. Journal of pharmaceutical sciences. 1994;83(12):1700-5.

45. LaFountaine JS, Prasad LK, Brough C, Miller DA, McGinity JW, Williams III RO. Thermal processing of PVP-and HPMC-based amorphous solid dispersions. AAPS PharmSciTech. 2016;17(1):120-32.

46. Huang S, Williams RO. Effects of the Preparation Process on the Properties of Amorphous Solid Dispersions. AAPS PharmSciTech. 2017.

47. Hu J, Rogers TL, Brown J, Young T, Johnston KP, Williams Iii RO. Improvement of dissolution rates of poorly water soluble APIs using novel spray freezing into liquid technology. Pharmaceutical Research. 2002;19(9):1278-84.

48. Tam JM, McConville JT, Williams RO, Johnston KP. Amorphous cyclosporin nanodispersions for enhanced pulmonary deposition and dissolution. Journal of pharmaceutical sciences. 2008;97(11):4915-33.

49. Dong Z, Chatterji A, Sandhu H, Choi DS, Chokshi H, Shah N. Evaluation of solid state properties of solid dispersions prepared by hot-melt extrusion and solvent co-precipitation. International Journal of Pharmaceutics. 2008;355(1):141-9.

50. Wurster DE, Taylor PW. Dissolution Rates. Journal of Pharmaceutical Sciences. 1965;54(2):169-75.

51. Korsmeyer RW, Gurny R, Doelker E, Buri P, Peppas NA. Mechanisms of solute release from porous hydrophilic polymers. International Journal of Pharmaceutics. 1983;15(1):25-35.

52. Cardamone JM. Keratin sponge/hydrogel II: Active agent delivery. Textile research journal. 2013;83(9):917-27.

53. Brouwers J, Brewster ME, Augustijns P. Supersaturating drug delivery systems: The answer to solubility-limited oral bioavailability? Journal of pharmaceutical sciences. 2009;98(8):2549-72.

54. Tuleu C, Andrieux C, Boy P, Chaumeil J. Gastrointestinal transit of pellets in rats: effect of size and density. International journal of pharmaceutics. 1999;180(1):123-31.

55. Miller DA, Keen, Justin M, Brough, Chris, Kucera, Sandra U, and Ellenberger, Daniel J, inventorImproved Formulations of Vemurafenib and Methods of Making the Same2016.

56. Leuner C, Dressman J. Improving drug solubility for oral delivery using solid dispersions. European Journal of Pharmaceutics and Biopharmaceutics. 2000;50(1):47-60.

57. Larkin J, Ascierto PA, Dréno B, Atkinson V, Liszkay G, Maio M, et al. Combined vemurafenib and cobimetinib in BRAF-mutated melanoma. New England Journal of Medicine. 2014;371(20):1867-76.

58. Ribas A, Hodi FS, Callahan M, Konto C, Wolchok J. Hepatotoxicity with combination of vemurafenib and ipilimumab. New England Journal of Medicine. 2013;368(14):1365-6.

59. Hong DS, Morris VK, Fu S, Overman MJ, Piha-Paul SA, Kee BK, et al. Phase 1B study of vemurafenib in combination with irinotecan and cetuximab in patients with BRAF-mutated advanced cancers and metastatic colorectal cancer. American Society of Clinical Oncology; 2014.

60. Flaherty KT, Yasothan U, Kirkpatrick P. Vemurafenib. Nature reviews Drug discovery. 2011;10(11):811-3.

61. Ellenberger DJ, Miller DA, Williams RO. Demonstration of KinetiSol® as a superior process for preparation of vemurafenib amorphous solid dispersions. AAPS PharmSciTech. 2017 (Accepted).

Chapter 3: Generation of a Weakly Acidic Amorphous Solid Dispersion of the Weak Base Ritonavir with Equivalent In-Vitro and In-Vivo Performance to Norvir Tablet

3.1 ABSTRACT

Ritonavir is an anti-viral compound that has also been employed extensively as a CYP3A4 and Pgp inhibitor to boost the pharmacokinetic performance of compounds that undergo first pass metabolism. For use in combination products, there is desire to minimize the mass contribution of the ritonavir system to reduce patient pill burden in these multi-agent products. In this study, KinetiSol® processing was utilized to produce an amorphous solid dispersion of ritonavir at double the drug load of the commercially available form of ritonavir and was subsequently developed into a tablet dose. The amorphous intermediate was demonstrated to be amorphous by x-ray powder diffraction and 13C solid-state nuclear magnetic resonance and an intimately mixed single-phase system by modulate differential scanning calorimetry and 1H T1/1H T1ρ solid-state nuclear magnetic resonance relaxation. In-vitro transmembrane flux analysis showed similar permeation rates for the KinetiSol-based tablet and the reference dosage form, Norvir®. In-vivo pharmacokinetic comparison between the two dosage forms resulted in equivalent exposure with approximately 20% Cmax reduction for the KinetiSol tablet. The performance gains were realized with a concurrent reduction of 45% dosage form mass.

3.2 INTRODUCTION

The active pharmaceutical ingredient ritonavir was initially employed as an anti-viral agent and protease inhibitor in the treatment of advanced HIV-1. (1, 2) However, in subsequent years, the value of ritonavir has expanded to serve as a potent P-glycoprotein and CYP3A4 inhibitor. (3-5) Many compounds have been identified as CYP3A4 substrates and their pharmacokinetic performance is often limited as a result of metabolism. (6) Ritonavir has been utilized for co-administration with other anti-HIV compounds such as saquinavir (7), indinavir (8), amprenavir (9), and lopinavir (10) to boost the pharmacokinetic performance of these molecules by inhibition of metabolism . Combination of ritonavir with anti-virals is a leading strategy in drug product development for the treatment of the hepatitis C virus (11, 12) and oncology products are being actively pursued as well. (13-15)

Ritonavir is commercially available as the standalone marketed product, Norvir® tablet. This product includes an amorphous solid dispersion containing 100 mg of ritonavir processed by hot melt extrusion. In the amorphous solid dispersion, ritonavir is present at 15% drug load (w/w) with copovidone as the water-soluble polymeric carrier and sorbitan monolaurate as a surfactant. (16) The amorphous dispersion represents a 667 mg contribution to total tablet mass of 789 mg. (17) This represents a substantial mass, especially in the context of application as a pharmacokinetic boosting component. Thus, there is a driver to increase drug load to support a more patient-centric combination product, i.e., reduced tablet number and/or size.

KinetiSol® processing represents an emerging technology for the production of amorphous solid dispersions. The process utilizes high shear to rapidly process amorphous solid dispersions on a short time scale and at temperatures often below the melting points and/or glass transitions of the included components. (18) The process has the ability to produce amorphous solid dispersions at drug loads as high as 50% w/w. (19) This capability makes the KinetiSol process an appealing technology in the context of creating high drug load amorphous solid dispersions for use in combination products. For weakly basic molecules like ritonavir, anionic polymers have been demonstrated to be an attractive option as their acidic groups interact with and stabilize weakly basic molecules in solution. (20-22) The polymeric carrier hypromellose acetate succinate (HPMCAS) is of note as strong interactions between its succinyl and especially acetyl groups with weakly basic drugs promotes in-solution stabilization. (23) This benefit has borne out in numerous examples. (24-26) Ritonavir is both thermally (27) and acid labile (28) which limits the application of thermal processing techniques such as hot melt extrusion as ritonavir degradation would be accelerated during processing. However, KinetiSol processing has been demonstrated to process amorphous solid dispersions of compounds susceptible to thermal and acidic degradation. (29, 30) In a previous study, a ritonavir-HPMCAS amorphous solid dispersion was produced by KinetiSol processing to enhance the delivery of the CYP3A4 metabolized AKBA compound at 30% drug load of ritonavir. (15) However, this study focused on the in-vivo AKBA exposure and did not explore broader application and utility of the ritonavir amorphous solid dispersion as a standalone dosage for CYP3A4 inhibition. In Figure 3.1 from the initial study, a specific challenge was identified in that the reference Norvir amorphous intermediate behaved as a weak base during pH change dissolution testing (release predominantly in acid phase) but the ritonavir-HPMCAS amorphous solid dispersion behaved as

a weak acid formulation (release predominantly in neutral phase). For this new study, it was hypothesized that the amorphous solid dispersion of ritonavir and HPMCAS at double the drug load of Norvir and with different pH solubility profiles could be demonstrated to behave equivalently by in-vitro and in-vivo analysis.

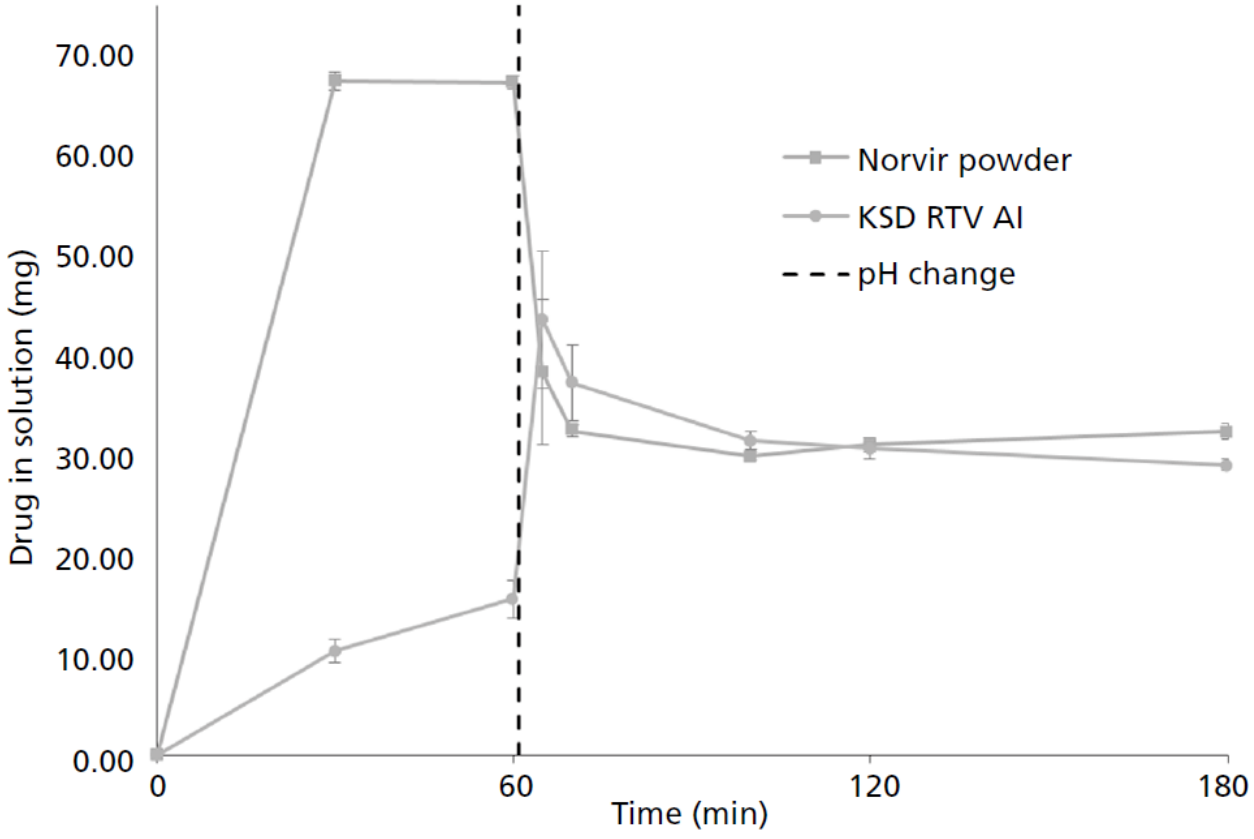

Figure 3.1: pH Change Dissolution of Crushed Norvir Tablets and Amorphous Solid Dispersion of Ritonavir Processed by KinetiSol. Reprinted from (15) with permission.

3.3 MATERIALS AND METHODS

3.3.1 Materials:

Ritonavir used in these studies was provided by Abbvie, Inc. (Chicago, IL, USA). Hypromellose acetate succinate (HPMCAS) used was Affinisol 912 granular grade acquired from Dow Chemical Company (Midland, MI, USA). Docusate sodium salt granular was acquired from Cytec Industries (Woodland Park, NJ, USA). All other excipients used in tableting or analysis were reagent grade except where otherwise noted.

3.3.2 KinetiSol Processing and Milling:

Ritonavir, HPMCAS, and docusate sodium salt were dispensed at a 30:65:5 ratio. Material blend was prepared by mixing components in a plastic bag by hand for approximately 2 minutes. KinetiSol processing was performed in a manufacturing scale KBC250 Batch Compounder (DisperSol Technologies, Georgetown, TX, USA). Batch size was 90 g and the sample was processed at 1500 rpm to an ejection temperature of 110°C. The ejected material was manually quenched between two metal plates. Quenched material was milled with a L1A Fitzmill (Fitzpatrick, Waterloo, ON, CA) at 9,000 rpm with blades forward and a 0.02” screen. Milled sample was passed through a #60 mesh (250 µm) screen.

3.3.3 X-Ray Powder Diffraction (XRPD):

X-Ray powder diffraction was performed on a MiniFlex 600 (Rigaku, The Woodlands, TX, USA). Sample was packed into circular sample holders and leveled prior to loading in the instrument. The unit utilized a Cu alpha radiation tube powered at a voltage of 40 kV and a current of 15 mA. A D/teX Ultra high-speed detector was used for data acquisition. Method parameters used a scan rate of 5.0 degrees/minute at a step size of 0.02 degrees from 2.5 to 40 2theta. Data was analyzed with the PDXL software package (Rigaku, The Woodlands, TX, USA).

3.3.4 Modulated Differential Scanning Calorimetry (mDSC):

Modulated differential scanning calorimetry was performed on a Q20 DSC unit (TA Instruments, New Castle, DE, USA). 5-10 mg of amorphous solid dispersion was evenly distributed in the bottom of a Tzero pan prior to compaction with a Tzero lid. Sample was equilibrated at 0°C for 5 minutes. After equilibration, sample was heated at a rate of 5°C/minute to 220°C with modulation at an amplitude of 0.5°C and frequency of 30 seconds. Thermal analysis was performed with a purge gas of dry nitrogen. Data analysis was performed with Universal Analysis software (TA Instruments, New Castle, DE, USA).

3.3.5 High Performance Liquid Chromatography (HPLC):

Sample purity and dissolution concentration was analyzed by HPLC. Data was collected on a Dionex Ultimate 3000 instrument (Thermo Electron, Sunnyvale, CA, USA) with Chromeleon 7 software used for data acquisition and analysis. HPLC grade water and acetonitrile were used for mobile phase A and B respectively. The column used for separation was an Acclaim™ 120, C18, 5µm, 120A, 4.6x150mm, P/N: 059148 (Thermo Fisher Scientific, Waltham, MA, USA). For dissolution analysis, samples were run with isocratic 30/70 water/acetonitrile flowed at 1.5 mL/minute for a 5 minute run time. For purity analysis, a 40 minute gradient was used with flow rate of 1 mL/minute. Purity sample was prepared at a nominal concentration 0.2 mg/mL and filtered through a 0.2 µm polyvinylidene fluoride (PVDF) syringe filter (Whatman, Piscataway, NJ, USA). Sample and column compartments were maintained at ambient conditions. An ultraviolet detector was used for data collection at a single wavelength of 240 nm.

3.3.6 Solid State Nuclear Magnetic Resonance (SSNMR):

Solid State Nuclear Magnetic Resonance was performed by Kansas Analytical Services (Loveland, CO, USA) on a Avance I Spectrometer (Bruker, Billerica, MA, USA). A Chemagnetics Apex probe refitted with a 7 mm Magic Angle Spinning (MAS) module (Revolutions NMR, Fort Collins, CO) was installed using 3-methylglutaric acid (MGA). Samples were packed into a 7 mm zirconia rotor. The instrument was operated at 399.67 MHz for 1H and 100.51 MHz for 13C. All experiments utilized MAS at 5 kHz, cross polarization (CP), and total suppression of spinning sidebands (TOSS).

3.3.7 Tableting:

Tablets were prepared per the formulation information provided in Table 3.1. A larger blend of material was prepared with 439 mg aliquots weighed out per tablet. Individual tablets were charged into a 04-17, 0.3126" x 0.4724", modified oval die (Natoli, St. Charles, MO, USA) and compressed with a Manual Tablet Compaction Machine (GlobePharma, New Brunswick, NJ, USA) to a target compression pressure of 5,000 psi. Tablet dimensions were measured with a calibrated digital caliper and fracture force was measured by a TBH 125 Tablet Hardness Tester (Erweka, Heusenstamm, Germany) to calculate the tensile strength of the tablet. Tablet disintegration time was measured by dosing tablet to a beaker containing deionized water with mixing provided by an overhead impeller.

Component	Amount/Tablet (mg)	Weight Percentage (%)
KSD-RTV Amorphous Intermediate	333	75.9
Microcrystalline cellulose	45	10.2
Mannitol	30	6.8
Croscarmellose	25	5.7
Colloidal silicon dioxide	2	0.5
Sodium stearyl fumarate	4	0.9
Total	439	100

Table 3.1: 100mg KSD-RTV Tablet Composition Containing 30% (w/w) Amorphous Solid Dispersion of Ritonavir

3.3.8 In-Vitro pH Change Dissolution:

Tablets containing KinetiSol produced ritonavir amorphous solid dispersion were analyzed by an in-vitro pH change dissolution method against the reference tablet, Norvir®. Tablets containing 100 mg of ritonavir were introduced into each vessel at the initiation of analysis. During the initial acid phase of the test, the dissolution media was 750 mL of 0.1N hydrochloric acid (HCl), pH 1.1. After 1 hour, the media was converted to 50 mM phosphate, pH 6.8 by rapid addition of 0.2M sodium phosphate tribasic as described by Miller et al. (31) The media temperature was maintained at 37°C throughout the test. The dissolution apparatus was a Distek 2500 (Distek, North Brunswick, NJ, USA) set up in paddle configuration per the United States Pharmacopeia 40, Chapter 711 Dissolution. Paddles were rotated at 50 rpm. 5 mL of sample was pulled via cannula at 30, 60, 65, 70, 75, 90, 120, 180, and 240 minutes. Pulled samples were filtered through a 1 µm glass membrane filter and diluted at a 1:1 ratio with acetonitrile. Diluted samples were analyzed by the HPLC method described previously.

3.3.9 MacroFLUX Dissolution:

Tablets containing KinetiSol produced ritonavir amorphous solid dispersion and the reference tablet Norvir were analyzed for trans-membrane flux by Pion Inc (Pion Inc., Billerica, MA, USA). A MacroFLUX dissolution setup was used for the analysis with a DT126 dissolution bath (Erweka, Heusenstamm, Germany). The donor compartment (dissolution vessel) utilized a media conversion dissolution from initially 800 mL of simulated gastric fluid (SGF), pH 1.6, to a final volume of 900 mL in fasted simulated intestinal fluid, (FaSSIF) pH 6.5. The acceptor

compartment contained Acceptor Sink Buffer (ASB), pH 7.4. An Parallel Artificial Membrane Permeability Assay (PAMPA) artificial membrane infused with GIT lipid served as the barrier between the donor and receiver compartments. Drug concentration was monitored in both the donor and receiver compartments by a Rainbow fiber optic UV system (Pion Inc., Billerica, MA, USA) with 5 mm path length probe tips on the donor side and 10 mm path length probe tips on the receiver side. A calibration curve was generated from 0-80 µg/mL in SGF, FaSSIF, and ASB media. In the case of FaSSIF media, solubility limitations of the drug required drug pre-dissolution in methanol with spiking into FaSSIF media to generate the curve. Total methanol content did not exceed 10% (v/v). Second derivative analysis was utilized to quantify ritonavir in solution with a range of 264-280 nm for quantification. Standard curves exhibited R2 values greater than 0.999. AU Pro software was utilized for all data analysis (Pion Inc., Billerica, MA, USA).

3.3.10 Pharmacokinetics in Male Beagle Dogs:

A pharmacokinetic study was conducted in male beagle dogs at Absorption Systems (Exton, PA, USA) to compare in-vivo performance of tablets containing KinetiSol produced ritonavir amorphous solid dispersion to Norvir. The study was non-crossover in design and each dog received one 100 mg tablet with three dogs per test article. All animals were fasted for 12 hours before dosing with food returned 4 hours post-dose. Tablets were provided by oral administration followed by a 40 mL flush with pH 2 acidified water. Blood samples were collected at 15 and 30 minutes and 1, 1.5, 2, 3, 4, 6, 9, and 12 hours post-dose. Sodium heparin was used as an anti-coagulant and samples were spun down to collect plasma. Plasma was analyzed by a LC-MS/MS

method for ritonavir content. Pharmacokinetic parameters were calculated using Phoenix WinNonlin v7.0 (Certara, Princeton, NJ, USA).

3.3.11 Statistical Analysis:

Statistical bioequivalence analysis between the test article, RTV-KSD, and the reference article, Norvir, was calculated following the procedures outlined in FDA Guidance for Industry: Bioequivalence Guidance. (32) All data was log transformed to stabilize variance in the sample data and preclude the need for distribution testing. Analysis of Variance (ANOVA) was utilized to determine the error mean square term. The 90% confidence interval was calculated for difference in log transformed mean of the reference and test articles and an alpha level of 0.05 was used. The lower and upper bounds were back-transformed to provide the confidence interval for the ratio of the geometric mean of the RTV-KSD tablet over the geometric mean of the Norvir tablet. These confidence intervals were compared to the bioequivalence limits which were defined as 80-125%. Statistically significant bioequivalence was obtained when the complete confidence interval for a pharmacokinetic parameter resided in the range of 80-125%. The described statistical analysis was performed on $AUC_{0\rightarrow 12}$, $AUC_{0\rightarrow\infty}$, and C_{max}.

3.4 RESULTS

3.4.1 KinetiSol Processing and Chemical Purity:

The KinetiSol processing profile for processing the amorphous solid dispersion of ritonavir is shown in Figure 3.2. The total processing time was 11.5 seconds with 5.2 seconds at elevated temperature.

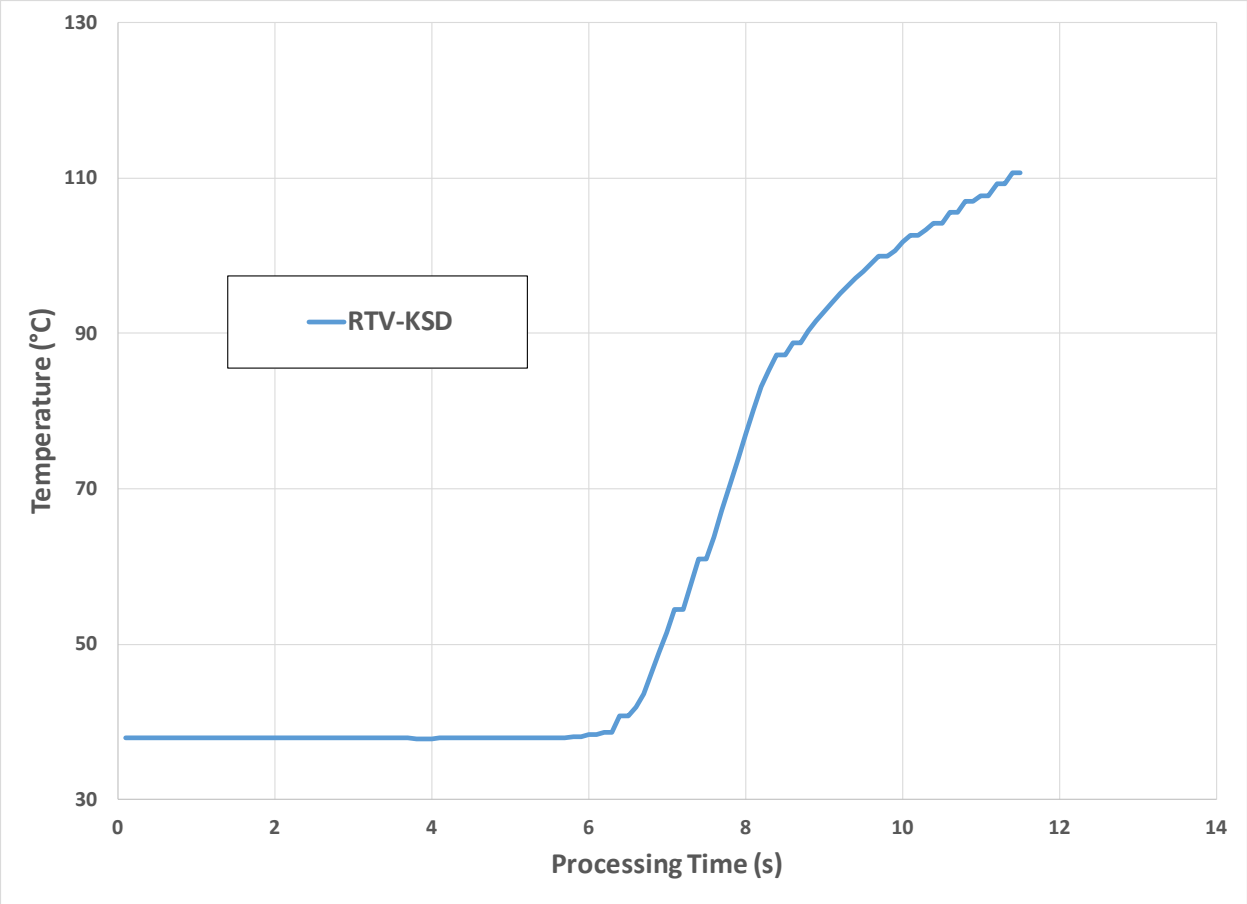

Figure 3.2: KinetiSol Processing Profile for Processing an Amorphous Solid Dispersion of Ritonavir at 1500 rpm

Chemical purity by HPLC for the RTV-KSD sample was found to be 98.81%. The majority of the observed impurities is constituted in one peak at a relative retention time of 0.83 and at a level of 1.14%.

3.4.2 Solid State-Characterization – mDSC and SSNMR:

When examined by XRD, the RTV-KSD amorphous solid dispersion lacked peaks associated with crystalline ritonavir and was fully amorphous (data not shown). For mDSC, the reversing heat flow thermogram and it is derivative with respect to time are shown in Figure 3.3 for the amorphous solid dispersion of ritonavir processed by KinetiSol. A single glass transition temperature (Tg) was observed at 61.16°C in the reverse heat flow plots. No melting point associated with crystalline ritonavir was observed in the heat flow thermogram (data not shown).

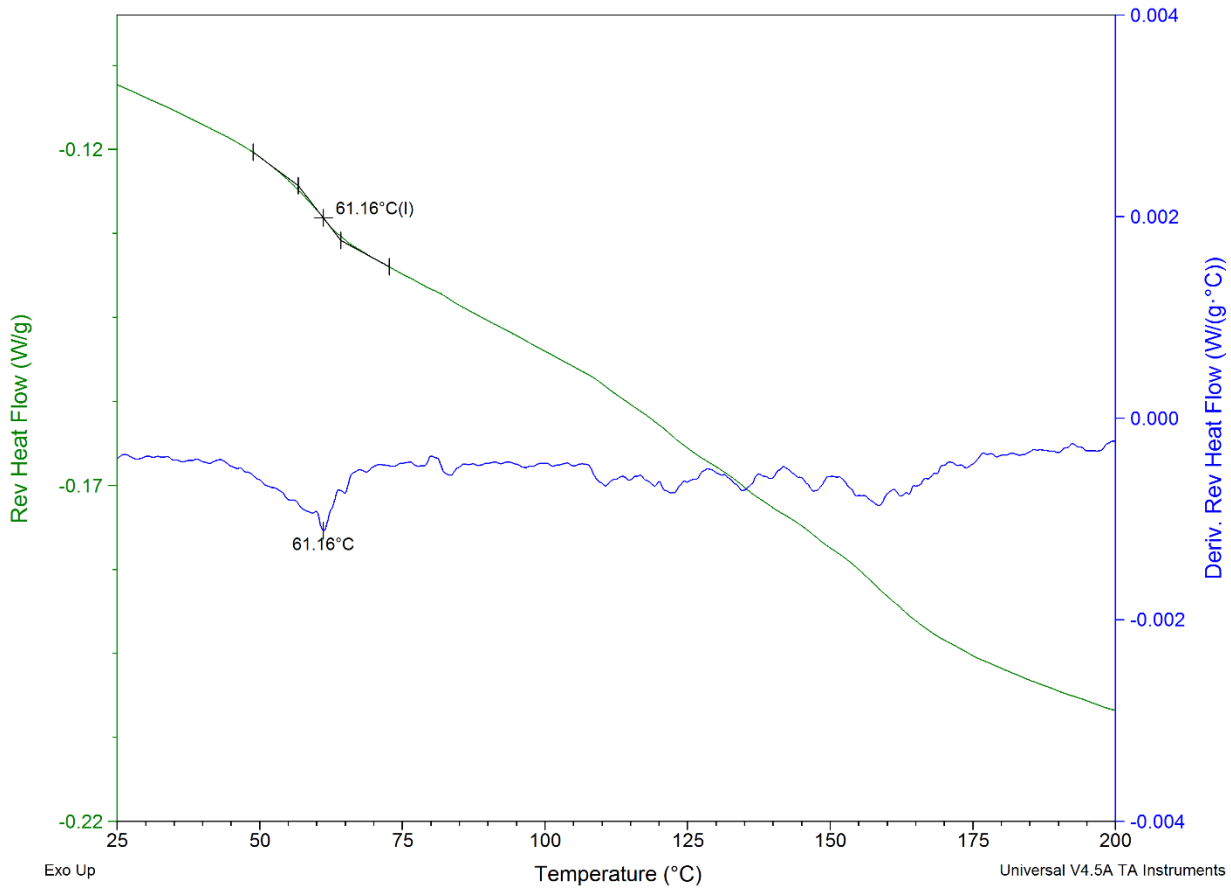

Figure 3.3: Modulated Differential Scanning Calorimetry of Amorphous Solid Dispersions Containing Ritonavir Made by the KinetiSol Process

In the SSNMR analysis for 13C, regions of 150-160 ppm for ritonavir and 100-110 ppm for HPMCAS were determined to only contain peaks for those compounds. These regions were used for subsequent analysis. No peaks associated with crystalline ritonavir were observed. The 13C SSNMR spectrum for the neat components and sample made by KinetiSol is overlaid in Figure 3.4.

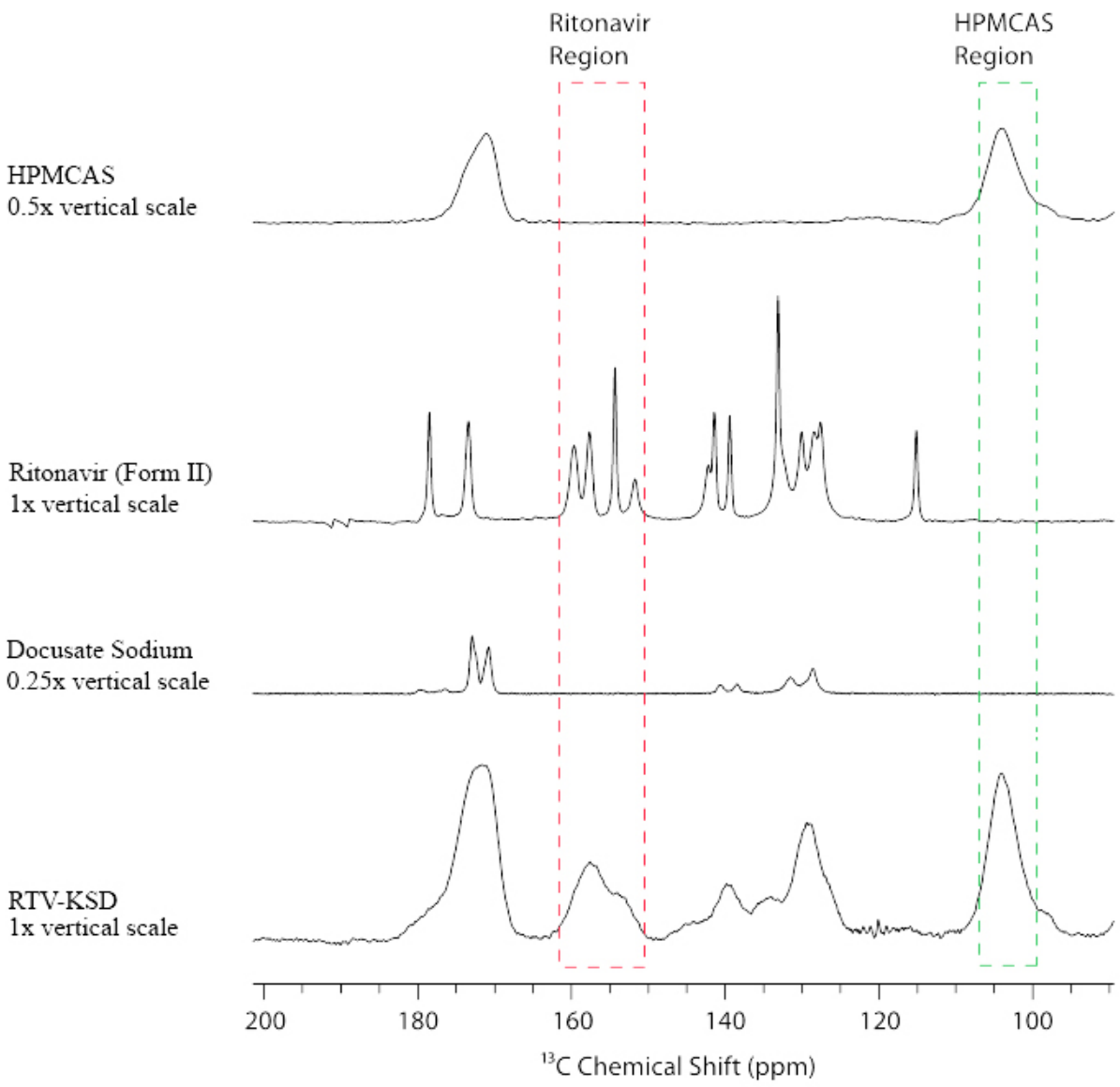

Figure 3.4: SSNMR 13C Spectra for Neat Materials and Ritonavir Amorphous Solid Dispersion with Isolated Regions Marked for the Primary Components, Ritonavir and HPMCAS

Table 3.2 summarizes the data for 1H T1 and 1H T1ρ for each of the samples generated by KinetiSol processing. For 1H T1, the sample exhibited values of 1.70 ± 0.05 and 1.76 ± 0.05

seconds for ritonavir and HPMCAS, respectively. For 1H T1ρ, the sample exhibited values of 7.68 ± 0.43 and 7.51 ± 0.19 seconds for ritonavir and HPMCAS, respectively.

Sample	**1H T1 (seconds)**	**1H T1ρ (ms)**
Docusate Sodium	1.15 ± 0.04	5.34 ± 0.14
HPMCAS-MF	4.34 ± 0.13	6.82 ± 0.10
Ritonavir	1.36 ± 0.04	87.35 ± 5.35
RTV-KSD	Drug: 1.70 + 0.05 Polymer: 1.76 + 0.05	Drug: 7.68 ± 0.43 Polymer: 7.51 ± 0.19

Table 3.2: SSNMR Relaxation Parameters 1H T1 and 1H T1ρ Spectra for Neat Materials and Ritonavir Amorphous Solid Dispersions

3.4.3 Tableting:

Using the KinetiSol processed amorphous solid dispersion, tablet blend was prepared per the formulation set forth in Table 3.1. Tablets were compressed at a target pressure of 2500 psi with modified oval dies and punches. On a representative tablet, calibrated calipers measured tablet dimensions as 7.95 mm wide by 12.02 mm long by 6.62 mm high. Tablet fracture force was measured as 146.1 N. The calculated tensile strength for the tablet was 1.38 MPa. Another

representative tablet was measured for disintegration time with the disintegration time in unbuffered water as 14 seconds.

3.4.4 pH Change In-Vitro Dissolution:

Figure 3.5 shows the pH change dissolution profile for the RTV-KSD tablet against the reference Norvir tablet. In the acid phase of the test conducted in 0.1 N hydrochloric acid, Norvir released to an average level of 82.2 µg/mL by the 60 minute pH change. In the same time frame and media, the tablet made from a KinetiSol processed sample released to an average level of 31.6 µg/mL. During the neutral phase of the test at pH 6.8, the Norvir tablets precipitated from its acid maximum drug concentration to a maximum observed neutral concentration of 44.7 µg/mL at 15 minutes after pH change or 75 minutes total. The RTV-KSD tablets released to a maximum drug concentration of 70.4 µg/mL at 5 minutes after pH change or 65 minutes total. The RTV-KSD tablet dissolution precipitated over time. In neutral pH 6.8 media, RTV-KSD tablets had a higher drug in solution concentration than Norvir through the 180 minute time point where RTV-KSD had an in-solution ritonavir concentration of 36.3 µg/mL and Norvir had a ritonavir concentration of 35.5 µg/mL.

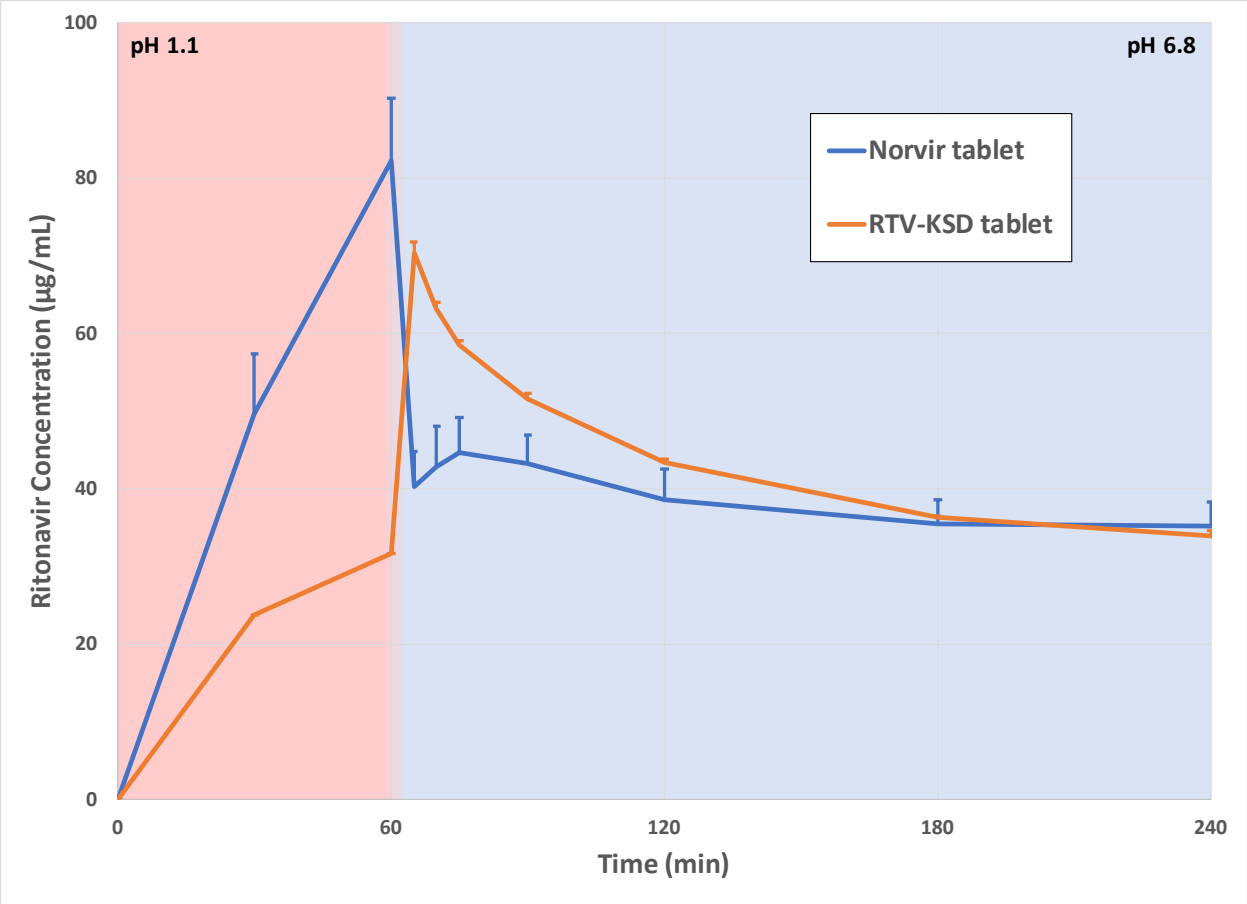

Figure 3.5: pH Change Dissolution of Tablet Made from KinetiSol Amorphous Solid Dispersion and Norvir Tablet

3.4.5 MacroFLUX Assay:

During the MacroFLUX assay, data and observations were collected on both the donor and receiver compartments. In the donor compartment, data collected in the neutral phase was not reliable due to high observed levels of Tyndall turbidity. However, turbidity onset occurred later

and to a lesser extent in RTV-KSD sample. Additionally, spectral shifts were observed in RTV-KSD sample but were not observed in Norvir donor compartments.

In the receiver compartment, appearance of drug was monitored throughout the test. During the SGF phase of the text (10-30 min.), the calculated average FLUX was 0.285 µg/(min. cm2) for Norvir and -0.015 µg/(min. cm2) for the RTV-KSD sample. In early phase of FaSSIF exposure (70-180 min.), the calculated average FLUX was 1.229 µg/(min. cm2) for Norvir and 1.145 µg/(min. cm2) for the RTV-KSD sample. In late phase of FaSSIF exposure (800-1000 min.), the calculated average FLUX was 0.403 µg/(min. cm2) for Norvir and 0.420 µg/(min. cm2) for RTV-KSD. The profile for the appearance of ritonavir in the receiver compartment is shown in Figure 3.6.

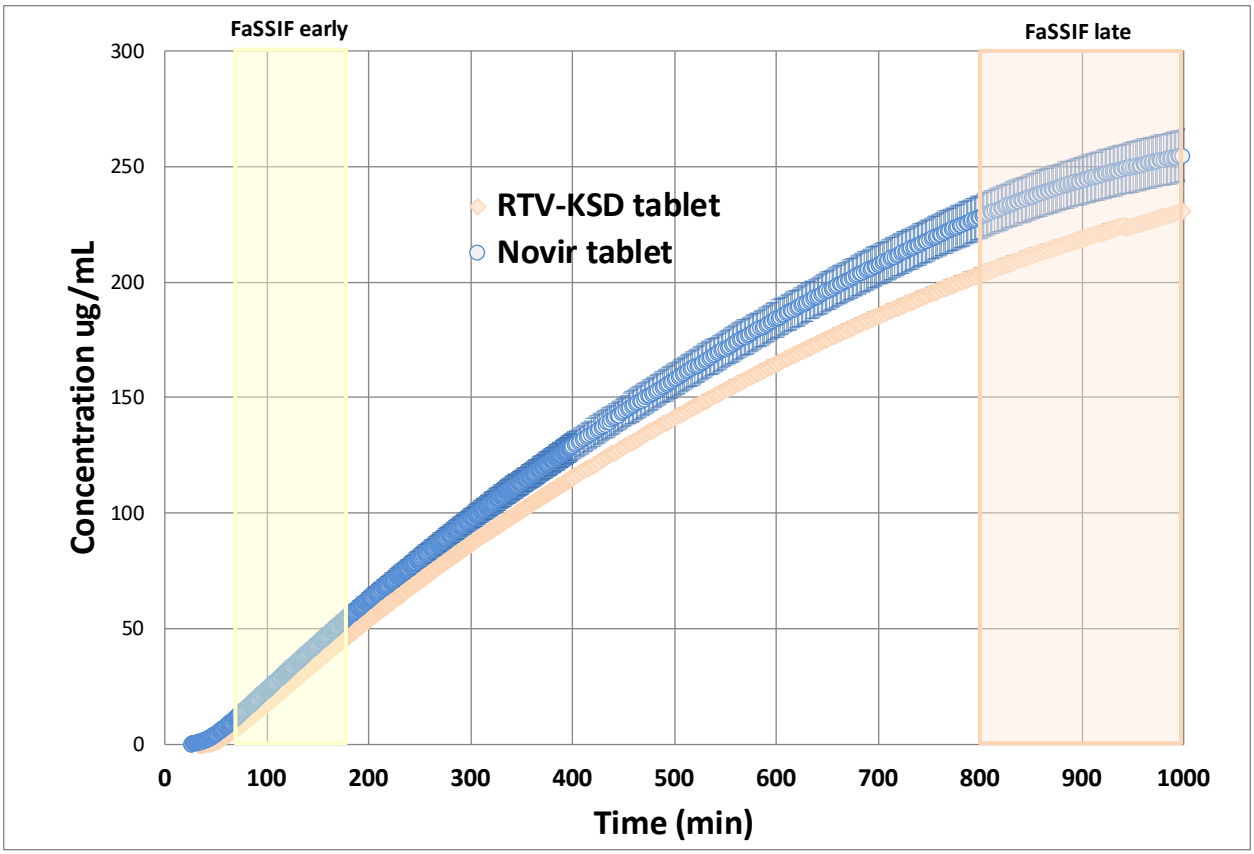

Figure 3.6: Ritonavir Concentration in Acceptor Compartment During pH Change Dissolution Conducted with MacroFLUX Permeability Apparatus

3.4.6 In-Vivo Pharmacokinetic Testing in Fasted Dog Model:

The average plasma concentration profiles for Norvir and RTV-KSD tablets are shown in Figure 3.7. The calculated tmax for both samples was 1.5 ± 0.5 hours. Cmax for the Norvir sample was 8490 ± 2316 ng/mL and the Cmax for the RTV-KSD tablets was 7037 ± 2713 ng/mL. Area under the curve at the last collected time point (AUC0→12) for each sample was calculated as 22560 ± 8885 hr*ng/mL for the Norvir tablets and 21993 ± 7438 hr*ng/mL for the RTV-KSD

tablets, respectively. AUC extrapolated to infinity (AUC0→∞) for each sample was calculated as 22612 ± 8927 hr*ng/mL for the Norvir tablets and 22115 ± 7494 hr*ng/mL for the RTV-KSD tablets, respectively. These parameters are summarized in Table 3.3.

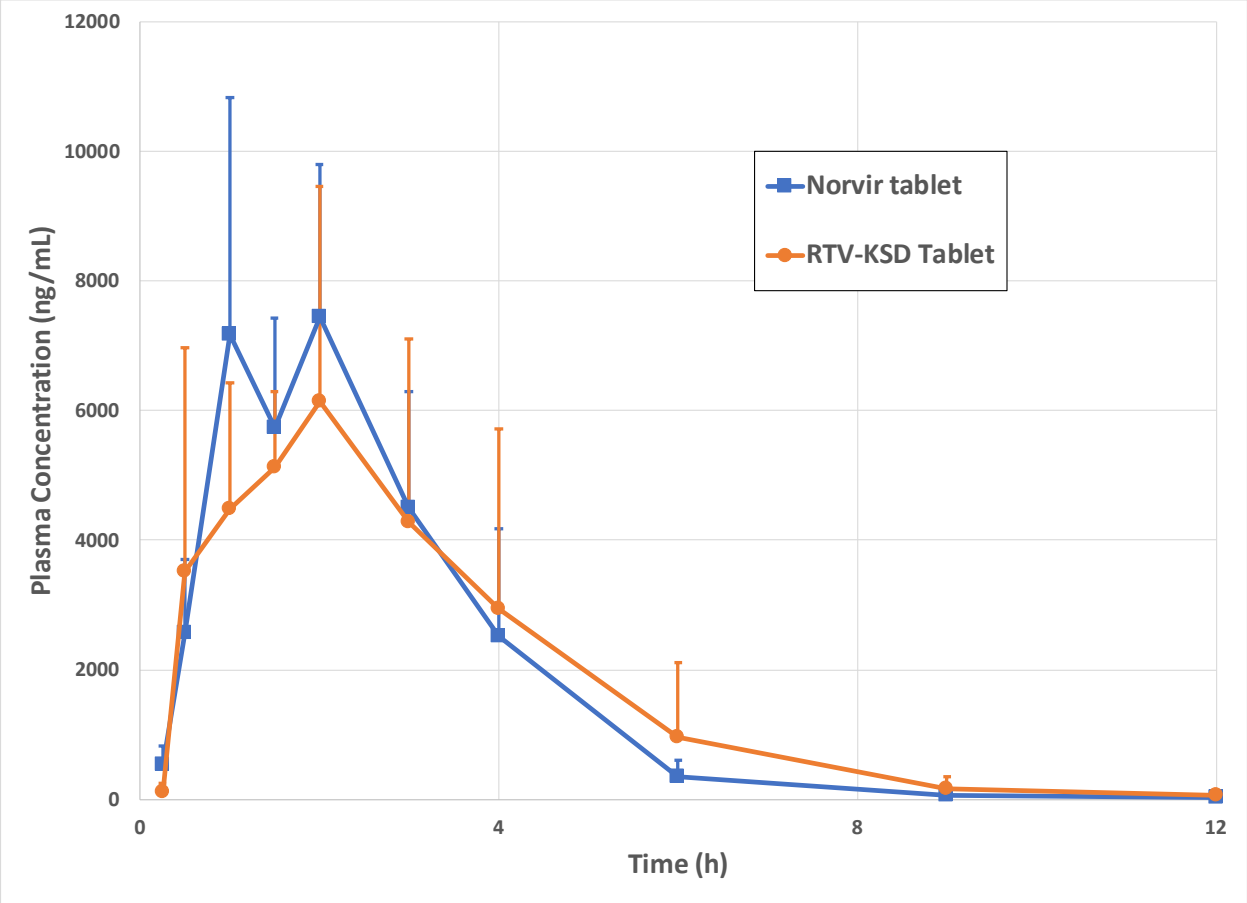

Figure 3.7: Ritonavir Plasma Concentration in Male Beagle Dogs After Oral Administration of 100 mg Norvir and RTV-KSD Tablets

Sample	Norvir	KSD Tablet	RTV-KSD Relative to Norvir
Dose (mg)	100	100	
tMax (h)	1.5 ± 0.5	1.5 ± 0.5	
CMax (ng/mL)	8490 ± 2316	7037 ± 2713	83%
Average AUC0→12 (hr·ng/mL)	22560 ± 8885	21993 ± 7438	97%
Average AUC0→∞ (hr·ng/mL)	22612 ± 8927	22115 ± 7494	98%

Table 3.3: Summary of Calculated Pharmacokinetic Values for Oral Administration of Ritonavir Tablets in Male Beagle Dogs For statistical bioequivalence analysis, the 90% confidence intervals for AUC0→12, AUC0→∞, and Cmax were 62-156%, 62-156%, and 54-121% respectively.

3.5 DISCUSSION

3.5.1 Characterization of KinetiSol Produced Amorphous Intermediate:

Conventional solid-state characterization was performed by XRD and mDSC to assess the system's crystallinity and phases present, respectively. Both techniques confirmed that the amorphous solid dispersion produced by KinetiSol was amorphous with respect to ritonavir. mDSC also exhibited a single Tg at 61.16°C. The glass transition temperature of amorphous ritonavir is 50°C (33), amorphous HPMCAS is 122°C. (34) The subsequent equation has been proposed (35) as a means of theoretically predicting the glass transition temperature for a glass system:

$$\frac{1}{T_g} = \sum \frac{w_i}{T_{g,i}}$$

where Tg is the glass transition temperature of the system, wi is the weight fraction of component i, and Tg,i is the glass transition temperature of component i. By this equation, the expected theoretical Tg for the ritonavir system processed by KinetiSol is 85°C. It should be noted that the equation proposed by Fox assumes that all components contribute equally to the glass transition of the system. Experimental results can be combined with the Gordon-Taylor equation to more accurately predict a system's glass transition. (36) However, that analysis is beyond the scope of this work. The mostly likely cause for the reduction in glass transition against the theoretical value is that docusate sodium can act as a plasticizer in some systems (37) which can result in depression of the glass transition temperature. (38) In 1995, Hancock et al. established a guideline that the glass transition temperature of a system should be at least 50

degrees higher than the intended storage condition due to risk of phase separation and subsequent recrystallization of material during pharmaceutically relevant timelines. (39) However, this guideline was developed utilizing rapid crystallizer drugs which are kinetically unstable and the guideline has been updated in recent years. In 2017, Hancock established a classification for crystallization propensity based a molecule's molecular weight and number of rotatable bonds. In the case of ritonavir (721 Daltons and 18 rotatable bonds), the classification describes it as having low propensity for crystallization. (40) Similar results were obtained in experimental work by Baird et al. classified ritonavir as a molecule with high glass forming ability and exhibited no recrystallization during heating. (41) Additionally, it has been demonstrated that weak base molecules like ritonavir have strong favorable interactions with anionic polymers like HPMCAS that promote improved thermodynamic stability of the system. (42, 43)
Finally, Chokshi et al. reported an accelerated (40°C/75% R.H.) stability study of amorphous solid dispersions containing weakly acidic indomethacin and cationic Eudragit EPO with glass transition temperatures as low as 46°C remained physically stable whereas non-ionic polymers were unstable in the same timeframe. All of these factors lead to the expectation that the RTV-KSD amorphous solid dispersion described in this work would be physically stable, although verification of physical stability at accelerated conditions is a critical future study.

When the reverse heat flow thermogram is examined, it was noted that there exist a number of disturbances in the signal beyond the primary Tg, including in the region where the Tg's for HPMCAS and docusate sodium reside. Despite being broadly applied in analysis of amorphous solid dispersions, mDSC and XRD are limited by their limits of detection. In the case of XRD, the limit of detection is typically 0.9% (44) and for mDSC the limit of detection for phase

separation is 30 nm. Practically, this means that phase separation into domains smaller than 30 nm will not be detectable by mDSC. (45) Additionally, the KinetiSol process is a short duration process typically lasting less than 30 seconds in total run time. In the case of the RTV-KSD amorphous solid dispersion, the maximum temperature of the process (110°C) is below the glass transition temperature of the polymeric carrier, HPMCAS (122°C). In the context of the thermogram appearance and the short duration, relatively low temperature KinetiSol process, a risk existed for an incompletely mixed system to exist and it was imperative to evaluate the amorphous solid dispersion with a more sensitive analytical technique. SSNMR is one such technique and it has been reported to have a minimum detectable domain size as low as 5 nm (46), compared to 30 nm for an ideal mDSC analysis.

Initially, 13C SSNMR analysis was performed as a confirmatory test for detection of crystallinity in the RTV-KSD sample and no evidence of crystallinity was detected. Thus, the RTV-KSD sample is confirmed as amorphous. For the phase separation analysis, the relaxation times for 1H T1 and 1H T1ρ analysis were conducted on the samples with the values determined for both the API and the polymer. As is readily apparent from the data in Table 3.2 for both 1H T1 and 1H T1ρ, the API and polymer relaxation parameters are in good agreement with the values overlapping within 1 standard deviation of the reported results. Previous work with this technique and amorphous solid dispersions has shown that when 1H T1 values agree for two components that they are intimately mixed at the 20-50 nm domain size and for 1H T1ρ the same is true at the 2-5 nm domain size. (46) Thus, it was concluded that the RTV-KSD amorphous solid dispersion was an intimately mixed system by SSNMR analysis of both 13C and 1H relaxation times. It is important to note that a processing speed of 1500 rpm is on the low end of

the processing range for the KinetiSol process (1000-3400 rpm) (18) with a total processing time of less than 12 seconds. Additionally, the ejection temperature of 110°C is below the reported melting point of ritonavir (120°C) (27) and the glass transition temperature of HPMCAS (122°C). (34) In a study with the high melting point drug meloxicam, Hughey et al. proposed that the high shear imparted by the KinetiSol process reduced the Noyes-Whitney boundary layer thickness and enabled the drug to be solubilized but drug dissolution into the polymer as opposed to melting and mixing of the drug as seen in other thermal processes. (47) If SSNMR shows that the amorphous solid dispersion can be intimately mixed in a short, relatively low intensity process below the melting point and glass transitions of the formulation, then it is expected that amorphous solid dispersions processed at more aggressive conditions will be similarly intimately mixed.

The chemical purity of the sample is similar to work previously reported for this amorphous composition. In that study, it was found that the one major degradant observed is also found in the reference tablet, Norvir, and at levels that would be beyond typical International Conference on Harmonization (ICH) guidelines. (15) Thus, it is expected that this degradant represents an impurity that has been qualified to higher acceptable limits via toxicology studies.

3.5.2 In-Vitro Performance Characterization:

When two formulations have different solubility properties, conventional dissolution methodologies are challenging to apply as was shown in previous work reproduced in Figure 3.1. (15) The employed pH shift methodology is often a frontline approach for assessment of the

performance a weakly basic formulation as it can simulate in-vivo transfer of the drug from the stomach to the intestinal compartment. (48) For the crushed reference Norvir product, the dissolution profile behaved as expected for the weakly basic ritonavir with extensive release in acid phase followed by substantial and rapid precipitation after conversion to neutral media. The non-ionic copovidone polymer did not impede the release of ritonavir during the acid phase of the test, as reported by Tho et al. (49) In the RTV-KSD amorphous solid dispersion, HPMCAS retarded the release of ritonavir during the acid phase of the test, followed by rapid dissolution of the drug and polymer when exposed to neutral phase conditions. Thus, the formulation released with a profile similar to a weak acid. After initial dissolution, HPMCAS slowed precipitation and helped maintain supersaturation, as reported elsewhere in literature. (24, 25) The disparity in performance across the test and in its individual phases suggests that conventional dissolution was inadequate when applied to the amorphous solid dispersions. Figure 3.5 shows a repeat of the analysis for tablet dosage forms and the analysis verified that the results hold for the final dosage form.

The addition of an acceptor or absorptive compartment to dissolution analysis has been shown to increase the predictive power of the analysis. (48) A two compartment biphasic dissolution apparatus that employs an octanol as the acceptor phase has been extensively reported in the literature. (50-52) In a common configuration, the dosage form is loaded into a USP IV flow through apparatus which is connected as a loop to a USP II dissolution bath containing an aqueous lower phase and an octanol upper, absorption mimicking phase. Specific to weak bases, the USP IV flow through cell apparatus often exists as a closed loop containing acidified media that is opened to the neutral media in the USP II apparatus 30-60 minutes after test initiation. In

the context of the systems of interest in this study, the two-compartment biphasic approach is not without limitations. For certain formulations, octanol absorbed into the aqueous phase at concentrations of 1% or less has been shown limit release of the drug to as low as 40% release compared to media without absorbed octanol. (53) Octanol absorption into media is particularly problematic when using biorelevant media (e.g. FaSSGF, FaSSIF or FeSSIF) as the surfactant enriched media can promote incorporation of octanol. (54) Specific to HPMCAS and octanol, a study by Sarode et al. reported high levels of aqueous supersaturation of itraconazole:HPMCAS amorphous solid dispersion in a single-phase dissolution, but nearly zero partitioning of itraconazole into the octanol layer of a separate biphasic dissolution. (55) The lack of partitioning of this formulation is surprising as itraconazole:HPMCAS formulations have been extensively studied and shown to have superior in-vivo performance over many other polymeric carriers. (25, 56) Additionally, it has been reported that two-compartment portion of the setup can restrict or delay the release of formulations that are pH dependent and/or erode. (53) In the case of RTV-KSD and the reference Norvir, it would be expected that ritonavir from Norvir would undergo significant dissolution during the acid phase of the test and be ready for transfer into the neutral compartment at the end of the 30 minute closed loop phase of the test. By contrast, RTV-KSD would undergo minimal dissolution during the closed loop portion of the test and would have a delay in release as the HPMCAS particles would slowly dissolve as the pH is gradually increased in the USP IV cell. Finally, in other studies, weak acid molecules have received different treatment from weak bases with their entire test conducted in neutral media. (57) The same application should be considered for a formulation that behaves like a weak acid. A biphasic test that included the acid phase would be expected to bias results towards Norvir whereas a test conducted without acid phase would be expected to bias results towards RTV-

KSD. Thus, another in-vitro test was deemed necessary for comparison of the formulations in this study.

Another example of an absorptive compartment joined to a conventional dissolution is transmembrane flux. One example is the MacroFLUX apparatus from Pion Inc. In this configuration, a traditional dissolution apparatus is used and an acceptor compartment containing acceptor sink media is lowered into the top of the media in the dissolution vessel. A parallel artificial membrane permeability assay (PAMPA) barrier forms a boundary between the dissolution media and the acceptor compartment and drug concentration in the acceptor compartment is monitored by a UV probe. (58) The PAMPA membrane has been demonstrated to correlate well with octanol-water partitioning measurements. (59) For the systems at hand, the advantages to a transmembrane flux analysis is that it removes octanol absorption into aqueous medias as a potential issue and eliminates the need for multiple compartments to facilitate pH shift during analysis. However, a limitation that exists for membrane systems like FLUX is that the limited surface area of the membrane is not representative of the total absorption and extent of mass transfer of the system being studied. (60) However, the rate of transfer across the membrane can be assessed and used to compare absorption rate of drug. (61) This form of analysis was expected to be able to compare the formulations of interest without biasing the test to favor one formulation or the other.

A MacroFLUX apparatus with conversion from SGF to FaSSIF after 30 minutes was used to collected data on both donor and receiver compartments for dissolution and absorption of RTV-KSD and the Norvir reference tablet. In the donor compartment, Norvir released more rapidly

and to a greater extent than the RTV-KSD sample during the 30 minute SGF phase. After pH change, both formulations exhibited extensive turbidity, although it was observed that the RTV-KSD had a delayed onset of turbidity and to a lesser extent. This observation corroborated the pH change dissolution testing. However, the donor compartment data is not reliable due to high levels of Tyndall turbidity. The acceptor compartment showed slight flux (0.285 µg/min/cm2) of ritonavir from the Norvir sample whereas the RTV-KSD sample had a slightly negative flux value within the baseline drift of the of the analysis. This was expected from the known release profiles of the two formulations in acidified media. After media conversion, flux increased for Norvir and RTV-KSD to 1.229 µg/min/cm2 and 1.145 µg/min/cm2 during early the early stage of FaSSIF analysis and 0.403 µg/min/cm2 and 0.420 µg/min/cm2 during the late stage of FaSSIF analysis. These represented RTV-KSD flux ratios of 94% in early stage FaSSIF and 104% in late stage FaSSIF. Based the measured rate of drug presentation in the acceptor compartment, it was expected that the two dosage forms should behave similarly in-vivo.

3.5.3 In-Vivo Pharmacokinetic Testing in Dogs and Statistical Analysis:

When selection of an in-vivo model was considered, similar issues related to differences in the formulations surfaced. Human gastric pH in the fasted state has been reported to range from 1-5 with the most common values occurring in the range of 1-2. (62-64) Compared to humans, dogs are poor acid secretors which can result in differences in performances for pH dependent formulations. (65) In the case of male beagle dogs, gastric pH has been reported across a wide range from 0.9-8.3, with most results occurring at extremes of the range. (62, 66) This range can have a significant impact on formulation performance, particularly for compounds exhibit pH

dependent solubility (66), such as ritonavir. To overcome high pH animals and variability in the dog model, there's a long history of dog PK testing in literature involving pretreatment with pentagastrin and histamine to control dog gastric pH. (4, 66, 67) While the in-vivo effects of pH modification on gastric conditions have been reported extensively in literature (65), there has been minimal in-vivo work to evaluate the effect of gastric pH modifiers on pH in the upper intestinal region of the animal model where significant absorption often occurs. However, an in-vitro analysis conducted with an artificial stomach and duodenum dissolution model demonstrated that buffered phosphate pretreatment (to represent in-vivo pentagastrin pretreatment) showed a reduction in the duodenum compartment pH to less than 5, and as low as 3, for approximately 1.5 hours. By contrast, an acidified suspension lowered duodenum pH for substantially less time, in the order 10-20 minutes. (68) This observed effect would be expected to boost duodenum performance of a formation with weakly basic behavior (such as Norvir) while limiting the performance of a weakly acidic formulation (such as RTV-KSD) in the same region.

To overcome these challenges, the conducted study utilized a 40 mL post-dose acidified water (pH 2) flush. The acidified flush was expected to reduce the stomach pH initially to allow for rapid dissolution of the Norvir tablet without a significant cascading pH effect that would lower pH in the duodenum region and blunt the release of RTV-KSD in this region. The study results found the pharmacokinetic data in good agreement between the formulations with equivalent tmax values of 1.5 hours and a RTV-KSD:Norvir AUC ratio of 97-98%. These congruent results were obtained despite formulating the dose to perform as a weak acid. A reduction in Cmax was observed at 83% for RTV-KSD relative to Norvir. This could represent an advantageous

situation for RTV-KSD as peak concentration (Cmax) reduction while maintaining overall drug exposure (AUC) is an important means of reducing or eliminating drug side-effects. Specific to ritonavir, neurological and gastrointestinal side-effects have been correlated to Cmax of the pharmacokinetic performance. (69)

Statistical analysis was performed to assess the RTV-KSD formulation for bioequivalence to the Norvir reference product. The United States Food and Drug Administration has established that formulation is deemed bioequivalent when the AUC and Cmax are statistically within 80-125% of the reference product. (32, 70) In the case of this analysis, the 90% confidence intervals for Cmax and AUC were not contained within the bounds of the 80-125% requirement. However, it should be noted that the pharmacokinetic study was not sufficiently powered to demonstrate bioequivalence. Additional analysis in more animals would be required to demonstrate bioequivalence.

3.6 CONCLUSION

A drug loading enhanced amorphous solid dispersion of ritonavir was produced by the KinetiSol® process. The formulation demonstrated adequate chemical purity, a lack of crystallinity, and homogeneity as a single-phase system. Additional analysis conducted by SSNMR showed that the amorphous solid dispersion was intimately mixed to a 2-5 nm scale despite a processing time on the order of second and at temperature below relevant thermal transitions for the formulation components. After formulation into a tablet, in-vitro analysis by transmembrane flux resulted in similar rates of drug transfer across a PAMPA membrane when

compared to the commercially available Norvir tablet. In-vivo pharmacokinetic analysis in a fasted dog model showed congruent exposure between the two dosages with approximately 20% Cmax reduction. The KinetiSol-based dosage form demonstrated essentially equivalent performance but with a reduction in tablet mass from 789 mg to 439 mg, a reduction of approximately 45%. The mass reduction is directly beneficial for combination product applications to reduce pill burden, thereby improving patient convenience and compliance.

3.7 REFERENCES:

1. Cameron DW, Heath-Chiozzi M, Danner S, Cohen C, Kravcik S, Maurath C, et al. Randomised placebo-controlled trial of ritonavir in advanced HIV-1 disease. The Lancet. 1998;351(9102):543-9.

2. Markowitz M, Saag M, Powderly WG, Hurley AM, Hsu A, Valdes JM, et al. A preliminary study of ritonavir, an inhibitor of HIV-1 protease, to treat HIV-1 infection. New England Journal of Medicine. 1995;333(23):1534-40.

3. Kageyama M, Namiki H, Fukushima H, Terasaka S, Togawa T, Tanaka A, et al. Effect of chronic administration of ritonavir on function of cytochrome P450 3A and P-glycoprotein in rats. Biological and Pharmaceutical Bulletin. 2005;28(1):130-7.

4. Law D, Schmitt EA, Marsh KC, Everitt EA, Wang W, Fort JJ, et al. Ritonavir–PEG 8000 amorphous solid dispersions: in vitro and in vivo evaluations. Journal of pharmaceutical sciences. 2004;93(3):563-70.

5. Eagling VA, Back D, Barry M. Differential inhibition of cytochrome P450 isoforms by the protease inhibitors, ritonavir, saquinavir and indinavir. British journal of clinical pharmacology. 1997;44(2):190-4.

6. CYP2C9 CC, CYP2D6 CA. The effect of cytochrome P450 metabolism on drug response, interactions, and adverse effects. Am Fam Physician. 2007;76:391-6.

7. Merry C, Barry MG, Mulcahy F, Ryan M, Heavey J, Tjia JF, et al. Saquinavir pharmacokinetics alone and in combination with ritonavir in HIV-infected patients. Aids. 1997;11(4):F29-F33.

8. van Heeswijk RP, Veldkamp AI, Hoetelmans RM, Mulder JW, Schreij G, Hsu A, et al. The steady-state plasma pharmacokinetics of indinavir alone and in combination with a low dose of ritonavir in twice daily dosing regimens in HIV-1-infected individuals. Aids. 1999;13(14):F95-F9.

9. Decker CJ, Laitinen LM, Bridson GW, Raybuck SA, Tung RD, Chaturvedi PR. Metabolism of amprenavir in liver microsomes: role of CYP3A4 inhibition for drug interactions. Journal of pharmaceutical sciences. 1998;87(7):803-7.

10. Crommentuyn K, Kappelhoff B, Mulder J, Mairuhu A, Van Gorp E, Meenhorst P, et al. Population pharmacokinetics of lopinavir in combination with ritonavir in HIV-1-infected patients. British journal of clinical pharmacology. 2005;60(4):378-89.

11. Andreone P, Colombo MG, Enejosa JV, Koksal I, Ferenci P, Maieron A, et al. ABT-450, ritonavir, ombitasvir, and dasabuvir achieves 97% and 100% sustained virologic response with or without ribavirin in treatment-experienced patients with HCV genotype 1b infection. Gastroenterology. 2014;147(2):359-65. e1.

12. Brayer SW, Reddy KR. Ritonavir-boosted protease inhibitor based therapy: a new strategy in chronic hepatitis C therapy. Expert review of gastroenterology & hepatology. 2015;9(5):547-58.

13. van Erp NP, Gelderblom H, Karlsson MO, Li J, Zhao M, Ouwerkerk J, et al. Influence of CYP3A4 inhibition on the steady-state pharmacokinetics of imatinib. Clinical Cancer Research. 2007;13(24):7394-400.

14. de Weger V, Stuurman F, Mergui-Roelvink M, Nuijen B, Huitema A, Beijnen J, et al. A phase I dose-escalation trial of bi-daily (BID) weekly oral docetaxel as ModraDoc006 in combination with ritonavir. Annals of Oncology. 2016;27(suppl_6).

15. Miller DA, Keen JM, Brough C, Ellenberger DJ, Cisneros M, Williams RO, et al. Bioavailability enhancement of a BCS IV compound via an amorphous combination product containing ritonavir. Journal of Pharmacy and Pharmacology. 2015.

16. Rosenberg J, Reinhold U, Liepold B, Berndl G, Breitenbach J, Alani L, et al., inventors; Abbott Laboratories, assignee. Solid pharmaceutical dosage form. United States patent 8268349. 18 Sep 2012.

17. Berndl G, Rosenberg J, Liepold B, Fastnacht K, Jung T, Roth W, et al., inventors; Abbott Laboratories, assignee. Solid pharmaceutical dosage formulations. United States patent application 11/939,640. 31 Jul 2008.

18. Ellenberger DJM, Dave A; and Williams, Robert O. Expanding the Application and Formulation Space of Amorphous Solid Dispersions with KinetiSol®: A Review. AAPS PharmSciTech. 2017 (Accepted).

19. Miller DA, Keen JM, Kucera SU, inventors; DisperSol Technologies, LLC, assignee. Formulations of deferasirox and methods of making the same. United States patent application 15/185,888. 2016 Jun 17.

20. Kohri N, Yamayoshi Y, Xin H, Iseki K, SATO N, TODO S, et al. Improving the oral bioavailability of albendazole in rabbits by the solid dispersion technique. Journal of pharmacy and pharmacology. 1999;51(2):159-64.

21. Miller DA, DiNunzio JC, Yang W, McGinity JW, Williams III RO. Enhanced in vivo absorption of itraconazole via stabilization of supersaturation following acidic-to-neutral pH transition. Drug development and industrial pharmacy. 2008;34(8):890-902.

22. Beten D, Gelbcke M, Diallo B, Moes A. Interaction between dipyridamole and Eudragit S. International journal of pharmaceutics. 1992;88(1-3):31-7.

23. Ueda K, Higashi K, Yamamoto K, Moribe K. Inhibitory effect of hydroxypropyl methylcellulose acetate succinate on drug recrystallization from a supersaturated solution assessed using nuclear magnetic resonance measurements. Molecular pharmaceutics. 2013;10(10):3801-11.

24. Friesen DT, Shanker R, Crew M, Smithey DT, Curatolo W, Nightingale J. Hydroxypropyl methylcellulose acetate succinate-based spray-dried dispersions: an overview. Molecular pharmaceutics. 2008;5(6):1003-19.

25. DiNunzio JC, Hughey JR, Brough C, Miller DA, Williams III RO, McGinity JW. Production of advanced solid dispersions for enhanced bioavailability of itraconazole using KinetiSol® Dispersing. Drug development and industrial pharmacy. 2010;36(9):1064-78.

26. Curatolo W, Nightingale JA, Herbig SM. Utility of hydroxypropylmethylcellulose acetate succinate (HPMCAS) for initiation and maintenance of drug supersaturation in the GI milieu. Pharmaceutical research. 2009;26(6):1419-31.

27. LaFountaine JS, Jermain SV, Prasad LK, Brough C, Miller DA, Lubda D, et al. Enabling thermal processing of ritonavir–polyvinyl alcohol amorphous solid dispersions by KinetiSol® Dispersing. European Journal of Pharmaceutics and Biopharmaceutics. 2016;101:72-81.

28. Rao RN, Ramachandra B, Vali RM, Raju SS. LC–MS/MS studies of ritonavir and its forced degradation products. Journal of pharmaceutical and biomedical analysis. 2010;53(4):833-42.

29. DiNunzio JC, Brough C, Hughey JR, Miller DA, Williams RO, McGinity JW. Fusion production of solid dispersions containing a heat-sensitive active ingredient by hot melt extrusion and Kinetisol® dispersing. European Journal of Pharmaceutics and Biopharmaceutics. 2010;74(2):340-51.

30. Hughey JR, DiNunzio JC, Bennett RC, Brough C, Miller DA, Ma H, et al. Dissolution enhancement of a drug exhibiting thermal and acidic decomposition characteristics by fusion processing: a comparative study of hot melt extrusion and KinetiSol® dispersing. AAPs Pharmscitech. 2010;11(2):760-74.

31. Miller DA, Gamba M, Sauer D, Purvis TP, Clemens NT, Williams RO. Evaluation of the USP dissolution test method A for enteric-coated articles by planar laser-induced fluorescence. International journal of pharmaceutics. 2007;330(1):61-72.

32. FDA Guidance. Statistical approaches to establishing bioequivalence. Center for Drug Evaluation and Research United States Food and Drug Administration. 2001.

33. Zhou D, Grant DJ, Zhang GG, Law D, Schmitt EA. A calorimetric investigation of thermodynamic and molecular mobility contributions to the physical stability of two pharmaceutical glasses. Journal of pharmaceutical sciences. 2007;96(1):71-83.

34. LaFountaine JS, McGinity JW, Williams III RO. Challenges and strategies in thermal processing of amorphous solid dispersions: a review. AAPS PharmSciTech. 2016;17(1):43-55.

35. Fox TG. Influence of diluent and of copolymer composition on the glass temperature of a polymer system. Bull Am Phs Soc. 1952;1:123.

36. Brostow W, Chiu R, Kalogeras IM, Vassilikou-Dova A. Prediction of glass transition temperatures: binary blends and copolymers. Materials Letters. 2008;62(17):3152-5.

37. Ghebremeskel AN, Vemavarapu C, Lodaya M. Use of surfactants as plasticizers in preparing solid dispersions of poorly soluble API: stability testing of selected solid dispersions. Pharmaceutical research. 2006;23(8):1928-36.

38. Chow T. Molecular interpretation of the glass transition temperature of polymer-diluent systems. Macromolecules. 1980;13(2):362-4.

39. Hancock BC, Shamblin SL, Zografi G. Molecular mobility of amorphous pharmaceutical solids below their glass transition temperatures. Pharmaceutical research. 1995;12(6):799-806.

40. Hancock BC. Predicting the Crystallization Propensity of Drug-Like Molecules. Journal of pharmaceutical sciences. 2017;106(1):28-30.

41. Baird JA, Van Eerdenbrugh B, Taylor LS. A classification system to assess the crystallization tendency of organic molecules from undercooled melts. Journal of pharmaceutical sciences. 2010;99(9):3787-806.

42. Song Y, Yang X, Chen X, Nie H, Byrn S, Lubach JW. Investigation of drug–excipient interactions in lapatinib amorphous solid dispersions using solid-state NMR spectroscopy. Molecular pharmaceutics. 2015;12(3):857-66.

43. Sarode AL, Sandhu H, Shah N, Malick W, Zia H. Hot melt extrusion for amorphous solid dispersions: temperature and moisture activated drug–polymer interactions for enhanced stability. Molecular pharmaceutics. 2013;10(10):3665-75.

44. Surana R, Suryanarayanan R. Quantitation of crystallinity in substantially amorphous pharmaceuticals and study of crystallization kinetics by X-ray powder diffractometry. Powder Diffraction. 2000;15(1):2-6.

45. Newman A, Engers D, Bates S, Ivanisevic I, Kelly RC, Zografi G. Characterization of amorphous API: Polymer mixtures using X-ray powder diffraction. Journal of pharmaceutical sciences. 2008;97(11):4840-56.

46. Yuan X, Sperger D, Munson EJ. Investigating miscibility and molecular mobility of nifedipine-PVP amorphous solid dispersions using solid-state NMR spectroscopy. Molecular pharmaceutics. 2013;11(1):329-37.

47. Hughey JR, Keen JM, Brough C, Saeger S, McGinity JW. Thermal processing of a poorly water-soluble drug substance exhibiting a high melting point: the utility of KinetiSol® dispersing. International journal of pharmaceutics. 2011;419(1):222-30.

48. Bevernage J, Brouwers J, Brewster ME, Augustijns P. Evaluation of gastrointestinal drug supersaturation and precipitation: strategies and issues. International journal of pharmaceutics. 2013;453(1):25-35.

49. Tho I, Liepold B, Rosenberg J, Maegerlein M, Brandl M, Fricker G. Formation of nano/micro-dispersions with improved dissolution properties upon dispersion of ritonavir melt extrudate in aqueous media. European Journal of Pharmaceutical Sciences. 2010;40(1):25-32.

50. Frank KJ, Locher K, Zecevic DE, Fleth J, Wagner KG. In vivo predictive mini-scale dissolution for weak bases: Advantages of pH-shift in combination with an absorptive compartment. European Journal of Pharmaceutical Sciences. 2014;61:32-9.

51. Heigoldt U, Sommer F, Daniels R, Wagner K-G. Predicting in vivo absorption behavior of oral modified release dosage forms containing pH-dependent poorly soluble drugs using a novel pH-adjusted biphasic in vitro dissolution test. European Journal of Pharmaceutics and Biopharmaceutics. 2010;76(1):105-11.

52. Vangani S, Li X, Zhou P, Del-Barrio M-A, Chiu R, Cauchon N, et al. Dissolution of poorly water-soluble drugs in biphasic media using USP 4 and fiber optic system. Clinical Research and Regulatory Affairs. 2009;26(1-2):8-19.

53. Thiry J, Broze G, Pestieau A, Tatton AS, Baumans F, Damblon C, et al. Investigation of a suitable in vitro dissolution test for itraconazole-based solid dispersions. European Journal of Pharmaceutical Sciences. 2016;85:94-105.

54. Phillips DJ, Pygall SR, Cooper VB, Mann JC. Overcoming sink limitations in dissolution testing: a review of traditional methods and the potential utility of biphasic systems. Journal of Pharmacy and Pharmacology. 2012;64(11):1549-59.

55. Sarode AL, Wang P, Obara S, Worthen DR. Supersaturation, nucleation, and crystal growth during single- and biphasic dissolution of amorphous solid dispersions: Polymer effects and implications for oral bioavailability enhancement of poorly water soluble drugs. European Journal of Pharmaceutics and Biopharmaceutics. 2014;86(3):351-60.

56. Stewart AM, Grass ME, Brodeur TJ, Goodwin AK, Morgen MM, Friesen DT, et al. Impact of Drug-rich Colloids of Itraconazole and HPMCAS on Membrane Flux In Vitro and Oral Bioavailability in Rats. Molecular Pharmaceutics. 2017.

57. Shi Y, Gao P, Gong Y, Ping H. Application of a biphasic test for characterization of in vitro drug release of immediate release formulations of celecoxib and its relevance to in vivo absorption. Molecular pharmaceutics. 2010;7(5):1458-65.

58. Narang AS, Tang D, Jennings SP, Mathias N, Tsinman KL, Dohoda DJ, et al., inventors; Pion Inc., assignee. Apparatus and Method for the Assessment of Concentration Profiling and Permeability Rates. United States patent application 15/098,514. 20 Oct 2016.

59. Avdeef A, Bendels S, Di L, Faller B, Kansy M, Sugano K, et al. PAMPA—critical factors for better predictions of absorption. Journal of Pharmaceutical Sciences. 2007;96(11):2893-909.

60. Hate SS, Reutzel-Edens SM, Taylor LS. Absorptive Dissolution Testing of Supersaturating Systems: Impact of Absorptive Sink Conditions on Solution Phase Behavior and Mass Transport. Molecular Pharmaceutics. 2017.

61. Borbás E, Sinkó Bl, Tsinman O, Tsinman K, Kiserdei Ev, Démuth Bz, et al. Investigation and mathematical description of the real driving force of passive transport of drug molecules from supersaturated solutions. Molecular pharmaceutics. 2016;13(11):3816-26.

62. Sagawa K, Li F, Liese R, Sutton SC. Fed and fasted gastric pH and gastric residence time in conscious beagle dogs. Journal of pharmaceutical sciences. 2009;98(7):2494-500.

63. Zane P, Guo Z, MacGerorge D, Vicat P, Ollier C. Use of the pentagastrin dog model to explore the food effects on formulations in early drug development. European Journal of Pharmaceutical Sciences. 2014;57:207-13.

64. Dressman JB. Comparison of canine and human gastrointestinal physiology. Pharmaceutical Research. 1986;3(3):123-31.

65. Akimoto M, Nagahata N, Furuya A, Fukushima K, Higuchi S, Suwa T. Gastric pH profiles of beagle dogs and their use as an alternative to human testing. European journal of pharmaceutics and biopharmaceutics. 2000;49(2):99-102.

66. Zhou R, Moench P, Heran C, Lu X, Mathias N, Faria TN, et al. pH-dependent dissolution in vitro and absorption in vivo of weakly basic drugs: development of a canine model. Pharmaceutical research. 2005;22(2):188-92.

67. Fancher RM, Zhang H, Sleczka B, Derbin G, Rockar R, Marathe P. Development of a canine model to enable the preclinical assessment of ph-dependent absorption of test compounds. Journal of pharmaceutical sciences. 2011;100(7):2979-88.

68. Bhattachar SN, Perkins EJ, Tan JS, Burns LJ. Effect of gastric pH on the pharmacokinetics of a bcs class II compound in dogs: Utilization of an artificial stomach and duodenum dissolution model and gastroplus,™ simulations to predict absorption. Journal of pharmaceutical sciences. 2011;100(11):4756-65.

69. Gatti G, Di Biagio A, Casazza R, De Pascalis C, Bassetti M, Cruciani M, et al. The relationship between ritonavir plasma levels and side-effects: implications for therapeutic drug monitoring. Aids. 1999;13(15):2083-9.

70. Haidar SH, Davit B, Chen M-L, Conner D, Lee L, Li QH, et al. Bioequivalence approaches for highly variable drugs and drug products. Pharmaceutical research. 2008;25(1):237-41.

Chapter 4: The Utility of Pharmaceutical Lubricants in Amorphous Solid Dispersions as a Tool to Promote Improved In-vitro Dissolution and In-vivo Pharmacokinetic Performance

4.1 Abstract

In this work, an investigation was conducted on an unexpected in-vivo benefit observed with the inclusion of the lubricant magnesium stearate in an amorphous solid dispersion. Lubricants like magnesium stearate are understood to negatively affect dissolution and pharmacokinetic performance of poorly soluble drugs and are used sparingly or avoided altogether. In this study, amorphous solid dispersions containing various lubricants in the amorphous solid dispersion were evaluated for their impacts on in-vitro and in-vivo drug performance. Improved dissolution was observed when the weakly acidic deferasirox, the neutral etravirine, and the weakly basic ritonavir drug molecules. Solubility benefits were observed with a large range of lubricants encompassing pharmaceutical fatty alcohols, fatty carboxylic acids, glyceryls, stearates, and other lubricants. Benefits were demonstrated with amorphous solid dispersions processed by the fusion process of KinetiSol dispersing and melt-quenching. In one example, the positive effect of a lubricant was observed when included in addition to a traditional surfactant. Positive effects observed in-vitro were corroborated by an in-vivo pharmacokinetic study with etravirine in fasted male beagle dogs. It was concluded that pharmaceutical lubricants can be utilized for solubility and in-vivo performance benefits when included internally in amorphous solid dispersions.

4.2 INTRODUCTION

In the current pharmaceutical development world, it is estimated that as high as 90% of drug molecules in development are solubility challenged. (1) The same holds true for approved drugs where drugs approved in 2012 were on average ten times less soluble than drugs approved in 1983. (2) To address these solubility challenged molecules, amorphous solid dispersions are applied with increasing frequency to allow for efficacious delivery of these molecules. As illustrated in Figure 4.1, only 4 orally administered amorphous drug products were approved prior to 2007, but in the time interval 2007-2017 there have been 19 approved amorphous oral dosage forms. (3) Additionally, a March 2015 survey found that there were at least 76 amorphous solid dispersion products in development pipelines at that point in time. (4) Despite the extensive use of amorphous solid dispersions in current product development, new chemical entities are increasingly outside Lipinski's rule-of-5 (5, 6) and attrition rates of remain high. (7) Even when an approved amorphous solid dispersion product is successfully launched, patient pill burdens remain high in some instances. Examples such as Zelboraf® (4 tablets, twice daily) (8) and Incivek® (2 tablets, thrice daily). (9) In the case of Zelboraf, there is evidence that the need for a high dose is at least partially caused by poor absorption of vemurafenib as 94% of the dosed active substance is recovered in fecal matter. (10) Thus, in addition to enabling drug delivery through generation of an amorphous solid dispersions, there is a demonstrated need to expand the formulation space for amorphous solid dispersions to better enable their delivery. (11)

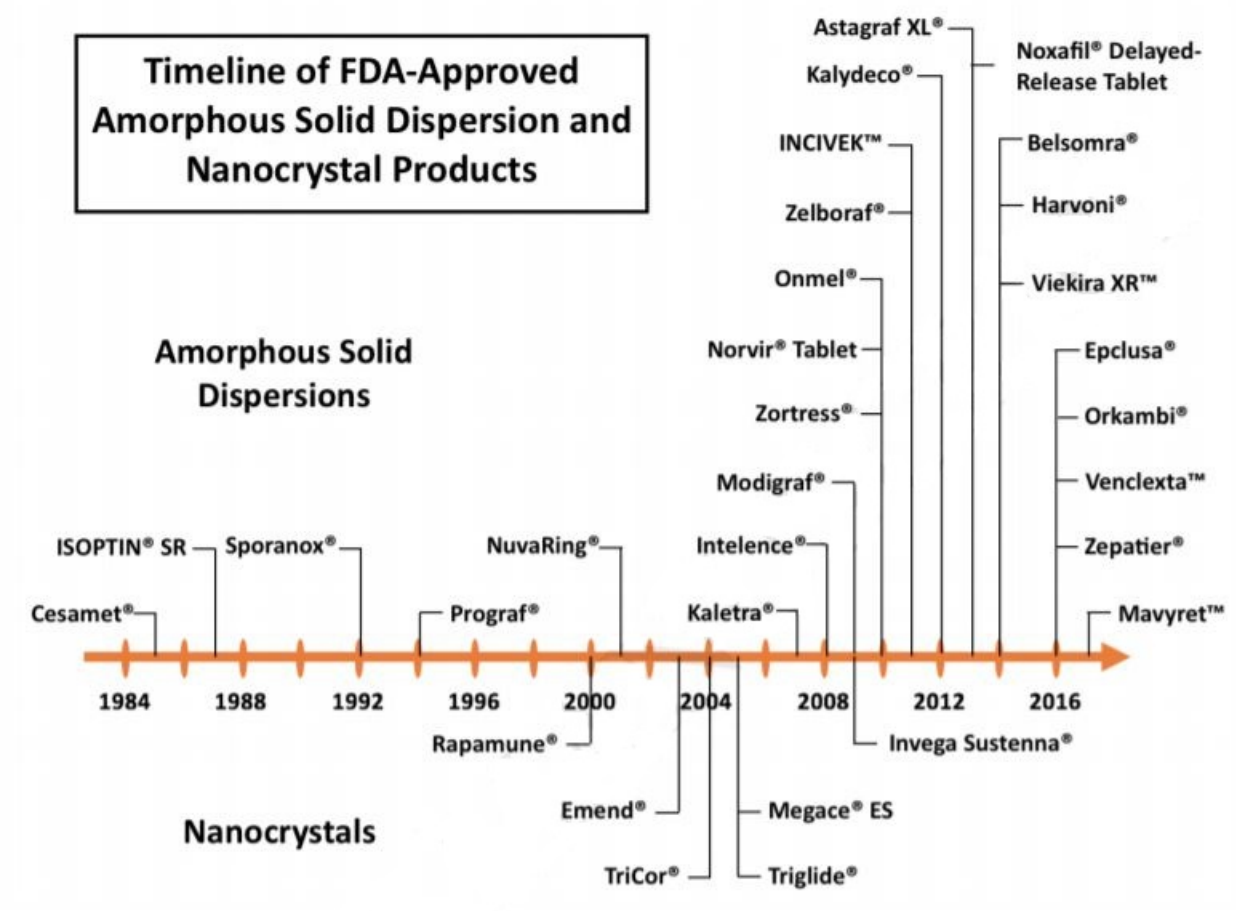

Figure 4.1: Approved Products Developed as Amorphous Solid Dispersions or Nanocrystals Reproduced from (3) with permission.

In a study of amorphous solid dispersions of deferasirox by the authors, a surprising positive result was obtained when the lubricant magnesium stearate was included in the amorphous solid dispersion. Initially, amorphous solid dispersions containing deferasirox with polymers as copovidone or copovidone/Eudragit® L100-55 were prepared by KinetiSol processing. To increase product yield, magnesium stearate was included as an optional lubricant in both formulations. The resulting formulations were prepared into tablet dosage forms described in Table 4.1.

Phase	Component	Lot 25	Lot 52	Lot 28	Lot 53
Amorphous Intermediate	Deferasirox	40%	40%	40%	40%
	Copovidone	20%	19.8%	40%	39.6%
	Methacrylic Acid and Ethyl Acrylate Copolymer	20%	19.8%	0%	0%
	Magnesium Stearate	0%	0.4%	0%	0.4%
External /tableting	Microcrystalline Cellulose	13%	13%	13%	13%
	Croscarmellose Sodium	6%	6%	6%	6%
	Colloidal Silicon Dioxide	0.5%	0.5%	0.5%	0.5%
	Magnesium Stearate	0.5%	0.5%	0.5%	0.5%

Table 4.1: Tablet Formulation Information for Deferasirox Tablets Prepared for Dosing in Dog Pharmacokinetic Study. All tablets prepared 900 mg total weight with 360 mg of deferasirox (active pharmaceutical ingredient). Amorphous intermediate prepared by KinetiSol process.

To assess the effects of lubricant inclusion in the amorphous solid dispersion, an in-vivo pharmacokinetic study was conducted in fasted male beagle dogs. Blood plasma concentrations are shown in Figure 4.2 and the pharmacokinetic parameters are summarized in Table 4.2.

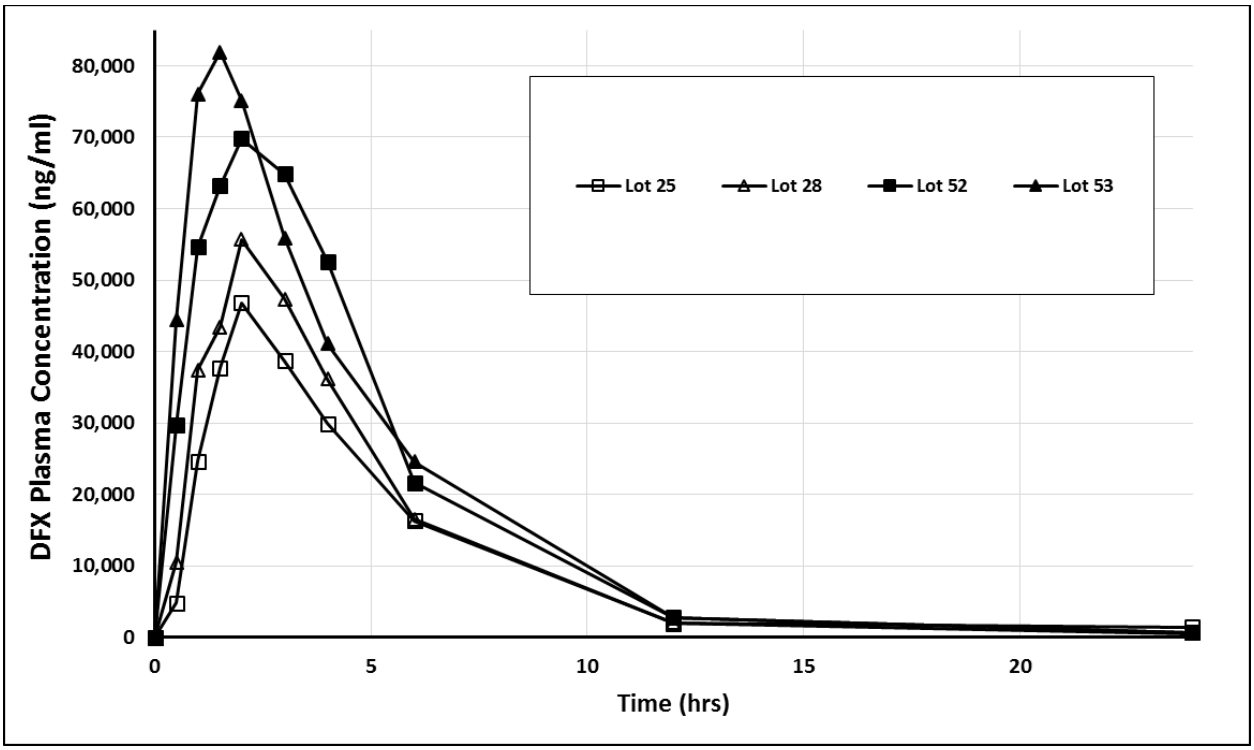

Figure 4.2: Deferasirox Plasma Concentration in Dog Pharmacokinetic Study Dosed at 360 mg of Deferasirox Per Tablet with 1 Tablet Per Dog

PK Parameter	Lot 25	Lot 52	Lot 28	Lot 53
AUC (ng*hr/ml)	262,333±61,028	394,815±101,967	283,375±39,668	409,369±133,071
Cmax (ng/ml)	48,550±17,337	75,750±25,364	59,775±5,480	88,300±32,129
tmax (hr)	1.75±0.29	2.13±0.63	2.00±0.82	1.50±0.41

Table 4.2: Pharmacokinetic Parameters From Dog Pharmacokinetic Study Dosed at 360 mg of Deferasirox Per Tablet with 1 Tablet Per Dog

For both polymeric systems, the inclusion of lubricant resulted in a 44-50% increase in average AUC and a 48-56% increase in average maximum plasma concentration.

The results obtained in the deferasirox-lubricant in-vivo study were unexpected and surprising. Lubricants are well established to be detrimental to performance of poorly soluble drugs when utilized as lubricants in their crystalline form. (12-14) The negative effect on dosage performance has been observed with increasing lubricant concentrations as shown in dissolution profiles in Figure 4.3. As magnesium stearate concentration was increased, dissolution rate and extent of nitrofurantoin was decreased.

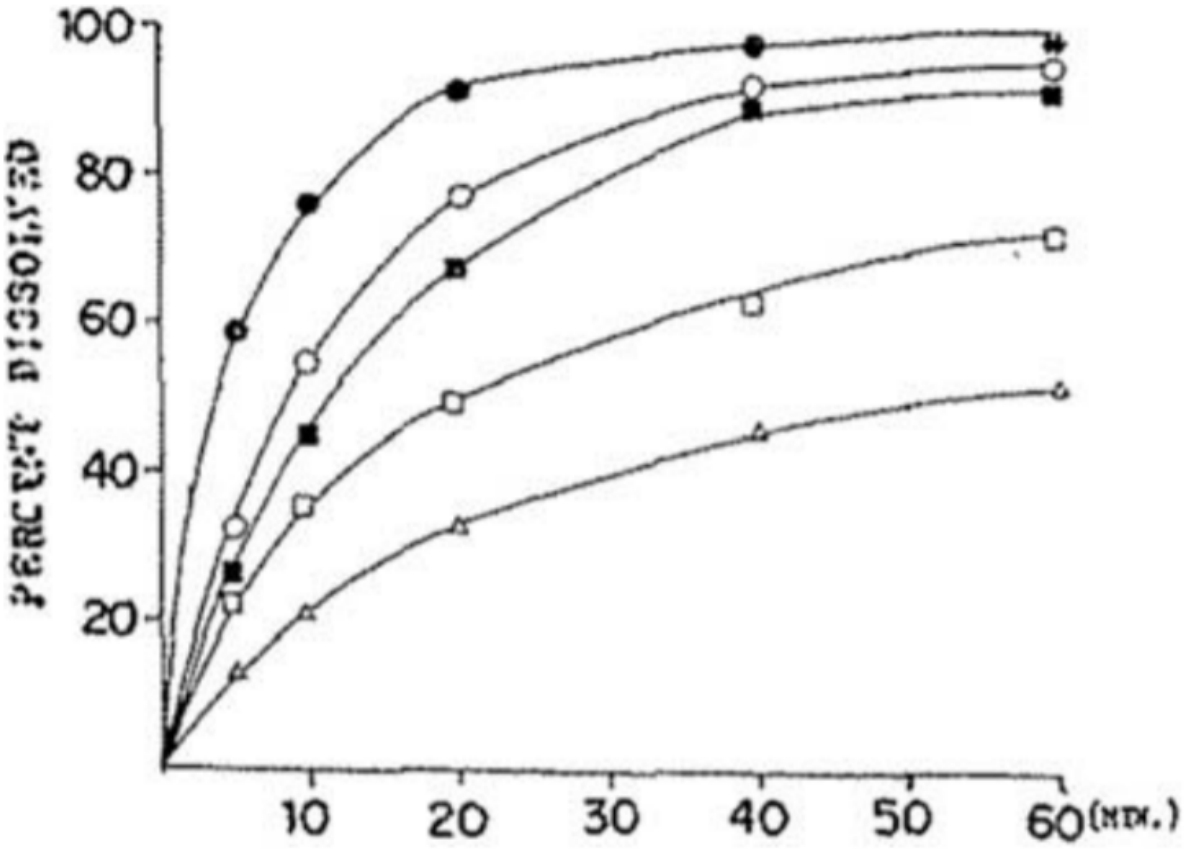

Figure 4.3: Effect of Magnesium Stearate Concentration on Dissolution Performance of Nitrofurantoin Tablets Granulated with Starch Paste. Magnesium stearate concentration (% w/w): closed circles – 0.5%, open circles – 1.0%, closed squares – 1.5%, open squares – 2.0%, open triangles – 3.0%. Reproduced from (32) with permission.

In the case of stearate lubricants, the effect has been demonstrated to be dependent on the particular stearate lubricant utilized as shown in Figure 4.4. In this analysis, magnesium stearate was found to be the worst-case lubricant for SQ37256 performance which further increased the surprise of the deferasirox result.

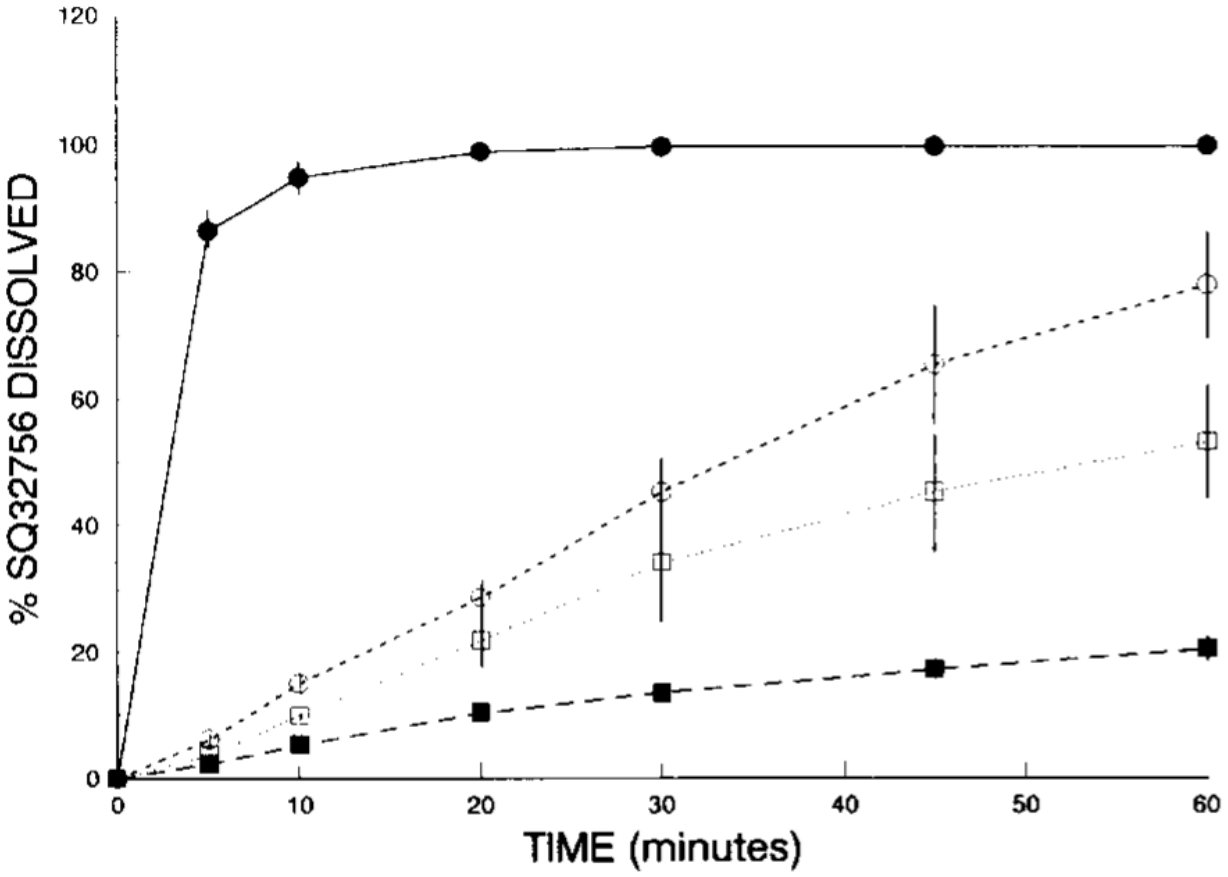

Figure 4.4: Effect of Various Lubricants on 0.1N Hydrochloric Acid Dissolution Performance of SQ32756. Closed circles contain no lubricant, open circles contain calcium stearate, open squares contain zinc stearate, and closed squares contain magnesium stearate. Reproduced from (33) with permission.

Sodium stearyl fumarate, another lubricant, is promoted as an alternative to magnesium stearate with reduced negative effects on drug delivery (15-17), but many examples exist where its presence also limited drug performance. (18-20) Another interesting aspect of the deferasirox with magnesium stearate example is that the large performance benefits were observed with the

inclusion of only 0.5% w/w lubricant in amorphous solid dispersion. There was a significant benefit to formulation enhancement without a corresponding substantial increase in mass of the dosage form. This aspect is important for high dose drugs where patient pill burden is already a significant challenge. (21) In this instance, magnesium stearate greatly improved the performance of the deferasirox formulation and opportunity was recognized to apply it and similar molecules as formulation solutions in amorphous solid dispersions.

It was hypothesized that water insoluble molecules with properties like magnesium stearate could be used to enhance the in-vitro and in-vivo performance of poorly water soluble drugs when co-formulated internally in an amorphous solid dispersion. To test the hypothesis, there were a several key areas to consider. First, it was imperative to assess that the inclusion of lubricants in the amorphous solid dispersion was beneficial to multiple classes of active pharmaceutical ingredients. To meet this need, deferasirox was selected as a weakly acidic molecule, ritonavir was selected as a weakly basic molecule, and etravirine was selected as a non-ionic molecule. Second, it was important to assess the breadth of molecules that could be applied in this manner. Molecules with properties like magnesium stearate and their classifications are discussed in the following paragraph. Another important consideration was if the performance gains could be realized in systems that already benefited from the inclusion of a surfactant to promote solubility enhancement. Finally, since the initial surprising result was discovered on amorphous solid dispersions processed by KinetiSol, it was deemed important to verify that the performance enhancement is not limited to amorphous solid dispersions prepared in this manner and that an amorphous solid dispersion processed by another technique could impart a similar effect. However, it is important to note that a review of magnesium stearate and

compounds with similar properties found that all of these compounds are practically insoluble in common organic solvents. Thus, solvent-based approaches represented limited opportunity for solubility enhancement through this formulation modification strategy and were not pursued.

When magnesium stearate was examined to identify similar molecules for assessment for amorphous solid dispersion performance enhancement, four criteria were applied: insoluble in water, melting point amenable to thermal processes, crystalline, and non-polymeric. After extensive review, several pharmaceutical additives were identified that met these criteria and were further classified based on common functional groups. These groups were fatty alcohols (Table 4.3), fatty carboxylic acids (Table 4.4), glyceryls (Table 4.5), stearates (Table 4.6), and three other compounds (Table 4.7) that did not fit the functional categories of the other compounds. Excluding menthol, all other compounds included long fatty carbon chains with one or more functional groups at the head (e.g. hydroxyl for fatty alcohols). Thus, if the carbon chain is important to the solubility enhancing performance of these lubricants, then menthol could represent a negative control for the performance of these systems.

Component	Aqueous Solubility	Physical Form @ Room Temperature	Melting Point (°C)
Myristyl Alcohol	Practically insoluble	Waxy solid	38
Cetyl alcohol	Practically insoluble	Waxy flakes or granules	49
Stearyl Alcohol	Practically insoluble	Waxy flakes or granules	59
Cetostearyl alcohol	Practically insoluble	Waxy flakes or granules	48-55

Table 4.3: Pharmaceutical Fatty Alcohols with Properties Similar to Magnesium Stearate. Chemical properties adapted from (31).

Component	Aqueous Solubility	Physical Form @ Room Temperature	Melting Point (°C)
Myristic Acid	Practically Insoluble	Waxy solid	54.5
Palmitic Acid	Practically Insoluble	Powder	63-64
Stearic Acid	Practically Insoluble	Powder	69-70

Table 4.4: Pharmaceutical Fatty Carboxylic Acids with Properties Similar to Magnesium Stearate. Chemical properties adapted from (31).

Component	Aqueous Solubility	Physical Form @ Room Temperature	Melting Point (°C)
Glyceryl Monostearate	Practically Insoluble	Waxy Solid	55-60
Glyceryl Behenate	Practically Insoluble	Powder	65-77
Glyceryl Palmitostearate	Practically Insoluble	Powder	52-55

Table 4.5: Pharmaceutical Glyceryls with Properties Similar to Magnesium Stearate. Chemical properties adapted from (31).

Component	Aqueous Solubility	Physical Form @ Room Temperature	Melting Point (°C)
Magnesium Stearate	Practically Insoluble	Powder	126-130
Calcium Stearate	Practically Insoluble	Powder	149-160
Zinc Stearate	Practically Insoluble	Powder	120-122
Aluminum Monostearate	Practically Insoluble	Powder	220-225
Aluminum Distearate	Practically Insoluble	Powder	150-165
Aluminum Tristearate	Practically Insoluble	Powder	117-120

Table 4.6: Pharmaceutical Stearates with Properties Similar to Magnesium Stearate (Including Magnesium Stearate). Chemical properties adapted from (31).

Component	Aqueous Solubility	Physical Form @ Room Temperature	Melting Point (°C)
Ascorbyl Palmitate	Practically Insoluble	Powder	107-117
Sodium Stearyl Fumarate	1 in 20,000	Powder	224-225
Menthol	Practically insoluble	Powder	34

Table 4.7: Other Pharmaceutical Excipients with Properties Similar to Magnesium Stearate. Chemical properties adapted from (31).

4.3 MATERIALS AND METHODS

4.3.1 Materials:

Deferasirox and etravirine active pharmaceutical ingredients were sourced from Teva Active Pharmaceutical Ingredients (Teva TAPI, Petah Tikva, Israel). Copovidone, glyceryl monostearate, and crospovidone were sourced from BASF (BASF, Ludwigshafen, Germany). Glyceryl dibehenate was sourced from Gattefosse (Gattefosse, Paramus, NJ, USA). Sodium stearyl fumarate, microcrystalline cellulose, and aerosil were sourced from FMC Biopolymer (FMC, Philadelphia, PA, USA). Ascorbyl palmitate, stearic acid, stearyl alcohol, menthol, cetyl alcohol, menthol, sodium acetate, sodium chloride, sodium hydroxide, monobasic sodium phosphate monohydrate, and hydrochloric acid were sourced from Fisher Scientific (Hampton,

NH, USA). Magnesium stearate was sourced from Mutchler (Harrington Park, NJ, USA). Hypromellose capsules size 00EL were sourced from Capsugel (Capsugel, Morristown, NJ, USA). Hypromellose methocel E5 was sourced from Dow (Petaluma, CA, USA). Vitamin E polyethylene glycol succinate was sourced from Antares (Ewing Township, NJ, USA). Mannitol was sourced from Millipore Sigma (Millipore Sigma, St. Louis, MO, USA). FaSSGF, FaSSIF, FeSSIF powder was sourced from Biorelevant (Biorelevant.com, London, UK). Ritonavir was sourced from a confidential supplier. PEG 8000 was sourced from Letco Medical (Decatur, AL, USA).

4.3.2 X-Ray Diffraction Analysis for All Samples:

Powder X-ray diffraction was performed on a MiniFlex 600 XRD unit (Rigaku, The Woodlands, TX, USA). Samples were loaded into metal sample holders and leveled prior to analysis. The instrument was configured with a Cu alpha radiation tube and was operated at 40 kV and 15 mA. The detector was a D/teX Ultra unit. A scan speed of 5.0 degrees/minute was used with a step size of 0.02 degrees across a range of 2-30 2theta. PDXL software package was used for data analysis (Rigaku, The Woodlands, TX, USA).

4.3.3 KinetiSol Processing of DFX-Lubricant Examples:

Samples containing deferasirox, copovidone, and an appropriate lubricant were processed into amorphous solid dispersions by KinetiSol processing. Formulation information is contained in

Table 4.8. Materials were dispensed into a plastic bag and mixed by hand for at least 1 minute. 10 grams of sample blend was loaded into a KBC20 KinetiSol Research Formulator (DisperSol Technologies, Georgetown, TX, USA) and processed at 7000 rpm to an ejection temperature of 150°C. Ejected material was manually quenched between two metal plates into an amorphous sheet. The amorphous material was milled in an IKA tube mill 100 (IKA, Staufen, Germany) at 5000 rpm in 30 second intervals. Between intervals, samples were passed through a No. 60 mesh screen (250 μm) with the coarse particles recycled into the tube mill. All samples processed until fully milled and all samples were confirmed as x-ray amorphous by the XRD method previously described.

Component	Lot 2	Lot 3	Lot 4	Lot 5	Lot 6	Lot 7	Lot 8	Lot 9	Lot 23	Lot 25
Deferasirox (DFX)	50	50	50	50	50	50	50	50	50	50
Copovidone	49	49	49	49	49		49	49	50	49
Glyceryl dibehenate	1									
Sodium stearyl fumarate		1								
Ascorbyl palmitate			1							
Stearic acid				1						
Stearyl alcohol					1					
Menthol						1				
Glyceryl monostearate							1			
Cetyl alcohol								1		
Magnesium stearate										1

Table 4.8: Formulation Information for DFX-Lubricant Compositions Processed by KinetiSol. Numerical Values are % w/w.

4.3.4 Dissolution Testing of Deferasirox-Lubricant Examples:

Dissolution testing was performed on Distek 2500 dissolution system (Distek, North Brunswick, NJ, USA). The unit was configured as Apparatus 2 with paddle speed at 50 rpm. 750 mL of 50 mM sodium acetate buffer, pH 5 was added to each vessel and heated to 37°C. 150 mg of deferasirox amorphous intermediate was loaded into size 00EL hypromellose capsules. One capsule per sample was dropped into each vessel using stainless steel sinkers just prior to test initiation. A Spectra fiber optic UV-Vis probe (Pion Inc, Billerica, MA, USA) monitored drug concentration in solution with data points collected every 5 minutes for 4 hours total run time. A wavelength of 295 nm was used for data acquisition with a baseline correction of 400 nm. Data was analyzed by AU Pro software (Pion Inc., Billerica, MA, USA).

4.3.5 KinetiSol Processing and Tableting of Etravirine-Lubricant Examples:

Samples containing etravirine, hypromellose E5, and vitamin E polyethylene glycol succinate with sodium stearyl fumarate in one iteration were processed into amorphous solid dispersions by KinetiSol processing. Formulation information is contained in Table 4.9. Materials were dispensed into a plastic bag and mixed by hand for at least 1 minute. 100 grams of sample blend was loaded into a KBC250 KinetiSol Batch Compounder (DisperSol Technologies, Georgetown, TX, USA) and processed at 2500 rpm to an ejection temperature of 170°C. Ejected material was quenched in a pneumatic chill press (DisperSol Technologies, Georgetown, TX, USA) into an amorphous sheet. The amorphous material was milled in a L1A Fitzmill (Fitzpatrick, Waterloo,

ON, CA) at 9000 rpm with hammers forward and passed through a 250 µm screen. All samples were confirmed as x-ray amorphous by the XRD method previously described.

Component	Lot 30025	Lot 30026
Etravirine (ETV)	20	20
Hypromellose, E5 grade (HPMC E5)	75	74
Vitamin E Polyethylene Glycol Succinate (TPGS)	5	5
Sodium stearyl fumarate (SSF)	0	1

Table 4.9: Formulation Information for Amorphous Solid Dispersions Containing Etravirine and With or Without Sodium Stearyl Fumarate. Numerical values are % w/w.

Tablet blends were prepared per Table 4.10 with amorphous intermediate screened through a 125 µm screen. Tablets were compressed using a single-station automated tablet press and were prepared at strengths of 25, 100, and 200 mg strengths.

Component	Lot 30025	Lot 30026
Etravirine (ETV)	14.29	14.29
Hypromellose, E5 grade (HPMC E5)	53.57	52.86
Vitamin E Polyethylene Glycol Succinate (TPGS)	3.57	3.57
Sodium stearyl fumarate (SSF)	0.00	0.71
Mannitol	10.00	10.00
Microcrystalline cellulose	10.00	10.00
Crospovidone	7.07	7.07
Colloidal silicon dioxide	0.50	0.50
Magnesium stearate	1.00	1.00

Table 4.10: Formulation Information for Tablets Containing Etravirine Amorphous Solid Dispersions With or Without Sodium Stearyl Fumarate. Numerical values are % w/w.

4.3.6 Dissolution Testing of Etravirine-Lubricant Examples:

Dissolution testing was performed on Vankel 7000 dissolution system (Agilent, Santa Clara, CA, USA). The unit was configured as Apparatus 2 with paddle speed at 70 rpm. FaSSIF dissolution media was prepared per the procedure provided with the FaSSGF, FaSSIF, and FeSSIF powder and with sodium chloride, sodium hydroxide, and monobasic sodium phosphate monohydrate as salts for the buffer precursor preparation. 900 mL of FaSSIF media was added to each vessel and heated to 37°C. One tablet per sample was dropped into each vessel just prior to test initiation.

100 mg and 200 mg tablets were used in dissolution testing. A Spectra fiber optic UV-Vis probe (Pion Inc, Billerica, MA, USA) monitored drug concentration in solution with data points collected every 5 minutes for 6 hours total run time. A wavelength of 310 nm was used for data acquisition with a baseline correction at 380 nm. Data was analyzed by AU Pro software (Pion Inc., Billerica, MA, USA).

4.3.7 In-Vivo Pharmacokinetic Analysis of Etravirine-Lubricant Examples:

An in-vivo pharmacokinetic study was conducted in fasted male beagle dogs at Charles Rivers Laboratories (Charles Rivers, Wilmington, MA, USA). Each animal was dosed with one 25 mg tablet followed by a 40 mL sterile water flush by oral gavage. Five dogs were used per arm. At time points of 0.5, 1, 1.5, 2, 3, 4, 6, and 12 hours, 1 mL of whole blood was collected with sodium heparin as an anticoagulant. Plasma was isolated and analyzed by a bioanalytical LC-MS/MS method for etravirine concentration. Pharmacokinetic analysis was conducted by Watson pharmacokinetic software (Fisher Scientific, Hampton, NH, USA).

4.3.8 Melt-Quenching of Ritonavir-Lubricant Examples:

In suitably sized beakers, PEG 8000 was slowly heated with stirring from an overhead impeller until fully melted. With stirring, ritonavir and sodium stearyl fumarate (when applicable) were slowly added to the melted PEG 8000 per the formulations summarized in Table 4.11. Composition was stirred with slight heat until a clear solution was formed. The melted

dispersions were dispensed into chilled pans to rapidly quench. Material collected from the pan was milled to form powder with an IKA tube mill 100 (IKA, Staufen, Germany) at 5000 rpm for 30 second intervals. Between intervals, sample was passed through a No. 60 mesh screen (250 μm) with the coarse particles recycled into the tube mill. All samples processed until fully milled. All samples were confirmed as x-ray amorphous with respect to ritonavir by the XRD method previously described.

Component	Lot 13	Lot 14
Ritonavir (RTV)	30	30
Polyethylene Glycol (PEG 8000)	70	69
Sodium Stearyl Fumarate (SSF)	0	1

Table 4.11: Formulation Information for Amorphous Solid Dispersions Containing Etravirine and With or Without Sodium Stearyl Fumarate. Numerical values are % w/w.

4.3.9 Dissolution Testing of Ritonavir-Lubricant Examples:

Dissolution testing was performed on Distek 2500 dissolution system (Distek, North Brunswick, NJ, USA). The unit was configured as Apparatus 2 with paddle speed at 50 rpm. 750 mL of 0.1N hydrochloric acid was added to each vessel and heated to 37°C. 333 mg of ritonavir amorphous intermediate representing 100 mg of ritonavir was dispersed on the surface of the dissolution

media. Three vessels were analyzed per test article. At time points of 10, 20, 30, 45, and 60 minutes, 5 mL of sample was sampled by cannula and filtered through 0.45 µm PVDF syringe filters with glass membrane pre-filters. Filtered samplers were diluted 1:1 with acetonitrile and transferred to HPLC vials after mixing. An isocratic water/acetonitrile HPLC method was used for analysis with an Acclaim™ 120, C18, 5µm, 120A, 4.6x150mm, P/N: 059148 (Thermo Fisher Scientific, Waltham, MA, USA) HPLC column for separation. The ritonavir peak was analyzed at 240 nm.

4.4 RESULTS

4.4.1 X-ray Powder Diffraction:

All samples analyzed were fully x-ray amorphous except for the ritonavir/PEG-8000 solid dispersions. Peaks associated with PEG-8000's crystalline structure were observed, but no peaks associated with crystalline ritonavir were observed.

4.4.2 Deferasirox-Lubricants:

The dissolution figures for deferasirox amorphous solid dispersions with various lubricants are shown in Figure 4.5. The sample containing magnesium stearate as the additive had the highest release, followed by a cluster of release profiles that contained glyceryl dibehenate, sodium stearyl fumarate, ascorbyl palmitate, stearic acid, stearyl alcohol, glyceryl monostearate, and

cetyl alcohol. The sample without lubricant released to lower extent than the cluster followed by the sample that contained menthol which exhibited the lowest overall release.

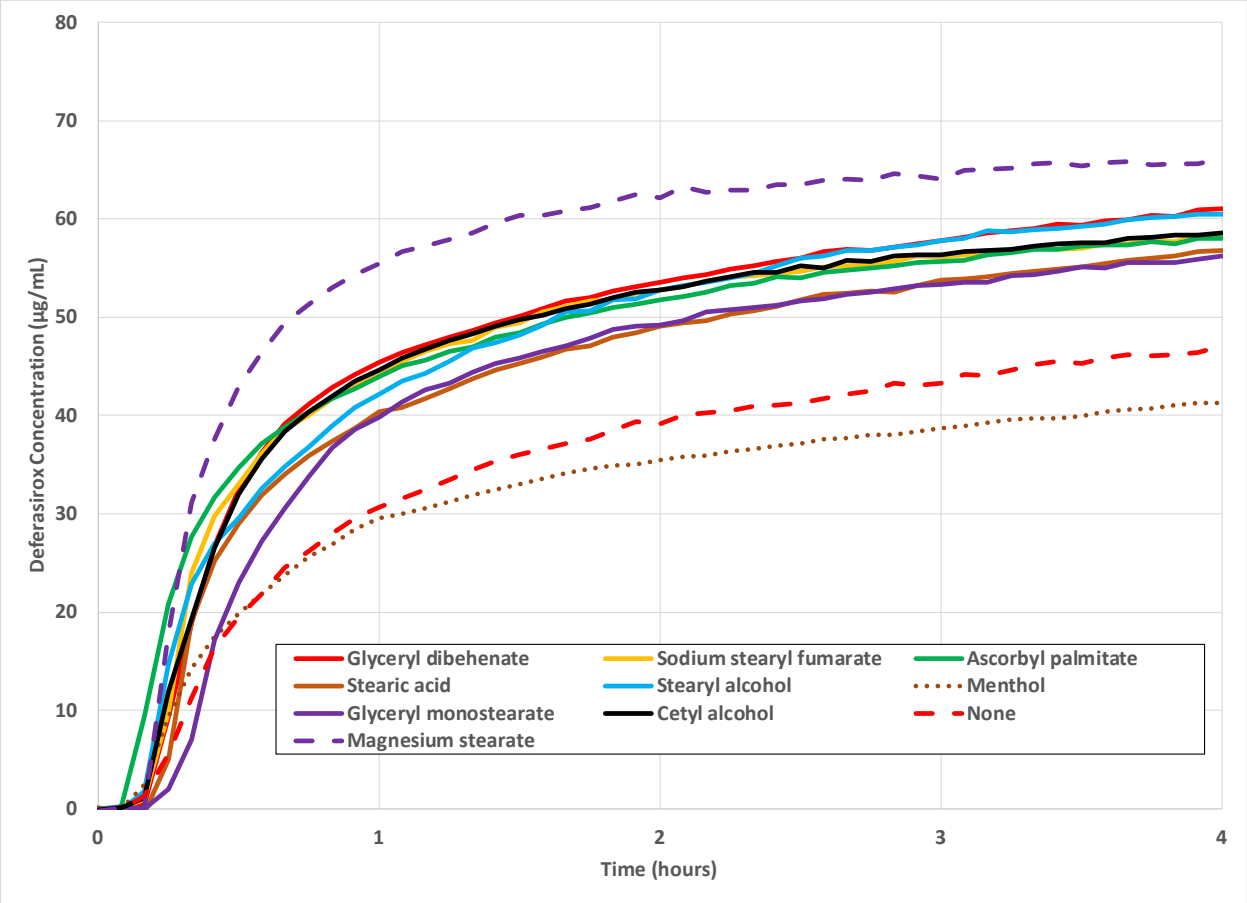

Figure 4.5: Dissolution Testing of Amorphous Solid Dispersions Containing Deferasirox and Various Pharmaceutical Excipients with Lubricant-like Properties

4.4.3 Etravirine-Sodium Stearyl Fumarate with a Surfactant:

The dissolution figures for 100 and 200 mg etravirine tablets with and without sodium stearyl fumarate in the amorphous solid dispersion are shown in Figures 4.6a and 4.6b. For both tablet strengths, the sample containing sodium stearyl fumarate in the amorphous solid dispersion released to a greater extent and maintained a higher degree of supersaturation than the sample that did not contain sodium stearyl fumarate in the amorphous solid dispersion.

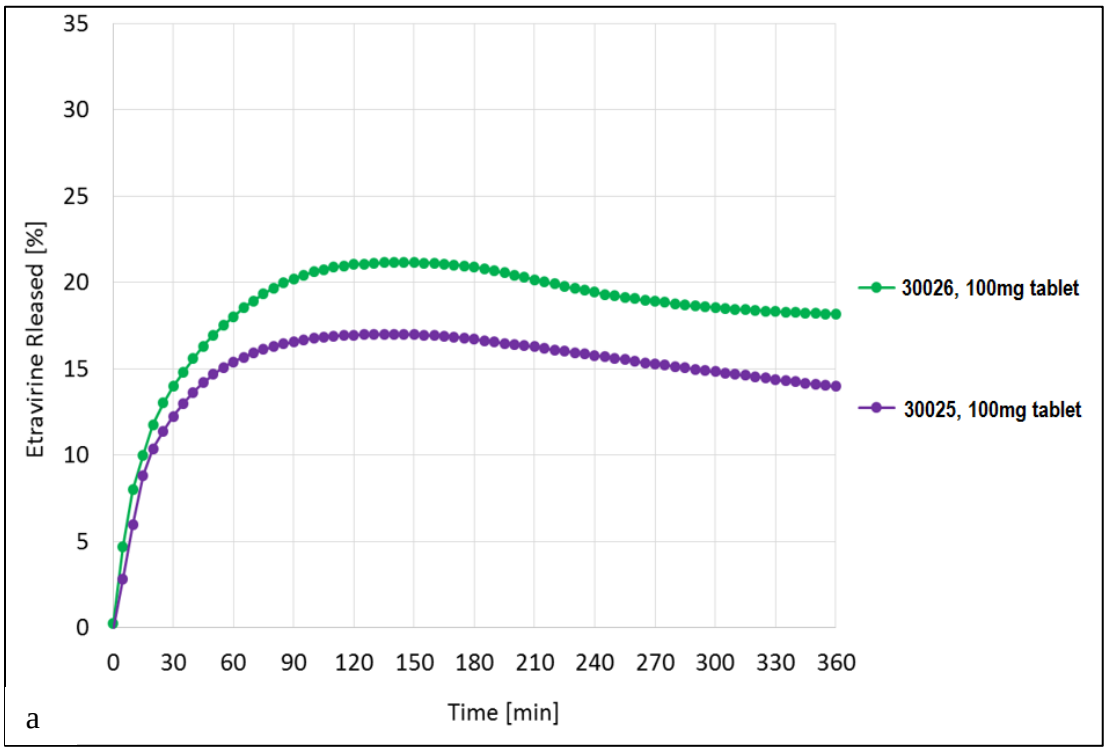

Figure 4.6: Dissolution Profiles for Etravirine from Tablets With (30026) and Without (30025) Sodium Stearyl Fumarate. a. 100 mg Tablets and b. 200 mg Tablets

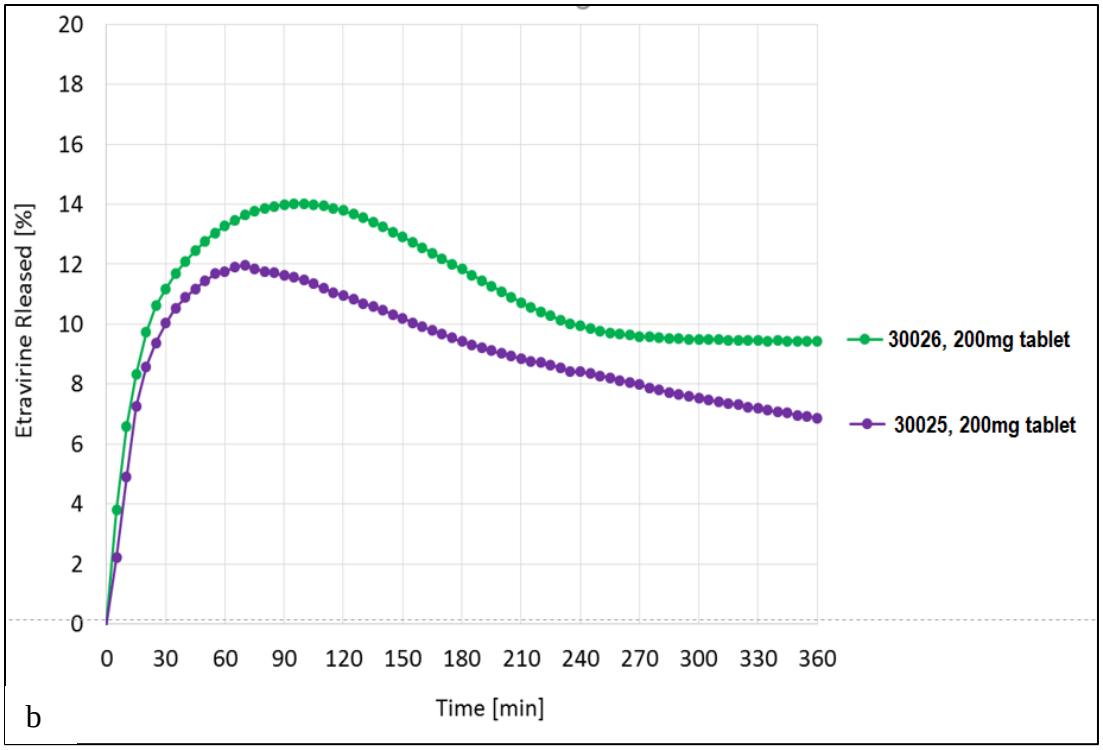

Figure 4.6, cont.

Etravirine blood plasma concentrations in the in-vivo pharmacokinetic study in fasted male beagle dogs is shown in Figure 4.7. The pharmacokinetic parameters are summarized in Table 4.12. The blood concentration reached an average Cmax of 433 ng/mL in the dogs dosed with the tablets that included sodium stearyl fumarate in the amorphous solid dispersion and to a Cmax of 327 ng/mL in the dogs dosed with the tablets did not include sodium stearyl fumarate. Similarly, AUC0-12 was 2486 ng*hr/mL in the sample with sodium stearyl fumarate and 2079 ng*hr/mL in the samples without. tmax values were 2.4 hours and 2.2 hours respectively.

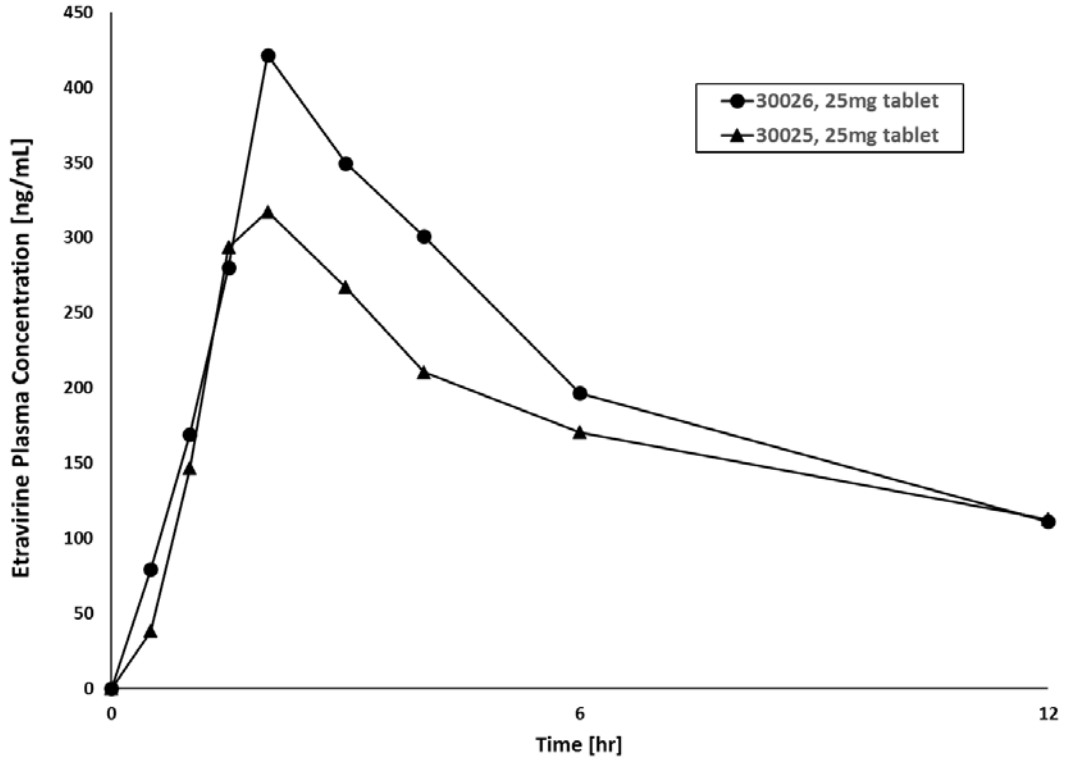

Figure 4.7: Etravirine Plasma Concentration for Pharmacokinetic Analysis of 25 mg Etravirine Tablet With (30026) and Without (30025) Sodium Stearyl Fumarate

Parameter	**30025**	**30026**
Cmax (ng/mL)	327 ± 120	433 ± 147
Tmax (hr)	2.2 ± 0.6	2.4 ± 0.9
AUC0→12 (ng*hr/mL)	2,080 ± 581	2,486 ± 946

Table 4.12: Summary of Pharmacokinetic Parameters for Analysis of Etravirine Tablets With (30026) and Without (30025) Sodium Stearyl Fumarate

4.4.4 Ritonavir-Sodium Stearyl Fumarate by Melt Quenching:

The dissolution profiles for the ritonavir-PEG 8000 solid dispersions are shown in Figure 4.8. The sample that contained sodium stearyl fumarate exhibited a faster release rate and a greater maximum concentration (129 µg/mL) than the sample without sodium stearyl fumarate (104 µg/mL).

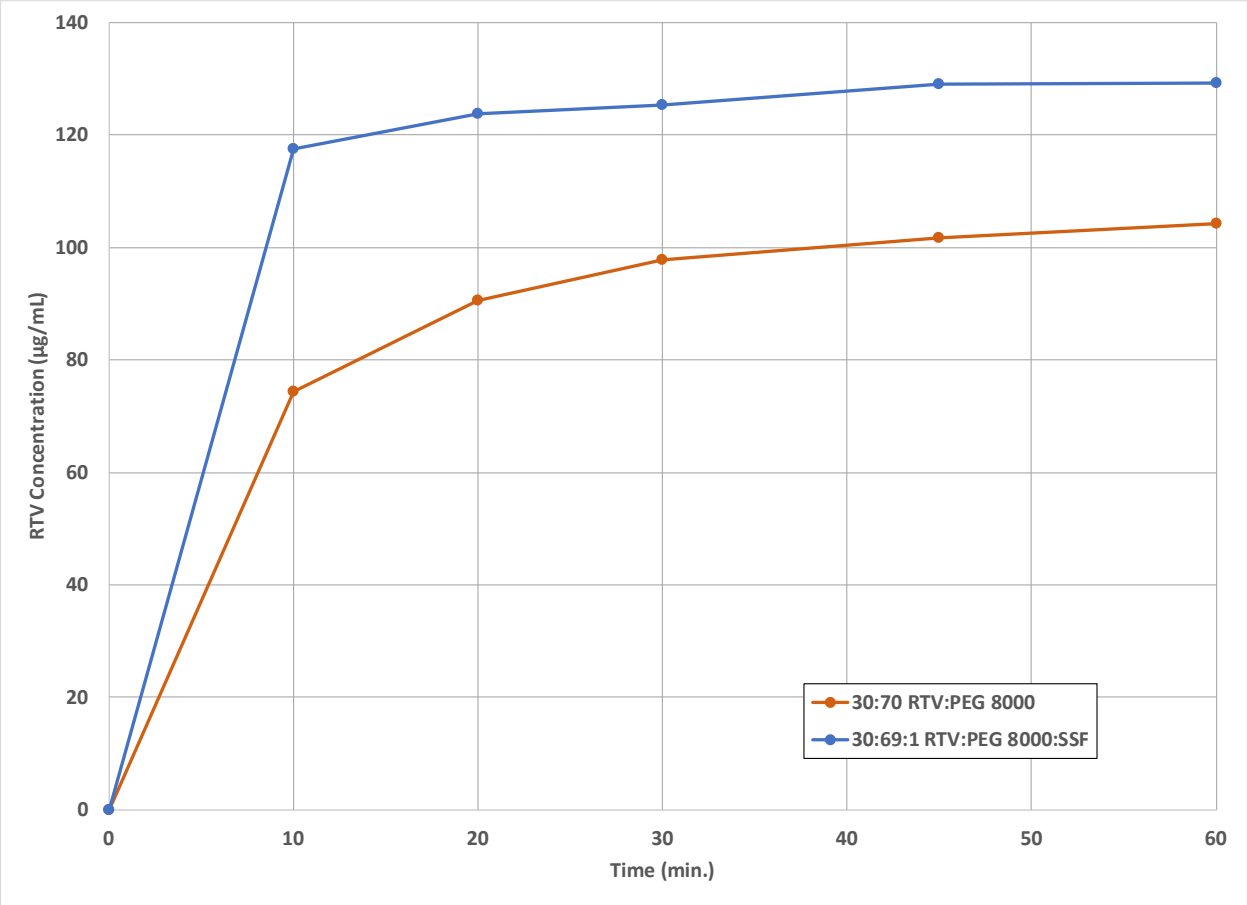

Figure 4.8: Dissolution Profiles for Ritonavir-PEG 8000 Melt-Quench Amorphous Solid Dispersions With and Without Sodium Stearyl Fumarate

4.5 DISCUSSION

4.5.1 Deferasirox-Lubricants:

For amorphous solid dispersions of deferasirox, in-vitro dissolution performance was enhanced for nearly all lubricants evaluated (see Figure 4.5). For all of these enhanced results, dissolution rate and concentration at 4 hours was higher than the sample that lacked a lubricant. These results substantiated the in-vivo pharmacokinetic result for deferasirox and magnesium stearate previously described. Deferasirox is a weak acid molecule and this example represents the opportunity to apply this formulation approach to other molecules in this classification. While weak acids are not as commonly benefitted by amorphous solid dispersions due to their increased solubility in media resembling intestinal pH (22), deferasirox is administered at high doses (>30 mg/kg) (23) and solubility enhanced formulations can reduce patient pill burden while maintaining overall exposure. (24)

In-vitro solubility enhancement was observed for stearyl alcohol, cetyl alcohol, stearic acid, glyceryl dibehenate, glyceryl monostearate, magnesium stearate, sodium stearyl fumarate, and ascorbyl palmitate. These positive results demonstrated the advantage of included fatty alcohols, fatty carboxylic acids, glyceryls, and stearates in amorphous solid dispersions for solubility benefits. By contrast, menthol represented a negative case in which in-vitro performance was diminished after its addition. While menthol shares many properties in common with the other entities explored, it lacks fatty acid chains present in all other examples. This likely speaks to the important role of the fatty chain to the performance of the amorphous solid dispersions.

Interestingly, magnesium stearate demonstrated a boosted effect beyond that observed for the other lubricants evaluated. Of note is that magnesium stearate possesses two fatty acid chains per molecule due to the +2 charge of the magnesium metal ion. However, this effect was not investigated further in this study.

4.5.2 Etravirine-Sodium Stearyl Fumarate with a Surfactant:

For amorphous solid dispersions containing etravirine and the lubricant sodium stearyl fumarate, both in-vitro and in-vivo performance enhancement were observed over the same formulation without lubricant in the amorphous solid dispersion (Figures 4.6a and 4.6b). During in-vitro analysis, drug release rate was faster for tablets containing amorphous solid dispersions with sodium stearyl fumarate and a higher dissolution Cmax was observed. Thus, the lubricant aided in spring portion of the spring-parachute model for the system. (25) Additionally, the tablets with sodium stearyl fumarate in the amorphous solid dispersion appeared to reach equilibrium concentrations of about 18% release and 9.5% release in the 100 mg and 200 mg tablets respectively. By contrast, the tablets without sodium stearyl fumarate appeared to not be at equilibrium after 6 hours of analysis with release values of approximately 14% and 6.5%, respectively, and declining. The higher in-solution concentration and achievement of equilibrium demonstrates the value of the sodium stearyl fumarate lubricant as an effective solubility maintaining parachute for etravirine. In the in-vivo pharmacokinetic analysis shown in Figure 4.7 and Table 4.12, the tablet with 1% sodium stearyl fumarate in the amorphous solid dispersion had 32% greater Cmax and 19.5% greater AUC0-12 than the tablet with the formulation that did

not include the lubricant in the amorphous solid dispersion. The positive results observed during in-vitro analysis translated to the in-vivo analysis.

At pharmaceutically relevant pH, etravirine is a non-ionic molecule with pH independent solubility. (26) These results suggest that lubricants can be applied to this classification of non-ionic drug molecules as well. Interestingly, the benefit was observed in a system where solubility was already expected to be benefitted by the inclusion of the tradition surfactant. (27) This result represents the advantage of a lubricant even for formulations benefitted by a surfactant. Finally, the demonstrated performance gains are both for in-vitro solubility enhancement and in-vivo drug absorption.

4.5.3 Ritonavir-Sodium Stearyl Fumarate by Melt-Quenching:

For the amorphous solid dispersion containing ritonavir and sodium stearyl fumarate, superior in-vitro dissolution performance was observed when compared to a formulation that did not include sodium stearyl fumarate in the dispersion (see Figure 4.8). The sample containing sodium stearyl fumarate released much more rapidly than the sample without sodium stearyl fumarate. 91% of observed release occurred by the 10 minute time point for sodium stearyl fumarate sample compared to 71% at the same time point. Additionally, 24% higher in-solution concentration was observed for the sodium stearyl fumarate sample compared to the one without lubricant at the 1 hour time point of dissolution analysis. Release rate and extent of ritonavir in 0.1N hydrochloric acid has been shown to correlate well with in-vivo results for ritonavir:PEG 8000 amorphous solid dispersions. (28)

This positive example for the weakly basic ritonavir molecule represents the potential value of including lubricants in amorphous solid dispersions for the weakly basic compounds. Weak base molecules are of high interest for development into amorphous solid dispersions due to their inherently poor aqueous solubility at intestinal absorption sites. (29, 30) Of note is that prior examples were generated with KinetiSol processing, but this ritonavir:PEG 8000 system utilized melt-quenching to process the material into an amorphous solid dispersion. Melt quenching (or melt cooling) can be used to represent fusion based processes such as hot-melt extrusion or KinetiSol processing. (4) Thus, a successful result with a lubricant via the melt-quench process lends itself to the expectation that inclusion of a lubricant would benefit other fusion based processes. As mentioned previously, solvent processing of amorphous solid dispersions containing lubricants would represent a significant challenge as these components are practically insoluble in solvents typically utilized for solvent evaporation processes.

4.6 CONCLUSION

As a result of the work conducted in this study, it was concluded that inclusion of lubricants internally in an amorphous solid dispersion can be utilized as a tool for enhancing the in-vitro and in-vivo performance of poorly water soluble drugs. The benefit was observed in drug molecules that represented weak acid, neutral, and weak base compounds. Lubricants that presented a performance advantage include fatty alcohols, fatty acids, glyceryls, stearates, sodium stearyl fumarate and ascorbyl palmitate. The performance advantage was observed in systems that included a traditional surfactant which promises the opportunity to use lubricants in

conjunction with systems that contain these components. Successful demonstration by melt-quenching in addition to KinetiSol processing showed that the process was applicable to a multitude of thermal and fusion processes utilized in the production of amorphous solid dispersions.

4.7 REFERENCES:

1. Loftsson T, Brewster ME. Pharmaceutical applications of cyclodextrins: basic science and product development. Journal of pharmacy and pharmacology. 2010;62(11):1607-21.
2. Crew M. BIOAVAILABILITY ENHANCEMENT - A New Year for Solubility Enhancement. Drug Development and Delivery. 2014.
3. Jermain SV, Brough C, Williams RO. Amorphous Solid Dispersions and Nanocrystal Technologies for Poorly Water-Soluble Drug Delivery–An Update. International Journal of Pharmaceutics. 2017.
4. He Y, Ho C. Amorphous solid dispersions: utilization and challenges in drug discovery and development. Journal of pharmaceutical sciences. 2015;104(10):3237-58.
5. Lipinski CA. Drug-like properties and the causes of poor solubility and poor permeability. Journal of pharmacological and toxicological methods. 2000;44(1):235-49.
6. Bergström CA, Charman WN, Porter CJ. Computational prediction of formulation strategies for beyond-rule-of-5 compounds. Advanced drug delivery reviews. 2016;101:6-21.
7. Leeson PD. Molecular inflation, attrition and the rule of five. Advanced drug delivery reviews. 2016;101:22-33.

8. Zelboraf® Tablets, Roche 2011 [cited FDA. Available from: https://www.accessdata.fda.gov/drugsatfda_docs/nda/2011/202429Orig1s000ClinPharmR.pdf.

9. Ghany MG, Nelson DR, Strader DB, Thomas DL, Seeff LB. An update on treatment of genotype 1 chronic hepatitis C virus infection: 2011 practice guideline by the American Association for the Study of Liver Diseases. Hepatology. 2011;54(4):1433-44.

10. Goldinger SM, Rinderknecht J, Dummer R, Kuhn FP, Yang KH, Lee L, et al. A single-dose mass balance and metabolite-profiling study of vemurafenib in patients with metastatic melanoma. Pharmacology research & perspectives. 2015;3(2).

11. Ellenberger DJM, Dave A; and Williams, Robert O. Expanding the Application and Formulation Space of Amorphous Solid Dispersions with KinetiSol®: A Review. AAPS PharmSciTech. 2017 (Accepted).

12. Li J, Wu Y. Lubricants in pharmaceutical solid dosage forms. Lubricants. 2014;2(1):21-43.

13. Llusa M, Levin M, Snee RD, Muzzio FJ. Measuring the hydrophobicity of lubricated blends of pharmaceutical excipients. Powder Technology. 2010;198(1):101-7.

14. Shah A, Mlodozeniec A. Mechanism of surface lubrication: Influence of duration of lubricant-excipient mixing on processing characteristics of powders and properties of compressed tablets. Journal of pharmaceutical sciences. 1977;66(10):1377-82.

15. Chowhan Z, Chi LH. Drug-excipient interactions resulting from powder mixing IV: Role of lubricants and their effect on in vitro dissolution. Journal of pharmaceutical sciences. 1986;75(6):542-5.

16. Shah N, Stiel D, Weiss M, Infeld M, Malick A. Evaluation of two new tablet lubricants-sodium stearyl fumarate and glyceryl behenate. Measurement of physical parameters

(compaction, ejection and residual forces) in the tableting process and the effect on the dissolution rate. Drug Development and Industrial Pharmacy. 1986;12(8-9):1329-46.

17. Hölzer AW, Sjögren J. Evaluation of sodium stearyl fumarate as a tablet lubricant. International Journal of Pharmaceutics. 1979;2(3):145-53.

18. Serajuddin A, Thakur AB, Ghoshal RN, Fakes MG, Ranadive SA, Morris KR, et al. Selection of solid dosage form composition through drug–excipient compatibility testing. Journal of pharmaceutical sciences. 1999;88(7):696-704.

19. Westerberg M, Nyström C. Physicochemical aspects of drug release. XII. The effect of some carrier particle properties and lubricant admixture on drug dissolution from tableted ordered mixtures. International journal of pharmaceutics. 1991;69(2):129-41.

20. Kuno Y, Kojima M, Nakagami H, Yonemochi E, Terada K. Effect of the type of lubricant on the characteristics of orally disintegrating tablets manufactured using the phase transition of sugar alcohol. European Journal of Pharmaceutics and Biopharmaceutics. 2008;69(3):986-92.

21. Van den Mooter G. The use of amorphous solid dispersions: A formulation strategy to overcome poor solubility and dissolution rate. Drug Discovery Today: Technologies. 2012;9(2):e79-e85.

22. Aggarwal S, Gupta G, Chaudhary S. Solid dispersion as an eminent strategic approach in solubility enhancement of poorly soluble drugs. International journal of pharmaceutical sciences and research. 2010;1(8):1-13.

23. Taher A, Cappellini MD, Vichinsky E, Galanello R, Piga A, Lawniczek T, et al. Efficacy and safety of deferasirox doses of> 30 mg/kg per d in patients with transfusion-dependent anaemia and iron overload. British journal of haematology. 2009;147(5):752-9.

24. Miller DA, Keen JM, Kucera SU, inventors; DisperSol Technologies, LLC, assignee. Formulations of deferasirox and methods of making the same. United States patent application 15/185,888. 2016 Jun 17.

25. Guzmán HR, Tawa M, Zhang Z, Ratanabanangkoon P, Shaw P, Gardner CR, et al. Combined use of crystalline salt forms and precipitation inhibitors to improve oral absorption of celecoxib from solid oral formulations. Journal of pharmaceutical sciences. 2007;96(10):2686-702.

26. Mellaerts R, Fayad EJ, Van den Mooter G, Augustijns P, Rivallan Ml, Thibault-Starzyk Fdr, et al. In situ FT-IR investigation of etravirine speciation in pores of SBA-15 ordered mesoporous silica material upon contact with water. Molecular pharmaceutics. 2013;10(2):567-73.

27. Ramesh K, Shekar BC, Khadgapathi P, Bhikshapathi D, Gourav N. Enhancement of Solubility and Bioavailability of Etravirine Solid Dispersions by Solvent Evaporation Technique with Novel Carriers. IOSR Journal of Pharmacy and Biological Sciences. 2015;10(4):30-41.

28. Law D, Schmitt EA, Marsh KC, Everitt EA, Wang W, Fort JJ, et al. Ritonavir–PEG 8000 amorphous solid dispersions: in vitro and in vivo evaluations. Journal of pharmaceutical sciences. 2004;93(3):563-70.

29. Kostewicz ES, Wunderlich M, Brauns U, Becker R, Bock T, Dressman JB. Predicting the precipitation of poorly soluble weak bases upon entry in the small intestine. Journal of pharmacy and pharmacology. 2004;56(1):43-51.

30. Miller DA, DiNunzio JC, Yang W, McGinity JW, Williams III RO. Enhanced in vivo absorption of itraconazole via stabilization of supersaturation following acidic-to-neutral pH transition. Drug development and industrial pharmacy. 2008;34(8):890-902.

31. Rowe RC, Sheskey PJ, Weller PJ. Handbook of pharmaceutical excipients. 6th ed: Pharmaceutical press London; 2009.

32. Wang J, Wen H, Desai D. Lubrication in tablet formulations. European journal of pharmaceutics and biopharmaceutics. 2010;75(1):1-15.

33. Desai D, Rubitski B, Varia S, Newman A. Physical interactions of magnesium stearate with starch-derived disintegrants and their effects on capsule and tablet dissolution. International journal of pharmaceutics. 1993;91(2-3):217-26.

References

References:

1999. Mowiol Polyvinyl Alcohol. edited by Clariant.

2001. "FDA Guidance. Statistical approaches to establishing bioequivalence." Center for Drug Evaluation and Research. United States Food and Drug Administration.

2011a. "Food and Drug Administration. Center for Drug Evaluation and Research." Clinical Pharmacology and Biopharmaceutics Review (s) 202-429 (0).

2011b. "Zelboraf® Tablets, Roche." https://www.accessdata.fda.gov/drugsatfda_docs/nda/2011/202429Orig1s000ClinPharmR.pdf.

2016. AquaSolve Hydroxypropylmethylcellulose Acetate Succinate. edited by Ashland.

Aggarwal, Shikha, GD Gupta, and Sandeep Chaudhary. 2010. "Solid dispersion as an eminent strategic approach in solubility enhancement of poorly soluble drugs." International journal of pharmaceutical sciences and research 1 (8):1-13.

Akimoto, Masayuki, Naokazu Nagahata, Atsushi Furuya, Kiyomi Fukushima, Shohei Higuchi, and Toshio Suwa. 2000. "Gastric pH profiles of beagle dogs and their use as an alternative to human testing." European journal of pharmaceutics and biopharmaceutics 49 (2):99-102.

Albano, A.A., D. Desai, J. Dinunzio, Z. Go, R.M. Iyer, H.K. Sandhu, and N.H. Shah. Pharmaceutical composition with improved bioavailability for high melting hydrophobic compound. United States: Hoffmann-La Roche Inc.

Albano, A.A., D. Desai, J. Dinunzio, Z. Go, R.M. Iyer, H.K. Sandhu, and N.H. Shah. 2013. Pharmaceutical composition with improved bioavailability for high melting hydrophobic compound. WIPO Patent Application WO2013087546 A1.

Alexy, Pavol, Darina Kachova, Miroslav Kršiak, Dušan Bakoš, and Barbora Šimková. 2002. "Poly (vinyl alcohol) stabilisation in thermoplastic processing." Polymer Degradation and Stability 78 (3):413-421.

Alexy, Pavol, Igor Lacík, Barbora Šimková, Dušan Bakoš, Nad'a Prónayová, Tibor Liptaj, Silvia Hanzelová, and Mária Várošová. 2004. "Effect of melt processing on thermo-mechanical degradation of poly (vinyl alcohol) s." Polymer Degradation and stability 85 (2):823-830.

Ambike, Anshuman A, KR Mahadik, and Anant Paradkar. 2005. "Spray-dried amorphous solid dispersions of simvastatin, a low Tg drug: in vitro and in vivo evaluations." Pharmaceutical research 22 (6):990-998.

Amidon, Gordon L, Hans Lennernäs, Vinod P Shah, and John R Crison. 1995. "A theoretical basis for a biopharmaceutic drug classification: the correlation of in vitro drug product dissolution and in vivo bioavailability." Pharmaceutical research 12 (3):413-420.

Andreone, Pietro, Massimo G Colombo, Jeffrey V Enejosa, Iftihar Koksal, Peter Ferenci, Andreas Maieron, Beat Müllhaupt, Yves Horsmans, Ola Weiland, and Henk W Reesink. 2014. "ABT-450, ritonavir, ombitasvir, and dasabuvir achieves 97% and 100% sustained virologic response with or without ribavirin in treatment-experienced patients with HCV genotype 1b infection." Gastroenterology 147 (2):359-365. e1.

Andrews, Gavin P, David S Jones, Osama Abu Diak, Colin P McCoy, Alan B Watts, and James W McGinity. 2008. "The manufacture and characterisation of hot-melt extruded enteric tablets." European journal of pharmaceutics and Biopharmaceutics 69 (1):264-273.

Avdeef, Alex, Stefanie Bendels, Li Di, Bernard Faller, Manfred Kansy, Kiyohiko Sugano, and Yukinori Yamauchi. 2007. "PAMPA—critical factors for better predictions of absorption." Journal of Pharmaceutical Sciences 96 (11):2893-2909. doi: 10.1002/jps.21068.

Baert, Lieven Elvire Colette, Geert Verreck, and Dany Thoné. Antifungal compositions with improved bioavailability. United States: Janssen Pharmaceutica NV.

Baird, Jared A, Bernard Van Eerdenbrugh, and Lynne S Taylor. 2010. "A classification system to assess the crystallization tendency of organic molecules from undercooled melts." Journal of pharmaceutical sciences 99 (9):3787-3806.

Banerjee, Amrita, JooHee Lee, and Samir Mitragotri. 2016. "Intestinal mucoadhesive devices for oral delivery of insulin." Bioengineering & Translational Medicine.

Banik, Manas, Shanmukha Prasad Gopi, Somnath Ganguly, and Gautam R Desiraju. 2016. "Cocrystal and salt forms of furosemide: solubility and diffusion variations." Crystal Growth & Design 16 (9):5418-5428.

Basavoju, Srinivas, Dan Boström, and Sitaram P Velaga. 2008. "Indomethacin–saccharin cocrystal: design, synthesis and preliminary pharmaceutical characterization." Pharmaceutical research 25 (3):530-541.

Bashiri-Shahroodi, Amir, Parya Reisi Nassab, Piroska Szabó-Révész, and Róbert Rajkó. 2008. "Preparation of a solid dispersion by a dropping methodto improve the rate of dissolution of meloxicam." Drug development and industrial pharmacy 34 (7):781-788.

Benet, Leslie Z, Chi-Yuan Wu, and Joseph M Custodio. 2006. "Predicting drug absorption and the effects of food on oral bioavailability." Bulletin Technique Gattefosse 99:9-16.

Bennett, Ryan C, Chris Brough, Dave A Miller, Kevin P O'Donnell, Justin M Keen, Justin R Hughey, Robert O Williams III, and James W McGinity. 2015. "Preparation of amorphous solid dispersions by rotary evaporation and KinetiSol Dispersing: approaches to enhance solubility of a poorly water-soluble gum extract." Drug development and industrial pharmacy 41 (3):382-397.

Bergström, Christel AS, William N Charman, and Christopher JH Porter. 2016. "Computational prediction of formulation strategies for beyond-rule-of-5 compounds." Advanced drug delivery reviews 101:6-21.

Berndl, G., J. Rosenberg, B. Liepold, K. Fastnacht, T. Jung, W. Roth, J. Breitenbach, J. Morris, C.E. Klein, and Y. Cai. Solid pharmaceutical dosage formulations. United States: Abbott Laboratories.

Berndl, Gunther, Matthias Degenhardt, Markus Mäegerlein, and Gerrit Dispersyn. Itraconazole compositions with improved bioavailability. United States: Abbott Gmbh & Co. and Kg.

Beten, DB, Michel Gelbcke, Bilo Diallo, and AJ Moes. 1992. "Interaction between dipyridamole and Eudragit S." International journal of pharmaceutics 88 (1-3):31-37.

Bevernage, Jan, Joachim Brouwers, Marcus E Brewster, and Patrick Augustijns. 2013. "Evaluation of gastrointestinal drug supersaturation and precipitation: strategies and issues." International journal of pharmaceutics 453 (1):25-35.

Bhattachar, Shobha N, Everett J Perkins, Jeffrey S Tan, and Lee J Burns. 2011. "Effect of gastric pH on the pharmacokinetics of a bcs class II compound in dogs: Utilization of an

artificial stomach and duodenum dissolution model and gastroplus,™ simulations to predict absorption." Journal of pharmaceutical sciences 100 (11):4756-4765.

Bollag, Gideon, James Tsai, Jiazhong Zhang, Chao Zhang, Prabha Ibrahim, Keith Nolop, and Peter Hirth. 2012. "Vemurafenib: the first drug approved for BRAF-mutant cancer." Nature reviews. Drug discovery 11 (11):873.

Borbás, Enikő, Bálint Sinkó, Oksana Tsinman, Konstantin Tsinman, Éva Kiserdei, Balázs Démuth, Attila Balogh, Brigitta Bodák, András Domokos, and Gergő Dargó. 2016. "Investigation and mathematical description of the real driving force of passive transport of drug molecules from supersaturated solutions." Molecular pharmaceutics 13 (11):3816-3826.

Brayer, Samuel W, and K Rajender Reddy. 2015. "Ritonavir-boosted protease inhibitor based therapy: a new strategy in chronic hepatitis C therapy." Expert review of gastroenterology & hepatology 9 (5):547-558.

Broadhead, J, SK Edmond Rouan, and CT Rhodes. 1992. "The spray drying of pharmaceuticals." Drug Development and Industrial Pharmacy 18 (11-12):1169-1206.

Brostow, Witold, Rachel Chiu, Ioannis M Kalogeras, and Aglaia Vassilikou-Dova. 2008. "Prediction of glass transition temperatures: binary blends and copolymers." Materials Letters 62 (17):3152-3155.

Brough, Chris, James W McGinity, Dave A Miller, Jim C DiNunzio, and Robert O Williams. Thermo-kinetic mixing for pharmaceutical applications. United States: DisperSol Technologies, LLC.

Brough, Chris, Dave A Miller, Daniel Ellenberger, Dieter Lubda, and Robert O Williams III. 2016. "Use of Polyvinyl Alcohol as a Solubility Enhancing Polymer for Poorly Water-Soluble Drug Delivery (Part 2)." AAPS PharmSciTech 17 (1):180-190.

Brough, Chris, Dave A Miller, Justin M Keen, Shawn A Kucera, Dieter Lubda, and Robert O Williams III. 2016. "Use of polyvinyl alcohol as a solubility-enhancing polymer for poorly water soluble drug delivery (part 1)." AAPS PharmSciTech 17 (1):167-179.

Brough, Chris, and R. O. Williams Iii. 2013. "Amorphous solid dispersions and nano-crystal technologies for poorly water-soluble drug delivery." International Journal of Pharmaceutics 453 (1):157-166. doi: http://dx.doi.org/10.1016/j.ijpharm.2013.05.061.

Brouwers, Joachim, Marcus E Brewster, and Patrick Augustijns. 2009. "Supersaturating drug delivery systems: The answer to solubility-limited oral bioavailability?" Journal of pharmaceutical sciences 98 (8):2549-2572.

Brown, Chad, James DiNunzio, Michael Eglesia, Seth Forster, Matthew Lamm, Michael Lowinger, Patrick Marsac, Craig McKelvey, Robert Meyer, and Luke Schenck. 2014. "Hot-melt extrusion for solid dispersions: composition and design considerations." In Amorphous Solid Dispersions, 197-230. Springer.

Bruce, Caroline, Kurt A Fegely, Ali R Rajabi-Siahboomi, and James W McGinity. 2007. "Crystal growth formation in melt extrudates." International journal of pharmaceutics 341 (1):162-172.

Budha, NR, A Frymoyer, GS Smelick, JY Jin, MR Yago, MJ Dresser, SN Holden, LZ Benet, and JA Ware. 2012. "Drug Absorption Interactions Between Oral Targeted Anticancer Agents and PPIs: Is pH-Dependent Solubility the Achilles Heel of Targeted Therapy?" Clinical Pharmacology & Therapeutics 92 (2):203-213.

Cameron, D William, Margo Heath-Chiozzi, Sven Danner, Calvin Cohen, Stephen Kravcik, Clement Maurath, Eugene Sun, David Henry, Richard Rode, and Amy Potthoff. 1998. "Randomised placebo-controlled trial of ritonavir in advanced HIV-1 disease." The Lancet 351 (9102):543-549.

Cardamone, Jeanette M. 2013. "Keratin sponge/hydrogel II: Active agent delivery." Textile research journal 83 (9):917-927.

Cavalli, Roberta, Elena Peira, Otto Caputo, and Maria Rosa Gasco. 1999. "Solid lipid nanoparticles as carriers of hydrocortisone and progesterone complexes with β-cyclodextrins." International journal of pharmaceutics 182 (1):59-69.

Chandanais, Ryan. 2015. "Specialty drug approvals: Review of 2014 and a forecast for 2015." Pharmacy Today 21 (1):50-51.

Chen, Changyi, Xiang-Huai Lu, Shaoyu Yan, Hong Chai, and Qizhi Yao. 2005. "HIV protease inhibitor ritonavir increases endothelial monolayer permeability." Biochemical and biophysical research communications 335 (3):874-882.

Chhabda, Pawanjeet J, M Balaji, V Srinivasarao, and KM Ch Appa Rao. "Development and validation of a new simple and stability indicating RP-HPLC method for the determination of vemurafenib in presence of degradant products."

Chirnomas, Deborah, Amber Lynn Smith, Jennifer Braunstein, Yaron Finkelstein, Luis Pereira, Anke K Bergmann, Frederick D Grant, Carole Paley, Michael Shannon, and Ellis J Neufeld. 2009. "Deferasirox pharmacokinetics in patients with adequate versus inadequate response." Blood 114 (19):4009-4013.

Chow, TS. 1980. "Molecular interpretation of the glass transition temperature of polymer-diluent systems." Macromolecules 13 (2):362-364.

Chowhan, ZT, and Li-Hua Chi. 1986. "Drug-excipient interactions resulting from powder mixing IV: Role of lubricants and their effect on in vitro dissolution." Journal of pharmaceutical sciences 75 (6):542-545.

Coppens, Karen, Mark Hall, Pam Larsen, Shawn Mitchell, P Nguyen, Mike Read, Uma Shrestha, and Parvinder Walia. 2004. "Thermal and rheological evaluation of pharmaceutical excipients for hot melt extrusion." AAPS Annual Meeting and Exposition, Baltimore, MD.

Corbett, Amanda H, Michael L Lim, and Angela DM Kashuba. 2002. "Kaletra (lopinavir/ritonavir)." Annals of Pharmacotherapy 36 (7-8):1193-1203.

Crew, Marshall. 2014. "BIOAVAILABILITY ENHANCEMENT - A New Year for Solubility Enhancement." Drug Development and Delivery.

Crommentuyn, KML, BS Kappelhoff, JW Mulder, ATA Mairuhu, ECM Van Gorp, PL Meenhorst, ADR Huitema, and JH Beijnen. 2005. "Population pharmacokinetics of lopinavir in combination with ritonavir in HIV-1-infected patients." British journal of clinical pharmacology 60 (4):378-389.

Crowley, Michael M, Feng Zhang, Michael A Repka, Sridhar Thumma, Sampada B Upadhye, Sunil Kumar Battu, James W McGinity, and Charles Martin. 2007. "Pharmaceutical applications of hot-melt extrusion: part I." Drug development and industrial pharmacy 33 (9):909-926.

Curatolo, William, James A Nightingale, and Scott M Herbig. 2009. "Utility of hydroxypropylmethylcellulose acetate succinate (HPMCAS) for initiation and maintenance of drug supersaturation in the GI milieu." Pharmaceutical research 26 (6):1419-1431.

CYP2C9, CYP2C19, and CYP3A4 CYP2D6. 2007. "The effect of cytochrome P450 metabolism on drug response, interactions, and adverse effects." Am Fam Physician 76:391-6.

Dahan, Arik, Jonathan M Miller, and Gordon L Amidon. 2009. "Prediction of solubility and permeability class membership: provisional BCS classification of the world's top oral drugs." The AAPS journal 11 (4):740-746.

Darji, Mittal A, Rahul M Lalge, Sushrut P Marathe, Tarul D Mulay, Tasnim Fatima, Alia Alshammari, Hyung Kyung Lee, Michael A Repka, and S Narasimha Murthy. 2017. "Excipient Stability in Oral Solid Dosage Forms: A Review." AAPS PharmSciTech:1-15.

de Weger, VA, FE Stuurman, M Mergui-Roelvink, B Nuijen, ADR Huitema, JH Beijnen, JHM Schellens, and S Marchetti. 2016. "A phase I dose-escalation trial of bi-daily (BID) weekly oral docetaxel as ModraDoc006 in combination with ritonavir." Annals of Oncology 27 (suppl_6).

Decker, Caroline J, Leena M Laitinen, Gary W Bridson, Scott A Raybuck, Roger D Tung, and Pravin R Chaturvedi. 1998. "Metabolism of amprenavir in liver microsomes: role of CYP3A4 inhibition for drug interactions." Journal of pharmaceutical sciences 87 (7):803-807.

Dehghan, MH, and Mohammad Jafar. 2010. "Improving dissolution of meloxicam using solid dispersions." Iranian journal of pharmaceutical research:231-238.

Desai, DS, BA Rubitski, SA Varia, and AW Newman. 1993. "Physical interactions of magnesium stearate with starch-derived disintegrants and their effects on capsule and tablet dissolution." International journal of pharmaceutics 91 (2-3):217-226.

Di, Li, Paul V Fish, and Takashi Mano. 2012. "Bridging solubility between drug discovery and development." Drug Discovery Today 17 (9):486-495.

Dinunzio, J. 2016. "Applications of Melt-Extrusion for Continuous Manufacturing of Novel Drug Products." 2016 AAPS Annual Meeting & Exposition, Denver, CO.

DiNunzio, James C, Chris Brough, Justin R Hughey, Dave A Miller, Robert O Williams, and James W McGinity. 2010. "Fusion production of solid dispersions containing a heat-sensitive active ingredient by hot melt extrusion and Kinetisol® dispersing." European Journal of Pharmaceutics and Biopharmaceutics 74 (2):340-351.

DiNunzio, James C, Chris Brough, Dave A Miller, Robert O Williams, and James W McGinity. 2010a. "Applications of KinetiSol® dispersing for the production of plasticizer free amorphous solid dispersions." European Journal of Pharmaceutical Sciences 40 (3):179-187.

DiNunzio, James C, Chris Brough, Dave A Miller, Robert O Williams, and James W McGinity. 2010b. "Fusion processing of itraconazole solid dispersions by KinetiSol® dispersing: a comparative study to hot melt extrusion." Journal of pharmaceutical sciences 99 (3):1239-1253.

DiNunzio, James C, Justin R Hughey, Chris Brough, Dave A Miller, Robert O Williams III, and James W McGinity. 2010. "Production of advanced solid dispersions for enhanced bioavailability of itraconazole using KinetiSol® Dispersing." Drug development and industrial pharmacy 36 (9):1064-1078.

Dokoumetzidis, Aristides, and Panos Macheras. 2006. "A century of dissolution research: from Noyes and Whitney to the biopharmaceutics classification system." International journal of pharmaceutics 321 (1):1-11.

Dong, Zedong, Ashish Chatterji, Harpreet Sandhu, Duk Soon Choi, Hitesh Chokshi, and Navnit Shah. 2008. "Evaluation of solid state properties of solid dispersions prepared by hot-melt extrusion and solvent co-precipitation." International Journal of Pharmaceutics 355 (1):141-149. doi: https://doi.org/10.1016/j.ijpharm.2007.12.017.

Dressman, Jennifer B. 1986. "Comparison of canine and human gastrointestinal physiology." Pharmaceutical Research 3 (3):123-131.

Du, Qiaohong, Xinnuo Xiong, Zili Suo, Peixiao Tang, Jiawei He, Xia Zeng, Quan Hou, and Hui Li. 2017. "Investigation of the solid forms of deferasirox: solvate, co-crystal, and amorphous form." RSC Advances 7 (68):43151-43160.

Eagling, Vo A, DJ Back, and MG Barry. 1997. "Differential inhibition of cytochrome P450 isoforms by the protease inhibitors, ritonavir, saquinavir and indinavir." British journal of clinical pharmacology 44 (2):190-194.

El-Badry, M, and M Fathy. 2006. "Enhancement of the dissolution and permeation rates of meloxicam by formation of its freeze-dried solid dispersions in polyvinylpyrrolidone K-30." Drug development and industrial pharmacy 32 (2):141-150.

Ellenberger, Daniel J, Dave A Miller, and Robert O Williams. 2017 (Accepted). "Demonstration of KinetiSol® as a superior process for preparation of vemurafenib amorphous solid dispersions." AAPS PharmSciTech.

Ellenberger, Daniel J; Miller, Dave A; and Williams, Robert O. 2017 (Accepted). "Expanding the Application and Formulation Space of Amorphous Solid Dispersions with KinetiSol®: A Review." AAPS PharmSciTech.

Fancher, R Marcus, Hongjian Zhang, Bogdan Sleczka, George Derbin, Richard Rockar, and Punit Marathe. 2011. "Development of a canine model to enable the preclinical

assessment of ph-dependent absorption of test compounds." Journal of pharmaceutical sciences 100 (7):2979-2988.

Flaherty, Keith T, Uma Yasothan, and Peter Kirkpatrick. 2011. "Vemurafenib." Nature reviews Drug discovery 10 (11):811-813.

Fox, Thomas G. 1952. "Influence of diluent and of copolymer composition on the glass temperature of a polymer system." Bull. Am. Phs. Soc. 1:123.

Frank, Kerstin J, Kathrin Locher, Damir E Zecevic, Jeannine Fleth, and Karl G Wagner. 2014. "In vivo predictive mini-scale dissolution for weak bases: Advantages of pH-shift in combination with an absorptive compartment." European Journal of Pharmaceutical Sciences 61:32-39.

Fricker, Gert, Torsten Kromp, Armin Wendel, Alfred Blume, Jürgen Zirkel, Herbert Rebmann, Constanze Setzer, Ralf-Olaf Quinkert, Frank Martin, and Christel Müller-Goymann. 2010. "Phospholipids and lipid-based formulations in oral drug delivery." Pharmaceutical research 27 (8):1469-1486.

Friesen, Dwayne T, Ravi Shanker, Marshall Crew, Daniel T Smithey, WJ Curatolo, and JAS Nightingale. 2008. "Hydroxypropyl methylcellulose acetate succinate-based spray-dried dispersions: an overview." Molecular pharmaceutics 5 (6):1003-1019.

Fukuda, Mamoru, Nicholas A Peppas, and James W McGinity. 2006. "Floating hot-melt extruded tablets for gastroretentive controlled drug release system." Journal of controlled release 115 (2):121-129.

Gatti, Giorgio, Antonio Di Biagio, Rosetta Casazza, Cleta De Pascalis, Matteo Bassetti, Mario Cruciani, Stefano Vella, and Dante Bassetti. 1999. "The relationship between ritonavir

plasma levels and side-effects: implications for therapeutic drug monitoring." Aids 13 (15):2083-2089.

Ghany, Marc G, David R Nelson, Doris B Strader, David L Thomas, and Leonard B Seeff. 2011. "An update on treatment of genotype 1 chronic hepatitis C virus infection: 2011 practice guideline by the American Association for the Study of Liver Diseases." Hepatology 54 (4):1433-1444.

Ghareeb, Mowafaq M, Alaa A Abdulrasool, Ahmed A Hussein, and Mohammed I Noordin. 2009. "Kneading technique for preparation of binary solid dispersion of meloxicam with poloxamer 188." Aaps Pharmscitech 10 (4):1206-1215.

Ghebremeskel, Alazar N, Chandra Vemavarapu, and Mayur Lodaya. 2006. "Use of surfactants as plasticizers in preparing solid dispersions of poorly soluble API: stability testing of selected solid dispersions." Pharmaceutical research 23 (8):1928-1936.

Goldinger, Simone M, Jeannine Rinderknecht, Reinhard Dummer, Felix Pierre Kuhn, Kuo-Hsiung Yang, Lucy Lee, Ruben C Ayala, Jagdish Racha, Wanping Geng, and David Moore. 2015. "A single-dose mass balance and metabolite-profiling study of vemurafenib in patients with metastatic melanoma." Pharmacology research & perspectives 3 (2).

Gu, Shuang, Rui Cai, Ting Luo, Zhongwei Chen, Minwei Sun, Yan Liu, Gaohong He, and Yushan Yan. 2009. "A Soluble and Highly Conductive Ionomer for High-Performance Hydroxide Exchange Membrane Fuel Cells." Angewandte Chemie International Edition 48 (35):6499-6502.

Gupta, Piyush, and Arvind K Bansal. 2005. "Molecular interactions in celecoxib-PVP-meglumine amorphous system." Journal of pharmacy and pharmacology 57 (3):303-310.

Gupta, Simerdeep Singh, Anuprabha Meena, Tapan Parikh, and Abu TM Serajuddin. 2014. "Investigation of thermal and viscoelastic properties of polymers relevant to hot melt extrusion, I: Polyvinylpyrrolidone and related polymers." Journal of Excipients and Food Chemicals 5 (1):32-45.

Gupta, Vivek, Byeong Hee Hwang, JooHee Lee, Aaron C Anselmo, Nishit Doshi, and Samir Mitragotri. 2013. "Mucoadhesive intestinal devices for oral delivery of salmon calcitonin." Journal of Controlled Release 172 (3):753-762.

Guzmán, Héctor R, Mark Tawa, Zhong Zhang, Pasut Ratanabanangkoon, Paul Shaw, Colin R Gardner, Hongming Chen, Jean-Pierre Moreau, Örn Almarsson, and Julius F Remenar. 2007. "Combined use of crystalline salt forms and precipitation inhibitors to improve oral absorption of celecoxib from solid oral formulations." Journal of pharmaceutical sciences 96 (10):2686-2702.

Hadida, Sabine, Frederick Van Goor, Kirk Dinehart, Adam R Looker, Peter Mueller, and Peter DJ Grootenhuis. 2014. "Case history: Kalydeco®(VX-770, Ivacaftor), a CFTR potentiator for the treatment of patients with cystic fibrosis and the G551D-CFTR mutation." Annu Rep Med Chem 49:383-398.

Haidar, Sam H, Barbara Davit, Mei-Ling Chen, Dale Conner, LaiMing Lee, Qian H Li, Robert Lionberger, Fairouz Makhlouf, Devvrat Patel, and Donald J Schuirmann. 2008. "Bioequivalence approaches for highly variable drugs and drug products." Pharmaceutical research 25 (1):237-241.

Hancock, Bruno C. 2017. "Predicting the Crystallization Propensity of Drug-Like Molecules." Journal of pharmaceutical sciences 106 (1):28-30.

Hancock, Bruno C, Sheri L Shamblin, and George Zografi. 1995. "Molecular mobility of amorphous pharmaceutical solids below their glass transition temperatures." Pharmaceutical research 12 (6):799-806.

Haser, Abbe, James C DiNunzio, Charlie Martin, James W McGinity, and Feng Zhang. 2016. "Melt Extrusion." In Formulating Poorly Water Soluble Drugs, 383-435. Springer.

Haser, Abbe, Siyuan Huang, Tony Listro, David White, and Feng Zhang. 2017. "An approach for chemical stability during melt extrusion of a drug substance with a high melting point." International journal of pharmaceutics 524 (1):55-64.

Hate, Siddhi S, Susan M Reutzel-Edens, and Lynne S Taylor. 2017. "Absorptive Dissolution Testing of Supersaturating Systems: Impact of Absorptive Sink Conditions on Solution Phase Behavior and Mass Transport." Molecular Pharmaceutics.

He, Yan, and Chris Ho. 2015. "Amorphous solid dispersions: utilization and challenges in drug discovery and development." Journal of pharmaceutical sciences 104 (10):3237-3258.

Heigoldt, Ulrich, Florian Sommer, Rolf Daniels, and Karl-Gerhard Wagner. 2010. "Predicting in vivo absorption behavior of oral modified release dosage forms containing pH-dependent poorly soluble drugs using a novel pH-adjusted biphasic in vitro dissolution test." European Journal of Pharmaceutics and Biopharmaceutics 76 (1):105-111.

Hölzer, Arne W, and John Sjögren. 1979. "Evaluation of sodium stearyl fumarate as a tablet lubricant." International Journal of Pharmaceutics 2 (3):145-153.

Hong, David S, Van Karlyle Morris, Siqing Fu, Michael J Overman, Sarina Anne Piha-Paul, Bryan K Kee, Ralph Zinner, David R Fogelman, Reena Mistry, and Imad Shureiqi. 2014. Phase 1B study of vemurafenib in combination with irinotecan and cetuximab in patients

with BRAF-mutated advanced cancers and metastatic colorectal cancer. American Society of Clinical Oncology.

Horbert, Rebecca, Boris Pinchuk, Paul Davies, Dario Alessi, and Christian Peifer. 2015. "Photoactivatable prodrugs of antimelanoma agent vemurafenib." ACS chemical biology 10 (9):2099-2107.

Hu, Jiahui, True L Rogers, Judith Brown, Tim Young, Keith P Johnston, and Robert O Williams Iii. 2002. "Improvement of dissolution rates of poorly water soluble APIs using novel spray freezing into liquid technology." Pharmaceutical Research 19 (9):1278-1284.

Huang, Siyuan, and Robert O. Williams. 2017. "Effects of the Preparation Process on the Properties of Amorphous Solid Dispersions." AAPS PharmSciTech. doi: 10.1208/s12249-017-0861-7.

Hughey, Justin R, James C DiNunzio, Ryan C Bennett, Chris Brough, Dave A Miller, Hua Ma, Robert O Williams III, and James W McGinity. 2010. "Dissolution enhancement of a drug exhibiting thermal and acidic decomposition characteristics by fusion processing: a comparative study of hot melt extrusion and KinetiSol® dispersing." AAPs Pharmscitech 11 (2):760-774.

Hughey, Justin R, Justin M Keen, Ryan C Bennett, Sakae Obara, and James W McGinity. 2015. "The incorporation of low-substituted hydroxypropyl cellulose into solid dispersion systems." Drug development and industrial pharmacy 41 (8):1294-1301.

Hughey, Justin R, Justin M Keen, Chris Brough, Sophie Saeger, and James W McGinity. 2011. "Thermal processing of a poorly water-soluble drug substance exhibiting a high melting point: the utility of KinetiSol® dispersing." International journal of pharmaceutics 419 (1):222-230.

Hughey, Justin R, Justin M Keen, Dave A Miller, Chris Brough, and James W McGinity. 2012. "Preparation and characterization of fusion processed solid dispersions containing a viscous thermally labile polymeric carrier." International journal of pharmaceutics 438 (1):11-19.

Hughey, Justin R, Justin M Keen, Dave A Miller, Karl Kolter, Nigel Langley, and James W McGinity. 2013. "The use of inorganic salts to improve the dissolution characteristics of tablets containing Soluplus®-based solid dispersions." European Journal of Pharmaceutical Sciences 48 (4):758-766.

Hughey, Justin R, and James W McGinity. 2012. "Emerging Technologies to Increase the Bioavailability of Poorly Water-Soluble Drugs." In Formulating Poorly Water Soluble Drugs, 569-602. Springer.

Ilevbare, Grace A, Wei Xu, Christopher T John, James D Ormes, Jesse L Kuiper, Allen C Templeton, and Annette Bak. 2015. "Solubility and Dissolution Considerations for Amorphous Solid Dispersions." Pharmaceutical Sciences Encyclopedia.

Jain, Neera, and Samuel H Yalkowsky. 2001. "Estimation of the aqueous solubility I: Application to organic nonelectrolytes." Journal of pharmaceutical sciences 90 (2):234-252.

Jain, Shashank, Niketkumar Patel, and Senshang Lin. 2015. "Solubility and dissolution enhancement strategies: current understanding and recent trends." Drug development and industrial pharmacy 41 (6):875-887.

Janssens, Sandrien, Sophie Nagels, Hector Novoa de Armas, Ward D'Autry, Ann Van Schepdael, and Guy Van den Mooter. 2008. "Formulation and characterization of ternary solid dispersions made up of Itraconazole and two excipients, TPGS 1000 and PVPVA

64, that were selected based on a supersaturation screening study." European Journal of Pharmaceutics and Biopharmaceutics 69 (1):158-166. doi: https://doi.org/10.1016/j.ejpb.2007.11.004.

Jermain, Scott V, Chris Brough, and Robert O Williams. 2017. "Amorphous Solid Dispersions and Nanocrystal Technologies for Poorly Water-Soluble Drug Delivery–An Update." International Journal of Pharmaceutics.

Jinno, Jun-ichi, Naoki Kamada, Masateru Miyake, Keigo Yamada, Tadashi Mukai, Masaaki Odomi, Hajime Toguchi, Gary G Liversidge, Kazutaka Higaki, and Toshikiro Kimura. 2006. "Effect of particle size reduction on dissolution and oral absorption of a poorly water-soluble drug, cilostazol, in beagle dogs." Journal of controlled release 111 (1):56-64.

Kageyama, Michiharu, Hitomi Namiki, Hiroto Fukushima, Shuichi Terasaka, Tatsuya Togawa, Akina Tanaka, Yukako Ito, Nobuhito Shibata, and Kanji Takada. 2005. "Effect of chronic administration of ritonavir on function of cytochrome P450 3A and P-glycoprotein in rats." Biological and Pharmaceutical Bulletin 28 (1):130-137.

Kalepu, Sandeep, Mohanvarma Manthina, and Veerabhadhraswamy Padavala. 2013. "Oral lipid-based drug delivery systems–an overview." Acta Pharmaceutica Sinica B 3 (6):361-372.

Karlina, MV, ON Pozharitskaya, VM Kosman, and SA Ivanova. 2007. "Bioavailability of boswellic acids: in vitro/in vivo correlation." Pharmaceutical Chemistry Journal 41 (11):569-572.

Keen, Justin M. In press, forthcoming 2017. "Development of Itraconazole Tablets Containing Viscous KinetiSol® Solid Dispersions: in vitro and in vivo Analysis in Dogs." AAPS PharmSciTech.

Keen, Justin M, Justin R Hughey, Ryan C Bennett, Vincent Jannin, Yvonne Rosiaux, Delphine Marchaud, and James W McGinity. 2014. "Effect of tablet structure on controlled release from supersaturating solid dispersions containing glyceryl behenate." Molecular pharmaceutics 12 (1):120-126.

Keen, Justin M, James W McGinity, and Robert O Williams III. 2013. "Enhancing bioavailability through thermal processing." International journal of pharmaceutics 450 (1):185-196.

Kessler, T, J Breitenbach, C Schmidt, M Degenhardt, J Rosenberg, and H Krull. Process for producing a solid dispersion of an active ingredient. United States: Abbott Gmbh & Co., Kg.

Kohri, Naonori, Yasuko Yamayoshi, HE Xin, KEN Iseki, NAOKI SATO, SATORU TODO, and KATSUMI MIYAZAKI. 1999. "Improving the oral bioavailability of albendazole in rabbits by the solid dispersion technique." Journal of pharmacy and pharmacology 51 (2):159-164.

Kolter, K, M Karl, A Gryczke, and BASF Ludwigshafen am Rhein. 2012. Hot-melt extrusion with BASF pharma polymers: extrusion compendium: BASF.

Korsmeyer, Richard W., Robert Gurny, Eric Doelker, Pierre Buri, and Nikolaos A. Peppas. 1983. "Mechanisms of solute release from porous hydrophilic polymers." International Journal of Pharmaceutics 15 (1):25-35. doi: https://doi.org/10.1016/0378-5173(83)90064-9.

Kostewicz, Edmund S, Martin Wunderlich, Ulrich Brauns, Robert Becker, Thomas Bock, and Jennifer B Dressman. 2004. "Predicting the precipitation of poorly soluble weak bases upon entry in the small intestine." Journal of pharmacy and pharmacology 56 (1):43-51.

Krüger, Phillip, Rambod Daneshfar, Gunter P Eckert, Jochen Klein, Dietrich A Volmer, Ute Bahr, Walter E Müller, Michael Karas, Manfred Schubert-Zsilavecz, and Mona Abdel-Tawab. 2008. "Metabolism of boswellic acids in vitro and in vivo." Drug Metabolism and Disposition 36 (6):1135-1142.

Krüger, Phillip, Johanna Kanzer, Jessica Hummel, Gert Fricker, Manfred Schubert-Zsilavecz, and Mona Abdel-Tawab. 2009. "Permeation of Boswellia extract in the Caco-2 model and possible interactions of its constituents KBA and AKBA with OATP1B3 and MRP2." european journal of pharmaceutical sciences 36 (2):275-284.

Ku, M Sherry, and Wendy Dulin. 2012. "A biopharmaceutical classification-based Right-First-Time formulation approach to reduce human pharmacokinetic variability and project cycle time from First-In-Human to clinical Proof-Of-Concept." Pharmaceutical development and technology 17 (3):285-302.

Kuminek, Gislaine, Fengjuan Cao, Alanny Bahia de Oliveira da Rocha, Simone Gonçalves Cardoso, and Naír Rodríguez-Hornedo. 2016. "Cocrystals to facilitate delivery of poorly soluble compounds beyond-rule-of-5." Advanced drug delivery reviews 101:143-166.

Kuno, Yoshio, Masazumi Kojima, Hiroaki Nakagami, Etsuo Yonemochi, and Katsuhide Terada. 2008. "Effect of the type of lubricant on the characteristics of orally disintegrating tablets manufactured using the phase transition of sugar alcohol." European Journal of Pharmaceutics and Biopharmaceutics 69 (3):986-992.

Kwong, Ann D, Robert S Kauffman, Patricia Hurter, and Peter Mueller. 2011. "Discovery and development of telaprevir: an NS3-4A protease inhibitor for treating genotype 1 chronic hepatitis C virus." Nature biotechnology 29 (11):993-1003.

LaFountaine, Justin S ; Prasad, Leena K; Miller, Dave A; McGinity, James W; Williams, Robert O. 2017. "Mucoadhesive Amorphous Solid Dispersions for Sustained Release of Poorly Water Soluble Drugs." European Journal of Pharmaceutics and Biopharmaceutics 113:157-67.

LaFountaine, Justin S, Scott V Jermain, Leena Kumari Prasad, Chris Brough, Dave A Miller, Dieter Lubda, James W McGinity, and Robert O Williams. 2016. "Enabling thermal processing of ritonavir–polyvinyl alcohol amorphous solid dispersions by KinetiSol® Dispersing." European Journal of Pharmaceutics and Biopharmaceutics 101:72-81.

LaFountaine, Justin S, James W McGinity, and Robert O Williams III. 2016. "Challenges and strategies in thermal processing of amorphous solid dispersions: a review." AAPS PharmSciTech 17 (1):43-55.

LaFountaine, Justin S, Leena Kumari Prasad, Chris Brough, Dave A Miller, James W McGinity, and Robert O Williams III. 2016. "Thermal processing of PVP-and HPMC-based amorphous solid dispersions." AAPS PharmSciTech 17 (1):120-132.

Larkin, James, Paolo A Ascierto, Brigitte Dréno, Victoria Atkinson, Gabriella Liszkay, Michele Maio, Mario Mandalà, Lev Demidov, Daniil Stroyakovskiy, and Luc Thomas. 2014. "Combined vemurafenib and cobimetinib in BRAF-mutated melanoma." New England Journal of Medicine 371 (20):1867-1876.

Law, Devalina, Eric A Schmitt, Kennan C Marsh, Elizabeth A Everitt, Weili Wang, James J Fort, Steven L Krill, and Yihong Qiu. 2004. "Ritonavir–PEG 8000 amorphous solid dispersions: in vitro and in vivo evaluations." Journal of pharmaceutical sciences 93 (3):563-570.

Leeson, Paul D. 2016. "Molecular inflation, attrition and the rule of five." Advanced drug delivery reviews 101:22-33.

Leuner, Christian, and Jennifer Dressman. 2000. "Improving drug solubility for oral delivery using solid dispersions." European Journal of Pharmaceutics and Biopharmaceutics 50 (1):47-60. doi: https://doi.org/10.1016/S0939-6411(00)00076-X.

Li, Jinjiang, and Yongmei Wu. 2014. "Lubricants in pharmaceutical solid dosage forms." Lubricants 2 (1):21-43.

Lin, Shan-Yang, and Hui-Ling Yu. 1999. "Thermal stability of methacrylic acid copolymers of Eudragits L, S, and L30D and the acrylic acid polymer of carbopol." Journal of Polymer Science Part A: Polymer Chemistry 37 (13):2061-2067.

Lipinski, Christopher A. 2000. "Drug-like properties and the causes of poor solubility and poor permeability." Journal of pharmacological and toxicological methods 44 (1):235-249.

Llusa, Marcos, Michael Levin, Ronald D Snee, and Fernando J Muzzio. 2010. "Measuring the hydrophobicity of lubricated blends of pharmaceutical excipients." Powder Technology 198 (1):101-107.

Loftsson, Thorsteinn, and Marcus E Brewster. 2010. "Pharmaceutical applications of cyclodextrins: basic science and product development." Journal of pharmacy and pharmacology 62 (11):1607-1621.

Maniruzzaman, Mohammed, David J Morgan, Andrew P Mendham, Jiayun Pang, Martin J Snowden, and Dennis Douroumis. 2013. "Drug–polymer intermolecular interactions in hot-melt extruded solid dispersions." International journal of pharmaceutics 443 (1):199-208.

Mansuri, Shakir, Prashant Kesharwani, Keerti Jain, Rakesh K Tekade, and NK Jain. 2016. "Mucoadhesion: A promising approach in drug delivery system." Reactive and Functional Polymers 100:151-172.

Markowitz, Martin, Michael Saag, William G Powderly, Arlene M Hurley, Ann Hsu, Joaquin M Valdes, David Henry, Fred Sattler, Anthony La Marca, and John M Leonard. 1995. "A preliminary study of ritonavir, an inhibitor of HIV-1 protease, to treat HIV-1 infection." New England Journal of Medicine 333 (23):1534-1540.

Meena, Anuprabha, Tapan Parikh, Simerdeep Singh Gupta, and Abu TM Serajuddin. 2014. "Investigation of thermal and viscoelastic properties of polymers relevant to hot melt extrusion, II: Cellulosic polymers." Journal of Excipients and Food Chemicals 5 (1):46-55.

Mellaerts, Randy, Elie J Fayad, Guy Van den Mooter, Patrick Augustijns, Mickaël Rivallan, Frédéric Thibault-Starzyk, and Johan A Martens. 2013. "In situ FT-IR investigation of etravirine speciation in pores of SBA-15 ordered mesoporous silica material upon contact with water." Molecular pharmaceutics 10 (2):567-573.

Merry, Concepta, Michael G Barry, Fiona Mulcahy, Mairin Ryan, Jane Heavey, John F Tjia, Sara E Gibbons, Alasdair M Breckenridge, and David J Back. 1997. "Saquinavir pharmacokinetics alone and in combination with ritonavir in HIV-infected patients." Aids 11 (4):F29-F33.

Miller, Dave A, James C DiNunzio, Justin R Hughey, Robert O Williams III, and James W McGinity. 2012. "KinetiSol: a new processing paradigm for amorphous solid dispersion systems." Drug Dev Deliv 11 (2011):22-31.

Miller, Dave A, James C DiNunzio, Wei Yang, James W McGinity, and Robert O Williams III. 2008. "Enhanced in vivo absorption of itraconazole via stabilization of supersaturation following acidic-to-neutral pH transition." Drug development and industrial pharmacy 34 (8):890-902.

Miller, Dave A, Daniel Ellenberger, and Marco Gil. 2016. "Spray-Drying Technology." In Formulating Poorly Water Soluble Drugs, 437-525. Springer.

Miller, Dave A, Mirko Gamba, Dorothea Sauer, Troy P Purvis, Noel T Clemens, and Robert O Williams. 2007. "Evaluation of the USP dissolution test method A for enteric-coated articles by planar laser-induced fluorescence." International journal of pharmaceutics 330 (1):61-72.

Miller, Dave A, and Justin M Keen. 2014. "KinetiSol®-Based Amorphous Solid Dispersions." In Amorphous Solid Dispersions, 567-577. Springer.

Miller, Dave A, Justin M Keen, Chris Brough, Daniel J Ellenberger, Marshall Cisneros, Robert O Williams, and James W McGinity. 2015. "Bioavailability enhancement of a BCS IV compound via an amorphous combination product containing ritonavir." Journal of Pharmacy and Pharmacology.

Miller, Dave A, Justin M Keen, and Sandra U Kucera. Formulations of deferasirox and methods of making the same. United States: DisperSol Technologies, LLC.

Miller, Dave A, Keen, Justin M, Brough, Chris. 2015. Tetrabenazine Modified Release Formulation.

Miller, Dave A, Keen, Justin M, Brough, Chris, Kucera, Sandra U, and Ellenberger, Daniel J. 2016. Improved Formulations of Vemurafenib and Methods of Making the Same.

Miller, Dave Alan. 2007. Improved oral absorption of poorly water-soluble drugs by advanced solid dispersion systems: University of Texas

Miller, Jonathan M, Avital Beig, Robert A Carr, Julie K Spence, and Arik Dahan. 2012. "A win–win solution in oral delivery of lipophilic drugs: supersaturation via amorphous solid dispersions increases apparent solubility without sacrifice of intestinal membrane permeability." Molecular pharmaceutics 9 (7):2009-2016.

Moser, JD, J Broyles, L Liu, E Miller, and M Wang. 2008. "Enhancing bioavailability of poorly soluble drugs using spray dried solid dispersions Part I." Am Pharm Rev 11:70-71.

Mosharraf, Mitra, and Christer Nyström. 1995. "The effect of particle size and shape on the surface specific dissolution rate of microsized practically insoluble drugs." International Journal of Pharmaceutics 122 (1-2):35-47.

Narang, Ajit S, Dan Tang, Scott P Jennings, Neil Mathias, Konstantin L Tsinman, Deren J Dohoda, David A Kwajewski, and Michael G Kelly. Apparatus and Method for the Assessment of Concentration Profiling and Permeability Rates. United States: Pion Inc.

Newman, Ann, David Engers, Simon Bates, Igor Ivanisevic, Ron C Kelly, and George Zografi. 2008. "Characterization of amorphous API: Polymer mixtures using X-ray powder diffraction." Journal of pharmaceutical sciences 97 (11):4840-4856.

Newman, Ann, Gregory Knipp, and George Zografi. 2012. "Assessing the performance of amorphous solid dispersions." Journal of pharmaceutical sciences 101 (4):1355-1377.

Nikitine, Clémence, Elisabeth Rodier, Martial Sauceau, Jean-Jacques Letourneau, and Jacques Fages. 2010. "Controlling the structure of a porous polymer by coupling supercritical

CO2 and single screw extrusion process." Journal of applied polymer science 115 (2):981-990.

Parikh, Tapan, Simerdeep Singh Gupta, Anuprabha Meena, and Abu TM Serajuddin. 2014. "Investigation of thermal and viscoelastic properties of polymers relevant to hot melt extrusion, III: polymethacrylates and polymethacrylic acid based polymers." Journal of Excipients and Food Chemicals 5 (1):56-64.

Park, Byoungduck, Bokyung Sung, Vivek R Yadav, Sung-Gook Cho, Mingyao Liu, and Bharat B Aggarwal. 2011. "Acetyl-11-keto-β-boswellic acid suppresses invasion of pancreatic cancer cells through the downregulation of CXCR4 chemokine receptor expression." International journal of cancer 129 (1):23-33.

Paudel, Amrit, Zelalem Ayenew Worku, Joke Meeus, Sandra Guns, and Guy Van den Mooter. 2013. "Manufacturing of solid dispersions of poorly water soluble drugs by spray drying: formulation and process considerations." International journal of pharmaceutics 453 (1):253-284.

Phillips, Daniel J, Samuel R Pygall, V Brett Cooper, and James C Mann. 2012. "Overcoming sink limitations in dissolution testing: a review of traditional methods and the potential utility of biphasic systems." Journal of Pharmacy and Pharmacology 64 (11):1549-1559.

Qian, Feng, Jun Huang, and Munir A Hussain. 2010. "Drug–polymer solubility and miscibility: stability consideration and practical challenges in amorphous solid dispersion development." Journal of pharmaceutical sciences 99 (7):2941-2947.

Raghavan, SL, A Trividic, AF Davis, and J Hadgraft. 2001. "Crystallization of hydrocortisone acetate: influence of polymers." International journal of pharmaceutics 212 (2):213-221.

Rahman, Mohammad. 2012. "The Use of Hot Melt Extrusion and Comparative Technologies in Preparing Solid Amorphous Dispersions and Controlled Release Dosage Forms." Pharmaceutical Extrusion Seminar.

Ramesh, K, B Chandra Shekar, P Khadgapathi, DVRN Bhikshapathi, and N Gourav. 2015. "Enhancement of Solubility and Bioavailability of Etravirine Solid Dispersions by Solvent Evaporation Technique with Novel Carriers." IOSR Journal of Pharmacy and Biological Sciences 10 (4):30-41.

Rao, R Nageswara, B Ramachandra, R Mastan Vali, and S Satyanarayana Raju. 2010. "LC–MS/MS studies of ritonavir and its forced degradation products." Journal of pharmaceutical and biomedical analysis 53 (4):833-842.

Repka, Michael A, Sunil Kumar Battu, Sampada B Upadhye, Sridhar Thumma, Michael M Crowley, Feng Zhang, Charles Martin, and James W McGinity. 2007. "Pharmaceutical applications of hot-melt extrusion: Part II." Drug development and industrial pharmacy 33 (10):1043-1057.

Repka, Michael A, Thomas G Gerding, Staci L Repka, and James W McGinity. 1999. "Influence of plasticizers and drugs on the physical-mechanical properties of hydroxypropylcellulose films prepared by hot melt extrusion." Drug development and industrial pharmacy 25 (5):625-633.

Reynolds, Thomas D, Shawn A Mitchell, and Karen M Balwinski. 2002. "Investigation of the effect of tablet surface area/volume on drug release from hydroxypropylmethylcellulose controlled-release matrix tablets." Drug development and industrial pharmacy 28 (4):457-466.

Ribas, Antoni, F Stephen Hodi, Margaret Callahan, Cyril Konto, and Jedd Wolchok. 2013. "Hepatotoxicity with combination of vemurafenib and ipilimumab." New England Journal of Medicine 368 (14):1365-1366.

Rosenberg, J., U. Reinhold, B. Liepold, G. Berndl, J. Breitenbach, L. Alani, and S. Ghosh. Solid pharmaceutical dosage form. United States: Abbott Laboratories.

Rowe, Raymond C, Paul J Sheskey, and Paul J Weller. 2009a. Handbook of pharmaceutical excipients. 6th ed: Pharmaceutical press London.

Rowe, Raymond C, Paul J Sheskey, and Paul J Weller. 2009b. Handbook of Pharmaceutical Excipients. 6th ed.

Rustichelli, C, G Gamberini, V Ferioli, MC Gamberini, R Ficarra, and S Tommasini. 2000. "Solid-state study of polymorphic drugs: carbamazepine." Journal of pharmaceutical and biomedical analysis 23 (1):41-54.

Sacchetti, M. 2000. "Thermodynamic analysis of DSC data for acetaminophen polymorphs." Journal of thermal analysis and calorimetry 63 (2):345-350.

Safayhi, Hasan, THOMAS Mack, JOACHIM Sabieraj, MICHAEL I Anazodo, LAKSHMINARAYANAPURAM R Subramanian, and HP Ammon. 1992. "Boswellic acids: novel, specific, nonredox inhibitors of 5-lipoxygenase." Journal of Pharmacology and Experimental Therapeutics 261 (3):1143-1146.

Sagawa, Kazuko, Fasheng Li, Ryan Liese, and Steven C Sutton. 2009. "Fed and fasted gastric pH and gastric residence time in conscious beagle dogs." Journal of pharmaceutical sciences 98 (7):2494-2500.

Sarode, Ashish L, Sakae Obara, Fumie K Tanno, Harpreet Sandhu, Raman Iyer, and Navnit Shah. 2014. "Stability assessment of hypromellose acetate succinate (HPMCAS) NF for application in hot melt extrusion (HME)." Carbohydrate polymers 101:146-153.

Sarode, Ashish L, Harpreet Sandhu, Navnit Shah, Waseem Malick, and Hossein Zia. 2013. "Hot melt extrusion for amorphous solid dispersions: temperature and moisture activated drug–polymer interactions for enhanced stability." Molecular pharmaceutics 10 (10):3665-3675.

Sarode, Ashish L., Peng Wang, Sakae Obara, and David R. Worthen. 2014. "Supersaturation, nucleation, and crystal growth during single- and biphasic dissolution of amorphous solid dispersions: Polymer effects and implications for oral bioavailability enhancement of poorly water soluble drugs." European Journal of Pharmaceutics and Biopharmaceutics 86 (3):351-360. doi: https://doi.org/10.1016/j.ejpb.2013.10.005.

Sauceau, Martial, Jacques Fages, Audrey Common, Clémence Nikitine, and Elisabeth Rodier. 2011. "New challenges in polymer foaming: A review of extrusion processes assisted by supercritical carbon dioxide." Progress in Polymer Science 36 (6):749-766.

Savla, Ronak, Jeff Browne, Vincent Plassat, Kishor M Wasan, and Ellen K Wasan. 2017. "Review and analysis of FDA approved drugs using lipid-based formulations." Drug Development and Industrial Pharmacy:1-16.

Schilling, Bastian, Antje Sucker, Klaus Griewank, Fang Zhao, Benjamin Weide, André Görgens, Bernd Giebel, Dirk Schadendorf, and Annette Paschen. 2013. "Vemurafenib reverses immunosuppression by myeloid derived suppressor cells." International journal of cancer 133 (7):1653-1663.

Schopf, Clemens. Preparation of Quinolizine Derivatives. United States: E. Merck.

Serajuddin, Abu. 1999. "Solid dispersion of poorly water-soluble drugs: Early promises, subsequent problems, and recent breakthroughs." Journal of pharmaceutical sciences 88 (10):1058-1066.

Serajuddin, Abu, Ajit B Thakur, Rabin N Ghoshal, Michael G Fakes, Sunanda A Ranadive, Kenneth R Morris, and Sailesh A Varia. 1999. "Selection of solid dosage form composition through drug–excipient compatibility testing." Journal of pharmaceutical sciences 88 (7):696-704.

Shah, AC, and AR Mlodozeniec. 1977. "Mechanism of surface lubrication: Influence of duration of lubricant-excipient mixing on processing characteristics of powders and properties of compressed tablets." Journal of pharmaceutical sciences 66 (10):1377-1382.

Shah, Navnit, Raman M Iyer, Hans-Juergen Mair, Duk Soon Choi, Hung Tian, Ralph Diodone, Karsten Fähnrich, Anni Pabst-Ravot, Kin Tang, and Emmanuel Scheubel. 2013. "Improved human bioavailability of vemurafenib, a practically insoluble drug, using an amorphous polymer-stabilized solid dispersion prepared by a solvent-controlled coprecipitation process." Journal of pharmaceutical sciences 102 (3):967-981.

Shah, Navnit, Harpreet Sandhu, Wantanee Phuapradit, Rodolfo Pinal, Raman Iyer, Antonio Albano, Ashish Chatterji, Shalini Anand, Duk Soon Choi, and Kin Tang. 2012. "Development of novel microprecipitated bulk powder (MBP) technology for manufacturing stable amorphous formulations of poorly soluble drugs." International journal of pharmaceutics 438 (1):53-60.

Shah, NH, D Stiel, M Weiss, MH Infeld, and AW Malick. 1986. "Evaluation of two new tablet lubricants-sodium stearyl fumarate and glyceryl behenate. Measurement of physical parameters (compaction, ejection and residual forces) in the tableting process and the

effect on the dissolution rate." Drug Development and Industrial Pharmacy 12 (8-9):1329-1346.

Shi, Yi, Ping Gao, Yuchuan Gong, and Haili Ping. 2010. "Application of a biphasic test for characterization of in vitro drug release of immediate release formulations of celecoxib and its relevance to in vivo absorption." Molecular pharmaceutics 7 (5):1458-1465.

Shi, Yi, William Porter, Thomas Merdan, and Luk Chiu Li. 2009. "Recent advances in intravenous delivery of poorly water-soluble compounds." Expert opinion on drug delivery 6 (12):1261-1282.

Singh, Bhupinder, Shantanu Bandopadhyay, Rishi Kapil, and Ramandeep Singh. 2009. "Self-emulsifying drug delivery systems (SEDDS): formulation development, characterization, and applications." Critical Reviews™ in Therapeutic Drug Carrier Systems 26 (5).

Six, Karel, Hugo Berghmans, Christian Leuner, Jennifer Dressman, Kristof Van Werde, Jules Mullens, Luc Benoist, Mireille Thimon, Laurent Meublat, and Geert Verreck. 2003. "Characterization of solid dispersions of itraconazole and hydroxypropylmethylcellulose prepared by melt extrusion, part II." Pharmaceutical research 20 (7):1047-1054.

Song, Yang, Xinghao Yang, Xin Chen, Haichen Nie, Stephen Byrn, and Joseph W Lubach. 2015. "Investigation of drug–excipient interactions in lapatinib amorphous solid dispersions using solid-state NMR spectroscopy." Molecular pharmaceutics 12 (3):857-866.

Souto, EB, and RH Müller. 2005. "SLN and NLC for topical delivery of ketoconazole." Journal of microencapsulation 22 (5):501-510.

Stewart, Aaron M, Michael E Grass, Timothy J Brodeur, Aaron K Goodwin, Michael M Morgen, Dwayne T Friesen, and David T Vodak. 2017. "Impact of Drug-rich Colloids of

Itraconazole and HPMCAS on Membrane Flux In Vitro and Oral Bioavailability in Rats." Molecular Pharmaceutics.

Surana, Rahul, and Raj Suryanarayanan. 2000. "Quantitation of crystallinity in substantially amorphous pharmaceuticals and study of crystallization kinetics by X-ray powder diffractometry." Powder Diffraction 15 (1):2-6.

Taher, Ali, Maria D Cappellini, Elliott Vichinsky, Renzo Galanello, Antonio Piga, Tomasz Lawniczek, Joan Clark, Dany Habr, and John B Porter. 2009. "Efficacy and safety of deferasirox doses of> 30 mg/kg per d in patients with transfusion-dependent anaemia and iron overload." British journal of haematology 147 (5):752-759.

Tajarobi, Farhad, Anette Larsson, Hanna Matic, and Susanna Abrahmsén-Alami. 2011. "The influence of crystallization inhibition of HPMC and HPMCAS on model substance dissolution and release in swellable matrix tablets." European Journal of Pharmaceutics and Biopharmaceutics 78 (1):125-133.

Tam, Jasmine M, Jason T McConville, Robert O Williams, and Keith P Johnston. 2008. "Amorphous cyclosporin nanodispersions for enhanced pulmonary deposition and dissolution." Journal of pharmaceutical sciences 97 (11):4915-4933.

Tanaka, Nobuyuki, Keiji Imai, Kazuto Okimoto, Satoshi Ueda, Yuji Tokunaga, Rinta Ibuki, Kazutaka Higaki, and Toshikiro Kimura. 2006. "Development of novel sustained-release system, disintegration-controlled matrix tablet (DCMT) with solid dispersion granules of nilvadipine (II): in vivo evaluation." Journal of controlled release 112 (1):51-56.

Thiry, Justine, Guy Broze, Aude Pestieau, Andrew S Tatton, France Baumans, Christian Damblon, Fabrice Krier, and Brigitte Evrard. 2016. "Investigation of a suitable in vitro

dissolution test for itraconazole-based solid dispersions." European Journal of Pharmaceutical Sciences 85:94-105.

Tho, Ingunn, Bernd Liepold, Joerg Rosenberg, Markus Maegerlein, Martin Brandl, and Gert Fricker. 2010. "Formation of nano/micro-dispersions with improved dissolution properties upon dispersion of ritonavir melt extrudate in aqueous media." European Journal of Pharmaceutical Sciences 40 (1):25-32.

Tran, Phuong Ha-Lien, Thao Truong-Dinh Tran, Jun Bom Park, and Beom-Jin Lee. 2011. "Controlled release systems containing solid dispersions: strategies and mechanisms." Pharmaceutical research 28 (10):2353-2378.

Tuleu, C, C Andrieux, P Boy, and JC Chaumeil. 1999. "Gastrointestinal transit of pellets in rats: effect of size and density." International journal of pharmaceutics 180 (1):123-131.

Ueda, Keisuke, Kenjirou Higashi, Keiji Yamamoto, and Kunikazu Moribe. 2013. "Inhibitory effect of hydroxypropyl methylcellulose acetate succinate on drug recrystallization from a supersaturated solution assessed using nuclear magnetic resonance measurements." Molecular pharmaceutics 10 (10):3801-3811.

Van den Mooter, Guy. 2012. "The use of amorphous solid dispersions: A formulation strategy to overcome poor solubility and dissolution rate." Drug Discovery Today: Technologies 9 (2):e79-e85.

van Erp, Nielka P, Hans Gelderblom, Mats O Karlsson, Jing Li, Ming Zhao, Jan Ouwerkerk, Johan W Nortier, Henk-Jan Guchelaar, Sharyn D Baker, and Alex Sparreboom. 2007. "Influence of CYP3A4 inhibition on the steady-state pharmacokinetics of imatinib." Clinical Cancer Research 13 (24):7394-7400.

van Heeswijk, Rolf PG, Agnes I Veldkamp, Richard MW Hoetelmans, Jan W Mulder, Gerrit Schreij, Ann Hsu, Joep MA Lange, Jos H Beijnen, and Pieter L Meenhorst. 1999. "The steady-state plasma pharmacokinetics of indinavir alone and in combination with a low dose of ritonavir in twice daily dosing regimens in HIV-1-infected individuals." Aids 13 (14):F95-F99.

Vangani, Saroj, Xiaoling Li, Peter Zhou, Mary-Anne Del-Barrio, Rick Chiu, Nina Cauchon, Ping Gao, Cesar Medina, and Bhaskara Jasti. 2009. "Dissolution of poorly water-soluble drugs in biphasic media using USP 4 and fiber optic system." Clinical Research and Regulatory Affairs 26 (1-2):8-19.

Vasconcelos, Teofilo, Bruno Sarmento, and Paulo Costa. 2007. "Solid dispersions as strategy to improve oral bioavailability of poor water soluble drugs." Drug discovery today 12 (23):1068-1075.

Verreck, Geert, Annelies Decorte, Hongbo Li, David Tomasko, Albertina Arien, Jef Peeters, Patrick Rombaut, Guy Van den Mooter, and Marcus E Brewster. 2006. "The effect of pressurized carbon dioxide as a plasticizer and foaming agent on the hot melt extrusion process and extrudate properties of pharmaceutical polymers." The Journal of supercritical fluids 38 (3):383-391.

Vijaya Kumar, Sengodan Gurusamy, and Dina Nath Mishra. 2006. "Preparation and evaluation of solid dispersion of meloxicam with skimmed milk." Yakugaku Zasshi 126 (2):93-97.

Vo, Chau Le-Ngoc, Chulhun Park, and Beom-Jin Lee. 2013. "Current trends and future perspectives of solid dispersions containing poorly water-soluble drugs." European journal of pharmaceutics and biopharmaceutics 85 (3):799-813.

Wang, Jennifer, Hong Wen, and Divyakant Desai. 2010. "Lubrication in tablet formulations." European journal of pharmaceutics and biopharmaceutics 75 (1):1-15.

Westerberg, M, and C Nyström. 1991. "Physicochemical aspects of drug release. XII. The effect of some carrier particle properties and lubricant admixture on drug dissolution from tableted ordered mixtures." International journal of pharmaceutics 69 (2):129-141.

Williams, Hywel D, Natalie L Trevaskis, Susan A Charman, Ravi M Shanker, William N Charman, Colin W Pouton, and Christopher JH Porter. 2013. "Strategies to address low drug solubility in discovery and development." Pharmacological reviews 65 (1):315-499.

Witschi, Claudia, and Eric Doelker. 1997. "Residual solvents in pharmaceutical products: acceptable limits, influences on physicochemical properties, analytical methods and documented values." European Journal of Pharmaceutics and Biopharmaceutics 43 (3):215-242.

Wurster, Dale E., and Palmer W. Taylor. 1965. "Dissolution Rates." Journal of Pharmaceutical Sciences 54 (2):169-175. doi: https://doi.org/10.1002/jps.2600540202.

Wyttenbach, Nicole, Christine Janas, Monira Siam, Matthias Eckhard Lauer, Laurence Jacob, Emmanuel Scheubel, and Susanne Page. 2013. "Miniaturized screening of polymers for amorphous drug stabilization (SPADS): rapid assessment of solid dispersion systems." European Journal of Pharmaceutics and Biopharmaceutics 84 (3):583-598.

Xi, Ning, Yingjun Zhang, Zhaohe Wang, Taoxi Lin, and Qian Wang. 2014. Vemurafenib prodrugs suitable for oral and IV administration. AACR.

Yang, Yonglai, Bi, Vivian, and Durig, Thomas. 2015. "The Impact of HPMC Molecular Weight and Degree of Substitution on Crystallization Inhibition of Felodipine in Aqueous Media." AAPS.

Yoshioka, Minoru, Bruno C Hancock, and George Zografi. 1994. "Crystallization of indomethacin from the amorphous state below and above its glass transition temperature." Journal of pharmaceutical sciences 83 (12):1700-1705.

Yuan, Xiaoda, Diana Sperger, and Eric J Munson. 2013. "Investigating miscibility and molecular mobility of nifedipine-PVP amorphous solid dispersions using solid-state NMR spectroscopy." Molecular pharmaceutics 11 (1):329-337.

Zane, P, Z Guo, D MacGerorge, P Vicat, and C Ollier. 2014. "Use of the pentagastrin dog model to explore the food effects on formulations in early drug development." European Journal of Pharmaceutical Sciences 57:207-213.

Zhou, Deliang, David JW Grant, Geoff GZ Zhang, Devalina Law, and Eric A Schmitt. 2007. "A calorimetric investigation of thermodynamic and molecular mobility contributions to the physical stability of two pharmaceutical glasses." Journal of pharmaceutical sciences 96 (1):71-83.

Zhou, Deliang, Geoff GZ Zhang, Devalina Law, David JW Grant, and Eric A Schmitt. 2008. "Thermodynamics, molecular mobility and crystallization kinetics of amorphous griseofulvin." Molecular pharmaceutics 5 (6):927-936.

Zhou, Rong, Paul Moench, Christopher Heran, Xujin Lu, Neil Mathias, Teresa N Faria, Doris A Wall, Munir A Hussain, Ronald L Smith, and Duxin Sun. 2005. "pH-dependent dissolution in vitro and absorption in vivo of weakly basic drugs: development of a canine model." Pharmaceutical research 22 (2):188-192.